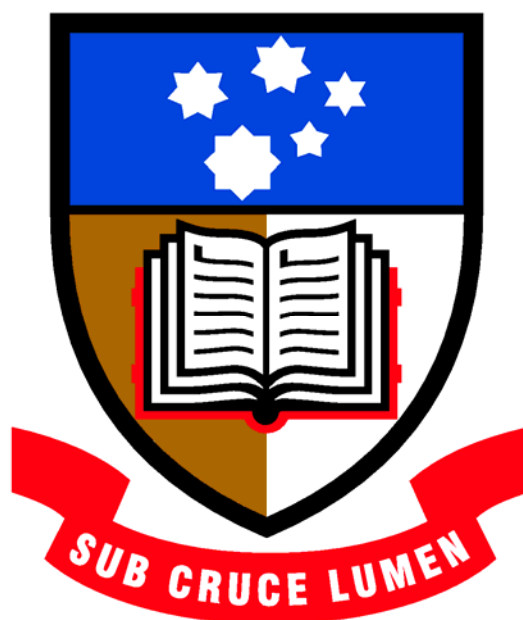# Synthesis of Glutamate Mimics as Neuropathic Pain Modulating Agents

A thesis submitted for the

Degree of Doctor of Philosophy

Nathan John Stanley

B.Sc. (Hons)

SUB CRUCE LUMEN

Department of Chemistry

The University of Adelaide

December 2009

Table of Contents

Abstract

As part of the vital search towards improved therapeutic agents for the treatment of neuropathic pain, the central nervous system ubiquitous glutamate receptors have become a major focus of research. As such, the discovery of glutamate receptor ligands with improved potency and selectivity has been an important area of study for many decades, though there is still much knowledge to be gained.

Outlined herein are the syntheses towards a series of potentially biologically active 3'-cycloalkyl-substituted carboxycyclopropylglycine analogues. These syntheses utilize novel synthetic chemistry to construct the cyclopropane core with all required stereochemistry. As a consequence of this work, two new cycloalkylcarboxycycloproplyglycine analogues were successfully synthesized, utilizing the reaction of 1,2-dioxines with protected phosphonates in a 20% overall yield for one diastereoisomer.

Secondly, the syntheses of a series of 1,4- and 1,5-substituted 1,2,3-triazole amino acids as a new class of potential glutamate receptor ligands. Briefly, a series of six 1,4- and 1,5-triazole amino acids were successfully synthesized utilizing both copper (I) and ruthenium-catalysed cycloaddition of functionalized azides and alkynes.

Furthermore, contained within Chapter 4 are the details and results of *in vitro* binding assays used in screening for possible active compounds. As an example, *in vitro* drug screening at NMDA, kainate and AMPA ionotropic glutamate receptor subtypes revealed activity of triazole amino acid **48** with an EC_{50} value of 49 μM at AMPA receptors. Also, drug screening at metabotropic glutamate receptor subtypes 1, 2 and 4 revealed potent agonist activity of cyclopropane amino acid **44a** at mGluR2 with an EC_{50} value of 0.05 μM. Cyclopropane amino acid **44a** was thus selected for further testing *in vivo* in a rodent model of neuropathic pain. The results indicated that cyclopropane amino acid **44a** significantly and dose-dependently decreased mechanical allodynia, one of the symptoms of neuropathic pain. It was suggested that this effect was due to activation of mGlu2 and 3 receptors located on both neuronal and glial cells within the dorsal horn of the spinal cord.

Lastly, in an effort to rationalize the *in vitro* binding data, the newly synthesized cyclopropane and triazole amino acids were docked *in silico* into the NMDA, AMPA, mGluR1 and mGluR3 receptors available as x-ray crystal structures. Only limited data was obtained regarding the mGluR1 and mGluR3 dockings. However, AMPA receptor docking of the new *in vitro* active triazole amino acids **45** and **48** revealed positive docking interactions in agreement with those seen for the endogenous ligand, glutamate and the selective agonist AMPA. The docking of these new compounds was also computed to be highly energetically favourable, thus suggesting plausible binding modes.

Declaration

This work contains no material which has been accepted for the award of any other degree or diploma in any university or other tertiary institution to Nathan Stanley and, to the best of my knowledge and belief, contains no material previously published or written by another person, except where due reference has been made in the text.

I give consent to this copy of my thesis, when deposited in the University Library, being made available for loan and photocopying, subject to the provisions of the Copyright Act 1968.

I also give permission for the digital version of my thesis to be made available on the web, via the University's digital research repository, the Library catalogue, the Australasian Digital Theses Program (ADTP) and also through web search engines, unless permission has been granted by the University to restrict access for a period of time.

Acknowledgements

I would like to extend sincere thanks to my supervisors Professor Dennis Taylor, Professor Andrew Abell and Associate Professor Rod Irvine who have encouraged me to keep pushing forward even when things were turning pear-shaped.

Special thanks goes out to Dr Thomas Avery and Dr Daniel Pedersen for all their invaluable help and practical tips in the lab. Without Dr Mark Hutchinson, the *in vivo* experiments and *in silico* docking work would not have happened; thankyou. Thanks also to Peter Grace for helping with the *in vivo* testing.

Many thanks to Birgitte Nielsen, Trine Kvist and especially Professor Hans Bräuner-Osborne at the University of Copenhagen in Denmark for kindly doing the *in vitro* receptor binding assays.

Gratitude is expressed to the Faculty of Sciences for providing the financial support necessary for this research to be undertaken.

Finally, to my beautiful wife, Penelope; I could not have made it through this without your support. Thankyou for putting up with me over the past four years throughout my PhD.

Abbreviations

Ac	acetyl
AcOH	acetic acid
Anal. Calcd.	analysis calculated
Bn	benzyl
Boc	*tertiary*-butoxycarbonyl
Cbz	carboxybenzyl
CCG	carboxy cyclopropyl glycine
CNS	central nervous system
COSY	correlated spectroscopy
Cp*	pentamethylcyclopentadiene
Δ	heat
DCM	dichloromethane
DCVC	dry column vacuum chromatography
DIAD	diisopropyl azodicarboxylate
DMSO	dimethyl sulfoxide
DPPA	diphenyl phosphoryl azide
EC_{50}	concentration which elicits a 50% maximal effect
EDC	1-ethyl-3-(3-dimethylaminopropyl) carbodiimide
ee	enantiomeric excess
EI	electron impact
ESI	electrospray ionisation
Et	ethyl
equiv.	equivalent(s)
de	diastereomeric excess
g	gram(s)
HOBt	*N*-Hydroxybenzotriazole
HRMS	high resolution mass spectrometry
h	hour(s)
hv	light
Hz	hertz
IC_{50}	concentration which elicits 50% maximum inhibition

iGluR	ionotropic glutamate receptor
IR	infrared
i.t.	intrathecal
J	coupling constant
lit.	literature
m	meta
M	moles per litre
m-CPBA	*meta*-chloroperbenzoic acid
m/z	mass to charge ratio
Me	methyl
MeOH	methanol
mGluR	metabotropic glutamate receptor
MIRC	Michael initiated ring closure
mol	mole(s)
mp	melting point
NIS	*N*-iodosuccinimide
NMR	nuclear magnetic resonance
PDC	pyridinium dichromate
Pd/C	palladium on carbon
Ph	phenyl
ppm	parts per million
R$_f$	retention factor
ROESY	Rotating Frame Overhauser Effect Spectroscopy
rt	room temperature
t-Bu, Bu^t	*tertiary*-butyl
TEA	triethylamine
TFAA	trifluoroacetic anhydride
THF	tetrahydrofuran
TLC	thin layer chromatography
TPP	triphenylphosphine
TPPO	triphenylphosphine oxide
UV	ultraviolet

Chapter 1 : Introduction

1.1 Introduction

The negative experience of pain embraces all of humankind, young and old, wealthy and poor and those of every land, culture and language. Yet even after many years of research, we are yet to alleviate ourselves completely of this universal burden. Not only is this an individual burden, but pain is a great economic burden also. It has been reported by the MBF Foundation that pain costs Australia an estimated total of $34 billion annually.[1]

1.2 What is Pain?

Pain can broadly be divided into two distinct types. Firstly, acute pain, such as common headache or pain associated with a temporary injury such as a laceration. Secondly, chronic pain, such as permanent spinal injury resulting in back pain or phantom limb pain. Pain can be described as the negative aversive sensation caused by an actual or perceived injury.[2]

1.3 Pain Pathways

Peripheral pain usually consists of a combination of either tactile or thermal along with affective sensory information. Referring to Figure 1.1, the tactile and thermal sensory pathways, consisting of Aβ and Aδ fibres, enter the central nervous system (CNS) via the dorsal horn of the spinal cord and from there, pathways ascend to the thalamus, where an involuntary reflex may be elicited in order to avoid injury and prevent ongoing pain. Pathways also ascend from the thalamus to the somatosensory cortex where the quality and location of the tactile or thermal stimulus is interpreted and suitable action is consciously decided. However, this is only half the story, since these pathways alone do not communicate anything about the noxious or painful nature of the stimulus. There are other pathways, consisting of C fibres, which also enter the CNS via the dorsal horn. Within the dorsal horn, the pain signals are integrated and a pathway ascends to the parabrachial area and from there, directly to the amygdala. The amygdala sends projections to the substantia innominata, which in turn projects to the thalamus and cortex; thus the painful or affective aspects of the painful stimulus are conveyed. It

is these pathways also that are involved in pairing context and aversive emotions with the noxious stimuli.[3-6]

Figure 1.1. Pain Pathways[3]

NOTE:
This figure is included on page 11 of the print copy of the thesis held in the University of Adelaide Library.

1.4 Neuropathic Pain

Chronic neuropathic pain affects a significant portion of the population worldwide[7] and decreases quality of life.[8,9] Many of the current medications used for neuropathic pain do not give adequate and effective pain relief in all cases[10-12] and so, much research has been focussed on finding alternative pain treatments.

Neuropathic pain results from tissue damage, inflammation or injuries in which affective pain pathways can become hypersensitive. Constant pain signalling causes neuroplastic changes, resulting in persistent pain even after the initial insult has healed or subsided.[13] This sensory disorder is characterized by hyperalgesia, the sensitization to painful stimuli, allodynia, the sensation of normal tactile stimuli as painful as well as other sensory disorders including hyperesthesia, paresthesia, dysesthesia and

hypoesthesia. Spontaneous pain is also sometimes evident.[13,14] Although the actual mechanistic causes behind neuropathic pain are poorly understood, it is known to be associated with direct nerve or spinal cord injury, herpes zoster infection, multiple sclerosis, diabetes, stroke and cancer.[12,14]

1.5 The Pain Control Loop

Spinal pain signalling is modulated by both descending inhibitory and facilitatory systems[15,16] (Figure 1.2). Ascending pathways from the dorsal horn project to the thalamus, however there are also descending pathways which project towards the periaqueductal grey and then to the rostral ventromedial medulla (RVM) and back to the dorsal horn via the dorsolateral funiculus. Animal behavioural experiments show activation of these systems via electrical or chemical stimulation of the PAG or areas of the RVM inhibits nociceptive reflexes such as the tail-flick and hotplate response.[17] Following these experiments, it has been found by electrophysiological studies that stimulation of either the RVM of PAG can cause inhibition of spinal nociceptive transmission via pathways descending back to the dorsal horn.[16,18] Of the projections from the RVM to the dorsal horn, one group of neurons has been labelled 'ON' cells, another group has been labelled 'OFF' cells and a final group labelled 'neutral' cells. These groups of neurons terminate in laminae I, II and V. As the labels suggest, 'neutral' cells have no effect on pain modulation, 'ON' cells are thought to be descending facilitatory neurons which potentiate dorsal horn pain signalling whereas the 'OFF' cells are descending inhibitory neurons which attenuate signalling.[18-20] There are also suggestions that descending pathways from the RVM and surrounding areas are not involved in pain signalling alone, but modulate a range of homeostatic functions and may play more of a role in stimulus-evoked arousal.[21] However, dysfunction of 'ON' cells has been implicated as part of the cause of neuropathic pain, whereby there is excess pain facilitation.[16,22]

Figure 1.2. The Pain Control Loop

1.6 Current Treatments

Opioids, with morphine as gold-standard, have traditionally been the mainstay of pain treatment. Be that as it may, these ancient therapeutics are generally considered to be less effective in alleviating the symptoms of neuropathic pain.[23] Though they do show some efficacy, there is a lot of inter-individual variation along with side-effects, particularly respiratory depression, sedation, tolerance and gastrointestinal upset, still remaining a problem.[24] Administered chronically, opioids can also cause adverse endocrine effects[25] and analgesic tolerance can also develop[26] which results in the need for dose escalation in the clinical setting and there is a well known risk of developing opioid dependence.[27] There is also evidence which implicates the endogenous opioid system in the induction and maintenance of chronic pain[28,29] and work which suggests that chronic opioids can actually cause apoptosis of certain inhibitory neurons in the dorsal horn, causing hyperalgesia which has the appearance of opioid tolerance in the clinical pain setting.[30] Further to this, individuals who are opioid dependent and who are

receiving opioids such as methadone and buprenorphine as substitution treatment often have problems with pain sensitivity.[26] This manifests itself in a similar way to neuropathic pain, being characterised by hyperalgesia and allodynia.[31] In this group of people, pain management can be difficult due to analgesic tolerance and opioid addiction, especially since there is strong evidence to suggest that chronic opioid use can actually be the cause of such sensory disorders.[30]

Owing to the fact that opioids have proved to lack efficacy in many types of chronic and neuropathic pain, much research has centred on finding alternative drugs. At present there are many drugs being used clinically to treat chronic pain (Figure 1.3) many of these are being used 'off-label' including antidepressants such as venlafaxine (**1**) and duloxetine (**2**) (Cymbalta®, Eli Lilly), NMDA antagonists like ketamine (**3**), anticonvulsant drugs like gabapentin (**6**) (Neurontin®, Pfizer), pregabalin (**7**) (Lyrica®, Pfizer) and lamotrigine (Lamictal®, GlaxoSmithKline), voltage-gated calcium channel blockers, for example ziconotide (**8**) (Prialt®, Elan Pharmaceuticals), adrenergic drugs such as clonidine (**9**) and more traditionally, opioids including tramadol (**4**) and oxycodone as well as topical medications.[12,32-35] There is often a lot of inter-individual variation in efficacy of these drugs in neuropathic pain patients. As such combination therapies are usually employed using several drugs with differing sites of action. Other underlying diseases or conditions also need to be taken into account such that the use of certain medications is prohibited due to drug interactions and the risk of serious side effects.[12,32]

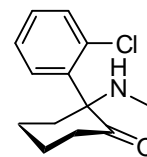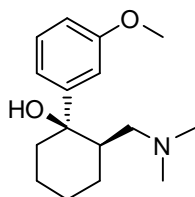**Figure 1.3.** Examples of Currently Used Chronic Pain Drugs
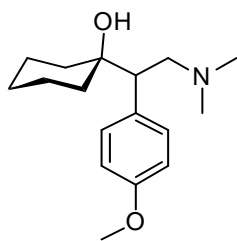
Venlafaxine
1
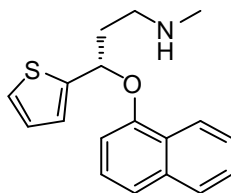
Duloxetine (Cymbalta®)
2

Ketamine
3

Tramadol
4
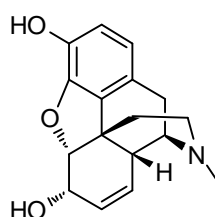
Morphine
5
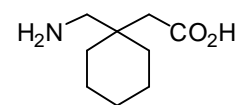
Gabapentin
(Neurontin®)
6
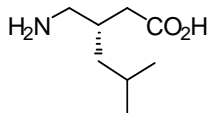
Pregabalin (Lyrica®)
7
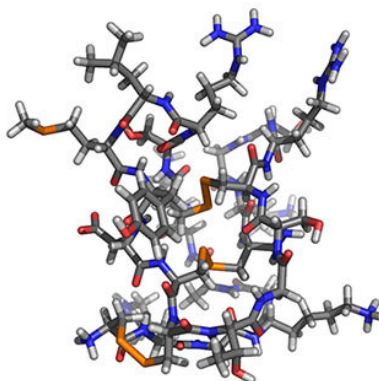
Ziconotide (Prialt®)
8
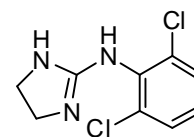
Clonidine
9

1.7 Glia and Pain

All currently used neuropathic pain therapeutics were, until relatively recently, thought to elicit their action purely though neuronal mechanisms, however it has been discovered that this is not the case. Much research has now been done into the involvement of central nervous system immune cells in modulation of pain signalling.

These cells, comprising mainly microglia and astrocytes (collectively known simply as 'glia'), are equivalent in number to neurons in the CNS and are known to be involved in the maintenance, support and immuno-protection of neurons.[36,37] However, mounting evidence indicates that glia can modulate the functional signalling and plasticity of neurons.[38-41] It has been shown that glia release a host of pro-inflammatory mediators which act on neurons to increase and sustain excitability. Further to this, it has been demonstrated that glia are intrinsically involved in opioid analgesic tolerance, hyperalgesia, allodynia and withdrawal symptoms.[42] Binding of opioids to toll-like receptors (TLR) located in association with glia, is proposed to cause activation of these cells which leads to increased levels of pro-inflammatory cytokines. It is becoming very clear that opioids such as morphine are a double edged sword, not only mediating analgesia in the short term, but actually increasing pain sensation in the longer term via two distinct mechanisms.[43] The excitatory neurotransmitter glutamate (**10**) is known to be involved in signalling between neurons and glia.[40] Crucially, metabotropic glutamate receptors, the target of this research, are also located in association with glial cells and as such activation or blockade of these receptors by external ligands may modulate how glial cells are behaving in the neuropathic pain state.[44]

Figure 1.4. Structure of L-Glutamate

10
L-Glutamate
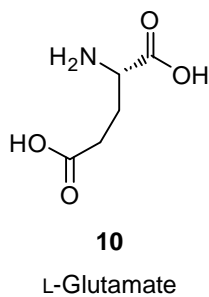
1.8 Glutamate Receptors

L-Glutamate (**10**) is the principal excitatory neurotransmitter in the central nervous system (CNS). It plays an important role in neuronal synaptic plasticity and in particular, changes to neuron signalling known as long-term potentiation and long-term depression.[45-47] A high density of glutamatergic projections are found in the hippocampus and neocortex where glutamate plays a vital role in learning and memory.[46,48,49] There are two main classes of glutamate receptors, the ionotropic and

the metabotropic. The ionotropic glutamate receptors (iGluRs) are ligand-gated sodium and calcium ion channels and consist of various forms of the *N*-methyl-D-aspartate (NMDA), α-amino-3-hydroxy-5-methyl-4-isoxazolepropionic acid (AMPA) and 2-carboxy-3-carboxymethyl-4-isopropenylpyrrolidine (kainate) receptors. The metabotropic glutamate receptors (mGluRs) are GTP-binding protein (G-protein) coupled receptors (GPCRs), having eight known subtypes divided into three groups depending on sequence homology, signal transduction mechanisms and agonist/antagonist interactions. These receptors consist of a 'venus fly trap' extracellular binding domain coupled to a heptahelical transmembrane domain, coupled to an intracellular signal transduction domain (Figure 1.5). Group I contains mGluR1 and mGluR5 and these receptors are excitatory, being coupled to $G_{q/11}$, leading to activation of phospholipase C (PLC). Group II contains mGluR2 and mGluR3 and group III contains mGluR4, R6, R7 and R8 and these are all inhibitory, being coupled to $G_{i/0}$, leading to inhibition of adenylyl cyclase and decreased cyclic adenosinemonophosphate (cAMP) production.[50]

Figure 1.5. A Representation of the Metabotropic Glutamate Receptor

NOTE:
This figure is included on page 17 of the print copy of the thesis held in the University of Adelaide Library.

Metabotropic glutamate receptors have been implicated as targets for a whole host of neurological disorders including neuropathic pain,[51-54] generalized anxiety disorder,[55-57] Parkinson's disease,[58-60] psychosis,[61,62] epilepsy,[63] depression,[64-66] dementia and Alzheimer's disease-related neuro-degeneration[67] and drug dependence.[68-70]

1.9 Glutamatergic Origins of Neuropathic Pain

Glutamate plays a significant role in the modulation of pain signalling.[71,72] There is substantial evidence to support the involvement of neuroplastic changes such as central sensitization and long term potentiation in the induction and maintenance of neuropathic pain[73,74] and previous studies have revealed that metabotropic glutamate receptors are important as modulators of neuroplasticity.[75] In the past, a large amount of research has been focussed on the possibility of targeting NMDA receptors which have been shown to be involved in the initiation and maintenance of neuropathic pain. The potential mechanism of treatment is by the use of NMDA antagonists such as ketamine[35] or dextromethorphan,[76] however, there are problems with side effects and lack of potency. The NMDA receptors are fast excitatory receptors as they are ligand-gated ion channels and as such, they elicit fast excitatory responses, whereas mGlu receptors are GTP-binding protein (G-protein) coupled receptors (GPCRs) which elicit a slower, more regulated response on nerve transmission. It has previously been shown that drugs targeting mGlu receptors show efficacy in various pain models, including those where allodynia and hyperalgesia are present.[71,77,78]

1.10 Distribution of Metabotropic Receptors

Metabotropic glutamate receptors have been identified in many key regions of the CNS known to play a role in pain signalling and processing. The main receptor sub-types present are those from Group I, mGluR1/R5 and those from Group II, mGluR2/R3 and it appears from second-messenger assays, electrophysiological studies and immunohistochemistry, that the Group I receptors act postsynaptically in an excitatory manner and the Group II receptors act presynaptically as inhibitory autoreceptors, in the case of mGluR3 or extrasynaptically, in the case of mGluR2 (Figure 1.6).[79,80]

Figure 1.6. A Representation of the Typical Synaptic Locations of Metabotropic Glutamate Receptors and Their Signalling Pathways[81]
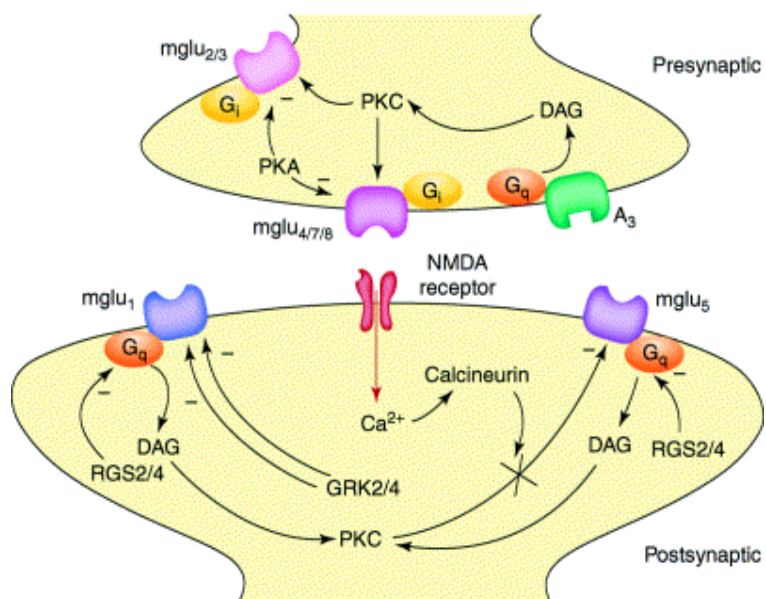
1.11 Pain Memory

There is recent research which points to the involvement of the amygdala in neuropathic pain through the spino-parabrachio-amygdaloid pathway.[82,83] The amygdala also sends descending projections to the PAG which in turn projects to the RVM, then to the dorsal horn (see Figure 1.2). The amygdala is involved in the emotional "colouring" of sensory information, for example fear conditioning, and has been implicated as playing a role in modulating the affective component of pain.[82-85] Pathways within the amygdala can undergo neuroplastic changes due to long-term potentiation of neuron signalling.[86] Glutamate is a key player in this process and mGlu receptors have been identified within the amygdala which are involved in synaptic plasticity and modulation of signalling.[87-89]

One aspect of neuropathic pain is the presence of the affective component of pain in the absence of any tactile or thermal insult or injury and the amygdala may well be involved in this signalling. The specific involvement of mGluR2 in the amygdala has been confirmed and early studies demonstrate that mGluR2 agonists can cause long term depression of synaptic transmission in this area.[90-92] Therefore, it is possible that

modulation of amygdala function by targeting mGlu receptors may result in alleviation of some aspects of neuropathic pain such as the negative feelings and depression associated with it and possibly alleviation of the 'pain' itself.

1.12 The Benefit of Targeting Metabotropic Glutamate Receptors

Glutamate is important for signal transmission in pain signalling structures and mGlu receptors are known to be involved in the RVM, the PAG[93,94] and the dorsal horn (see Figure 1.2).[95] Research found that activation of Group II mGlu receptors by DCG-IV (Figure 1.7, **11**) within the RVM produces a powerful inhibition of the spinal nociceptive tail-flick reflex.[17] However, DCG-IV also activates NMDA receptors which may have contributed to the antinociceptive effects.

Figure 1.7. Known mGluR Ligands

DCG-IV	(1S,3R)-ACPD	(2S)-α-Eglu	(R,S)-AIDA
11	**12**	**13**	**14**
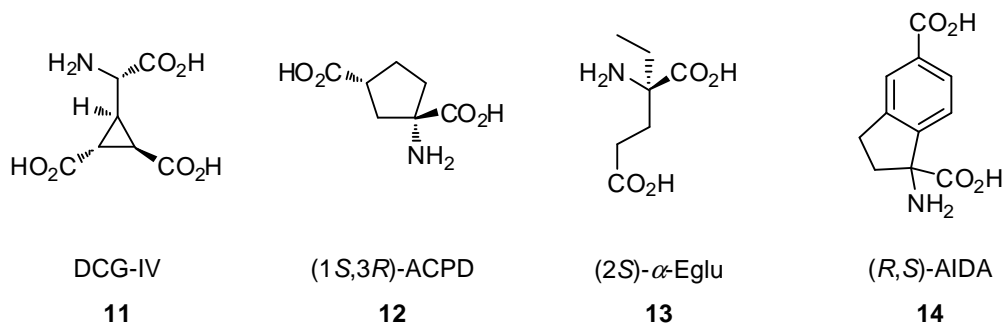
It has also been shown that microinjection of mGluR Group I and II agonist (1S,3R)-ACPD (Figure 1.7, **12**) into the PAG causes a dose-dependent increase in nociceptive response latency in the mouse hotplate test. Pre-treatment with a Group II antagonist, (2S)-α-Eglu (**13**), caused a brief but significant reversal of the antinociceptive effects, whereas pre-treatment with a Group I antagonist, (RS)-AIDA (**14**), caused a partial, yet significant potentiation of the antinociceptive effect produced by (1S,3R)-ACPD.[93] These results suggest that both Group I and II mGlu receptors are involved in thermal nociception and that blockade of Group I and activation of Group II receptors can elicit antinociception. A further study directly injected the Group I agonist, (S)-3,5-DHPG (Figure 1.8, **15**) and Group II agonist, L-CCG-I (Figure 1.8, **16**) into the PAG which decreased the late phase formalin-induced nociceptive response.[94] These results appear to be contradictory since here a Group I agonist was antinociceptive whereas results

found previously suggested that a Group I antagonist would be effective. However, several research groups have found activation of Group II receptors to be antinociceptive. This theory is also supported in experimental models of neuropathic pain, where hyperalgesia, allodynia and spontaneous pain are evident. Sharpe et al.[96] administered the Group II mGlu agonist, LY379268 (Figure 1.8, **17**), to both rats and mice and found a significant reduction in hyperalgesia both in models of thermal and neurogenic inflammation. Simmons et al.[52] found intraperitoneal injection of mGluR2 agonists resulted in antinociception in the late phase of the formalin test as well as significantly reducing neuropathic allodynia in a rat model. Activation of Group II mGluRs within the amygdala by agonist L-CCG-I, produced long term depression of synaptic transmission which points to such receptor modulation being potentially useful in targeting the affective component of pain.[91]

Figure 1.8

| (S)-3,5-DHPG	L-CCG-I	LY379268
15	**16**	**17**
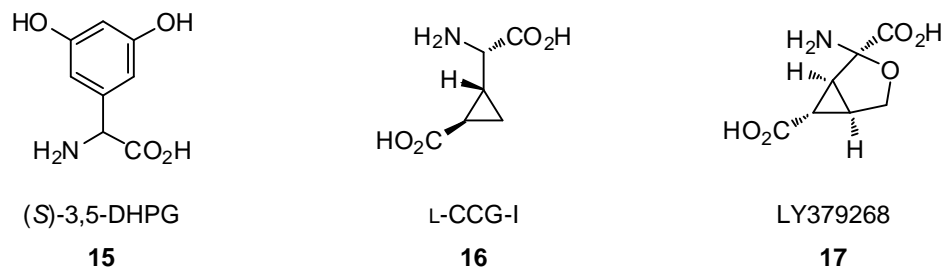
1.13 Structure Activity Relationship of Metabotropic Glutamate Ligands

Over the past twenty years, there has been an immense amount of research into the structure activity relationship of metabotropic glutamate receptor ligands and the search for more potent and selective compounds is far from over. Outlined herein is an overview of the advances made in understanding the structure and function relationship of the receptors themselves and how this relates to the design of new and improved ligands. The metabotropic class of glutamate receptors was first recognized in 1987 by Sugiyama and colleagues where it was shown that the potent AMPA receptor agonist, quisqualate (**18**) and the potent NMDA agonist, ibotenate (**19**) as well as glutamate could activate phosphoinositide hydrolysis in rat brain slices *in vitro*.[97] It was shown that this effect could not be replicated by using other ionotropic receptor agonists such as NMDA or kainate, nor blocked by known antagonists of these receptors.[98] This work

opened up the doorway to subsequent examination of the structures of quisqualate and ibotenate which will be discussed later.

Figure 1.9. Original Metabotropic Glutamate Receptor Ligands

| Quisqualate | Ibotenate |
| **18** | **19** |
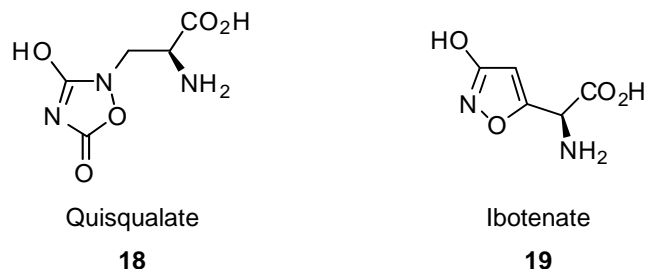
In 1989, the first mGluR selective agonist was reported. It was shown that (1*SR*,3*RS*)-1-aminocyclopentane-1,3-dicarboxylic acid ((1*SR*,3*RS*)-ACPD, also known as (±) *trans* ACPD) (Figure 1.10), could cause activation of phosphoinositide hydrolysis in the presence of antagonists of NMDA, kainate and AMPA (at the time known as quisqualate) receptors.[98]

Figure 1.10. (±) *trans* ACPD
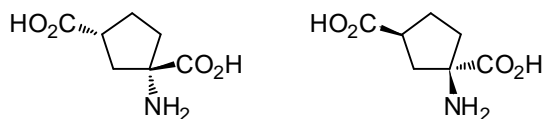
(1:1) mixture of enantiomers

With the cloning of the rat mGlu1a by two independent groups in 1991[99,100] it was now possible, by matching sequence homology, to identify a further seven subtypes, mGlu2, mGlu3, mGlu4, mGlu5, mGlu6, mGlu7 and mGlu8.[101-103] It also became apparent that the subtypes fell into three different groups owing to the fact that selective binding of quisqualate to mGlu1 and mGlu5 receptors potently activated phosphoinositide hydrolysis whereas selective binding of the compound L-CCG-I (**16**) to mGluR2 and mGluR3, potently inhibited adenylyl cyclase and decreased cAMP production and selective binding of the compound L-AP4 (**20**) to mGlu4, mGlu6, mGlu7 and mGlu8, also potently inhibited adenylyl cyclase and decreased cAMP production. Analysis of sequence homology revealed 60% conserved sequence identity within each group and

40-50% between groups.[101,103] Thus there was an obvious division into three groups based on sequence homology, ligand binding and second messenger systems.

Figure 1.11. Group II and III Ligands

L-CCG-I

16

L-AP4

20
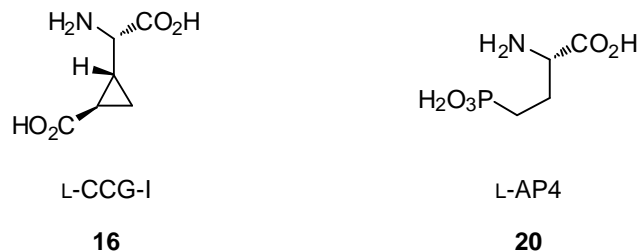
Metabotropic glutamate receptors (mGluRs) belong to the family of GTP-binding protein (G-protein) coupled receptors and can be divided between the extracellular *N*-terminal, comprising the ligand binding region (LBR) consisting of some 550 amino acid residues, tethered by a cysteine-rich domain (CR) to the heptahelical transmembrane domain (TM) which is linked to the intracellular C-terminal signal transduction domain. In 1993, the LBR of mGluR1 was found to be homologous to the known leucine/isoleucine/valine binding protein (LIVBP) which belongs to the bacterial periplasmic binding protein (PBP) family.[104] At the time, there were no x-ray crystal structures available for the LBR of any mGluR subtypes, but using the structure of LIVBP as a guide, it was possible to begin unravelling the details of mGluR ligand binding.

The mGlu receptor, when expressed on the cell surface, exists in the active conformation as a homodimer (MOL1 and MOL2) each of which have a bi-lobal ligand binding domain (LB1 and LB2) between which is the actual ligand binding region (Figure 1.12). The two protomers MOL1 and MOL2 are covalently connected by a disulfide bridge between Cys140 of each monomer, which has been shown by substitution with an alanine residue to be important for favouring the formation of the active dimer.[105]

Figure 1.12 Metabotropic Glutamate Receptor Domains[105]

As has been briefly discussed above, there is an ever-growing body of research focussed on the elucidation of the structure-function relationship and pharmacodynamics of the metabotropic glutamate receptors. This has in turn necessitated the development of improved ligands with greater subtype selectivity and potency as experimental tools. Outlined below are the classes of compounds that have been investigated thus far.

1.13.1 The Cyclopentane Analogues

The cyclopentane class of compounds were the first investigated, due to their relation to known iGluR ligands. Desai and Conn reported that (±) *trans* ACPD (1*SR*,3*RS*)-ACPD) (see Figure 1.10) stimulates phosphoinositide hydrolysis, an effect similar to the iGluR agonist ibotenate (**19**, Figure 1.9).[106] However, this effect was not blocked by NMDA, AMPA or kainate receptor antagonists indicating that the ligand was activating a different type of receptor. This new class of receptor was consequently labelled the metabotropic glutamate receptor after it was discovered to be a G-protein-coupled receptor. Although these compounds all bear a similar core structure, there is great diversity in their pharmacological profiles. Referring to Figure 1.13, (1*S*,3*R*)-ACPD (**12**), the active enantiomer of (±) *trans* ACPD, is a broad spectrum, non-selective agonist showing *in vitro* activity in the order: mGluR2 > mGluR5 > mGluR1 > mGluR8 > mGluR6 > mGluR4. Addition of a carboxylic acid group in the 4-position converts amino acid **12** into (3*S*,4*S*)-ACPT-III (**21**), a selective mGluR4 agonist. Introduction of a nitrogen atom into the cyclopentane ring of (1*S*,3*R*)-ACPD (**12**) at the 4-position increases affinity for the Group II receptors, mGluR2 and R3 and the compound

becomes the potent and selective agonist, (2*R*,4*R*)-APDC (**22**). This compound is approximately equipotent at both R2 and R3, however, if the nitrogen atom is substituted with an amine group, as in (2*R*,4*R*)-amino-APDC (**23**) this results in a compound which is about ten times more selective for mGluR2 over R3. If the nitrogen atom is substituted with a benzyl group, as in (2*R*,4*R*)-benzyl-APDC (**24**) this results in a compound which exhibits agonist activity at mGluR6, whilst being a weak antagonist at mGluR2 (EC$_{50}$: 200 µM) and mGluR5 (EC$_{50}$: 600 µM). Finally, homologation of (1*S*,3*R*)-ACPD (**12**) at the 3-position, produces (**25**) which increases the compound's affinity as an agonist for mGluR2 over all other subtypes.[107]

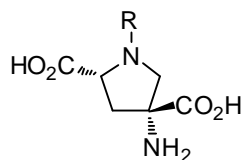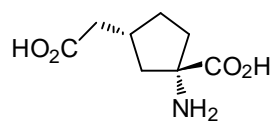**Figure 1.13.** Cyclopentane Analogues
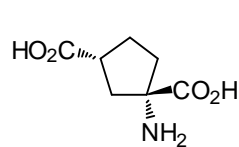
(1*S*,3*R*)-ACPD

12
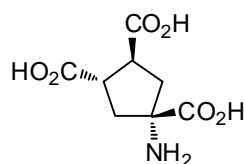
(3*S*,4*S*)-ACPT-III

21

22 R = H: (2*R*,4*R*)-APDC
23 R = NH$_3$:   (2*R*,4*R*)-amino-APDC
24 R = CH$_2$Ph: (2*R*,4*R*)-benzyl-APDC

(1*S*,3*R*)-Homo-ACPD

25

1.13.2 The mGluR Binding Site

The ligand binding region of all known metabotropic glutamate receptors consists of six conserved amino acid residues that are essential for binding L-glutamate and all known competitive ligands. The sequence of the amino acids varies slightly between the three receptor groups and the details of these are outlined in Table 1.1 below.

Table 1.1. Amino Acid Residues Involved in Ligand Binding

	Group I	Group II	Group III
distal carboxylate salt bridge	Arg78	Arg68	Arg78
	Lys409	Lys389	Lys407
proximal carboxylic hydrogen bonds	Ser165	Ser151	Ser159
	Thr188	Thr174	Thr182
amine salt bridge	Asp318	Asp301	Asp314
van der Waals and lone pair interaction with side group	Tyr236	Tyr222	Tyr230
hydrogen bond acceptor (phenolic)	Tyr236	Tyr222	Tyr230

However, simply knowing the residues involved in binding is not sufficient to predict ligand binding. It is now becoming apparent that the actual size of the binding region varies amongst the receptor subtypes. This is due to more or less bulky amino acid side chains occupying the region at the edge of the binding cleft. These residues alone can prevent entry of excessively bulky ligands into the respective receptor LBR.

Energetic and entropic effects also come into play. The LBR in the open form contains a concentration of solvent molecules that is at equilibrium with the surrounding. Binding of a ligand always requires displacement of some solvent molecules in order for the receptor to convert to the closed form. From an entropic point of view, the greater the number of solvent molecules that must be displaced in order for the ligand to bind, the less favourable the binding. Furthermore, in x-ray crystallography studies it has also been observed that some ligands actually require residual solvent molecules in order to facilitate binding.

1.13.3 Phenylglycine Derivatives

In the early 1990s, a group of selective mGluR antagonists was reported that were based on a phenylglycine core structure.[108-110] There are three main types of compound in this class, the hydroxyphenylglycines (Figure 1.14), the carboxyphenylglycines (Figure
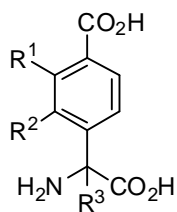
1.15) and the phosphonophenylglycines (Figure 1.16). The simplest compound in the first class is (*S*)-3-HPG (**26**) which is primarily an mGluR5 agonist, but also exhibits weak agonist activity at mGluR1. Addition of a second hydroxyl group at the 5-position gives (*S*)-3,5-DHPG (**15**) which has increased potency over compound **26**, however it has less selectivity for mGluR5 over mGluR1. Further addition of a chlorine atom to the 6-position results in (*R*,*S*)-CHPG (**27**), which is 100 times less potent than compound **15**, but is 10-fold more selective for mGluR1 over mGluR5. The simplest carboxyphenylglycine is (*S*)-4CPG (**28**) which is a selective mGluR1 antagonist, but also shows some weak agonist activity at mGluR2. The addition of a hydroxyl group at the 3-position of compound **28** gives (*S*)-4C3HPG (**29**), which is both an mGluR1 antagonist and an mGluR2 agonist with equal potency at both subtypes. Inclusion of a methyl group at the 2-position of compound **29** provides (*R*,*S*)-4C3H2MPG (**31**) which is solely a selective mGluR1 antagonist with no activity at mGluR2. The compound (+)-4C2MPG (**30**) exhibits equivalent activity to compound **31** at mGluR1. (*S*)-M4CPG (**32**) is compound **28** with methyl substitution on the alpha carbon and is also an mGluR1 antagonist along with LY367366 (**33**) which also shows mGluR5 antagonist activity. Finally, the phosphonophenylglycine analogues have a different pharmacological profile entirely. (*R*,*S*)-PPG (**34**) is a very potent mGluR8 agonist and also a moderately active mGluR4 and mGluR6 agonist, whereas (*R*,*S*)-MPPG (**35**) is an mGluR2 antagonist.
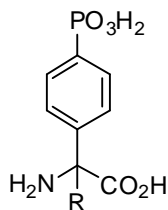
Figure 1.14. Hydroxyphenylglycine Compounds
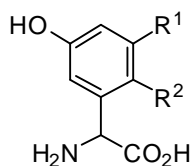
	R^1	R^2	
26	H	H	(*R*,*S*)-3-HPG
15	OH	H	(*S*)-3,5-DHPG
27	OH	Cl	(*R*,*S*)-CHPG

Figure 1.15. Carboxyphenylglycine Compounds

	R^1	R^2	R^3	
28	H	H	H	(*S*)-4CPG
29	OH	H	H	(*S*)-4C3HPG
30	H	Me	H	(+)-4C2MPG
31	OH	Me	H	(*R,S*)-4C3H2MPG
32	H	H	Me	(*S*)-M4CPG
33	H	H		LY367366

Figure 1.16. Phosphonophenylglycine Compounds

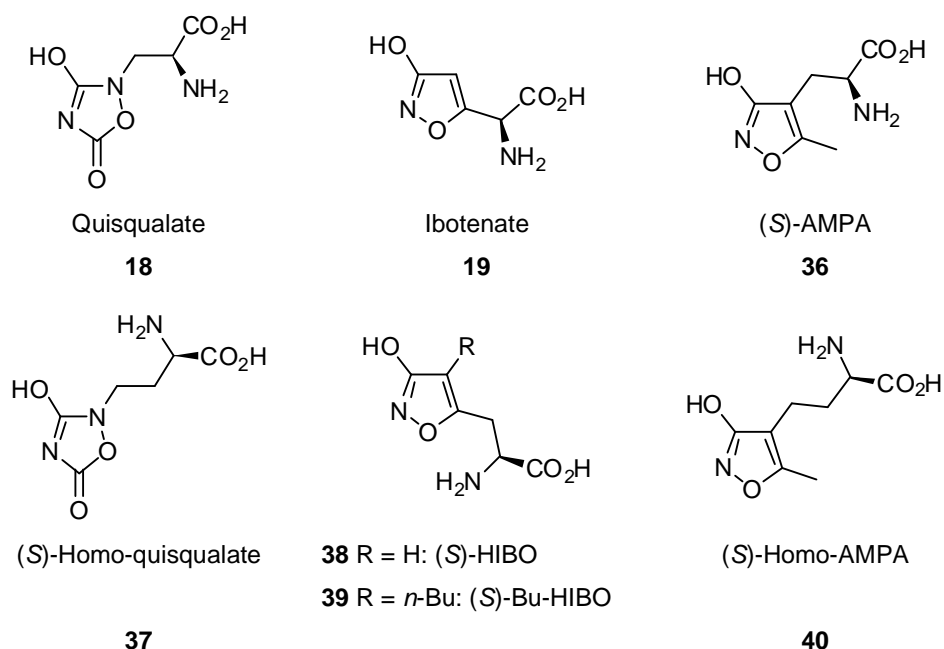|	R	
34	H	(*R,S*)-PPG
35	Me	(*R,S*)-MPPG

1.13.4 The Isoxazoles and Oxadiazoles

These compounds were amongst the first to be discovered as having activity at mGluRs. Most are also active at ionotropic glutamate receptors, such as the prototypes quisqualic acid (quisqualic acid, **18**) and ibotenate (ibotenic acid, **19**) as well as (*S*)-AMPA (**36**).

Figure 1.17. Isoxazoles and Oxadiazoles

Quisqualate
18

Ibotenate
19

(*S*)-AMPA
36

(*S*)-Homo-quisqualate

37

38 R = H: (*S*)-HIBO
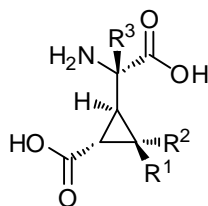**39** R = *n*-Bu: (*S*)-Bu-HIBO

(*S*)-Homo-AMPA

40

1.13.5 The Carboxycyclopropylglycines

Several isomers of 2-carboxycyclopropylglycine were first isolated as natural products from the seeds of *Blighia sapida* and later from the stems of *Ephedra altissima* and *Ephedra foeminea* where they were suggested to play a role as an anti-feeding agents.[111-114] Subsequent synthesis and testing revealed activity in L-glutamate pathways in the central nervous system. In particular, these compounds were found to be relatively selective for metabotropic glutamate receptors and were used as tools to gain insight into the molecular conformation required for subtype selectivity. It was found that NMDA receptor binding required the molecule to adopt a folded conformation, whereas metabotropic binding required an extended conformation.[115-117] In order to investigate this further, a hybrid molecule (2,3-dicarboxycyclopropyl)glycine (DCG-IV) (Figure 1.7, **11**), was synthesized which incorporated both the extended and folded conformations in the same molecule.[118] Further to this, certain types of substitution have been found to result in either agonist or antagonist activity (Table 1.2). It was found that addition of a methyl, phenyl, xanthenylmethyl or xanthenylethyl groups to the 2-position resulted in antagonist activity and phenyl, xanthenylmethyl or xanthenylethyl substitution at the 3'-position also resulted in antagonist activity.[119,120] The cyclopropane core is also a key element as its rigid nature holds the functional groups in

a conformation that very closely resembles L-glutamate's folded conformation as opposed to the fully extended conformation; this is vital for subtype selectivity. Examination of the relationship between substitution at the 3'-position and ligand potency as measured by the EC_{50} value suggests that a group comprising a one carbon chain with a lone pair donor atom attached, such as oxygen, gives the greatest potency of all tested CCGs thus far.[121] Simple methyl substitution is also fairly potent.[122]

**Table 1.2.** Known Carboxycyclopropylglycine Glutamate Receptor Ligands

Compound	R^1	R^2	R^3	EC$_{50}$ (µM)*	
				mGluR2	mGluR3
L-Glutamate[123]				26	6.1
L-CCG-I[121]	H	H	H	0.3	0.6
L-F2CCG-I[121]	F	F	H	0.09	
cis MCG-I[121]	H	CH$_2$OCH$_3$	H	0.1	
trans MCG-I[121]	CH$_2$OCH$_3$	H	H	0.3	
DCG-IV[121]	CO$_2$H	H	H	0.3	0.2
PCCG-4[124]	phenyl	H	H	**0.8**	
XM-CCG-I[119]	xanthenylmethyl	H	H	**6.4**	**1.3**
XE-CCG-I[119]	xanthenylethyl	H	H	**0.2**	**0.75**
LY341495[119]	H	H	xanthenylmethyl	**0.2**	**0.16**
HM-CCG-I[122]	CH$_2$OH	H	H	0.005	0.012
Thiolmethyl[122]	CH$_2$SH	H	H	0.047	0.059
Methyl[122]	CH$_3$	H	H	0.008	0.039
Ethyl[122]	CH$_2$CH$_3$	H	H	0.17	3.6
CN-CCG[122]	CN	H	H	0.19	0.064

*Values shown in bold indicate antagonist activity

It has been found that certain minimal elements of the carboxycyclopropyl glycine molecule are necessary for any binding to occur; this is known as the pharmacophore

(Figure 1.18). The requirements are a positively charged site (PA), two negatively charged sites (NA1/NA2) and two lone pair donating groups (DS1/DS2).[116] However, there are also other possible interactions, such as with a tyrosine residue as with LY404039 (Figure 1.20, **43**) as well as the potential for a ligand molecule to be excessively bulky in a certain region such that entry into the binding site it prohibited.

Figure 1.18. The mGluR Group II Pharmacophore
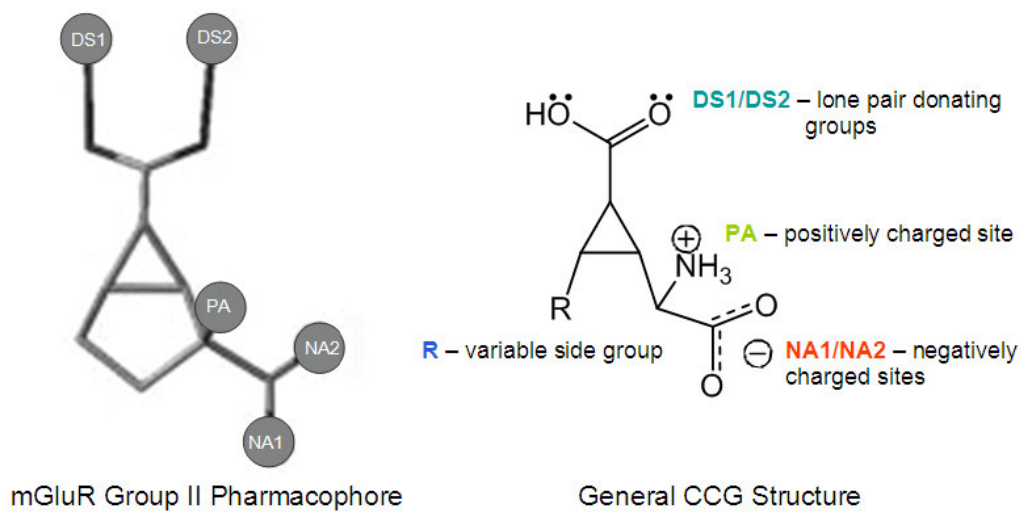
The x-ray crystal structures of the ligand binding domain of one subtype from each group of receptors have now been obtained, enabling identification of the amino acid residues making up the ligand binding region of the receptor and the possibility of screening new compounds via *in silico* docking simulations. An example is depicted in Figure 1.19 which illustrates the binding position and interactions of the group II agonist, DCG-IV (Figure 1.7, **11**) in the x-ray crystal structure of mGluR3.

Figure 1.19. Amino Acids in the Binding Region of mGlu3 Important for Binding
of the Agonist DCG-IV (**11**)
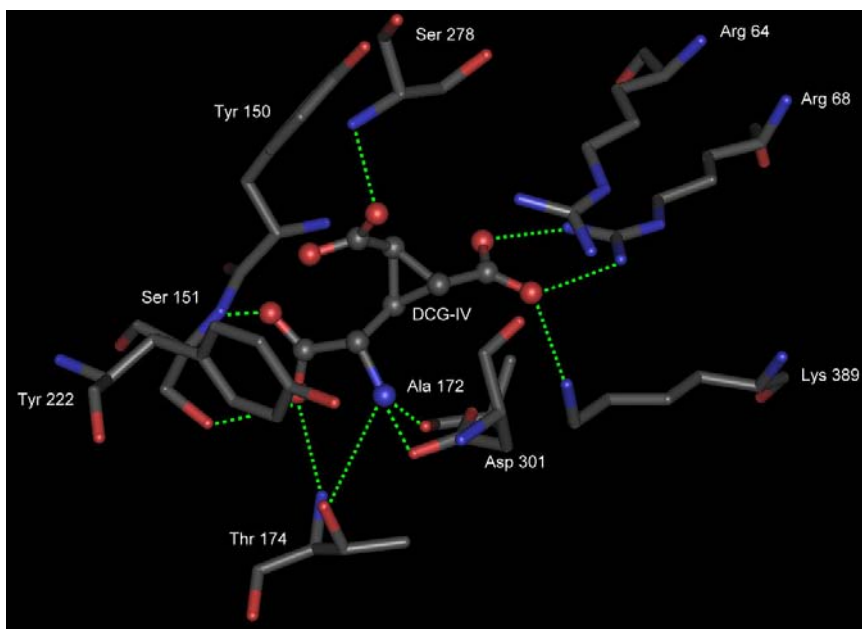
1.13.6 The Bicyclo[3.1.0]hexane Analogues

The next generation of compounds are based around a more rigid bicyclo[3.1.0]hexane
system. This system is a hybrid devised from the potent cyclopentane type ligands and
the cyclopropane type ligands. The general structure is shown in Figure 1.20. Designed
and synthesized by Eli Lilly, LY354740 (**41**) was the prototypical drug of this class and
much testing was done on this molecule.[125] However, on advancing into human drug
trials, it was found that this drug had a low oral bioavailability due to low absorption
and was not sufficiently blood-brain barrier penetrant. Owing to this, they designed the
sulfonyl compound, LY404039 (**43**), which showed a better human pharmacokinetic
profile, though having a slightly lower potency, it was more selective for mGluR2 and
mGluR3 over mGluR6 compared with the other structures (Figure 1.20).

Figure 1.20. Bicyclo[3.1.0]hexane Analogues[125-127]
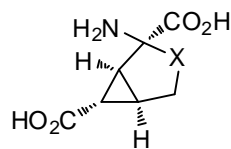
		EC$_{50}$ (µM)	mGlu1	mGlu2	mGlu3	mGlu4	mGlu5	mGlu6	mGlu7	mGlu8
41	LY354740	X = H	>100	0.011	0.038	>100	>100	3.0	>100	12
17	LY379268	X = O	>100	0.0027	0.0046	21	>100	0.40	>100	1.7
42	LY389795	X = S	>100	0.0039	0.0076	>100	>100	2.4	>100	7.3
43	LY404039	X = SO$_2$	>100	0.023	0.048	>100	>100	17	>100	10

Computer modelling suggested that upon binding, LY404039 (**43**) formed hydrogen bonding interactions via the sulfonyl oxygen lone pair with a phenolic proton located on tyrosine residue 222 (236 in mGluR1 as shown in Figure 1.21).

Figure 1.21. LY404039 (**43**) Interactions in the mGluR2 Binding Pocket (residue numbering is from mGluR1)
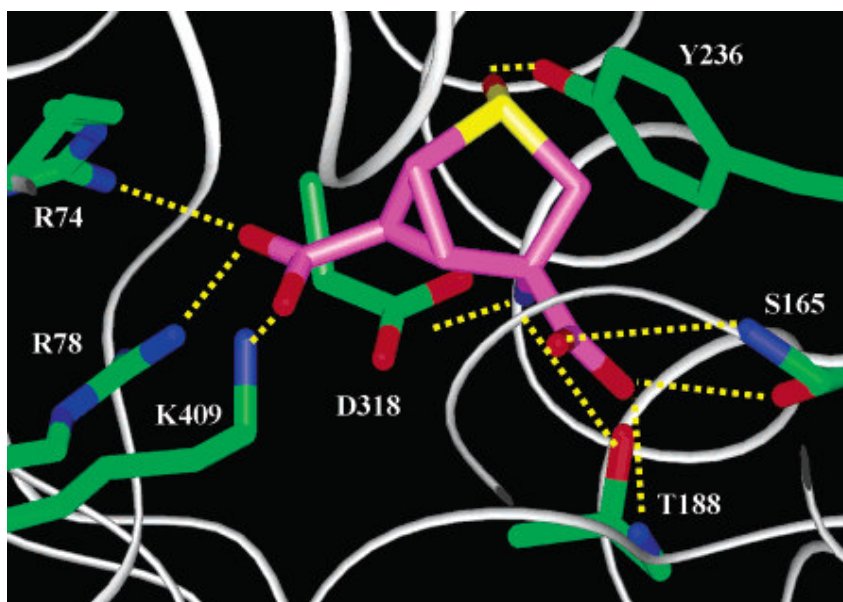
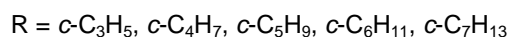
1.13.7 A Note on Bioisosteres

Several of the compounds mentioned possess alternative groups in place of the distal carboxylic acid moiety. A number of carboxylic acid bioisosteres have been examined

including a phenolic moiety as in the phenylglycine analogues (Figures 1.14-1.16), phosphonic acid as in L-AP4 (Figure 1.11, **20**) and variations on isoxazoles and oxadiazoles as in (*S*)-HIBO (Figure 1.17, **38**). Analogues of this kind not only retain potency, but also show increased subtype selectivity suggesting that the ligand binding region of each subtype is sufficiently different such that some can accept certain bioisosteric groups, whilst others cannot. This gives merit to the search for novel bioisosteric groups which may convey further subtype selectivity whilst maintaining ligand potency.
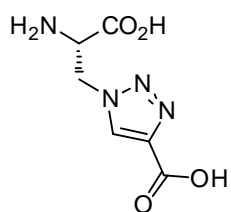
1.14 Current Research

In the search for new therapeutic agents for the treatment of neuropathic pain, outlined herein are the syntheses towards a series of potentially biologically active 3'-cycloalkyl-substituted carboxycyclopropylglycine analogues, utilizing novel synthetic chemistry to construct the cyclopropane core with all required stereochemistry (Figure 1.22). Secondly, the syntheses of a series of 1,4- and 1,5-substituted 1,2,3-triazole amino acids as a new class of potential glutamate receptor ligands (Figure 1.23). Also included are the details and results of *in vitro* binding assays used to screen for possible active compounds, investigations into *in silico* glutamate receptor docking analysis of the active and non-active test compounds in an effort to rationalize *in vitro* data and finally, the details of *in vivo* anti-allodynic activity of one compound in an animal model of neuropathic pain.
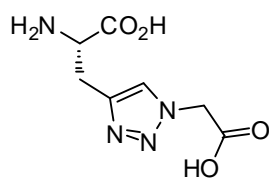
Figure 1.22. Proposed Cyclopropane Amino Acids

(*R*) **44b, d, f, h, j**   (*S*) **44a, c, e, g, i**

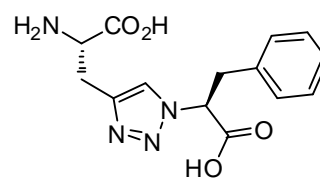R = *c*-C$_3$H$_5$, *c*-C$_4$H$_7$, *c*-C$_5$H$_9$, *c*-C$_6$H$_{11}$, *c*-C$_7$H$_{13}$
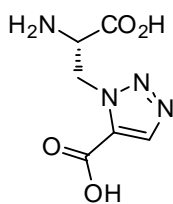
Figure 1.23. Proposed Triazole Amino Acids

45

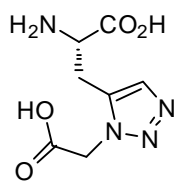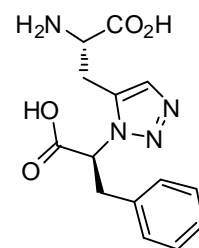**46**

47

48

49

50

Chapter 2 : Cyclopropane Amino Acids

2.1 Introduction

Over the past ten years, many new metabotropic glutamate receptor (mGluR) ligands have been synthesized both as experimental tools and potential therapeutic agents.[103] One potent class of compounds, the carboxycyclopropylglycines (CCGs) show potential for development as a new range of therapeutic agents. The CCGs bear structural resemblance to the neurotransmitter glutamate (Figure 2.1), however, due to the cyclopropane ring, they are conformationally restricted and CCGs can incorporate an additional side group (R) that may help to increase receptor specificity and selectivity for one mGluR subtype over another. Recent advances in synthetic chemistry have provided a general route for synthesis of cycloalkyl substituted CCGs, allowing exploration of their therapeutic potential.[128]

Figure 2.1. Structural Comparison between L-Glutamate and Carboxycyclopropylglycines

10

L-glutamate

R = H, F, CH_2OH, alkyl, aryl

(1S)-carboxycyclopropylglycines
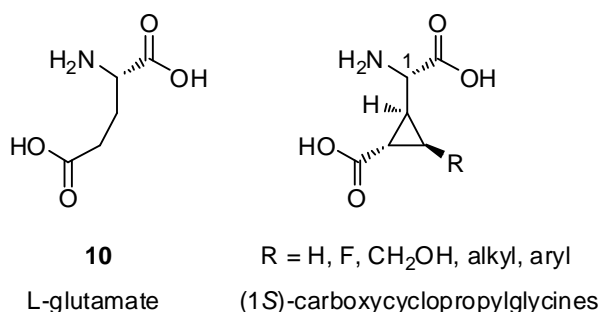
2.1 Construction of the Cyclopropane Motif

The cyclopropane moiety is found widely in nature and is a key feature of many bioactive molecules. Examples include curacin A, isolated from Caribbean marine cyanobacterium (blue-green algae) *Lyngbya majuscula* and found to have anti-cancer activity,[129,130] constanolactone A, extracted from the red alga *Constantinea simplex*[131] and FR-900848, produced by *Streptoverticillium fervens* and displaying potent antifungal activity (Figure 2.2).[132-134] Consequently, it is often employed in drug synthesis because of its constrained and rigid structure and due to the predictable geometry of substituent groups around the ring.

Figure 2.2. Cyclopropane-Containing Natural Products


curacin A

constanolactone A

FR-900848
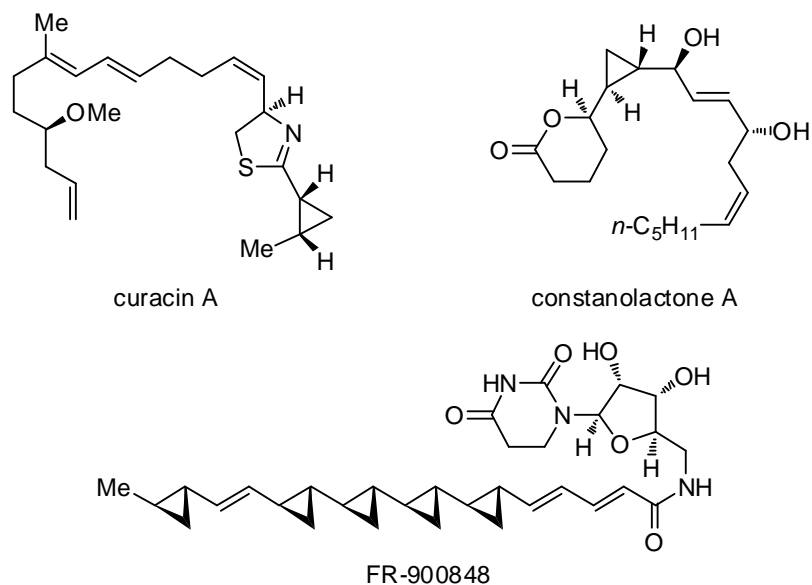
Over the years, many methods have been developed to enable construction and functionalization of the cyclopropane ring. However, obtaining the desired relative stereochemistry in high enantioselectivity and diastereoselectivity still remains a challenge.[135,136] Outlined following are some of the major types of reactions for construction of cyclopropanes which are of historical significance.

## 2.2 Simmons-Smith Cyclopropanation

The Simmons-Smith methodology revolves around the reaction of a Zn-Cu couple, Zn-Ag couple or diethylzinc generated diiodomethane carbenoid species with olefins (Scheme 2.1).[137-142] The use of *trans* olefins affords *trans* cyclopropanes and similarly *cis* olefins furnish *cis* cyclopropanes.

Scheme 2.1. General Outline of Simmons Smith Cyclopropanation

R^1, R^2, R^3, R^4 = H, alkyl, aryl
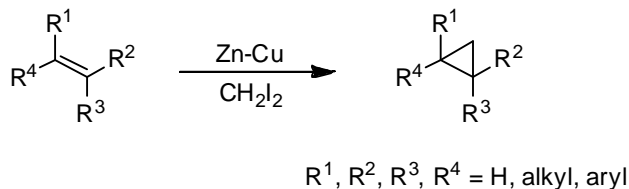
Scheme 2.2 outlines an example of the Simmons Smith cyclopropanation utilizing diethylzinc where a catalytic amount of the dipeptide *N*-Boc-L-Val-L-Pro-OMe (**51**), used as a chiral directing species, and ethylmethoxyacetate, used to prevent side reactions, provided a high yield of cyclopropane **53** with high enantioselectivity from olefin **52** which lacks directing groups.[143]

**Scheme 2.2.** Example of a Simmons Smith Cyclopropanation
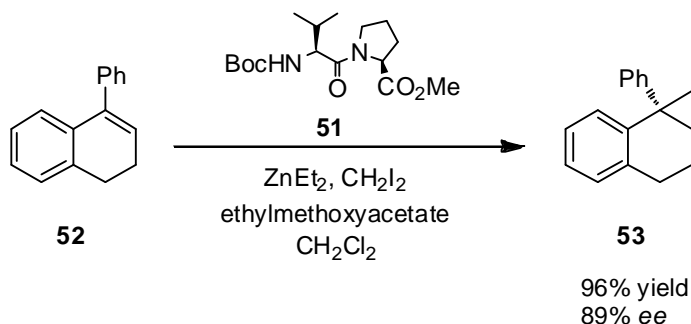
2.3 Transition Metal-Carbene Complexes

Carbene ligands can be transferred to olefins via a transition metal catalysed reaction to provide enantioenriched cyclopropanes.[139,142,144-148] In the literature it has been found that carbenes can be added across double bonds using a range of chiral metal complexes including iron, palladium, cobalt, ruthenium and rhodium. This manifold requires use of diazo-compounds which pose a potential explosion risk, making large scale synthesis difficult.[149]

Barluenga and colleges have outlined a procedure involving the use of a Fischer tungsten metal carbene complex (**54**) reacting with 2-methoxyfuran (**55**) to furnish a versatile tri-substituted cyclopropane building block in excellent yield and with high diastereoselectivity (**56**, Scheme 2.3).[150] Simple oxidation of the carbene product and subsequent elaboration gives access to alcohols, diols and cyclopropanecarbaldehydes.

Scheme 2.3. Illustration of a Transition Metal-Carbene Complex Cyclopropanation
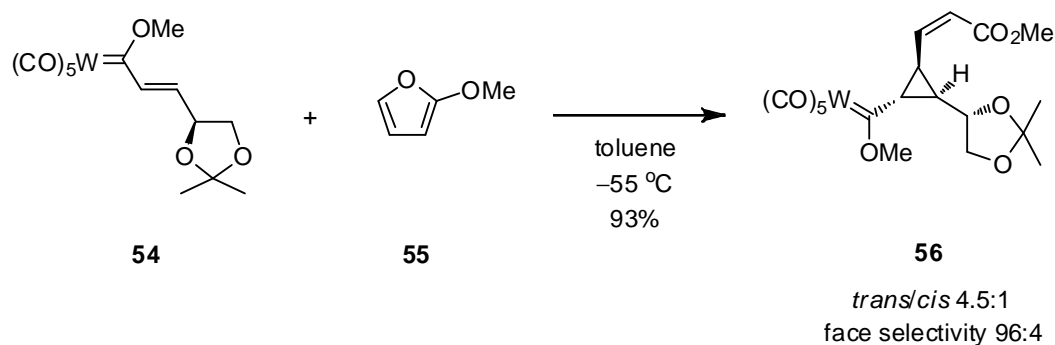

2.4 Michael Initiated Ring-Closure (MIRC)

Cyclopropane syntheses which entail tandem 1,4-conjugate nucleophilic addition followed by nucleophilic ring closure are placed under the MIRC class of reactions.[151,152] The leaving group may be located either on the conjugate acceptor (**A**) or on the nucleophile (**B**) in the reaction as depicted in Scheme 2.4.

**Scheme 2.4.** Mechanisms of Michael Initiated Ring-Closure
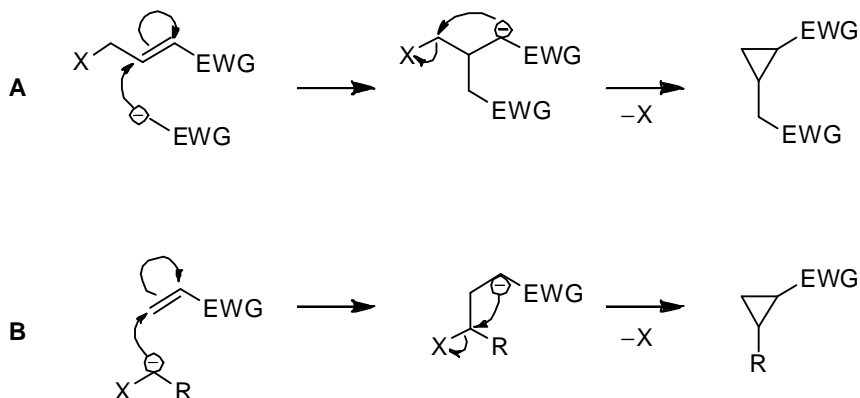
Su and colleagues have utilized a Michael initiated ring closing reaction based upon a simple alkene incorporating bromide as a leaving group and employing borohydride as a nucleophile to give a tetrasubstituted cyclopropane building block (Scheme 2.5).[153]

Scheme 2.5. A Michael Initiated Ring-Closure Reaction
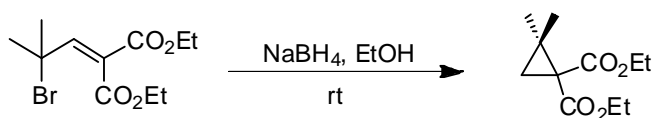
Work by Sun and Tang has found that cyclopropanes can be synthesized by use of telluronium ylides. Starting from methyl cinnamate and under basic conditions, chiral 1,2,3-trisubstituted cyclopropanes may be obtained in excellent yields and with high enantiomeric excess as outlined in Scheme 2.6.[154]

Scheme 2.6. Tri-substituted Cyclopropanes via Michael Initiated Ring-Closure
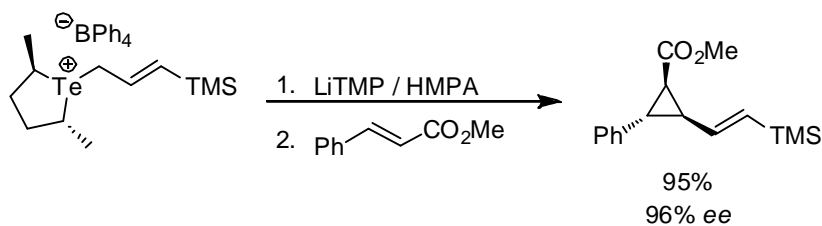

2.5 The Carboxycyclopropylglycines

As discussed earlier, several isomers of 2-carboxycyclopropylglycine have been isolated as natural products.[111-114] Up until now, few general routes for synthesis of di-substituted cyclopropyl glycines have been developed. Most syntheses have previously been aimed towards obtaining a single isomer, with no possibility of varying the substitution pattern and involve as many as 21 synthetic steps. This has hindered the pharmacological investigation of their therapeutic potential.

A previous enantioselective synthesis of 3'-alkyl substituted carboxycyclopropylglycines (CCGs) (**57, 58**) was carried out by an addition and then elimination of a chiral lithium bislactam ether anion to a racemic 4-alkyl-4-bromo-2-butenoate (**59**) as shown in Scheme 2.7.[155] However, all CCGs synthesized by this route had the R group *cis* to the carboxyl group on the cyclopropane ring and it was found that the more active isomers had the R group *anti* to the carboxyl group and these could not be synthesized via this route.

Scheme 2.7. Enantioselective Synthesis of 3'-Alkyl Substituted Carboxycyclopropylglycines
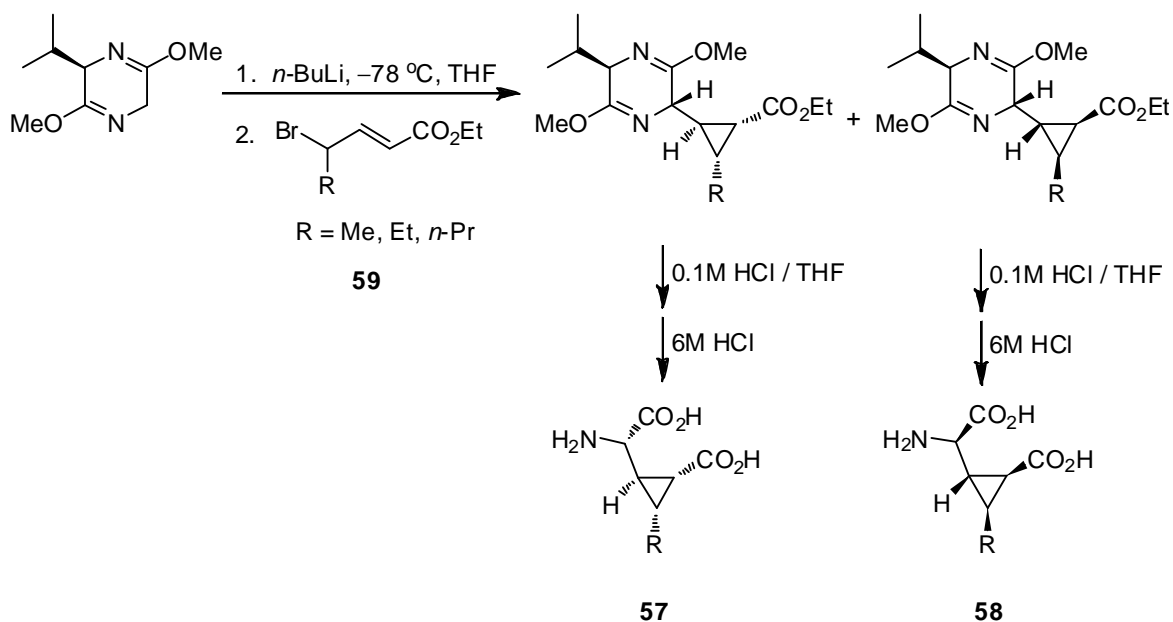
A stereo-specific synthesis of the group II metabotropic glutamate receptor antagonist (2S,3S,4S)-MCCG (**60**) was put forward by Pajouhesh *et al.*, starting with a chiral protected oxazolidinone (**61**).[156] A transition metal-carbene complex formed by use of diazomethane and palladium (II) acetate was employed to construct the cyclopropane core from chiral olefin **62**. This route afforded product with 99% *ee* (Scheme 2.8).

Scheme 2.8. Stereo-Specific Synthesis of (2S,3S,4S)-MCCG
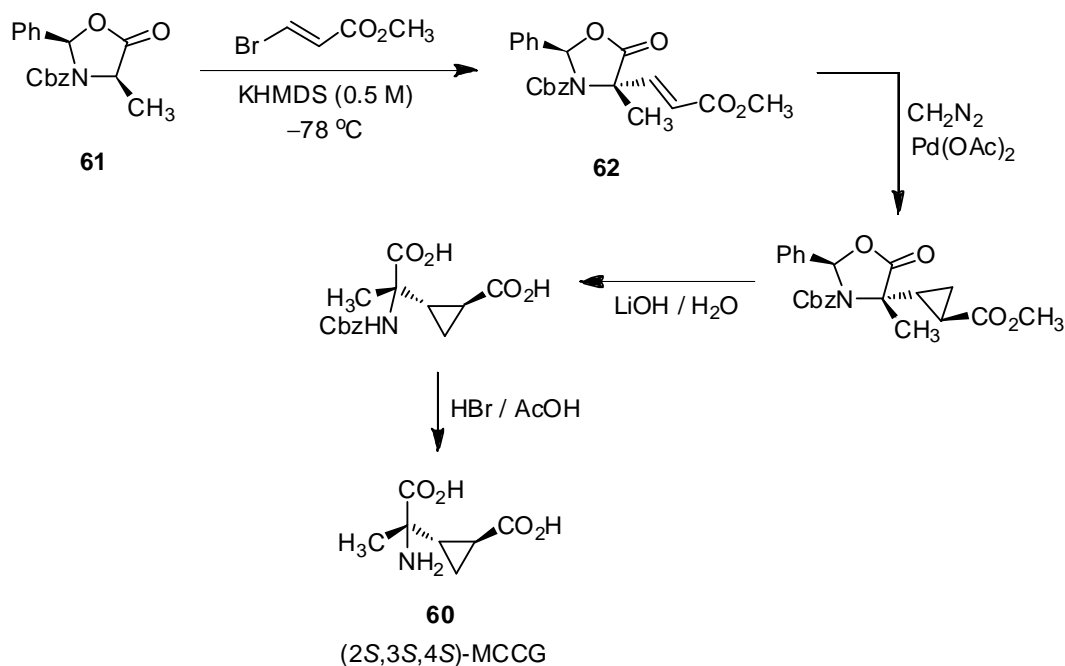
Further syntheses have been investigated by researchers at Eli Lilly to produce the 3'-alkyl substituted biologically active carboxycyclopropyl glycines (Scheme 2.9).[55] This time, starting from the readily available crotyl alcohol and building up the cyclopropane core by use of di-rhodium catalysed intramolecular carbene chemistry (step **c**).

Scheme 2.9. Eli Lilly Synthesis of 3'-Alkyl Substituted Biologically Active Carboxycyclopropyl Glycines
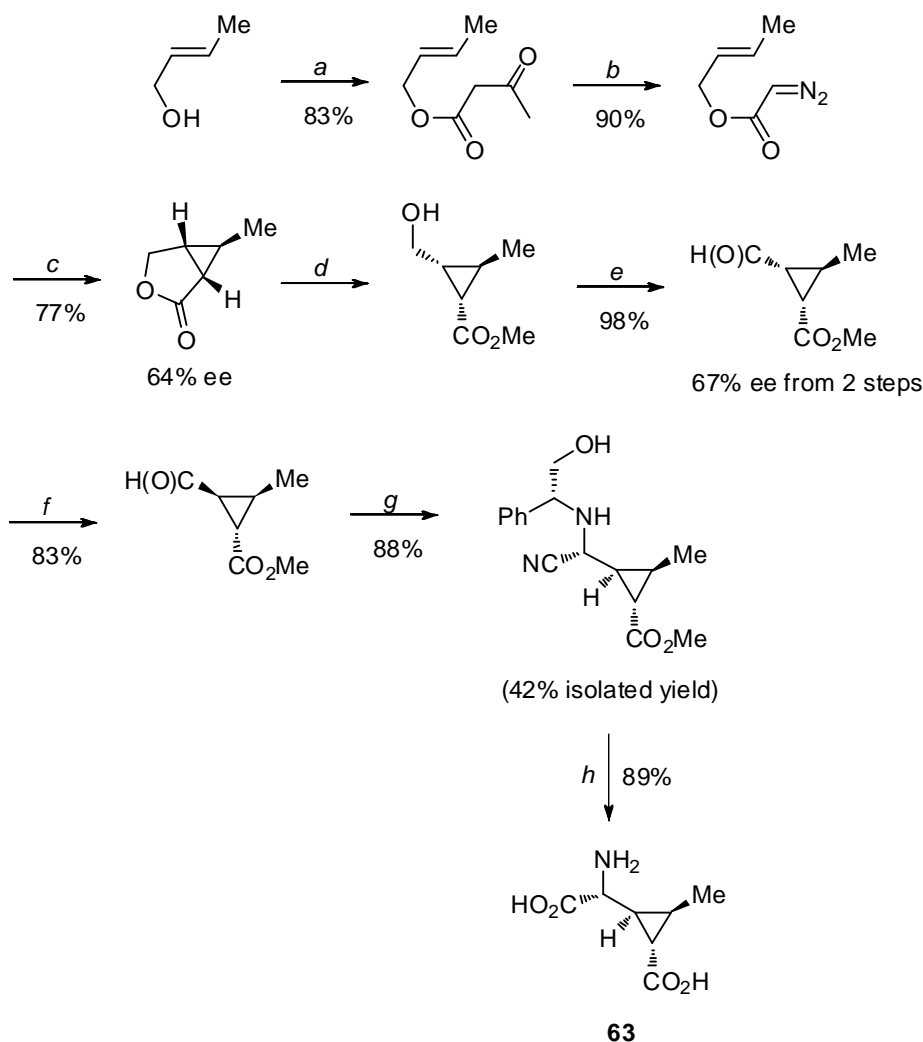
a: Diketene, AcONa, THF, reflux; **b:** (i) p-AcNHC$_6$H$_4$SO$_2$N$_3$, Et$_3$N, CH$_3$CN, rt, (ii) LiOH, H$_2$O, rt; **c:** Rh$_2$(5R-MEPY)$_4$, CH$_2$Cl$_2$, reflux; **d:** (i) 2.8 N LiOH, THF, rt, (ii) CH$_2$N$_2$, Et$_2$O, 0 °C; **e:** TPAP, NMO, mol sieves (4 Å), CH$_2$Cl$_2$, rt; **f:** (i) 10% NaOH, MeOH, rt, (ii) CH$_2$N$_2$, Et$_2$O, 0 °C; **g:** (i) (R)-Phenylglycinol, MeOH, rt, (ii) TMSCN, rt; **h:** (i) Pb(OAc)$_4$, CH$_2$Cl$_2$, MeOH, 0 °C, (ii) 6 N HCl, (iii) Dowex 50 x 8-100.

This enantioselective synthesis of the 3'-methyl substituted cyclopropane (**63**) was accomplished over a total of 14 steps with a 12% overall yield. The same synthetic strategy was used to synthesize the hydroxymethyl compound, using *cis* 4-benzyloxy-2-buten-1-ol in place of crotyl alcohol.[121]

A Michael-Initiated Ring Closure reaction based on asymmetric sulfonium ylide (**64**) chemistry was used in the synthesis of the related metabotropic glutamate receptor ligand, LY354740.[157] This molecule has a more rigid bicyclo[3.1.0]hexane core (Scheme 2.10).

Scheme 2.10. Synthesis of LY354740 via Michael-Initiated Ring Closure
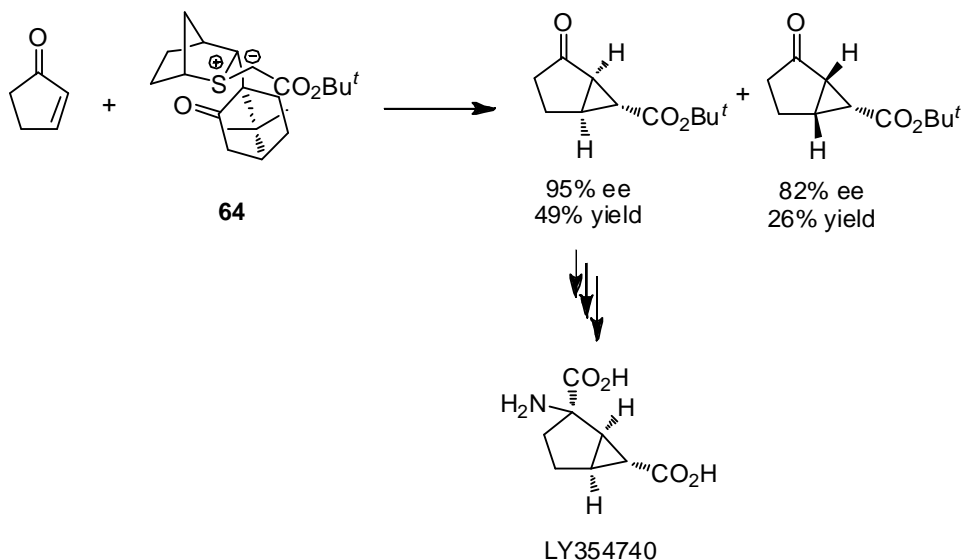
2.6 Construction of Cyclopropanes Using 1,2-Dioxines

The synthesis of 3,6-dihydro-1,2-dioxines or endoperoxides has undergone considerable research, with a vast library of analogues having been synthesized.[158-167] The most common method for preparing these compounds is the [4π + 2π] cycloaddition of singlet state oxygen onto a 1,3-butadiene. Singlet state oxygen is usually produced by irradiation of a saturated solution of triplet state oxygen in the presence of a dye acting as a photosensitizer. The most commonly used dyes are tetraphenylporphine or rose bengal.

Of particular interest is the base-catalysed rearrangement known as the Kornblum-DeLaMare decomposition of peroxides, which results in the formation of γ-hydroxyenone species (**65**, **66**) from 1,2-dioxines (**67**, Scheme 2.11).[168]

Scheme 2.11. Kornblum-DeLaMare Decomposition of Peroxides

67

R^1, R^2 = H, alkyl, aryl

65

cis

66

trans
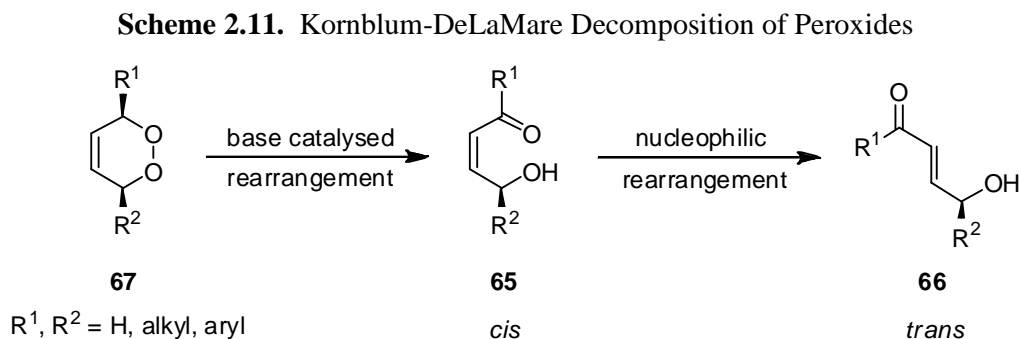
It has previously been discovered that bulky and non-bulky stabilised phosphorus ylides may react with *cis* γ-hydroxyenones to form tri-substituted cyclopropanes (**68**, **69**) in good yield. The *cis* γ-hydroxyenones can be conveniently prepared by ring-opening of 1,2-dioxines being catalysed by either base or using a cobalt (II)-catalysed radical rearrangement (Scheme 2.12).[159-161]

Scheme 2.12. Tri-substituted Cyclopropanes From Phosphorus Ylides and *cis* γ-Hydroxyenones

X = Y = H, alkyl, aryl

Ph$_3$P=CHCO$_2$R

R = Me, Et, Bn, 1-Ad, Bu^t

68
non-bulky ylide product

69
bulky ylide product
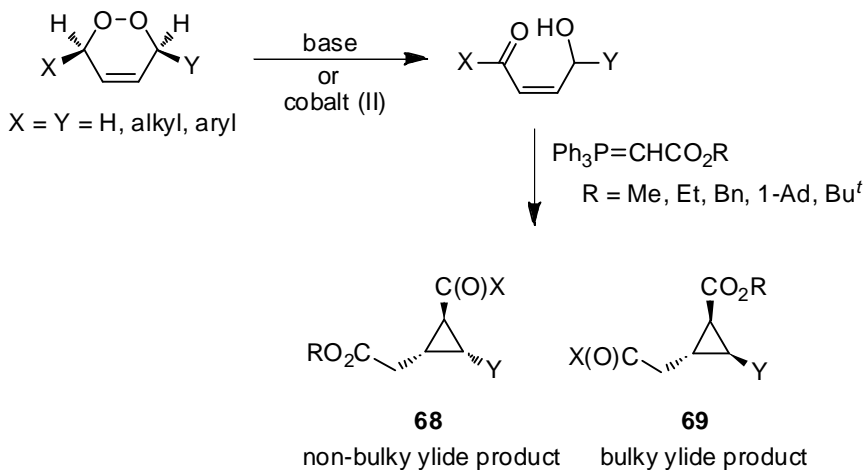
Further to this, Taylor *et al.* reported that 1,2-dioxines may react with stabilised Horner-Wadsworth-Emmons, cyano and Weinreb type phosphonates (**70**) under basic conditions to afford cyclopropanes (**71**) in excellent yields (Scheme 2.13).[167]

Scheme 2.13
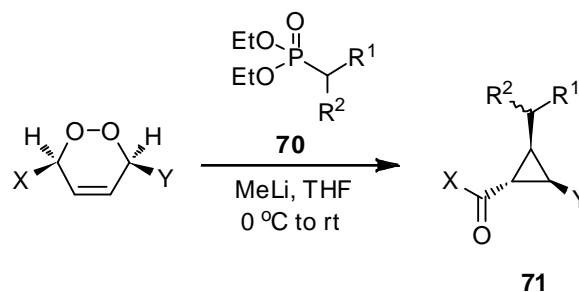
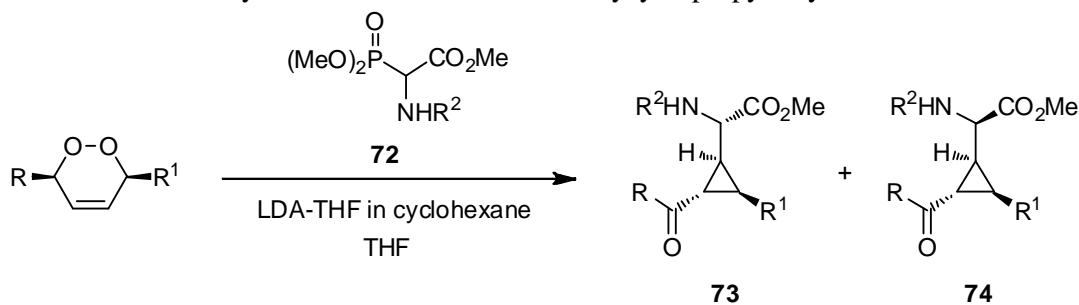|				Yield
X = Ph	Y = Ph	$R^1 = CO_2Me$	$R^2 = H$	81%
X = Ph	Y = Ph	$R^1 = CO_2t$-Bu	$R^2 = H$	75%
X = Ph	Y = Ph	$R^1 = CN$	$R^2 = H$	53%
X = Ph	Y = Ph	$R^1 = C(O)N(Me)OMe$	$R^2 = H$	91%
X = Ph	Y = H	$R^1 = CO_2Me$	$R^2 = H$	80%
X = Ph	Y = H	$R^1 = CN$	$R^2 = H$	51%
X = Ph	Y = Ph	$R^1 = CO_2Et$	$R^2 = Me$	30%

This methodology has subsequently been employed in the synthesis of CCGs through reaction with an aminophosphonate (**72**, Scheme 2.14). Base-catalysed ring opening of the 1,2-dioxine is followed by Michael addition of the phosphonate nucleophile and intramolecular ring closure to form the desired cyclopropanes as a 1:1 mixture of diastereoisomers (**73**, **74**), in good overall yield.[128]

Scheme 2.14. Synthesis of Substituted Carboxycyclopropyl Glycine Precursors[128]

			Total Yield
R = Ph	$R^1 = Ph$	$R^2 = Cbz$	47%
R = Ph	$R^1 = H$	$R^2 = Cbz$	54%
R = Ph	$R^1 = Me$	$R^2 = Cbz$	53%
R = Ph	$R^1 = CH_2OTBDMS$	$R^2 = Cbz$	67%
R = 2-MeOPh	$R^1 = CH_2OTBDMS$	$R^2 = Boc$	66%
R = Ph	$R^1 = c$-C_6H_{11}	$R^2 = Cbz$	50%

The cyclopropane diastereoisomers are easily separated by flash column chromatography and can then easily be converted to the desired biologically active 3'-cycloalkyl substituted carboxycyclopropylglycines. This synthetic route has several advantages over those found in the literature in that a total of only seven steps are required and the 3'-substitution can be altered simply by preparing the corresponding 1,2-dioxine.

2.7 3'-Cycloalkyl Carboxycyclopropylglycines

To extend the previous work and investigate novel carboxycyclopropyl glycines, investigations into the synthesis of new cyclopropyl compounds having cycloalkyl substitution were to be conducted. Based on previous structure-activity work found in the literature, it was hypothesized that these compounds may be potent agonists or antagonists at selected subtypes of metabotropic glutamate receptors. Scheme 2.15 below depicts the retro-synthetic strategy for making these compounds and follows work previously carried out by the Taylor group, with the exception of the starting 1,2-dioxines being cycloalkyl-substituted. The cyclopropane amino acids to be synthesized were to have cycloalkyl ring sizes ranging from a 3-membered cyclopropyl right through to a relatively bulky 7-membered cycloheptyl. Based on the structure-activity relationships of previously tested CCGs, it was hypothesized that the activity of these compounds may switch between agonist to antagonist as the ring size increases.

Scheme 2.15. Retrosynthetic Strategy

R = c-C$_3$H$_5$, c-C$_4$H$_7$,
c-C$_5$H$_9$, c-C$_6$H$_{11}$, c-C$_7$H$_{13}$
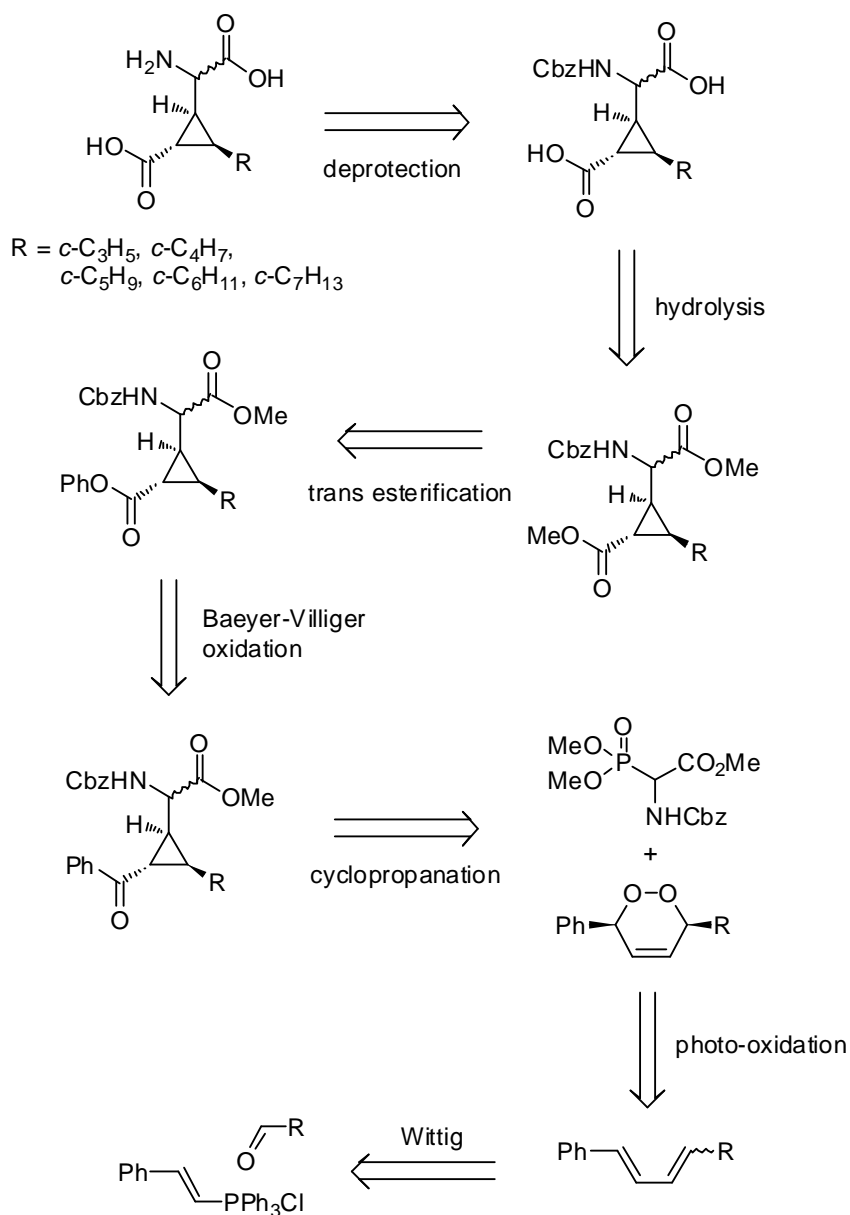
2.8 Synthesis of Target Cyclopropane Amino Acids

The requisite 1,3-butadienes (**75a–f**) were prepared in good to excellent yields using phosphorus ylide chemistry utilizing cycloalkanecarboxaldehydes and cinnamyl triphenylphosphonium chloride except for diene **75f** where (*E*)-2-methoxycinnamaldehyde (**76f**) and cycloheptylmethyl triphenylphosphonium iodide (**77b**) were employed (See Scheme 2.19). The cycloheptylmethyl triphenylphosphonium iodide was prepared from cycloheptyliodomethane (**78**) which

was conveniently synthesized from the corresponding alcohol via one of two routes (A[169] or B[170]) as illustrated in Scheme 2.16 following.

Scheme 2.16. Preparation of Cycloheptyliodomethane (**75**) Starting Material

A. NIS, PPh$_3$

B. I$_2$, imidazole, PPh$_3$

78a: 67% (A)
78b: 96% (B)
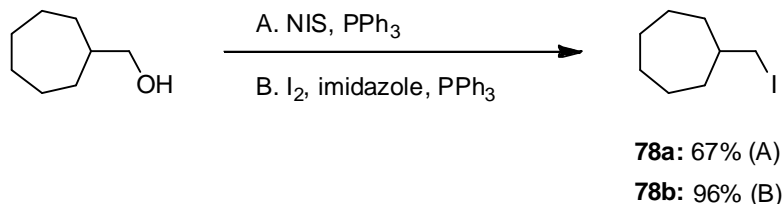
Where the required cycloalkanecarboxaldehyde was not available commercially, it was prepared from the carboxylic acid via lithium aluminium hydride reduction followed by oxidation with pyridinium dichromate. Some difficulty was experienced in obtaining the aldehydes due to over-oxidation and so Swern conditions[171] were investigated as well as Parikh-Doering conditions,[172,173] however, these proved to either produce mainly by-products or to be too mild and the reaction too slow to be satisfactory. The Swern oxidation of alcohol **79** produced only traces of aldehyde **76c**, but mainly a by-product which was determined by ^{1}H NMR analysis to most likely be ester **80** (Scheme 2.17).

Scheme 2.17. Attempted Swern Oxidation

DMSO, (COCl)$_2$

Et$_3$N

CH$_2$Cl$_2$

79

trace

76c

+

80
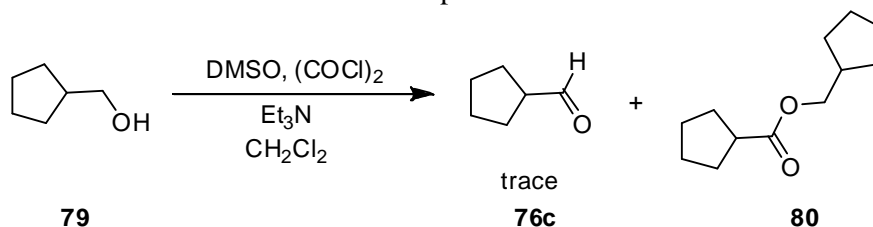
The Parikh-Doering oxidation of alcohol **79** also produced only a trace of aldehyde **76c** even after 24 hours reaction time and so this methodology was abandoned (Scheme 2.18).

Scheme 2.18. Attempted Parikh-Doering Oxidation

DMSO, SO$_3$.pyr

Et$_3$N

CH$_2$Cl$_2$

79

76c
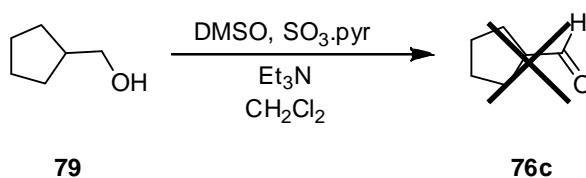
The crude 1,3-butadienes **75a–f** were obtained in high (58%) to excellent (97%) yields with the desired isomer being the (*E,E*) as this can undergo addition to singlet oxygen to form the 1,2-dioxine, whereas the (*E,Z*) isomer cannot. The reaction solvent used was either anhydrous diethyl ether or anhydrous THF, however, it was found that THF gave predominantly the (*E,E*) product whereas using ether afforded a mix of (*E,E*) and (*E,Z*). This was not a great problem as subjecting the diene to photolysis conditions induces isomerism from the (*E,Z*) to the desired (*E,E*) isomer.[174]

Scheme 2.19. Preparation of Butadienes via Wittig Reaction
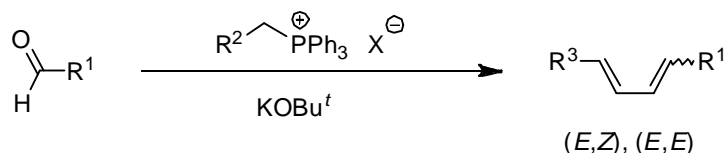
			Yield
76a: $R^1 = c\text{-}C_3H_5$	**77a:** $R^2 = (E)$-cinnamyl	**75a:** $R^1 = c\text{-}C_3H_5$ $R^3 = $ Ph	90%
76b: $R^1 = c\text{-}C_4H_7$	**77a:** $R^2 = (E)$-cinnamyl	**75b:** $R^1 = c\text{-}C_4H_7$ $R^3 = $ Ph	74%
76c: $R^1 = c\text{-}C_5H_9$	**77a:** $R^2 = (E)$-cinnamyl	**75c:** $R^1 = c\text{-}C_5H_9$ $R^3 = $ Ph	93%
76d: $R^1 = c\text{-}C_6H_{11}$	**77a:** $R^2 = (E)$-cinnamyl	**75d:** $R^1 = c\text{-}C_6H_{11}$ $R^3 = $ Ph	97%
76e: $R^1 = c\text{-}C_7H_{13}$	**77a:** $R^2 = (E)$-cinnamyl	**75e:** $R^1 = c\text{-}C_7H_{13}$ $R^3 = $ Ph	58%
76f: $R^1 = (E)$-2-MeO-cinnamyl	**77b:** $R^2 = c\text{-}C_7H_{13}$	**75f:** $R^1 = c\text{-}C_7H_{13}$ $R^3 = $ 2-MeO-Ph	86%

X = Cl or I

Photolysis (dye sensitised photo-oxidation) of the 1,3-butadienes **75a–f** employing rose bengal bis(triethylammonium) salt as the sensitiser, in the presence of oxygen, afforded the desired 3-cycloalkyl-6-phenyl-3,6-dihydro-1,2-dioxines **80a–f** in moderate (21%) to high (69%) yields, including the known compound **80d**[128] (Scheme 2.20). This reaction proceeds via a [4π + 2π] cycloaddition of singlet oxygen. Due to the inefficient and non-selective nature of this reaction, there were many side products formed (ene, cleavage) and this always meant that the maximum yield obtainable was reduced to a greater or lesser extent, depending on the substrate 1,3-butadiene. It was often necessary to carry out the photo-oxidation over several sessions in order to obtain a decent overall yield with reaction times ranging from a total of 8 to 18 hours. Highlighting the inefficiency of this photolysis process for these particular substrates, there was always a large amount of un-reacted starting material remaining, even after subjecting the reaction to photo-oxidation conditions for 8 hours or more.

Scheme 2.20. Photolysis (Photo-oxidation)
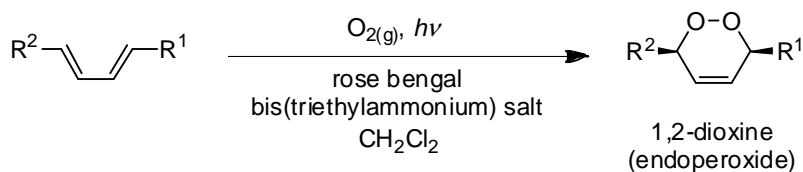
				Yield
75a: $R^1 = c\text{-}C_3H_5$	$R^2 = Ph$	**80a:** $R^1 = c\text{-}C_3H_5$	$R^2 = Ph$	69%
75b: $R^1 = c\text{-}C_4H_7$	$R^2 = Ph$	**80b:** $R^1 = c\text{-}C_4H_7$	$R^2 = Ph$	40%
75c: $R^1 = c\text{-}C_5H_9$	$R^2 = Ph$	**80c:** $R^1 = c\text{-}C_5H_9$	$R^2 = Ph$	21%
75d: $R^1 = c\text{-}C_6H_{11}$	$R^2 = Ph$	**80d:** $R^1 = c\text{-}C_6H_{11}$	$R^2 = Ph$	59%
75e: $R^1 = c\text{-}C_7H_{13}$	$R^2 = Ph$	**80e:** $R^1 = c\text{-}C_7H_{13}$	$R^2 = Ph$	44%
75f: $R^1 = c\text{-}C_7H_{13}$	$R^2 = 2\text{-MeO-Ph}$	**80f:** $R^1 = c\text{-}C_7H_{13}$	$R^2 = 2\text{-MeO-Ph}$	48%

The protected cyclopropane amino acids **81a–j** were prepared by reaction of the 1,2-dioxines (**80a–e**) with (±)-Cbz-α-phosphonoglycine trimethylester under basic conditions with yields ranging from moderate (60%) to poor (17%) (Scheme 2.21). This methodology has previously been used by Kimber *et al.* in the synthesis of 1,2,3-trisubstituted cyclopropanes using Horner-Wadsworth-Emmons phosphonates.

Scheme 2.21. Cyclopropanation

cyclopropyl phenyl ketones
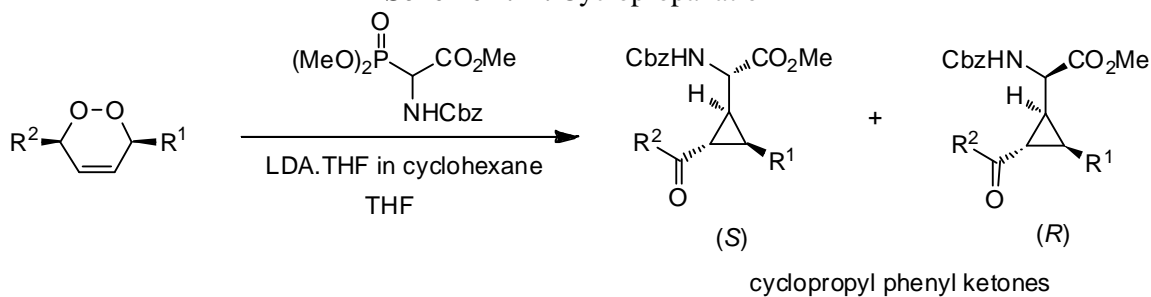
|						Yield*
80a:	$R^1 = c\text{-}C_3H_5$	$R^2 = Ph$	**81a,b:**	$R^1 = c\text{-}C_3H_5$	$R^2 = Ph$	60%
80b:	$R^1 = c\text{-}C_4H_7$	$R^2 = Ph$	**81c,d:**	$R^1 = c\text{-}C_4H_7$	$R^2 = Ph$	50%
80c:	$R^1 = c\text{-}C_5H_9$	$R^2 = Ph$	**81e,f:**	$R^1 = c\text{-}C_5H_9$	$R^2 = Ph$	38%
80d:	$R^1 = c\text{-}C_6H_{11}$	$R^2 = Ph$	**81g,h:**	$R^1 = c\text{-}C_6H_{11}$	$R^2 = Ph$	50%
80e:	$R^1 = c\text{-}C_7H_{13}$	$R^2 = Ph$	**81i,j:**	$R^1 = c\text{-}C_7H_{13}$	$R^2 = Ph$	17%
80f:	$R^1 = c\text{-}C_7H_{13}$	$R^2 = 2\text{-MeO-Ph}$	**81k,l:**	$R^1 = c\text{-}C_7H_{13}$	$R^2 = 2\text{-MeO-Ph}$	0%[a]

*Yield refers to total isolated yield of both diastereoisomers obtained as a 1:1 mix.

[a]No product could be detected by ^{1}H NMR.

However, it was shown that substitution even by a simple methyl group at the *α*-position on the phosphonate caused a decrease in yield from 81% to 30%. The reason for this was suggested to be the decreased nucleophilicity of the aminophosphonate.[167]

The attempted synthesis of cyclopropanes **81k** and **81l** was to investigate the effects of 2-methoxy substitution of the phenyl ketone on the rate of the subsequent reaction in the synthetic sequence. *Ortho*-methoxy substitution had previously been used by our research group to decrease reaction times of the Baeyer-Villiger oxidation, as this increases electron density of the phenyl ring and speeds up migration.[128] In this instance, the change in electronic character of the phenyl ring seems to have caused the reaction to fail. The cyclopropanation reaction was found to be generally unreliable, with fluctuating yields and corresponding changes in the number of by-products formed. Over the course of experimenting to optimize the reaction, different bases, reaction temperatures and reaction concentrations were studied by other members of our research group.[128] However, these all resulted in even poorer yields or no isolated product whatsoever. The reaction affords a 1:1 ratio of diastereoisomers which can be separated by one or two rounds of careful flash chromatography. The difference between the two R_f values for each isomer was approximately 0.05−0.10 and it was noted that the first isomer off the column for all the cyclopropanes was the (*S*) isomer, followed by the (*R*) isomer. Cyclopropanes **81g**, **h** have previously been synthesized by the Taylor group and our data was found identical to that reported.[128]

The main by-product that featured in these reactions was tetrahydrofurans (THFs) (Scheme 2.22, **82**), which were quite difficult to separate from the desired cyclopropane products in any of the tested solvent systems, due to similar polarities of the THFs and cyclopropanes.

Scheme 2.22. Formation of Tetrahydrofurans
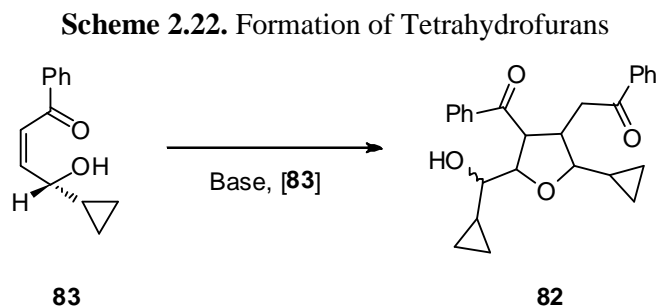
The details of the likely mechanistics of the cyclopropanation reaction have been elucidated by Avery *et al.* which sheds some light on some problems that were encountered in the present work.[128] Referring to the reaction mechanism in Scheme 2.23, it has been postulated that at -78 °C, upon addition of the 1,2-dioxine, *cis* γ-hydroxyenone (**83**) forms but then no further reaction occurs.

Scheme 2.23. Mechanism of the Cyclopropanation Reaction
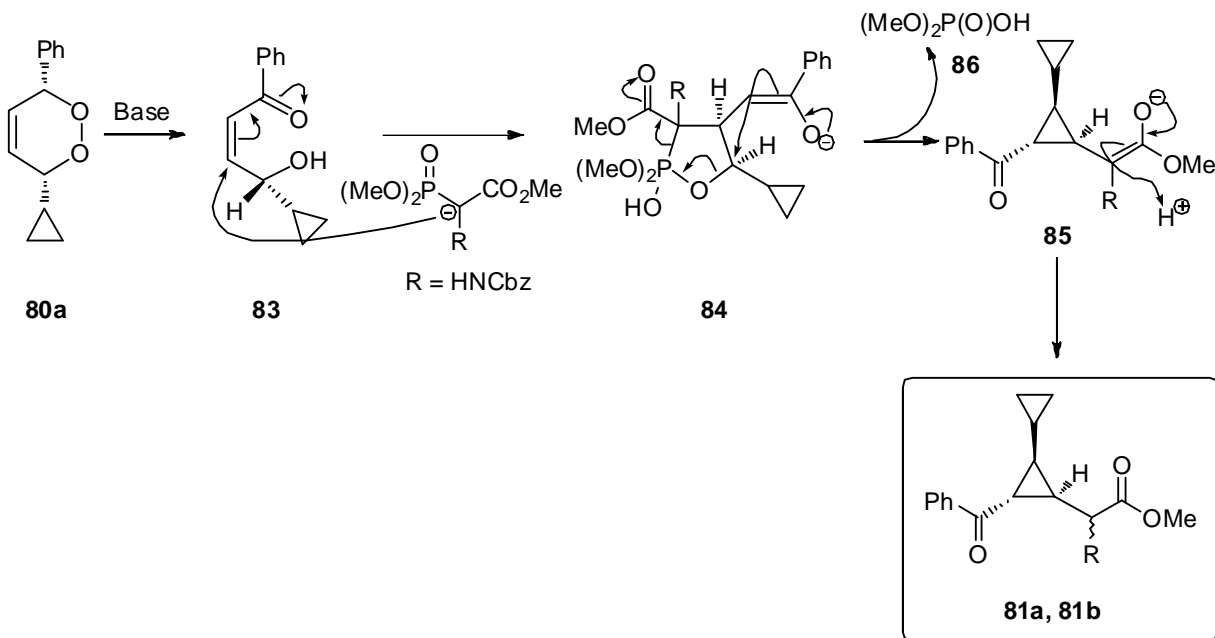
Based on previous experimentation, only once the reaction temperature reaches somewhere between -20 to -15 °C is there Michael addition of the aminophosphonate nucleophile to the *cis* γ-hydroxyenone (**83**), ring-closure and formation of the 1-2λ-oxaphospholane intermediate (**84**). Ring collapse of the intermediate to form the cyclopropane enolate (**85**) seems to occur between -15 °C and room temperature ($\sim$23 °C). Our methodology had involved maintaining the reaction at -78 °C and then letting it "slowly" warm to room temperature overnight before quenching with aqueous ammonium chloride. This meant that the reaction was left at -78 °C for a considerable amount of time and at these temperatures, if the solubility of the 1,2-dioxine in the reaction solvent (THF) is high, then these are very favourable conditions for formation of THFs and this is what was observed (Scheme 2.22).

The THFs form due to base-promoted self-condensation of two molecules of γ-hydroxyenone via an oxa-Michael/Michael ring-closing reaction; the mechanism is depicted in Scheme 2.24.

Scheme 2.24. Mechanism of Tetrahydrofuran Formation
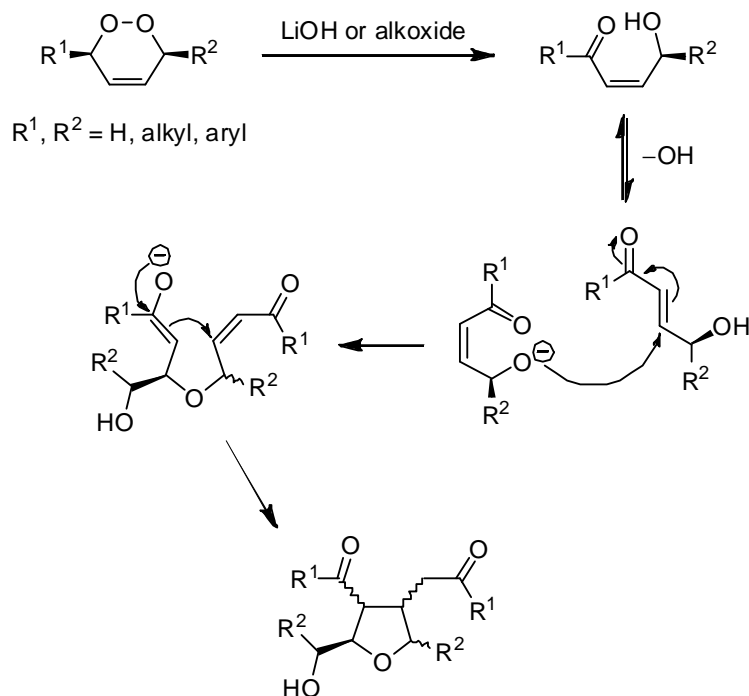
Eventually a procedure was found which requires addition of base and 1,2-dioxine at $-78\ ^{\circ}$C followed by warming to -15 to $-10\ ^{\circ}$C for about 4 hours and then slow warming to room temperature overnight. Using this protocol, it was possible to scale the reaction up to 2.5 g for some 1,2-dioxines with total isolated yield for both diastereoisomers ranging from 38 to 60%. Formation of the cyclopropane product was confirmed by the appearance of a strong IR absorption due to the phenyl ketone at 1648–1670 cm^{-1}. This absorption peak would be expected to appear around 1685 cm^{-1}, however, the frequency is lowered since the ketone is also adjacent to the cyclopropane ring, which exhibits a double bond character.[175] The relative stereochemistry of the cyclopropanes could not be determined using ^{1}H NMR or 2D NMR due to overlap of the cyclopropyl and cycloalkyl signals and identical ROESY interactions for both diastereoisomers. The relative stereochemistry of cyclopropanes **81a, 81b** and **81g** were determined by single crystal x-ray crystallography (Figures 2.3, 2.4, 2.5).

Figure 2.3. X-ray Crystal Structure of Cyclopropane **81a**
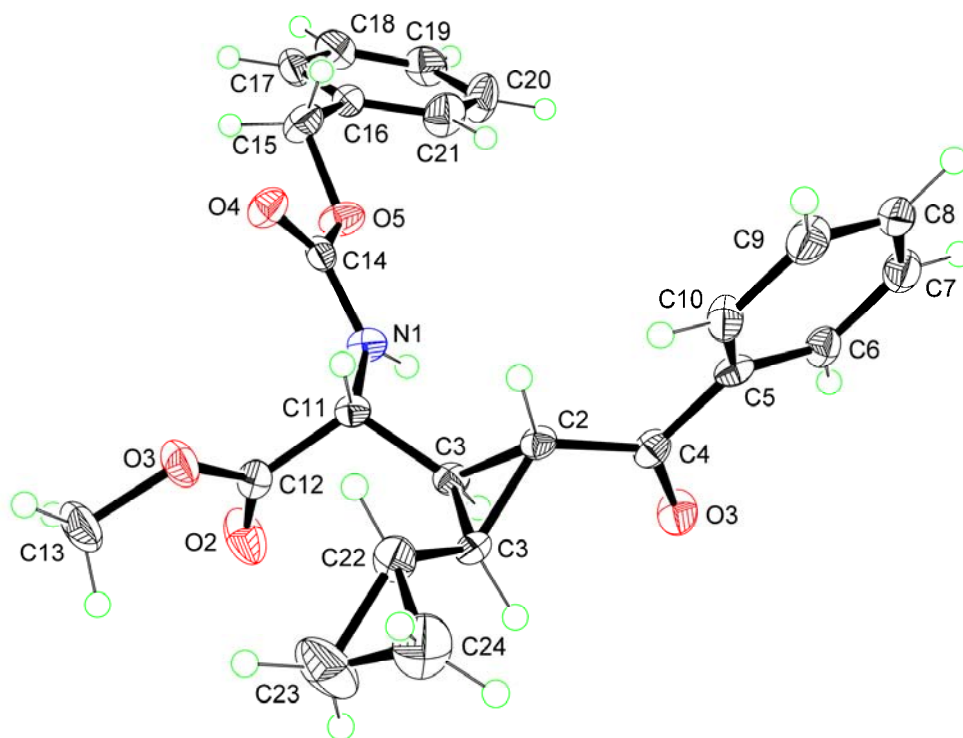
Molecular structure (50% probability ellipsoids) and crystallographic numbering scheme for
$C_{24}H_{25}NO_5$

Figure 2.4. X-ray Crystal Structure of Cyclopropane **81b**
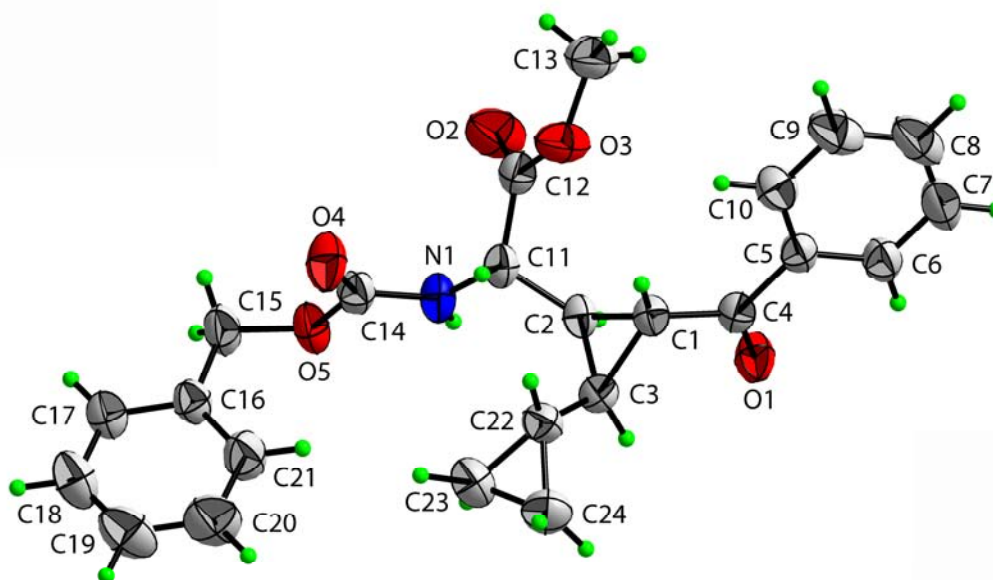
Molecular structure (50% probability ellipsoids) and crystallographic numbering scheme for
$C_{24}H_{25}NO_5$

Figure 2.5. X-ray Crystal Structure of Cyclopropane **81e**

Molecular structure (50% probability ellipsoids) and crystallographic numbering scheme for $C_{26}H_{29}NO_5$ (for reasons of clarity only one component of the disordered cyclopentane ring is shown)

Scheme 2.25. Baeyer-Villiger Oxidation

trifluoroperacetic acid[a]
OR
meta-chloroperbenzoic acid[b]

Yield

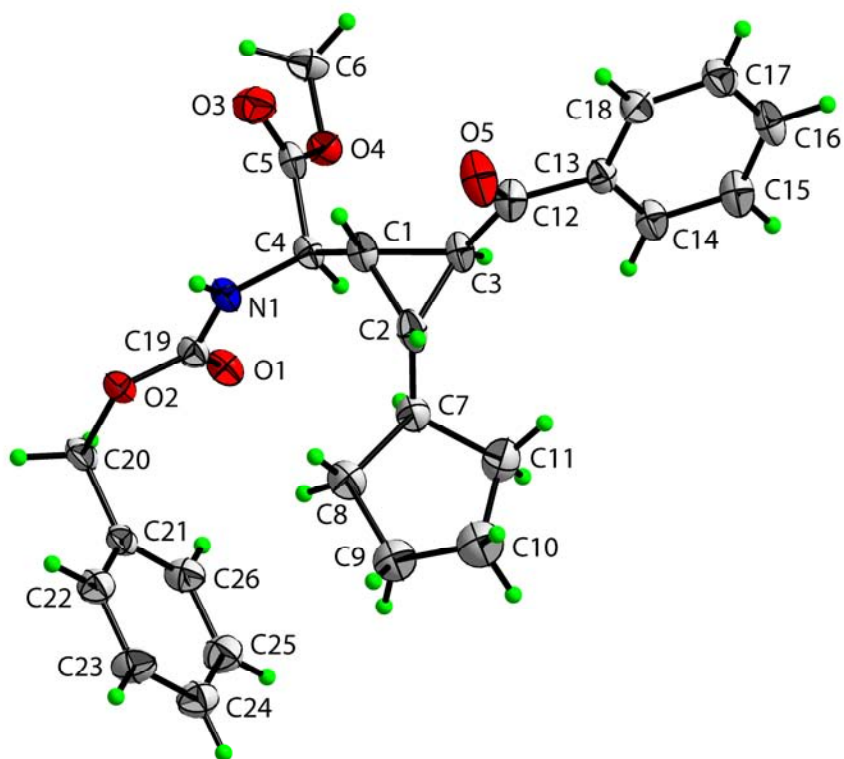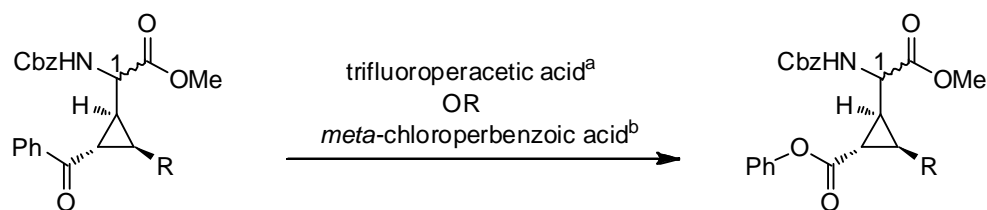|		
81a: (1*S*) R = *c*-C$_3$H$_5$	**87a:** (1*S*) R = *c*-C$_3$H$_5$	24%[a]* 77%[b]
81b: (1*R*) R = *c*-C$_3$H$_5$	**87b:** (1*R*) R = *c*-C$_3$H$_5$	11%[a]*
81c: (1*S*) R = *c*-C$_4$H$_7$	**87c:** (1*S*) R = *c*-C$_4$H$_7$	0%[b]*
81d: (1*R*) R = *c*-C$_4$H$_7$	**87d:** (1*R*) R = *c*-C$_4$H$_7$	47%[b]*
81e: (1*S*) R = *c*-C$_5$H$_9$	**87e:** (1*S*) R = *c*-C$_5$H$_9$	64%[a]
81f: (1*R*) R = *c*-C$_5$H$_9$	**87f:** (1*R*) R = *c*-C$_5$H$_9$	19%[a]
81g: (1*S*) R = *c*-C$_6$H$_{11}$	**87g:** (1*S*) R = *c*-C$_6$H$_{11}$	44%[a]
81h: (1*R*) R = *c*-C$_6$H$_{11}$	**87h:** (1*R*) R = *c*-C$_6$H$_{11}$	47%[a]

*Products readily decomposed under reaction conditions

The Baeyer-Villiger oxidation (Scheme 2.25) was performed using trifluoroperacetic acid produced *in situ* from trifluoroacetic anhydride and hydrogen peroxide as per Anastasia *et al.*[176] These harsher conditions were used in lieu of the conventional *m*-CPBA since the phenyl group is very slow to migrate when using *m*-CPBA, which results in greatly increased reaction times and lower yields. This method worked fairly well with the cyclohexyl-substituted cyclopropane (**81g, h**). However, yields decreased significantly when it was attempted with the cyclopropyl (**81a, b**) and cyclobutyl (**81c, d**) compounds where little or no product could be isolated. It was thought that the strongly acidic conditions had caused the product to decompose and so it was opted to try using *m*-CPBA, despite expecting a very long reaction time and potentially low yields. After 5 weeks phenyl ester **87a** was isolated in 77% yield. This methodology was subsequently employed in the attempt to form the cyclobutyl compounds **87c** and **87d**, however after workup and purification, ¹H NMR analysis revealed that the products were prone to decomposition. The exact nature of the instability is unknown. Owing to the long reaction times, an attempt was made to increase the speed of Baeyer-Villiger phenyl group migration by 2-methoxy substitution and thus avoiding the use of trifluoroperacetic acid as oxidant. The 2-methoxyphenyl cycloheptyl 1,2-dioxine was synthesized successfully, however all attempts to form the cyclopropane failed. Purification of the Baeyer-Villiger products was usually accomplished via flash column

chromatography without much difficulty. However, due to the fact that when using *m*-CPBA as oxidant, the reaction did not proceed to completion, it was sometimes not possible to fully separate the starting ketone from the desired ester product. In these cases, the impure product was simply carried through to the next step of the synthesis and fully purified after the next synthetic transformation. Formation of the phenyl ester could be confirmed by ^{1}H NMR as an obvious disappearance of aromatic and cyclopropane peaks associated with the protons adjacent to the ketone at approximately 8.0 ppm and 2.9 ppm respectively and the appearance of phenyl ester peaks at *ca.* 7.1 ppm. A corresponding shift was also observed in the ^{13}C NMR with a shift in the cyclopropyl carbonyl peak from approximately 198 ppm to *ca.* 172 ppm after conversion to the ester. Also noted in the IR spectra, was the disappearance of the absorption peak due to the phenyl ketone at 1648–1670 cm^{-1}, which was replaced by an ester carbonyl absorption that was largely obscured by the methyl ester absorption at approximately 1740 cm^{-1}.

Scheme 2.26. Trans-esterification

		Yield
87a: (1*S*) R = *c*-C$_3$H$_5$	**88a:** (1*S*) R = *c*-C$_3$H$_5$	96%
87e: (1*S*) R = *c*-C$_5$H$_9$	**88b:** (1*S*) R = *c*-C$_5$H$_9$	80%
87f: (1*R*) R = *c*-C$_5$H$_9$	**88c:** (1*R*) R = *c*-C$_5$H$_9$	82%
87g: (1*S*) R = *c*-C$_6$H$_{11}$	**88d:** (1*S*) R = *c*-C$_6$H$_{11}$	76%
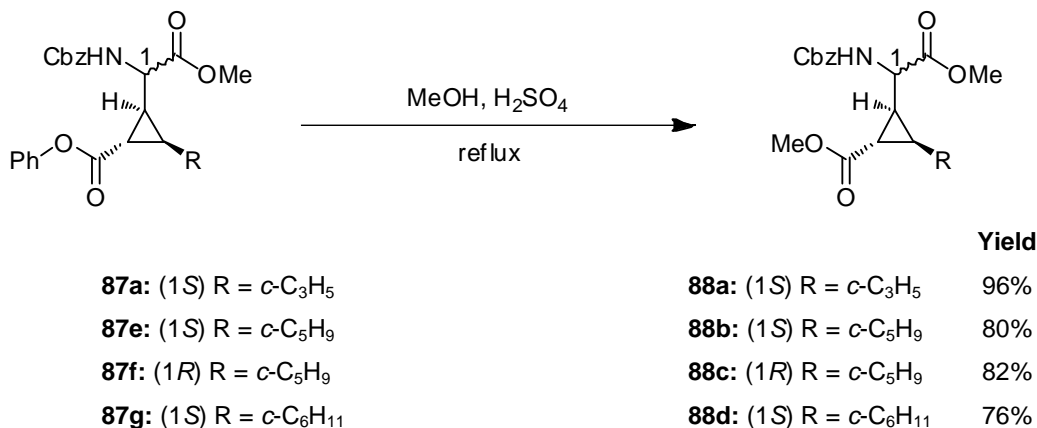
The trans-esterification reactions outlined in Scheme 2.26 went smoothly with yields ranging from good (76%) to excellent (96%). This step is necessary in order to separate the phenol by-product form the cyclopropanes, which would be difficult if the esters were simply hydrolysed. The phenol that was formed could be clearly visualized via TLC as a red spot, when developed with vanillin and was confirmation that the reaction was proceeding. It was not difficult to purify the products by flash column chromatography to remove all traces of the phenol by-product and residual starting

material. All the dimethyl esters (**88a–d**) were isolated as white solids and were easy to handle, except the cyclopropyl substituted compound (**88a**) which was a colourless, viscous, sticky gum. ^{1}H NMR revealed the presence of a single phenyl ring and the appearance of a second, sharp methyl ester peak at approximately 3.6 ppm. An IR absorption peak due to the new methyl ester carbonyl group could be distinguished at approximately 1720 cm^{-1}.

Scheme 2.27. Ester Hydrolysis

		Yield
88a: (1*S*) R = *c*-C$_3$H$_5$	**89a:** (1*S*) R = *c*-C$_3$H$_5$	92%
88b: (1*S*) R = *c*-C$_5$H$_9$	**89b:** (1*S*) R = *c*-C$_5$H$_9$	99%
88c: (1*R*) R = *c*-C$_5$H$_9$	**89c:** (1*R*) R = *c*-C$_5$H$_9$	96%
88d: (1*S*) R = *c*-C$_6$H$_{11}$	**89d:** (1*S*) R = *c*-C$_6$H$_{11}$	97%
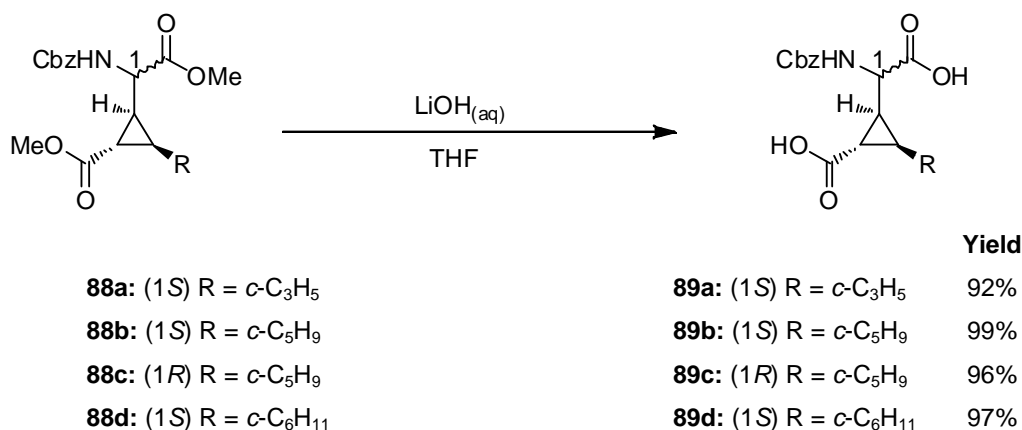
Ester hydrolysis gave almost quantitative yields of **89a–d** (Scheme 2.27), however due to the workup using ethyl acetate and concentrated hydrochloric acid, it was necessary to add toluene and then remove it *in vacuo* to remove all traces of acetic acid that was formed by hydrolysis of the solvent. The success of the hydrolysis was indicated by ^{1}H NMR by the disappearance of both methyl peaks. The IR spectra showed a shift in frequencies corresponding to the carboxylic acid groups at *ca.* 1694 and 1680 cm^{-1}. Yields were in the range of 92 to 99%.

Scheme 2.28. Hydrogenolysis (Amine Deprotection)

		Yield
89a: (1S) R = c-C$_3$H$_5$	**90a:** (1S) R = c-C$_3$H$_5$	95%
89b: (1S) R = c-C$_5$H$_9$	**90b:** (1S) R = c-C$_5$H$_9$	ND
89c: (1R) R = c-C$_5$H$_9$	**90c:** (1R) R = c-C$_5$H$_9$	ND
89d: (1S) R = c-C$_6$H$_{11}$	**90d:** (1S) R = c-C$_6$H$_{11}$	ND

ND: not determined
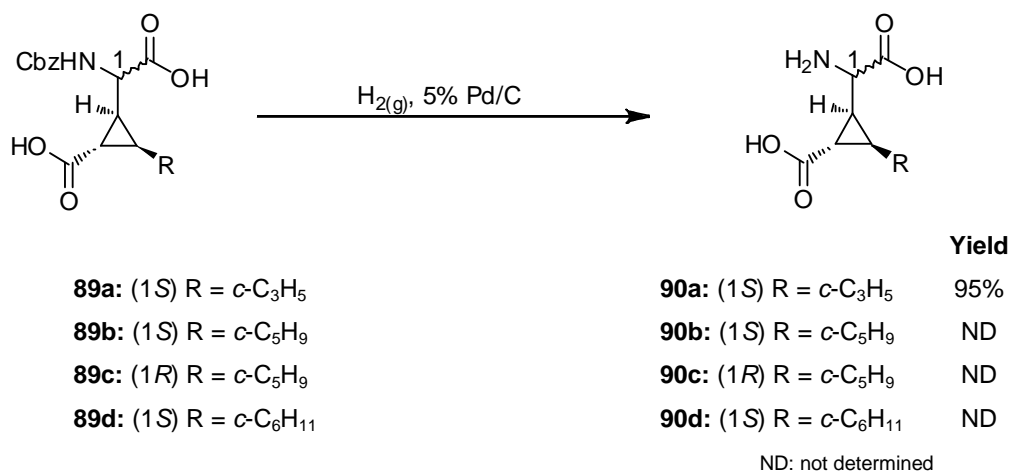
The carboxybenzyl (Cbz) amine protecting group was utilized so that amine deprotection could be done as the final step via a hydrogenolysis reaction, leaving the amine in need of minimal purification (Scheme 2.28). The method previously used for workup by our research group was to add water to the reaction followed by filtration though a pad of kenite, washing with ethyl acetate and evaporation of the water to give pure amino acid. This method depended on the product being fairly water soluble and it was found to be successful in the isolation of **90a**, however, it was found that the cyclopentyl- (**90b, c**) and cyclohexyl-substituted (**90d**) compounds were methanol soluble, which complicated their purification. Conversion of the requisite amino acid to the hydrochloride salt was needed in order to afford pure product, however as the free amino acid was desired, this necessitated removal of the HCl as the last step. The method employed to do this was the same as used by Collado[55] and required stirring a concentrated methanol solution of the hydrochloride salt with dry propylene oxide followed by filtration to obtain the solid product (Scheme 2.29). The HCl reacts with the propylene oxide to form 1-chloro-2-propanol which can be removed by drying the product under a hard vacuum.

Scheme 2.29. Removal of HCl
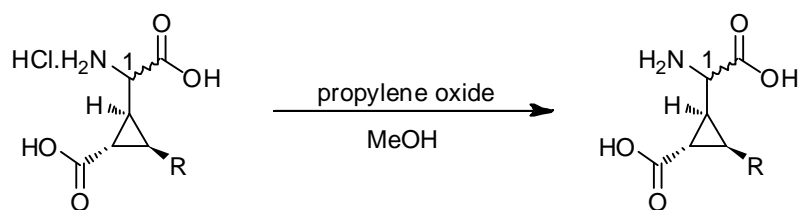
		Yield
90b: (1S) R = c-C$_5$H$_9$	**91b:** (1S) R = c-C$_5$H$_9$	0%
90c: (1R) R = c-C$_5$H$_9$	**91c:** (1R) R = c-C$_5$H$_9$	0%
90d: (1S) R = c-C$_6$H$_{11}$	**91d:** (1S) R = c-C$_6$H$_{11}$	16%

This protocol was attempted on the cyclopentyl (**90b, c**) and the cyclohexyl (**90d**) compounds. The cyclopropyl compound was sufficiently water soluble to negate its conversion to the hydrochloride salt for purification. It was found upon filtration of the cyclopentyl reactions that no product remained, presumably due to decomposition. Decomposition also occurred in the cyclohexyl reaction, however, a small amount of **91d** was able to be recovered upon filtration.

2.9 Summary

Two new cycloalkylcarboxycycloproplyglycine analogues were successfully synthesized utilizing the reaction of 1,2-dioxines with protected phosphonates to rapidly construct the cyclopropane core with all necessary stereochemistry of pendant groups, in a 20% overall yield for one diastereoisomer.

Chapter 3 : Triazole Amino Acids

3.1 Introduction

One class of compounds that have not been widely investigated as glutamate receptor ligands are the 1,2,3-triazoles. Thus, a series of basic analogues was designed which could be obtained in a synthetically straight-forward manner (Figure 3.1). Given the structural similarity between the proposed triazoles and known ionotropic glutamate receptor ligands, it was hypothesized that these new structures may also show biological activity (Figure 3.2). To this end, the library of synthesized compounds was screened *in vitro* against both ionotropic (NMDA, kainate and AMPA) and metabotropic (mGluR1, mGluR2, mGluR4 and mGluR5) glutamate receptors.

Figure 3.1. Proposed Triazole Amino Acids
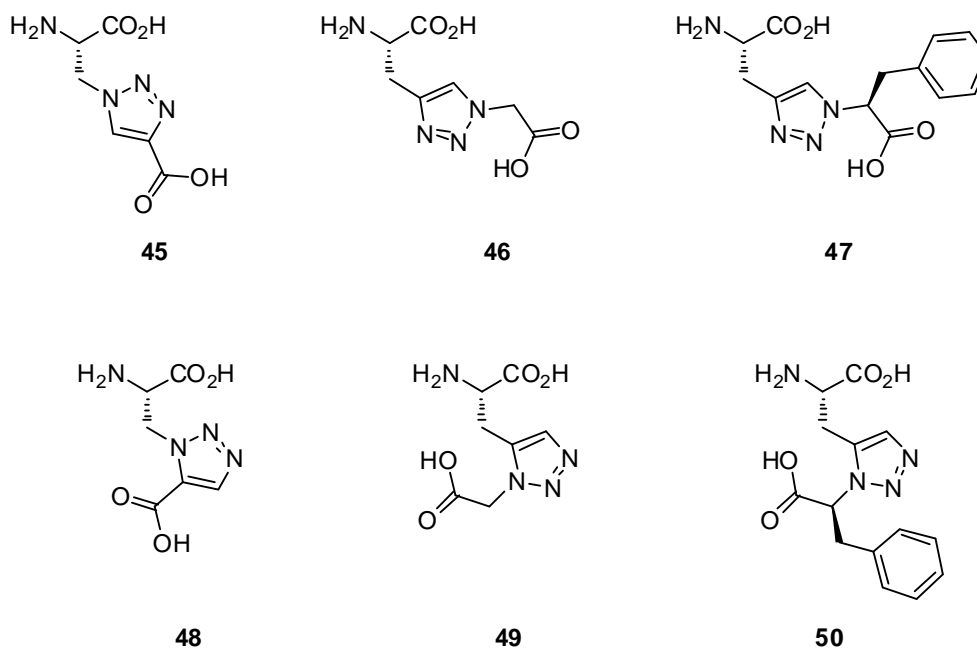
The triazole moiety is an aromatic five membered heterocycle containing 3 nitrogens; those being considered here are 1,2,3-triazoles.[177] When one of the nitrogens is substituted, the other two have lone pairs that can potentially act as hydrogen bond donors.

Figure 3.2. Structural Comparison Between Triazoles and Known Ligands
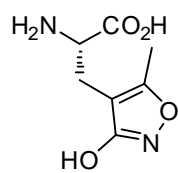
36
(*S*)-AMPA
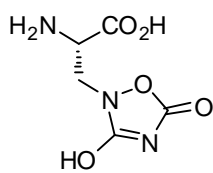
18
Quisqualate
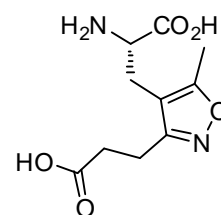
92
(*S*)-ACMP
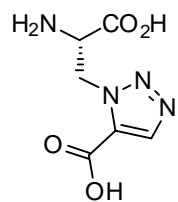
48
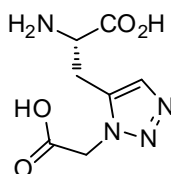
49
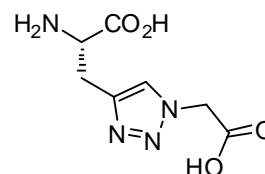
46
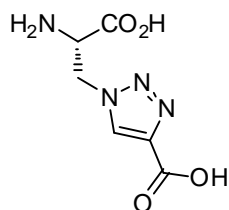
45
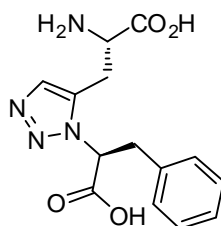
50
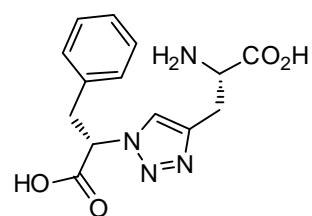
47
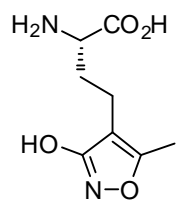
40
(*S*)-Homo-AMPA
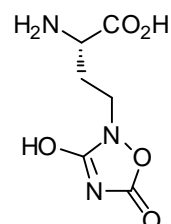
37
(*S*)-Homo-Quisqualate
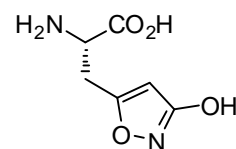
38
(*S*)-HIBO
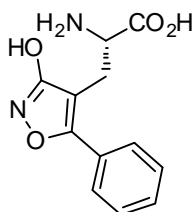
93
(*S*)-APPA

As is depicted in Figure 3.2, this configuration mimics the arrangement found in some competitive AMPA and NMDA receptor ligands such as (*S*)-AMPA (**36**), Quisqualate (**18**) and (*S*)-ACMP (**92**) where either an isoxazole or oxadiazolone ring is present.[107,178,179] Many of these known ligands incorporate hydroxyl substitution on the heterocycle, which bears an acidic proton and thus acts as a carboxylic acid bioisostere. However, one compound, (*S*)-ACMP (**92**) is a known AMPA receptor antagonist which bears a 2-carbon chain terminated with a carboxylic acid group.[180]

The current research was seeking novel metabotropic receptor ligands as opposed to ionotropic ligands and so it was chosen to employ carboxylic acid substitution on the heterocycle, instead of a hydroxyl group. This was done in an effort to increase affinity towards the mGluRs over the iGluRs. Another structural feature of some iGluR ligands, for example, the AMPA receptor agonist, (*S*)-APPA (**93**), is substitution on the heterocycle by another aromatic ring.[181] This is usually a simple phenyl or pyridinyl group. Compounds **47** and **50** were designed in order to probe the effects of phenyl substitution on the carboxylic acid chain adjacent to the heterocycle.

The 1,2,3-triazole core structure offers some advantages. Firstly, it is readily prepared by a high yielding copper or ruthenium catalysed cycloaddition reaction. Secondly, it is possible to establish a library of compounds for biological screening by cycloaddition of a few simple azide and alkyne building blocks in different combinations (Figure 3.3). Compounds **94**, **98** and **101** have previously been reported and our analytical data was found to be in agreement with the literature.[182-184]

Figure 3.3. Key Azide and Alkyne Building Blocks
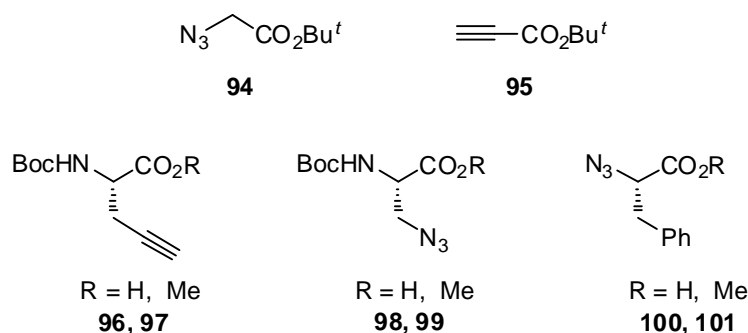
Thus, the following retro-synthetic strategies were devised (Scheme 3.1-Scheme 3.4). The desired triazolyl amino acid hydrochloride salts (**45a**, **46a**, **47a**, **48a**, **49a**, **50a**) could be obtained from the Boc-protected amino acids via treatment with HCl. These in turn could be obtained from the methyl or *t*-butyl ester protected carboxylic acids by alkaline hydrolysis. Formation of the protected triazoles is accomplished either by a 'click'-style copper-catalysed cycloaddition (Schemes 3.1, Scheme 3.2) or a ruthenium-catalysed cycloaddition (Schemes 3.3, Scheme 3.4) involving the reaction between a functionalized azide (**94**, **98**, **99**, **100**, **101**) and alkyne (**95**, **96**, **97**).

Scheme 3.1. Retro-Synthetic Strategies
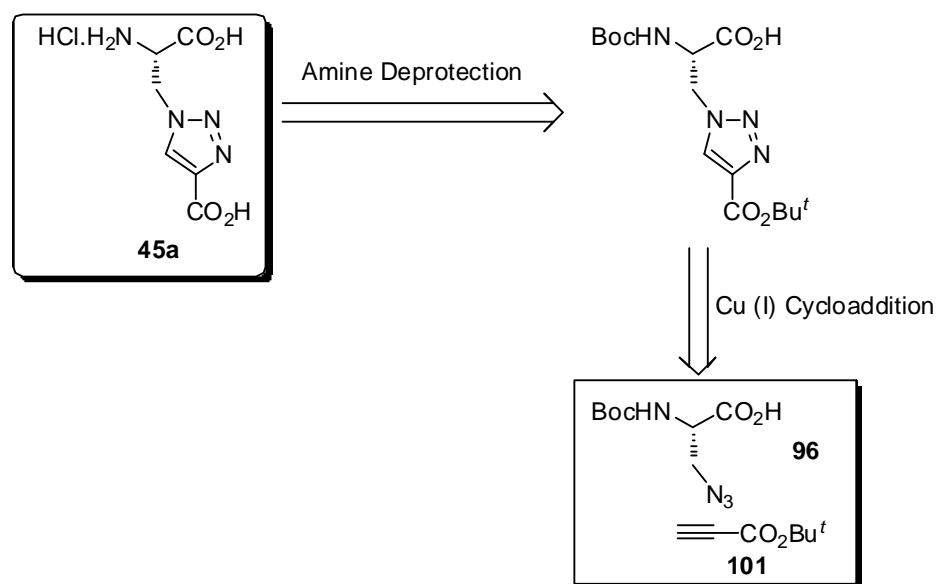
Scheme 3.2. Retro-Synthetic Strategies
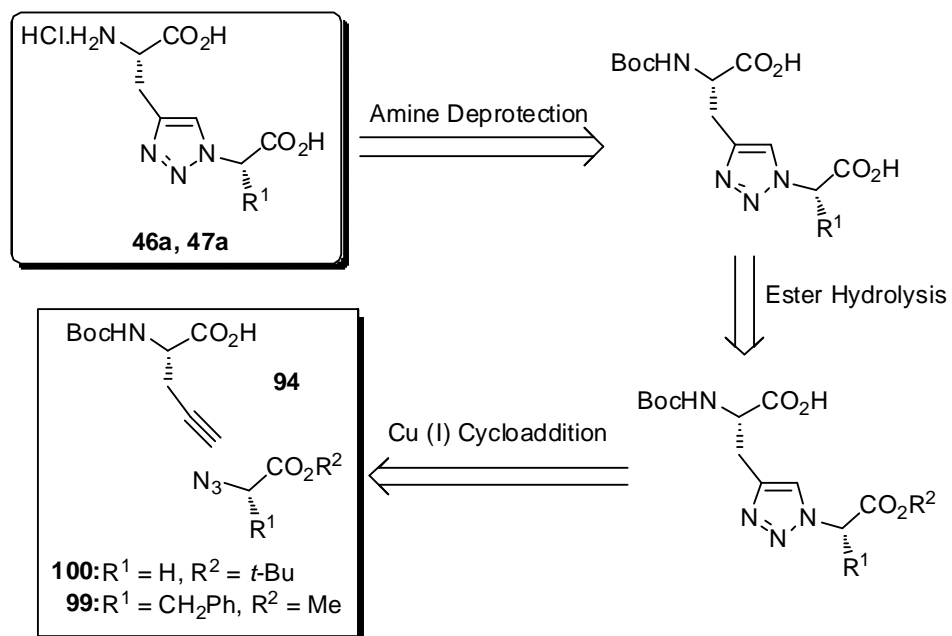
Scheme 3.3. Retro-Synthetic Strategies
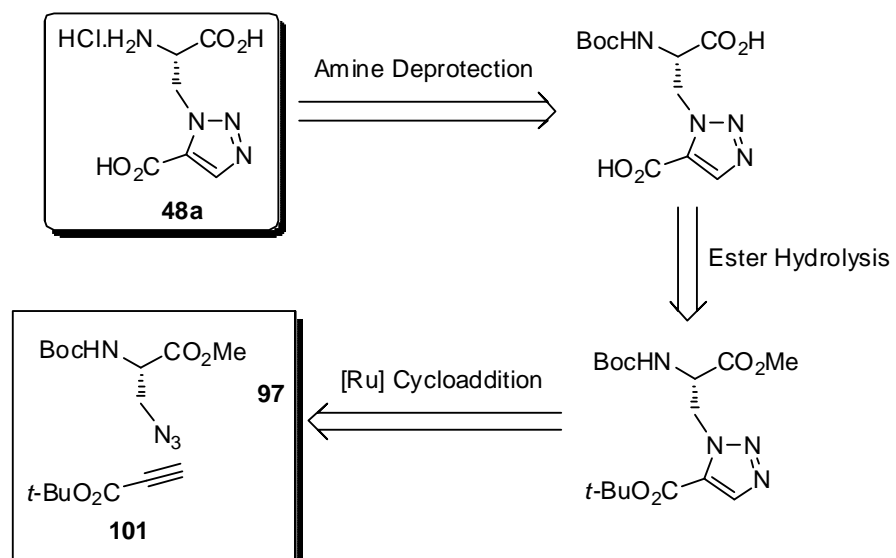
Scheme 3.4. Retro-Synthetic Strategies
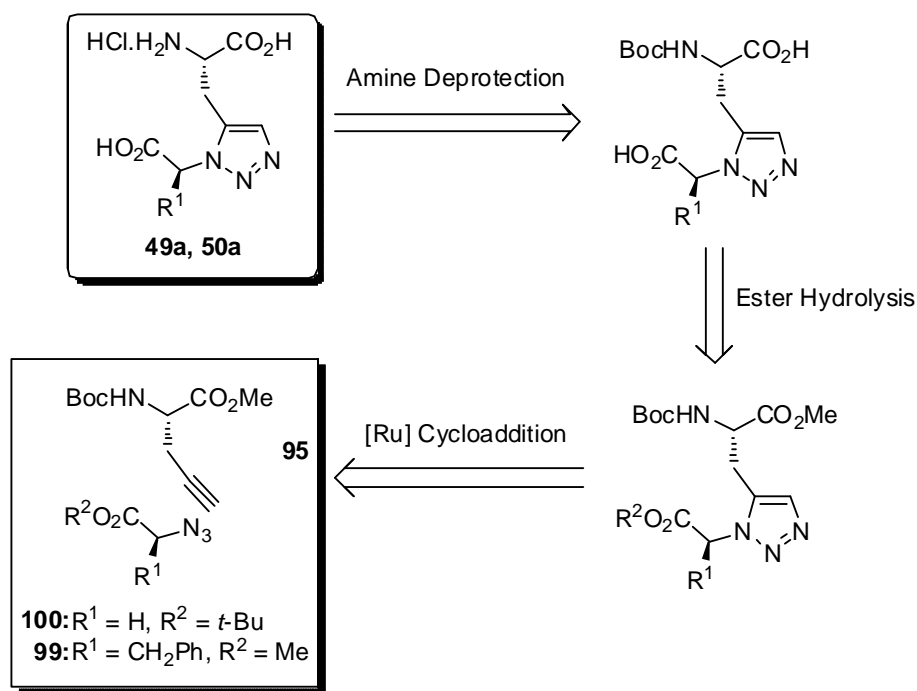
3.2 Triazoles in Drug Discovery

Examination of the current literature reveals that there have been relatively few efforts to investigate 1,2,3-trizoles as potential drug molecules.[185-188] Gajewski and co-workers have reported the design and synthesis of several triazolyl amino acids as potential inhibitors of the neutral amino acid transporter SN1 (Figure 3.4).[185] This transporter is an L-glutamine shuttle responsible for transporting the endogenous amino acid in and out of cells. Six potential ligands (**45**, **102–106**) were synthesized including compound **45** that was investigated in the present work, however, none showed significant inhibitory activity in the amino acid transporter assay.[185]

An interesting advance put forward by Sharpless and co-workers is the synthesis of an acetylcholinesterase inhibitor by *in situ* click chemistry. The process involved incubation of the enzyme from *Torpedo californica* with azide-functionalized tacrine, a known main binding site ligand, and allowing a variety of acetylene-functionalized phenylphenanthridinium derivatives (with known activity) to interact with peripheral binding sites (Figure 3.5). Triazoles are only formed when there is a favourable interaction between the enzyme and both the azide and alkyne.

Figure 3.4. Triazolyl Amino Acids as Amino Acid Transporter Inhibitors[185]

102

103

104

45

105

106
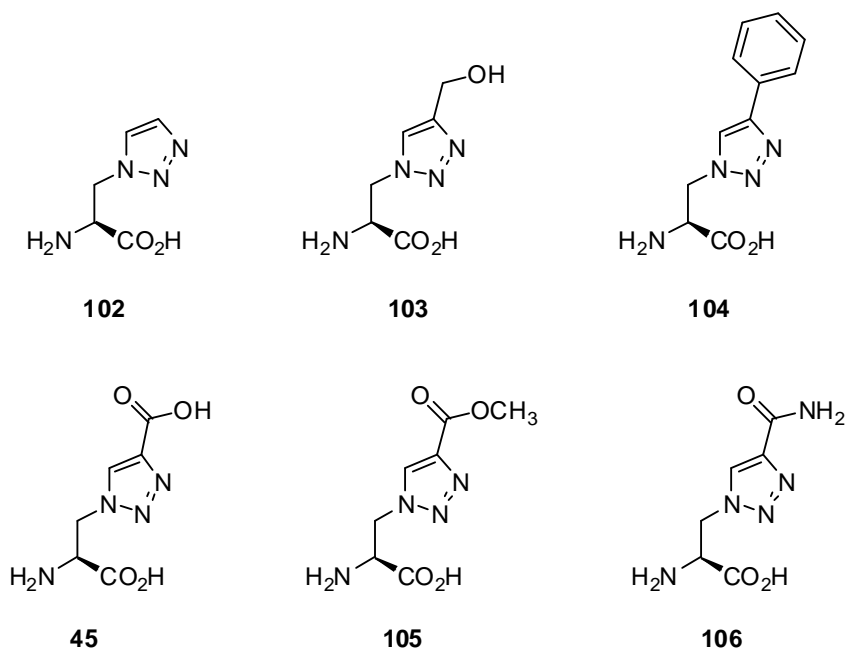
Figure 3.5. Triazole Acetylcholinesterase Inhibitor Synthesized *In Situ*[189,190]

syn-1

107
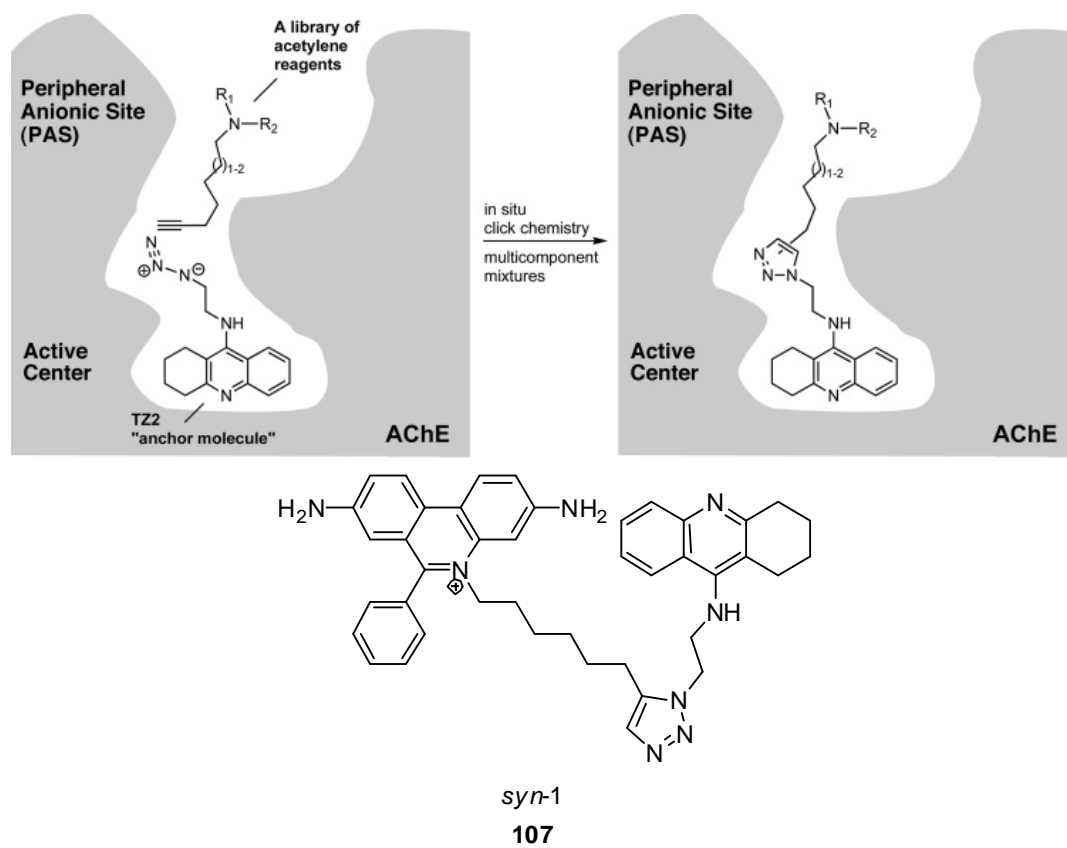
The interactions cause an energy barrier lowering effect which catalyses the reaction. Through this methodology, it was possible to find several hit structures that showed increased activity and better enzyme kinetics than either of the known lead compounds. The most potent new compound identified was *syn*-1 (**107**)[189,190]

3.3 Background on the Synthesis of 1,2,3-Triazoles

The original preparation of this class of heterocycle, reported by Huisgen in 1963, involved a thermally promoted cycloaddition of an azide to a terminal alkyne resulting in both 1,4- and 1,5-substituted products (Scheme 3.5). The energy barrier for the thermally driven reaction has been calculated to be a very high +26 kcal/mol due to the inherent stability of both azides and alkynes. For this reason, these reactions necessitate high temperatures and long reaction times in order to furnish reasonable yields.

Scheme 3.5. Huisgen 1,3-Dipolar Cycloaddition

It was soon discovered that the energy barrier for the cycloaddition reaction could be lowered significantly by use of copper (I) catalysis. Catalysed cycloaddition of an azide to a terminal alkyne (CuCAA) was subsequently made famous by Barry K. Sharpless and co-workers under its 'Click Chemistry' moniker.[191,192] It has since been employed as a versatile coupling reaction, especially in polymer chemistry and in the attachment of long chain linkers and pendant groups.[192-196] However, as stated earlier, it has been used in relatively few drug discovery applications, until recently.[185-188] It should be noted that copper catalysis only affords the 1,4-substituted triazoles, however, ruthenium catalysis allows access to the 1,5-substituted and tri-substituted 1,2,3-triazoles (Figure 3.6).

Figure 3.6. 1,4- and 1,5-Substituted 1,2,3-Triazoles
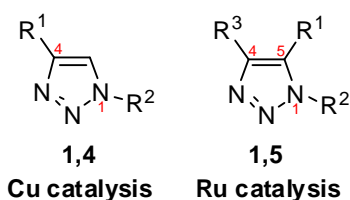
The catalytic cycle for the cycloaddition has been elucidated and is outlined in Scheme 3.6. Briefly, the Cu(I) displaces a proton from the acetylene followed by coordinate bonding of the azide to the copper. The binding of the acetylene to the copper increases the electrophilicity of the alkyne, enabling attack by the azide to form a six-membered cupro-cycle. Ring-collapse followed by proton displacement of the copper releases the final 1,2,3-triazole product.

Scheme 3.6. Copper Azide Alkyne Cycloaddition Catalytic Cycle[197,198]

R^1 = alkyl, aryl, CO_2H, NH_2
R^2 = alkyl, aryl
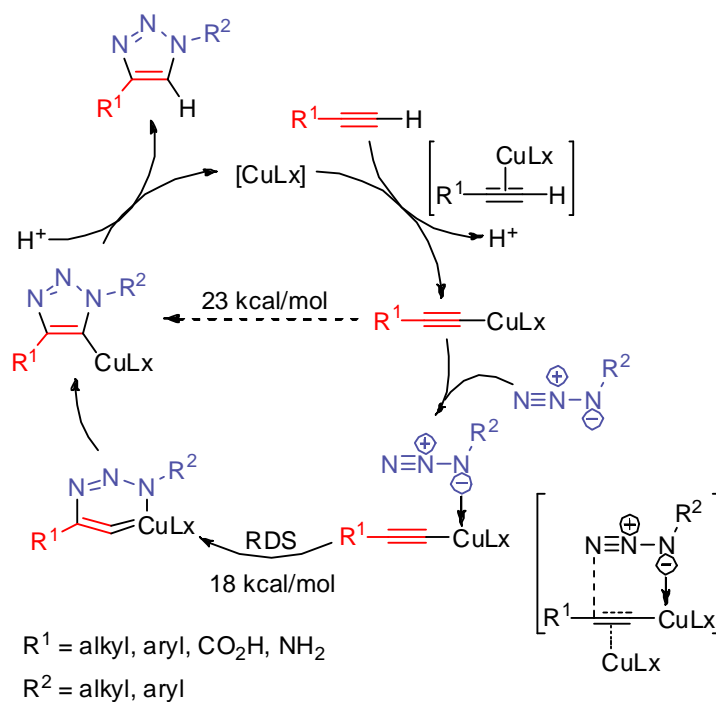
It is possible to obtain 1,5-substituted triazoles as the sole product by use of ruthenium catalysis. Several catalysts have been investigated including those outlined in Table 3.1.

Table 3.1. Ruthenium (II) catalysis product distribution of benzyl azide and phenyl acetylene cycloaddition[199]

Ru catalyst	1,5-Substitution	1,4-Substitution
$RuCl_2(PPh_3)_3$	-	1.7%
$Ru(OAc)_2(PPh_3)_3$	-	46.5%
$RuHCl(CO)(PPh_3)_3$	-	2.5%
$RuH_2(CO)(PPh_3)_3$	-	55.8%
$CpRuCl(PPh_3)_2$	12.9%	1.3%
$Cp*RuCl(COD)$	100%	-
$Cp*RuCl(NBD)$	93.5%	-
$[Cp*RuCl]_4$ (**108**)	100%	-
$Cp*RuCl(PPh_3)_2$ (**109**)	100%	-

As summarized in Table 3.1 above, in order to obtain 1,5-substituted triazoles in good yields, a pentamethylcyclopentadiene (Cp*) ruthenium catalyst must be used. $[Cp*RuCl]_4$ (**108**) is the most potent catalyst thus far reported and can be used to produce tri-substituted triazoles. Ruthenium complex **109** is also very potent and shows complete selectivity for 1,5-cycloaddition. However, this catalyst has an advantage over more potent catalyst **108** in that it can be stored for prolonged periods and does not have to be prepared each time it is required.

The mechanism for ruthenium catalysis is shown in Scheme 3.7. Briefly, both the azide and alkyne coordinate to the metal centre simultaneously, thus displacing two ligands. This causes activation of both the azide and alkyne allowing them to form a cyclic intermediate which collapses to form the tethered triazole which is subsequently displaced from the metal centre by re-coordination to the starting ligands.

Scheme 3.7. Ruthenium Azide Alkyne Cycloaddition Catalytic Cycle[199]

R^1 = alkyl, aryl, CO_2Me, NHBoc

R^2 = alkyl, aryl
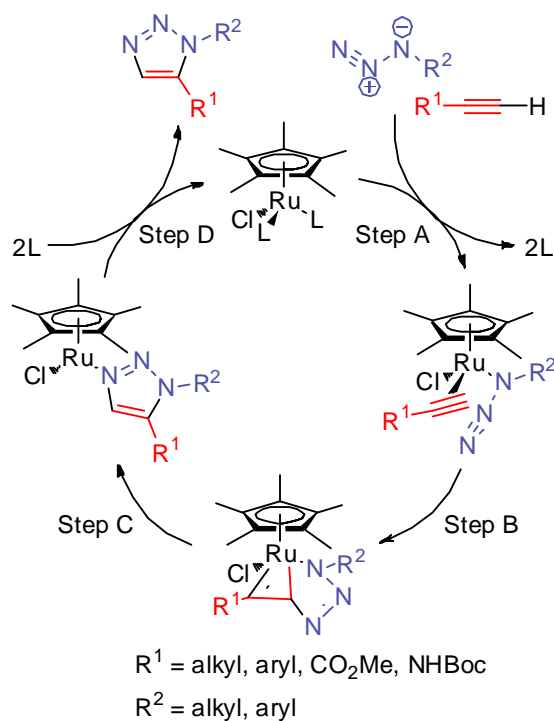
3.4 Synthesis of the Target Triazole Amino Acids

As stated previously, the target molecules for synthesis were the 1,4- and 1,5-substituted 1,2,3-triazole amino acids depicted in Figure 3.7.

Figure 3.7. Proposed Triazole Amino Acids

| **45** | **46** | **47** |

| **48** | **49** | **50** |
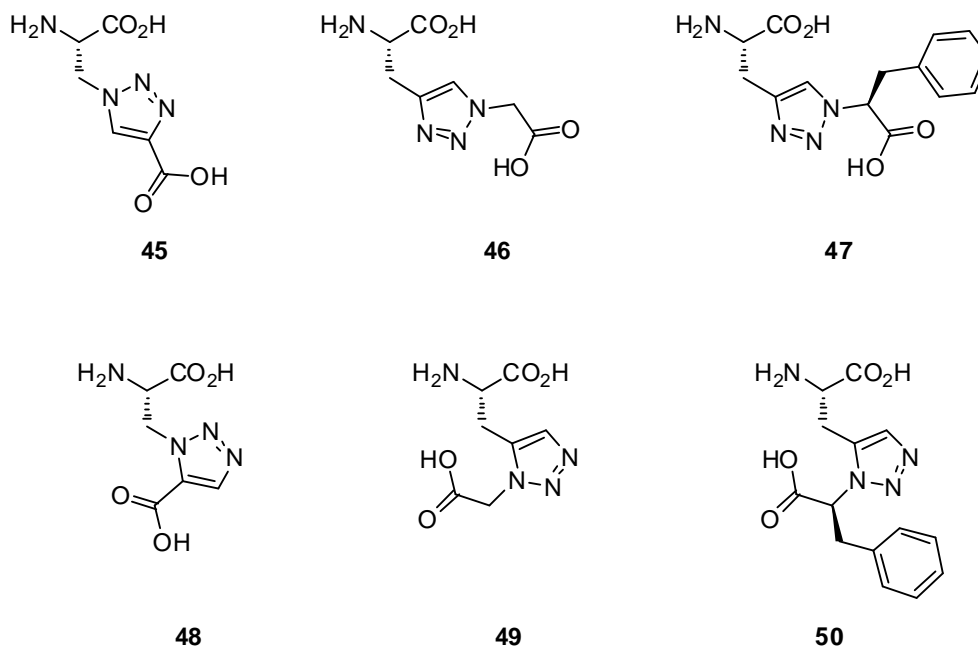
Following is a discussion on the synthesis of the starting materials required in these syntheses. The most basic azide building block was *tert*-butyl azidoacetate (**94**) which was prepared from bromo ester **110** by reaction with sodium azide (Scheme 3.8). This reaction employed chloroform as solvent, however, these conditions can give rise to some diazidomethane formation, which is dangerously explosive.[200] One literature synthesis reports dimethylformamide as solvent, however, due to its high boiling point, this would make purification difficult, since the product is volatile. A more suitable method has been reported by Vollmar and Dunn where the reaction is carried out in aqueous acetone, followed by removal of the acetone and ether extraction.[201] Nevertheless, the azide was obtained, albeit in low yield (38%). During TLC analysis, it was expected that it would be possible to visualize the product using UV light, due to the p-orbital conjugation of the azide moiety. Contrary to this, it was discovered that the bromo starting material was actually fluorescent under UV light. This caused confusion during isolation and purification, until IR analysis was carried out on the suspected desired product and no diagnostic azide peak was observed. The presence of the desired product in the other major fraction with an IR spectrum revealing a strong absorption peak at approximately 2100 cm^{-1}.

Scheme 3.8. Preparation of *tert*-Butyl Azidoacetate (**94**)
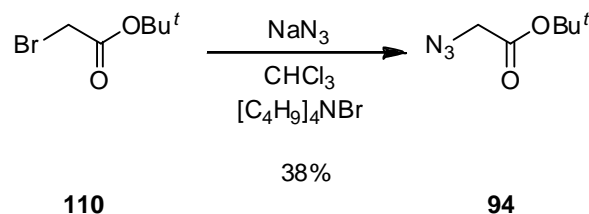
Preparation of Boc-protected propargyl glycine (**96**) was accomplished by reaction of amino acid **111** with di-*tert*-butyl dicarbonate with aqueous sodium hydroxide as base (Scheme 3.9). Initially, the base used for this reaction was triethylamine, however, after workup the desired product was not evident in the ^{1}H NMR. It's possible that the triethylamine salt formed and was more resistant to re-protonation with acid during the workup than would be expected.

Scheme 3.9. Synthesis of Boc-Propargylglycine (**96**)
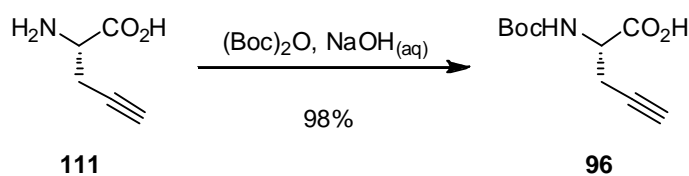
The methyl ester **97** was prepared in 83% yield from **111** by a literature procedure consisting of a two step, one pot synthesis employing thionyl chloride and forming the methyl ester hydrochloride salt as an intermediate (Scheme 3.10).[202]

Scheme 3.10. Synthesis of Boc-Propargylglycine Methyl Ester (**97**)
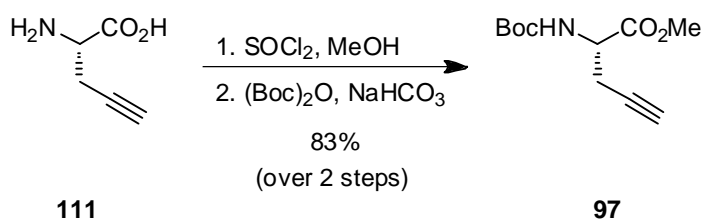
Boc-protected azide (**98**) was prepared from Boc-L-2,3-diaminopropionic acid (**112**) using freshly prepared triflyl azide as an azide transfer reagent (Scheme 3.11). This method of diazotransfer, devised by Yan and colleagues, has significant advantages over other methods.[184] For example, it is usually carried out using water as co-solvent, however, this requires the use of a large excess of the relatively expensive and highly toxic triflic anhydride. By generating the triflyl azide in acetonitrile, it is possible to decrease the amount of triflic anhydride required; the amount of sodium azide required is also reduced compared to other methods. The main by-product of this reaction (trifyl amine) is quite difficult to remove completely. However, its low solubility in chloroform does allow separation from the target material. Due to the difficultly in purification of this starting material, a quite low 32% yield was obtained. The IR spectrum showed the expected sharp azide absorption at 2111 cm^{-1}.

Scheme 3.11. Synthesis of Boc-Azidoalanine (**98**)
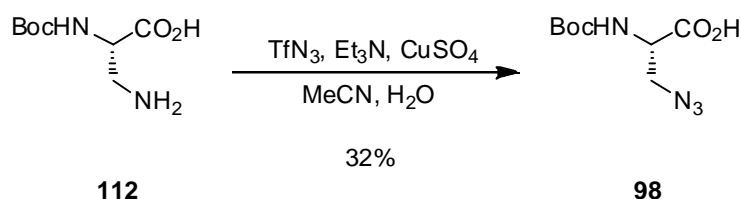
An alternative procedure to prepare **99** was sought, owing to the difficulty in purification and low yield when using triflyl azide, as for synthesis of **98**. Hydroxyl groups are conveniently transformed into azides by means of a Mitsunobu reaction (Scheme 3.12).[203] Thus, Boc-serine methyl ester (**113**) was converted to azide **99** under basic, anhydrous conditions. However, it was found that purification of this reaction was more difficult that the previous method due to similar polarities of starting material and desired product, even so the overall yield was significantly improved over that for the synthesis of azide **98**. The product was confirmed as an azide by appearance of a diagnostic sharp IR absorption around 2108 cm^{-1}.

Scheme 3.12. Synthesis of Boc-Azidoalanine Methyl Ester (**99**)
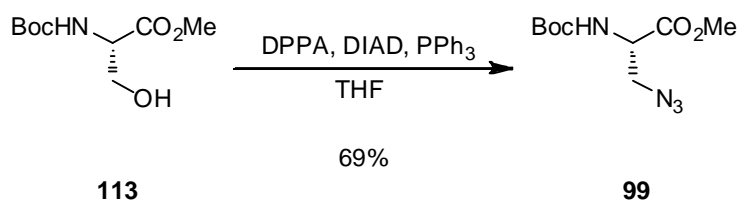
The use of triflyl azide as an azide transfer reagent smoothly converted L-phenylalanine (**114**) to provide azide **100** as a pale yellow gum (Scheme 3.13). The presence of the azide functionality was indicated by IR absorption at 2118 cm^{-1}.

Scheme 3.13. Synthesis of 2-Azido-3-Phenyl-Propanoic Acid (**100**)
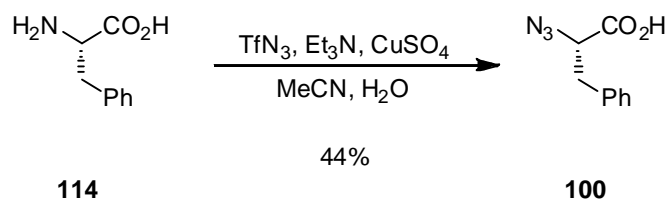
The corresponding known methyl ester **101** was prepared by dissolving compound **100** in methanol and adding minimal thionyl chloride (Scheme 3.14).[184] Infrared spectroscopy analysis revealed expected absorptions for the azide moiety at 2112 cm^{-1} and for the ester carbonyl at 1747 cm^{-1}.

Scheme 3.14. Synthesis of Methyl 2-Azido-3-Phenyl-Propanoate (**101**)
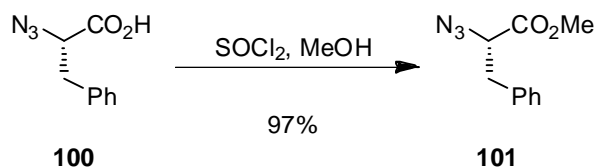
It was brought to our attention that there was a possibility that in the preparation of azides **99** and **101** and alkyne **97**, some racemisation may have occurred. In order to investigate this, it was necessary to deprotect the molecules and couple them to another optically pure amino acid (Schemes 3.15, 3.16). By doing this, if the starting materials were not optically pure, then diastereoisomers would be formed, which could be detected by ^{1}H NMR analysis. For simplicity of the resulting spectra, it was opted to couple to L- and D-valine to provide both isomers for analysis. Thus, alkyne **97** was stirred in anhydrous dichloromethane to which was added 0.6 mL of concentrated HCl. After stirring at room temperature overnight, the solvent and excess HCl were removed under reduced pressure to furnish hydrochloride salt **115**. This was coupled to Boc-L-valine (**116**) using HOBt and EDC under basic conditions to provide di-peptide **117** in 89% yield over two steps. Azide methyl esters **99** and **101** were dissolved in THF and treated with 2M LiOH overnight to provide the free carboxylic acids. These were coupled separately to both L-valine methyl ester (**118**) and D-valine methyl ester (**119**) using HOBt and EDC under basic conditions to provide di-peptides **120**, **121**, **122** and **123** in 69 to 92% yield over two steps.

Scheme 3.15. Synthesis of Dipeptide **117**
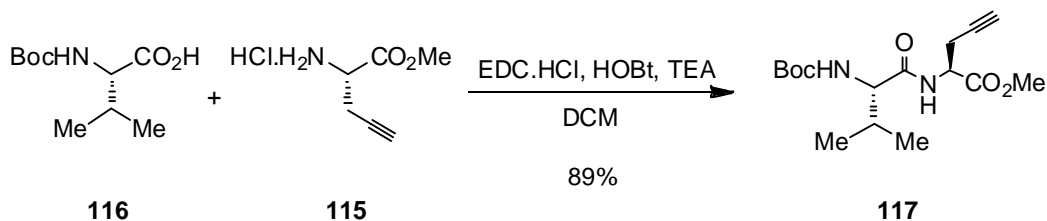
Scheme 3.16. Synthesis of Dipeptides **120–123**

					Yield
118	120:R^1 = N_3	R^2 = Ph	(*S*,*S*)	69%	
119	121:R^1 = N_3	R^2 = Ph	(*S*,*R*)	86%	
118	122:R^1 = NHBoc	R^2 = N_3	(*S*,*S*)	92%	
119	123:R^1 = NHBoc	R^2 = N_3	(*S*,*R*)	77%	
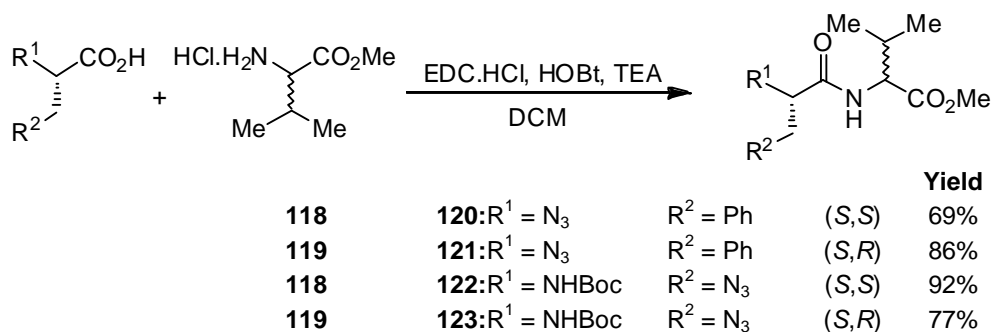
After coupling and workup, no crude ^{1}H NMR of the di-peptides revealed more than 8% diastereoisomer. Examples of excerpts from the ^{1}H NMR spectra for compounds **121** and **122** are found in Figure 3.8. The ratio of diastereoisomers was determined by comparison of the relative areas of the peaks corresponding to the methoxy groups (highlighted in yellow) found between 3.60 and 3.80 ppm. Considering that the conditions used for the amino acid coupling can also induce some epimerization, the presence of this amount of optical impurity in the starting materials was not considered to be a major problem.

Figure 3.8. Expansions from the ^{1}H NMR Spectra Used for Determination of the Relative Diasteromeric Ratios

NJS-02-80 in CDCl3, 9/2/09

Sample Name:
  NJS0280
Data Collected on:
  chemnmr.chemistry.adelaide.edu.au-inova600
Archive directory:
  /home/dtaylor/vnmrsys/data
Sample directory:
  NJS0280_20090205_01
FidFile: data_s2pul_001

Pulse Sequence: PROTON (s2pul)
Solvent: CDCl3
Data collected on: Feb 9 2009

Compound 122
~8% other isomer
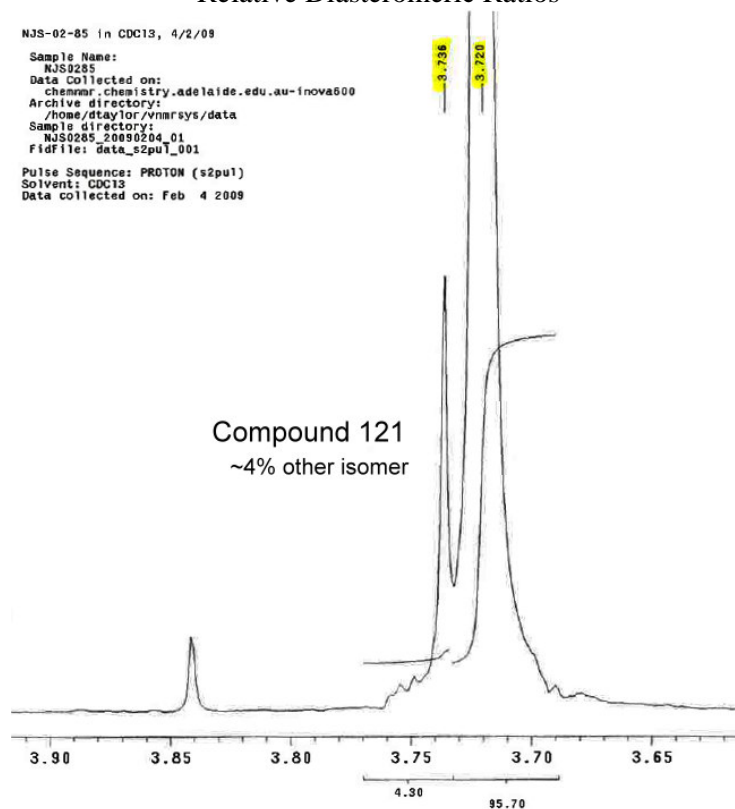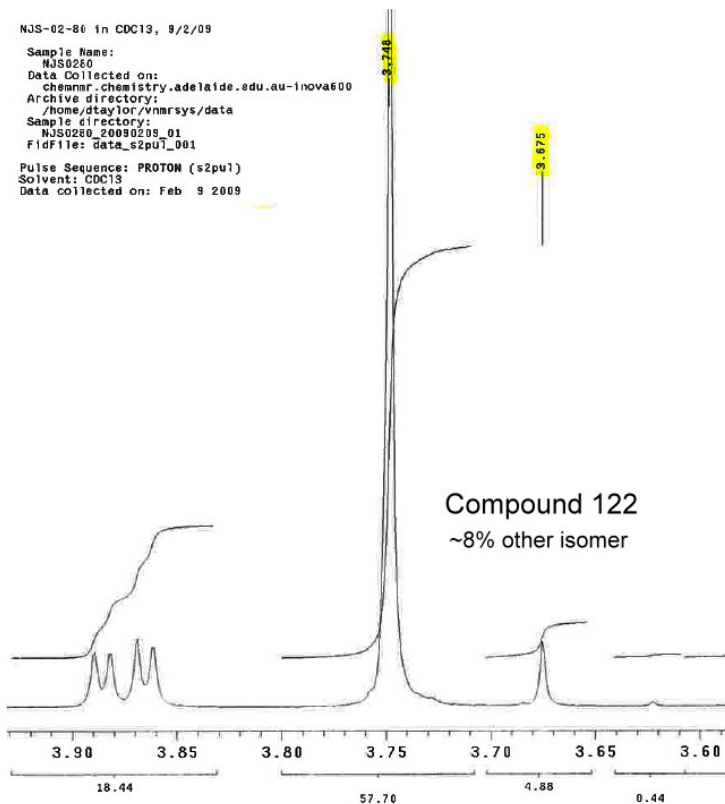
With the basic building blocks (Figure 3.3, **94–101**) in hand, we set about synthesizing a number of 1,2,3-triazole amino acid analogues. Referring to Scheme 3.17, alkyne **95** and azide **98** were dissolved in a 2:1 mix of *t*-butanol and water. Copper sulfate was added at 5 mol% loading followed by sodium ascorbate to enable the necessary reduction of Cu^{2+} to Cu^{1+} and enabling the cycloaddition to proceed. Stirring overnight at room temperature was usually sufficient to obtain maximal yield, however, the reaction time was occasionally extended to two days. After removal of solvents under vacuum, pure triazole **124** was usually obtained after a single pass of flash column chromatography. Likewise, referring to Scheme 3.18, azides **94** and **101** were allowed to react with alkyne **96** and pure triazoles **125** and **126** respectively, obtained in good yield.

Scheme 3.17. Synthesis of Triazole **124**

98 → **124**
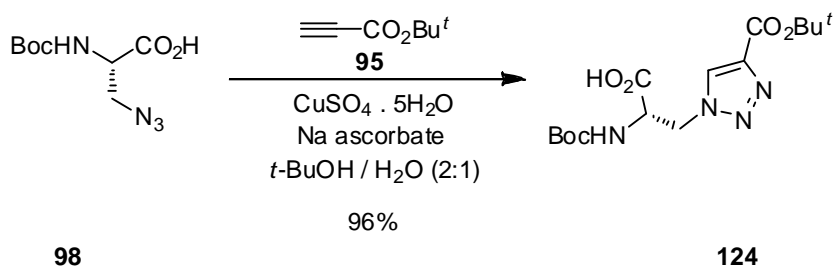
The reaction time ranged from 16 to 60 hours with yields of triazoles ranging from good (64%) to excellent (96%). Formation of the desired triazoles was indicated by the appearance in the ^{1}H NMR spectrum of a diagnostic aromatic triazole peak at *ca.* 7.50 ppm for compounds **125** and **126** and at *ca.* 8.04 ppm for compound **124**.

Scheme 3.18. Synthesis of 1,4-Triazoles **125, 126**

				Yield
94 R^1 = *t*-Bu	R^2 = H		**125**	85%
101 R^1 = Me	R^2 = CH$_2$Ph		(*S,S*)-**126**	64%
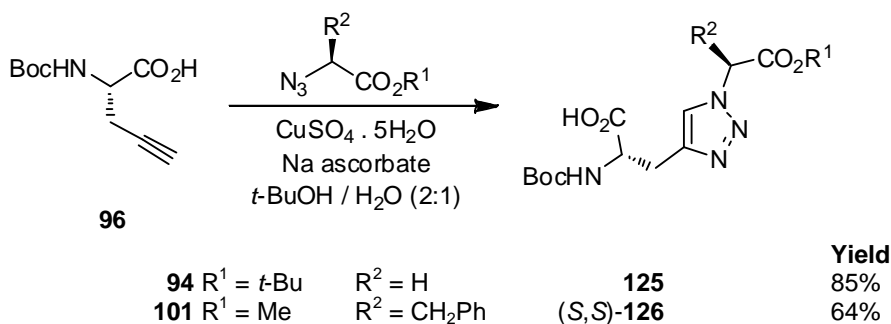
In pursuit of the 1,5-substituted triazoles obtainable by ruthenium catalysis, preparation of the most potent catalyst thus far reported, **108** from ruthenium compound **127** was attempted.[199,204] However, all attempts were unsuccessful (Scheme 3.19). This catalyst has the disadvantage that it must be freshly prepared each time it is required and cannot be stored.

Scheme 3.19. Attempted Preparation of Ruthenium Catalyst (**108**)

127 → **108**

No product isolated
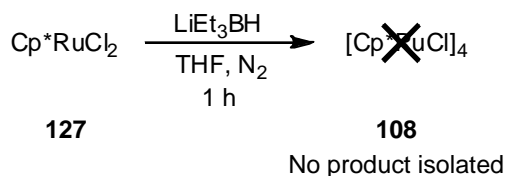
The literature procedure describes a colour change from orange to blue-green, however this was not observed.[204] One explanation is that excess oxygen in the reaction caused decomposition, though oxygen sensitivity has not been reported in the literature. Most likely the lithium triethylborohydride purchased from Aldrich was contaminated or not of sufficient concentration to enable the reaction to proceed. Owing to time constraints, synthesis of this particular catalyst was abandoned and the synthesis of ruthenium catalyst **109** pursued.

Ruthenium catalyst $Cp*Ru(PPh_3)_2Cl$ (**109**) was prepared from $Cp*RuCl_2$ (**127**) which was synthesized by another member of our research group, Dr. Daniel Pedersen (Scheme 3.20).[205] This catalyst has the advantage that, unlike the more potent catalyst **108**, it may be stored under an inert atmosphere for several weeks without significant decomposition occurring. Following Morandini *et al.*[205], the catalyst was obtained in moderate yield (49%) as a brick red / orange solid which was used without further analysis, as the catalyst is known to undergo decomposition in deuterated chloroform.

Scheme 3.20. Preparation of Ruthenium Catalyst (**109**)

$$Cp*RuCl_2 \xrightarrow[\substack{EtOH, \text{ reflux}, N_2 \\ 6\text{ h} \\ 49\%}]{PPh_3} Cp*Ru(PPh_3)_2Cl$$

127   **109**
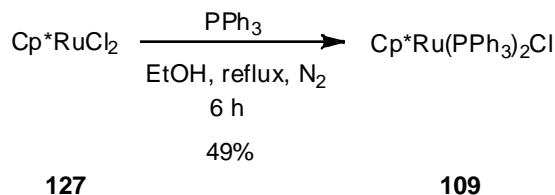
Unlike the copper-based chemistry, the ruthenium-catalysed reaction must be carried out under an inert atmosphere and under anhydrous reflux conditions. Initially, the reaction was attempted using azide **98** and alkyne **95**, as used for the copper-catalysed cycloaddition, but it was found that the ruthenium catalyst was sensitive to free carboxylic acid groups on the reaction substrates (Scheme 3.21). The presence of a carboxylic acid group (as in **98**), resulted in a complex mixture of products and signs of catalyst decomposition were evident (colour change from orange to brown). Although traces of the desired triazole product could be detected in the ^{1}H NMR, it was not possible to cleanly isolate the compound.

Scheme 3.21. Attempted Synthesis of 1,5-Triazole 111 (**128**)
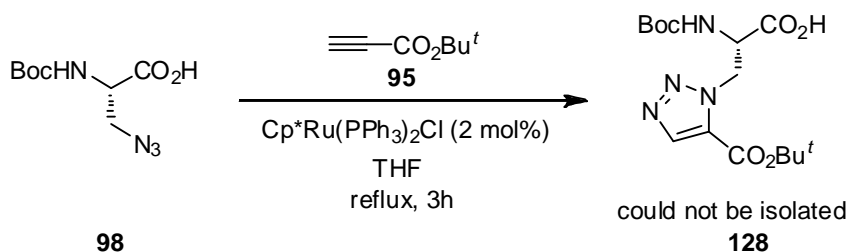
In order to avoid this, all carboxylic acid groups were protected as methyl esters. Thus, the reaction of azide **99** with alkyne **95** was carried out in refluxing anhydrous THF and using the ruthenium catalyst **109** at 2 mol% loading (Scheme 3.22). Though it has not been reported for this particular catalyst, organometallic ruthenium complexes are often sensitive to oxygen, which can oxidize the metal centre. Because of this, the THF was de-oxygenated by bubbling nitrogen through the solution just prior to use. The solution was heated at reflux for 3 hours and over the course of the reaction the colour of the solution changed from orange to brown indicating that the catalyst had undergone some decomposition. Following this, volatiles were removed *in vacuo* and the residue subjected to flash column chromatography. A second pass of column chromatography was necessary in order to remove all traces of brown-coloured ruthenium species. Protected 1,5-triazolyl amino acid **128** was obtained in low (33%) yield.

Scheme 3.22. Synthesis of 1,5-Triazole **128**
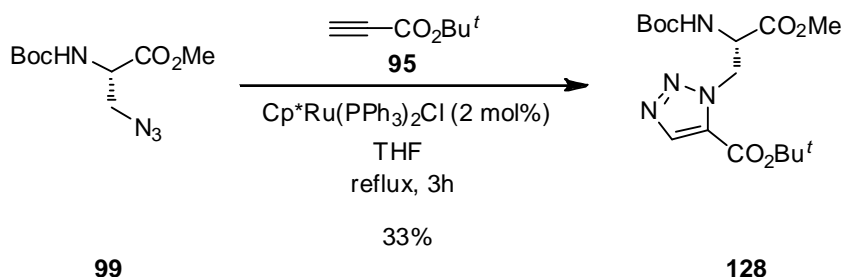
Employing the same methodology, azides **94** and **101** were allowed to react with alkyne **97** and the pure triazoles **129** and **130** were obtained in good yield (64% and 85% respectively) (Scheme 3.23). Formation of the desired triazoles was indicated by the appearance in the ^{1}H NMR spectrum of a diagnostic aromatic triazole peak at *ca.* 8.02 ppm for compound **128** and at *ca.* 7.50 ppm for compounds **129** and **130**.

Scheme 3.23. Synthesis of 1,5-Triazoles **129–130**

				Yield
94 R^1 = *t*-Bu	R^2 = H		(*S,S*)-**129**	85%
101 R^1 = Me	R^2 = CH$_2$Ph		(*S,S*)-**130**	64%
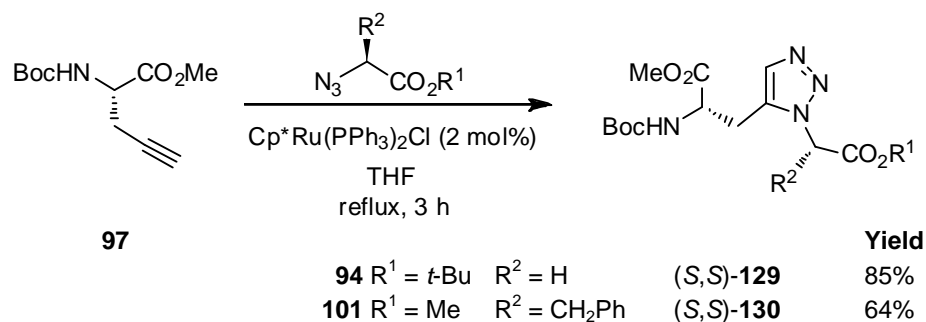
The methyl esters (**126**, **128**, **129** and **130**) were hydrolysed with LiOH. The reactions were stirred overnight at room temperature and the solvent removed *in vacuo* before being acidified with 1M HCl. The product was partitioned into ethyl acetate and solvents removed under vacuum to give the crude carboxylic acid. Traces of acetic acid formed during workup were removed azeotropically by repeated addition and removal *in vacuo* of benzene or toluene. The hydrolysis afforded the dicarboxylic acids **132** and **131** in excellent (96%) and quantitative yields, respectively (Schemes 3.24–3.27). It should be noted that the compounds **128** and **129** contained a *t*-butyl ester which resulted in a mixture of hydrolysis products, since the *t*-butyl ester group was partially hydrolysed during workup. These compounds were isolated as a mix of di-carboxylic acid and *t*-butyl ester (**133a,b** and **134a,b**, respectively) and were carried to the next deprotection step without further purification.

Scheme 3.24. Synthesis of Diacid **131**
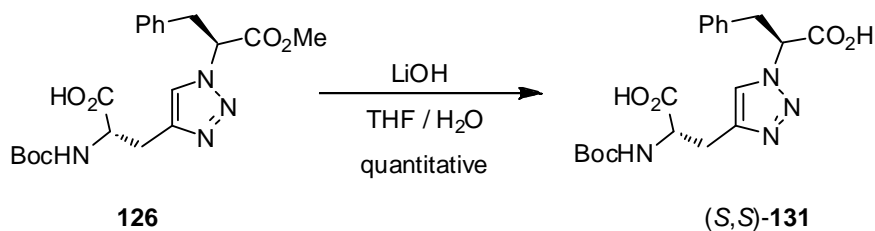
Scheme 3.25. Synthesis of Diacid **132**

$$130 \xrightarrow[\substack{\text{THF / H}_2\text{O} \\ 96\%}]{\text{LiOH}} (S,S)\text{-}132$$
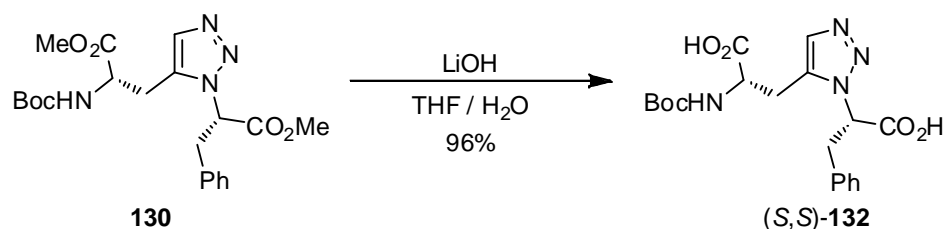
Scheme 3.26. Synthesis of Diacids **133a,b**

128

LiOH

THF / H₂O

quantitative

133a: R = H
133b: R = t-Bu
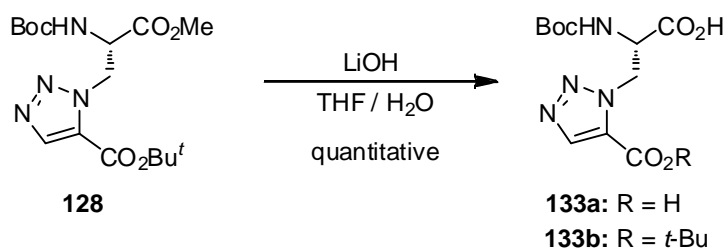
Scheme 3.27. Synthesis of Diacids **134a,b**

129

LiOH

THF / H₂O

65%

134a: R = H
134b: R = t-Bu
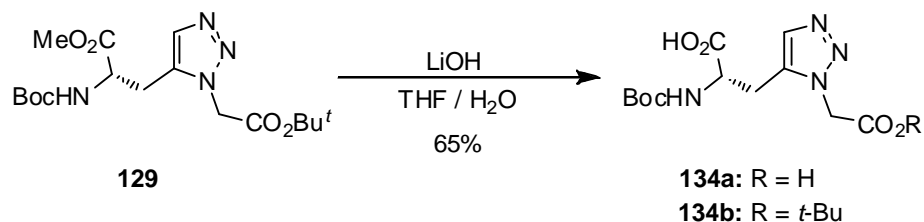
Deprotection of the amine and hydrolysis of the *t*-butyl ester was carried out under acidic conditions (Schemes 3.28−3.33). Triazole **124** was stirred at room temperature in 1,4-dioxane with 6M HCl (2:1) for 16 hours. Volatiles were removed under high vacuum and the residue washed with ethyl acetate and dichloromethane. Any traces of residual water and HCl were removed azeotropically by repeated addition and removal *in vacuo* of benzene and toluene. The residue was dried overnight under high vacuum to afford the final amino acid which was obtained as hydrochloride salt **45a** in quantitative yield. Following the same procedure, triazole **125** was hydrolysed to give hydrochloride salt **46a** in quantitative yield, triazole **126** was hydrolysed to give hydrochloride salt **47a** in quantitative yield, triazoles **133a** and **133b** were hydrolysed to give hydrochloride salt **48a** in quantitative yield, triazoles **134a and 134b** were hydrolysed to give hydrochloride salt **49a** in 90% yield over two steps and finally, triazole **132** was hydrolysed to give hydrochloride salt **50a** in 92% yield. Most of the hydrochloride salts

were extremely difficult to handle as they were very hygroscopic. Thorough drying under high vacuum provided dry solid material to allow yield determination. However, even after a few minutes in the air, the compounds became gummy as they absorbed water from the air, thus thorough characterisation was not attempted.

Scheme 3.28. Synthesis of Triazole Amino Acid **45a**
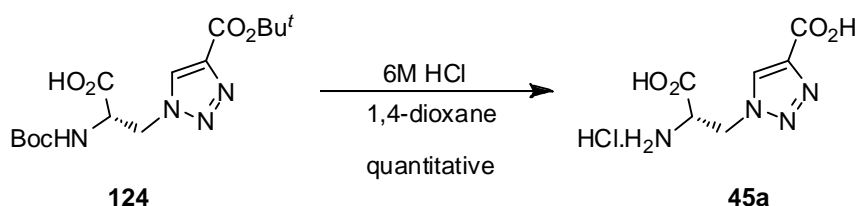
Scheme 3.29. Synthesis of Triazole Amino Acid **46a**
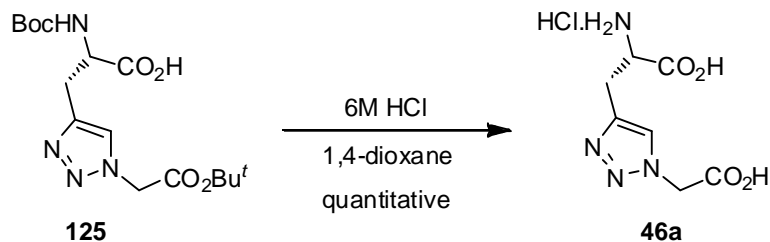
Scheme 3.30. Synthesis of Triazole Amino Acid **47a**
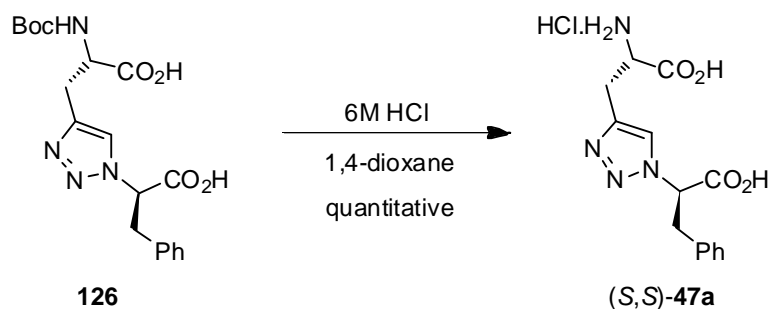
Scheme 3.31. Synthesis of Triazole Amino Acid **48a**
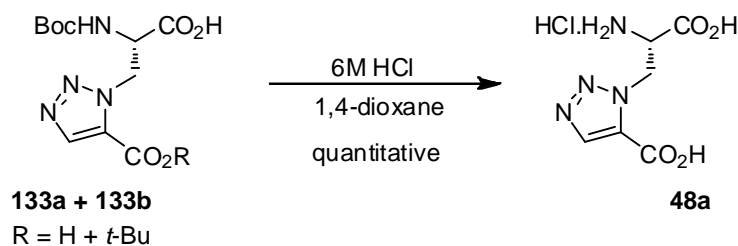
Scheme 3.32. Synthesis of Triazole Amino Acid **49a**

134a + 134b
R = H + *t*-Bu

49a
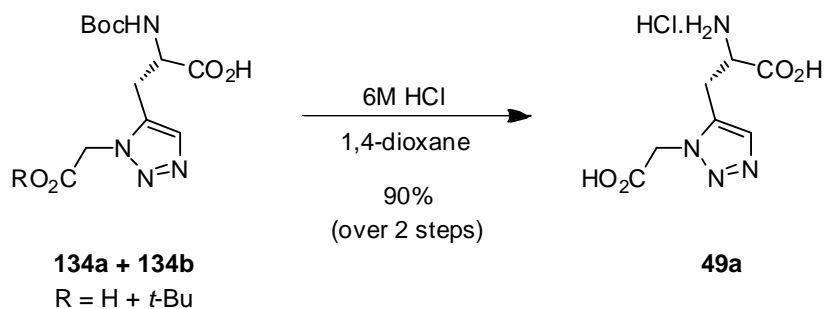
Scheme 3.33. Synthesis of Triazole Amino Acid **50a**

132

(*S,S*)-**50a**
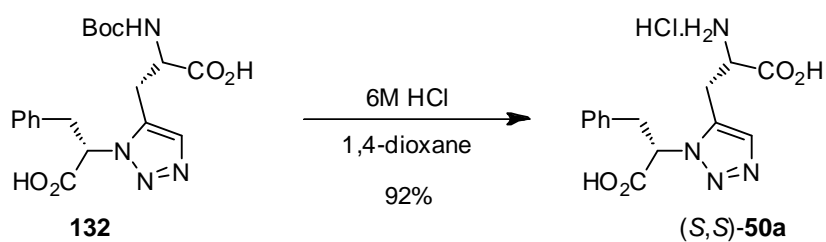
3.5 Summary

A series of six 1,4- and 1,5-triazole amino acids were synthesized utilizing both copper (I) and ruthenium catalysis. These compounds were obtained as the hydrochloride salts in good yields from the starting azides and alkynes. Subsequent *in vitro* receptor binding assays and *in silico* docking simulations are discussed in Chapters 4 and 5 respectively.

Chapter 4 : Pharmacology

4.1 Pharmacological Testing

With the cyclopropane and triazole amino acids in hand, it was necessary to determine their biological activity. This was accomplished by our collaborators at the University of Copenhagen, where *in vitro* glutamate receptor binding assays were carried out. It was desirable that the compounds be active only at the metabotropic receptor class, as opposed to the ionotropic glutamate receptors. The reason for this is that competitive metabotropic ligands show promise as potential neuropathic pain therapeutics,[52,54,78,206] whereas ionotropic ligands have been associated with lack of efficacy and unwanted side effects.[32,35]

Based on comparison with previously tested compounds, the cyclopropane amino acids were predicted to be active at metabotropic glutamate receptor 2 (mGluR2).[121,122] Research has made it clear that it is desirable for mGluR2 ligands to show agonist activity in order to effectively alleviate neuropathic pain symptoms.[17,52,54,71,207] As such, antagonists of this receptor would be excluded from *in vivo* testing. Antagonists at mGluR1 were also desirable, as studies have also shown their potential therapeutic benefit.[53,54,208] Any compounds showing activity at ionotropic receptors were also excluded from *in vivo* testing. Only compounds having EC_{50} values less than 10 μM would be considered for further study *in vivo* and compounds with EC_{50} greater than 100 μM were considered inactive.

The cyclopropane amino acid **44a** showed potent and selective activity in the *in vitro* binding assays. Based on this, **44a** was then tested *in vivo* in a neuropathic pain model, the chronic constriction injury of the sciatic nerve in Sprague-Dawley rats. Von Frey filaments were employed in order to test for neuropathic pain, as observed through the presence of mechanical allodynia. During this testing procedure, fine filaments of increasing diameter and bending force are touched to the underside of the hind paw until the animal shows a withdrawal response.

4.2 *In Vitro* Studies

The *in vitro* binding assays were performed by our collaborators at the University of Copenhagen according to the following methodology. The ionotropic assays measured the displacement of selective radio-labelled ligands from each of the sub-types, NMDA, AMPA and kainate, expressed natively in rat brain homogenates. This assay does not provide any insight into whether the compound is blocking or activating the receptors, but simply indicates the binding affinity. The metabotropic receptor assays, however, were functional assays, enabling the assessment of agonist or antagonist activity by measurement of concentrations of the second messengers cyclic AMP (cAMP) and inositol phosphates. Because of this, it is necessary to use recombinant receptors where a single receptor sub-type is expressed in a cell expressing no other similar receptors. Here, Chinese hamster ovary (CHO) cells were employed so as to provide a clear measurement of changes to inter-cellular cAMP and inositol second messenger concentrations and thus determine ligand activity.

4.2.1 Binding assays at native iGlu receptors
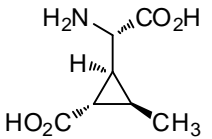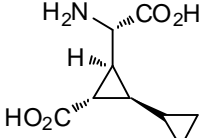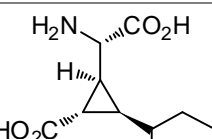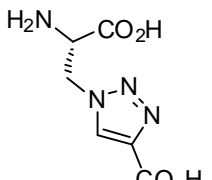
All binding assays were performed using rat brain synaptic membranes of cortex and the central hemispheres from adult male Sprague-Dawley rats with tissue preparation as earlier described.[209] Affinities for native AMPA, KAIN and NMDA receptors were determined using 5 nM [^{3}H]AMPA,[210] 5 nM [^{3}H]KAIN,[211] and 2 nM [^{3}H]CGP39653[212] with some modifications. On the day of experiments, frozen membranes were quickly thawed and homogenised in 40 volumes of ice-cold buffer (pH 7.4) (30 mM Tris-HCl containing 2.5 mM $CaCl_2$, 50 mM Tris-HCl, or 50 mM Tris-HCl containing 2.5 mM $CaCl_2$, for [^{3}H]AMPA, [^{3}H]KAIN, or [^{3}H]CGP39653 binding, respectively), and centrifuged ($48,000 \times g$ for 10 min). This step was repeated four times. In [^{3}H]AMPA binding experiments, 100 mM KSCN was added to the buffer during the final wash and during incubation. The final pellet was re-suspended in ice-cold buffer, corresponding to approx. 0.4–0.5 mg protein/mL. [^{3}H]AMPA, [^{3}H]KAIN, and [^{3}H]CGP39653 binding were carried out in aliquots consisting of 25 μL [^{3}H]ligand, 25 μL test solution, and 200 μL membrane suspension and incubated for 30 min, 60 min, and 60 min, respectively. Binding was terminated by filtration through GF/B filters using a 96-well Packard Filter-Mate Cell Harvester and washing with 3×250 μL buffer. After drying, 25 μL
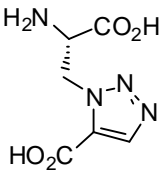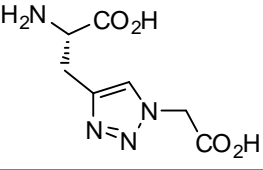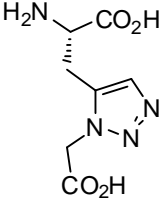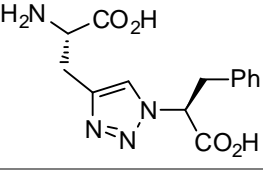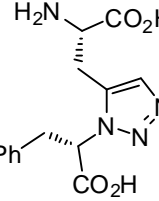
Microscint 0 (Perkin-Elmer) per well was added and the plate was counted on a Topcounter (Perkin-Elmer). Non-specific binding was determined using 1 mM (*S*)-Glu. The Bradford[213] protein assay was used for protein determination using bovine serum albumin as a standard, according to the protocol of the supplier (Bio-Rad, Milan, Italy).

4.2.2 Results

As shown in Table 4.1, *in vitro* drug screening at NMDA, kainate and AMPA ionotropic glutamate receptor subtypes revealed activity of compound **45** with an EC_{50} value of 63 µM and compound **48** with an EC_{50} value of 49 µM at AMPA receptors. All other compounds were inactive at all of the tested ionotropic receptor subtypes as indicated by IC_{50} / K_i > 100 µM.

Table 4.1. Ionotropic Glutamate Receptor Binding Data

	Structure	[^{3}H]AMPA	[^{3}H]Kainate	[^{3}H]CGP39653 (NMDA)
		IC_{50} (µM)	IC_{50} (µM)	K_i (µM)
Methyl (negative control)		> 100	> 100	> 100
44a		> 100	> 100	> 100
44d		> 100	> 100	> 100
45		63 [54;74]*	> 100	> 100

#	Structure			
48	H$_2$N, CO$_2$H triazole, HO$_2$C	49 [44;55]*	> 100	> 100
46	H$_2$N, CO$_2$H triazole, CO$_2$H	> 100	> 100	> 100
49	H$_2$N, CO$_2$H triazole, CO$_2$H	> 100	> 100	> 100
47	H$_2$N, CO$_2$H triazole, Ph, CO$_2$H	> 100	> 100	> 100
50	H$_2$N, CO$_2$H triazole, Ph, CO$_2$H	> 100	> 100	> 100

Values are expressed as the antilog to the log mean of three-four individual experiments.

*Numbers in brackets indicate maximum and minimum SEM.

4.2.3 Binding assays at recombinant mGlu receptors

Cell Culture

The Chinese hamster ovary (CHO) cell lines stably expressing mGlu1α, mGlu2 and mGlu4a receptors have previously been described.[214,215] Cell cultures were maintained at 37 °C in a humidified 5% CO$_2$ incubator in Dulbecco's Modified Eagle Medium (DMEM) containing a reduced concentration of (S)-glutamine (2 mM) and supplemented with 1% proline, penicillin (100 U/mL), streptomycin (100 mg/mL), and 10% dialyzed foetal calf serum (all GIBCO, Paisley, Scotland). For phosphatidylinositol 4,5-biphosphate hydrolysis assays, 1.8×10^6 cells were divided into the wells of 48 well

plates 2 days before assay. For cyclic AMP assays, 1×10^6 cells were divided into the wells of 96 well plates 2 days before assay.

Second Messenger Assays

Phosphatidylinositol 4,5-biphosphate hydrolysis was measured as described previously.[109,216] Briefly, the cells were labelled with [^{3}H]-inositol (2 μCi/mL) 24 h prior to the assay. For agonist assays, the cells were incubated with ligand dissolved in phosphate buffered saline (PBS)–LiCl for 20 min, and agonist activity was determined by measurement of the level of [^{3}H]-labelled mono-, bis- and tris-inositol phosphates by ion-exchange chromatography. For antagonist assays, the cells were pre-incubated with the ligand dissolved in PBS–LiCl for 20 min prior to incubation with ligand and 20 μM (S)-Glu for 20 min. The antagonist activity was then determined as the inhibitory effect of the (S)-Glu-mediated response. The assay of cyclic AMP formation was performed as described previously.[109,216] Briefly, the cells were incubated for 10 min in PBS containing the ligand and 10 μM forskolin and 1 mM 3-isobutyl-1-methylxanthine (IBMX) (both Sigma, St. Louis, MO). The agonist activity was then determined as the inhibitory effect of the forskolin-induced cyclic AMP formation. For antagonist assay, the cells were pre-incubated with ligand dissolved in PBS containing 1 mM IBMX for 20 min prior to a 10 min incubation in PBS containing the ligand, 30 μM (S)-Glu, 10 μM forskolin, and 1 mM IBMX.

Data Analysis
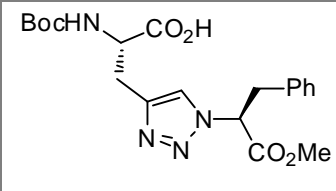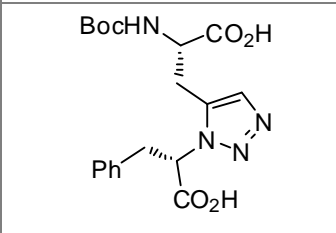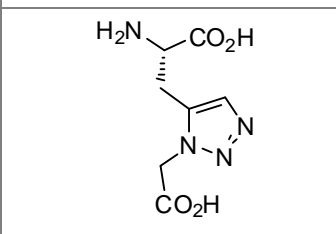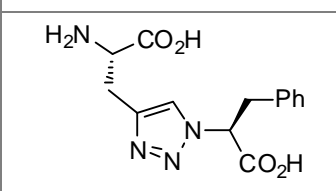
All experiments were performed in triplicate and the results are given as mean ± S.E.M. of at least two independent experiments. Antagonist potencies were calculated from inhibition curves using the 'functional equivalent' of the Cheng–Prusoff equation; $K_b = IC_{50} / (1 + ([A]/EC_{50}))$, where IC_{50} is the concentration of antagonist required to reduce the response to 50% of the maximal response, EC_{50} is the concentration of agonist which elicits 50% of the maximal response, and [A] is the fixed concentration of the agonist.[217]

4.2.4 Results

As shown in Table 4.2, compound **44a** was found to be an agonist at mGluR2 with an EC_{50} of 0.05 µM, whilst compound **44d** was found to be a weak antagonist at mGluR2 with an IC_{50} of 62 µM. All other assayed compounds were found to be inactive at the tested receptor subtypes ($EC_{50} > 100$ µM).

Table 4.2. Metabotropic Glutamate Receptor Binding Data

Compound	Structure	mGluR1	mGluR2	mGluR4
43 Methyl (positive control)		> 100	0.01	> 100
44a		> 100	0.05	> 100
44d		> 100	**62**	> 100
125		> 100	> 100	> 100
45		> 100	> 100	> 100
46		> 100	> 100	> 100

126		> 100	> 100	> 100
132		> 100	> 100	> 100
49		> 100	> 100	> 100
47		> 100	> 100	> 100

[a]Plain and bold text refer to agonist and antagonist potencies in μM, respectively.

4.3 *In Vivo* Studies

The *in vivo* drug testing in an animal model of neuropathic pain was performed in the Discipline of Pharmacology, University of Adelaide with the help of Dr. Mark Hutchinson.

4.3.1 Animals

Experiments were carried out on 12 male, pathogen-free Sprague-Dawley rats (325−500g) housed in groups of three per cage. Rats were given free access to food and water and maintained on a controlled 12/12 hour light/dark cycle with lights on at 0700 h.

4.3.2 Ethics

Ethical approval was obtained from the University of Adelaide Animal Ethics Committee for all animal tests and manipulations and care was taken to minimize the extent of suffering and duration of pain, where doing so would not interfere with the project. All experimental work involving animals abided by the guidelines found in the Australian Code of Practise for the Care and Use of Animals for Scientific Purposes.

4.3.3 Drugs

The test compound (±) (1*R*,2*S*,3*S*)-3-[(*S*)-amino(carboxy)methyl]-1,1'-bi(cyclopropyl)-2-carboxylic acid (**44a**) was synthesized in the Discipline of Chemistry, University of Adelaide and the positive control (2*R*,4*R*)-aminopyrrolidine-2,4-dicarboxylate (APDC) was purchased from Tocris Bioscience (Bristol, UK). Both drugs were administered intrathecally, compound **44a** as a suspension (500 nmols) or solution (50 and 250 nmols) and APDC as a solution in Milli-Q water containing 12 mM HCl. The method of acute intrathecal (i.t.) drug administration was based on that described previously.[218] Briefly, intrathecal operations were conducted under isoflurane anaesthesia (Phoenix Pharmaceuticals, St Joseph, MO, USA) by threading sterile polyethylene-10 tubing (PE-10 Intramedic Tubing; Becton Dickinson Primary Care Diagnostics, Sparks, MD, USA) guided by an 18-gauge needle between the L5 and L6 vertebrae. The catheter was inserted such that the proximal catheter tip lay over the lumbosacral enlargement. The catheters were pre-loaded with drugs at the distal end in a total volume of no greater than 25 μL and delivered over 20–30 s once the catheter was in position. The catheters were 17 cm in length, and were attached to a pre-loaded Hamilton syringe.

4.3.4 Chronic Constriction Injury (CCI)

Neuropathic pain was induced using the chronic constriction injury (CCI) model of partial sciatic nerve injury.[219] CCI was performed at the mid-thigh level of the left hind leg as previously described.[220] Animals were anesthetized with isoflurane. The shaved skin was treated with ethanol to cleanse and the surgery was aseptically performed. Animals were monitored post-operatively until fully ambulatory prior to return to their home cage, and checked daily for any sign of infection. No such cases occurred in this study. In brief, four sterile chromic gut sutures (cuticular 4-0 chromic gut, FS-2;

Ethicon, Somerville, NJ, USA) were loosely tied around the gently isolated sciatic nerve. Drug testing was delayed until 16 days after surgery to ensure that neuropathic pain was well established prior to the initiation of drug delivery.

4.3.5 Von Frey Testing

All testing was conducted blind with respect to group assignment. Rats received at least three 60-min habituations to the test environment prior to behavioural testing. The von Frey test[221] was performed within the sciatic innervation region of the hind paws as previously described in detail.[222,223] Assessments were made prior to (baseline) and at 1 and 3 hours after intrathecal (i.t.) drug dosing. A logarithmic series of 10 calibrated Semmes-Weinstein monofilaments (von Frey hairs; Stoelting, Wood Dale, IL, USA) was applied randomly to the left and right hind paws to define the threshold stimulus intensity required to elicit a paw withdrawal response. Log stiffness of the hairs was determined by $\log_{10}$ (milligrams $\times$ 10) and ranged from 3.61 (4.07 g) to 5.18 (15.136 g). The behavioural responses were used to calculate absolute threshold (the 50% paw withdrawal threshold) by fitting a Gaussian integral psychometric function using a maximum likelihood fitting method,[224] as described in detail previously.[223,225] This fitting method allows parametric analyses that otherwise would not be appropriate.[223,225]

4.3.6 Data Analysis

All data is reported as mean $\pm$ SEM. Von Frey data was analysed as the interpolated 50% thresholds (absolute threshold) in log base 10 of stimulus intensity (monofilament stiffness in milligrams $\times$ 10). Pre-drug baseline measures were analysed by one-way ANOVA. Post drug time course measures were analysed by repeated measures two-way ANOVAs followed by Bonferroni post hoc tests. The three hour time point data was compared to vehicle by one-way ANOVA followed by Dunnett's *t* test post hoc. Where appropriate, $P < 0.05$ was considered statistically significant.

4.3.7 Results
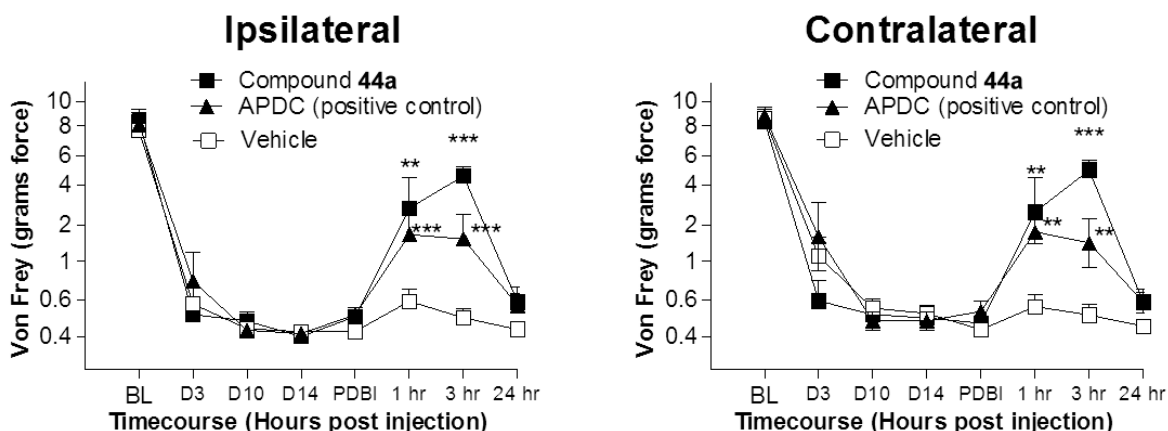
Figure 4.1. Effects of an acute dose of compound **44a** (500 nmols i.t.) and a positive control, APDC (500 nmols i.t.) on mechanical allodynia following chronic constriction injury of the sciatic nerve in Sprague-Dawley rats. Data are expressed as mean $\pm$ SEM, n = 6. BL = baseline, PDBl = pre-drug baseline. **P < 0.01, ***P < 0.001 compared to vehicle.

Illustrated in Figure 4.1, prior to surgery, all animals responded only at a bending force of about 9.0 g, both ipsilaterally and contralaterally as indicated at baseline (BL). Following surgery, subsequent von Frey testing on days 3, 10 and 14 revealed a decrease in response threshold to about 0.4 g bending force for both sides, indicating that all animals were allodynic. On the day of drug dosing, a pre-drug baseline (PDBl) measurement was also made to ensure the reliability of inter-day test results. One hour after an intrathecal dose of (2R,4R)-APDC, von Frey response thresholds were significantly increased up to about 1.6 g bending force on both sides, compared to animals receiving vehicle. Three hours after drug dosing, response thresholds were similar to the one hour post-drug time point at 1.5 g bending force. One hour after an intrathecal dose of compound **44a**, von Frey response thresholds of drug-treated animals were significantly increased up to about 3.0 g bending force on both sides, compared to animals receiving vehicle. Three hours after drug dosing, von Frey response thresholds of drug-treated animals were significantly increased up to about 5.0 g bending force on both sides, compared to animals receiving vehicle. After 24 hours, all animals had returned to responding to a bending force of 0.6 g, with positive control and drug-

treated animals no longer significantly different from vehicle-treated controls. No other behavioural effects of either drug were noted except very slight sedation.

Mechanical Thresholds
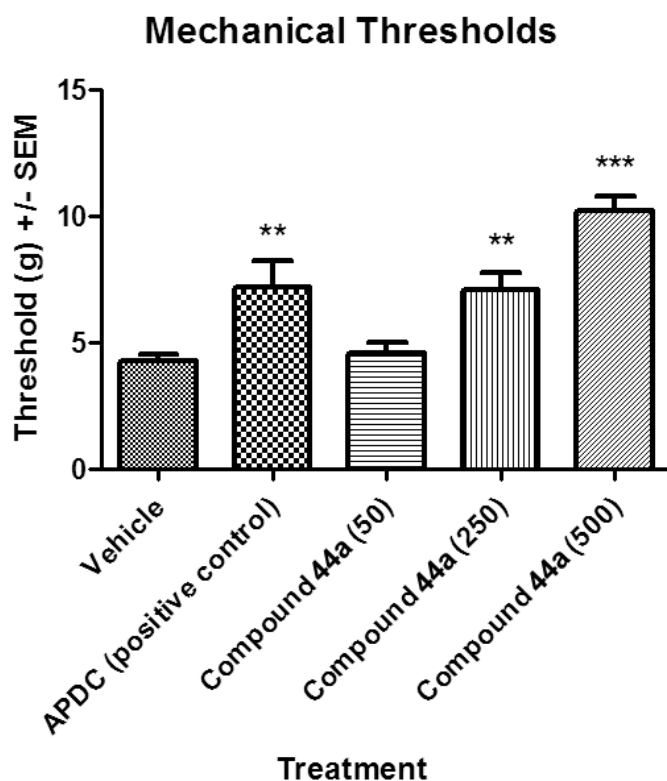
Figure 4.2. Comparison of the changes in mechanical threshold three hours after intrathecal administration of (2*R*,4*R*)-APDC (500 nmols), compound **44a** (50, 250 and 500 nmols) or vehicle. Data expressed in grams ± SEM, n = 6. **P < 0.01, ***P < 0.001 compared to vehicle.

In order to investigate any possible dose dependency of the anti-allodynic effect of **44a**, two lower doses, 50 nmols and 250 nmols, were also administered. For clarity, only the data relating to the three hour time point is shown in Figure 4.2. The data strongly indicated a dose dependency of compound **44a** with 50 nmols causing an increase in response threshold to 5.0 g, 250 nmols causing a significant increase to 7.5 g and 500 nmols causing a significant increase in response threshold to 10.0 g compared to vehicle.

4.4 Discussion

In Vitro Binding Assays

Referring to Table 4.1, the data obtained from the competitive binding assays at the ionotropic glutamate receptors indicates that only two compounds exhibited any bioactivity. Triazole amino acid **45** bound to the AMPA receptor with an IC_{50} of 63 μM and triazole **48** also bound to the AMPA receptor, but with an IC_{50} of 49 μM; these values indicate only weak activity. This is an interesting outcome considering the structural similarities between these compounds and some known ligands of these receptors. However, in order for the compounds to be potential candidates as neuropathic pain drugs, they must not be agonists at any of the iGluRs, as activation of these receptors is pro-nociceptive.[206] It also must be noted that the assays used cannot indicate agonist or antagonist activity of the active compounds **45** and **48**.

Referring to Table 4.2, the data obtained from functional assays at the metabotropic glutamate receptors indicates that only two of the new compounds exhibited any bioactivity. The second messenger assays to measure mGluR2 activity involved the radioimmunoassay detection of forskolin-stimulated cAMP concentrations. Agonists caused a decrease in cAMP, whereas antagonist activity was measured in the presence of the endogenous agonist, glutamate and indicated as an increase in cAMP levels. The methyl-substituted cyclopropyl amino acid was used as a positive control and had a measured EC_{50} value of 0.01 μM at mGluR2, which is comparable to, though slightly higher than, that reported previously by Collado *et al.*[55] Test compound **44a** showed agonist activity at mGluR2 which was approximately five-fold lower than the positive control, with a measured EC_{50} of 0.05 μM. Overall, the *in vitro* data indicates that compound **44a** is quite potent and is also selective for mGluR2 over mGluR1 and mGluR4 as well as having no activity at the ionotropic receptors. This made cyclopropyl amino acid **44a** a good candidate for further investigation *in vivo*. Finally, test compound **44d** showed weak antagonist activity at mGluR2 with an EC_{50} of 62 μM. The *in vitro* assays confirm the initial hypothesis where it was expected that the small ring size, as in compound **44a** would provide an agonist, whereas the large ring size, as in compound **44d**, would provide an antagonist. Compound **44a** is structurally quite similar to the positive control, however the cyclopropyl-substitution is slightly more bulky than a simple methyl group, which may account for the loss of potency. On the

other hand, compound **44d** is substituted with a comparatively bulky cyclohexyl group which seems to convey antagonist activity. Substitution by other bulky, hydrophobic groups, such as phenyl and xanthenyl has been reported previously to consistently produce receptor antagonists, thus this result is hardly surprising.[119,124] It was only possible to test the compounds at three of the eight sub-types of the metabotropic glutamate receptors; mGluR1, mGluR2 and mGluR4, representing the three groups of receptors. It's possible that these compounds may have also shown some activity at the five receptor sub-types which were not investigated; mGluR3, mGluR5, mGluR6, mGluR7 and mGluR8.

In Vivo Testing

Finally, work was carried out to ascertain the *in vivo* effects of the novel, selective Group II metabotropic glutamate receptor (mGluR) agonist **44a** in a rodent model of neuropathic pain. The model employed in this study was chronic constriction of the sciatic nerve, where the nerve bundle undergoes loose ligation with chromic gut at the mid-thigh level. The outcome is a neuropathic pain state that develops over a period of two weeks and persists for months thereafter.[219] This model results in reliably measurable allodynia which resembles that reported and measured in human neuropathic pain states.[219] Although the surgery manipulates the sciatic nerve on only one side of the animal, allodynia develops on both the operated side (ipsilateral) and the non-operated side (contralateral) as can be seen in Figure 4.1.[226] This phenomena is known as mirror-image allodynia and there is mounting evidence to suggest that it is caused by glial activation and the associated action of pro-inflammatory cytokines.[227-229]

Due to a lack of test compound, it was opted to administer the drugs via the intrathecal route, by lumbar puncture between the L5 and L6 vertebrae. Drugs that act at the spinal level have the advantage of avoiding CNS side effects and offer the possibility of chronic administration via an indwelling catheter in a chronic pain setting. However, Jones and colleagues have identified the potential for development of therapeutic tolerance to mGluR agonists upon repeated dosing, which could potentially limit their effectiveness as therapeutics.[230] Intrathecal administration also confines drug action to the spinal dorsal horn and thus limits the possible mechanisms responsible for drug effects, thus simplifying interpretation of the data obtained.

Although only *in vitro* receptor binding data relating to mGlu2 receptors was obtained, it is reasonable to assert that compound **44a** would also activate mGlu3 receptors, given that all known ligands in this compound class are approximately equipotent at mGluR2 and R3.[121,122] It is widely reported that agonists at these receptors can significantly decrease the behavioural signs associated with neuropathic pain, including thermal and mechanical hyperalgesia and mechanical allodynia.[52,54,206] The intrathecal route of drug administration employed in this study distributes the drug in the region of the dorsal horn of the spinal cord and so it is in this region that the test compounds are eliciting their pharmacological action. Several *in situ* hybridization studies have identified mRNA encoding for the mGlu3 receptor in the spinal dorsal horn, however, levels of mRNA encoding for the mGlu2 receptor were found to be very low.[207,231] Jia and co-workers used light and electron microscopic immunocytochemistry to show the presence of mGluR2/R3 in the inner part of lamina II and also the presence of these receptors pre-synaptically on GABAergic neurons within the dorsal horn.[79] These results were confirmed by Azkue and colleagues using an immunogold technique.[80] Finally, both Gerber *et al.* and Carlton *et al.* have provided evidence that mGlu2 and 3 receptors were also located pre-synaptically on glutamatergic primary afferent neurons within the dorsal horn.[207,232] The involvement of mGlu2 and 3 receptors on sensory transmission within the dorsal horn has been verified by a number of studies, including work by Dolan and Nolan, who showed an increase in mechanical nociception threshold in sheep after intrathecal administration of the selective Group II agonist, L-CCG-I.[233] The known selective Group II mGluR agonist, (2*R*,4*R*)-APDC, here used as a positive control, has previously been shown by Fisher and co-workers to prevent the development of mechanical allodynia, following loose ligation of the sciatic nerve chronic constriction injury, and using a repeated intrathecal dosing regime.[54] Similarly, we observed that this compound is capable of producing a significant reversal of mechanical allodynia with the greatest effect apparent at the 1 hour time point. There was no possibility to use receptor antagonism to verify that the anti-allodynic effects observed were indeed due to Group II mGluR activation, as receptor blockade would be pro-nociceptive, which was undesirable.[71]

Referring to Figure 4.1, the test compound **44a** was found to have greater *in vivo* anti-allodynic activity than the positive control, (2*R*,4*R*)-APDC. This result was expected given the EC$_{50}$ value of amino acid **44a** at mGluR2 is 8 times higher, indicating the

higher *in vitro* potency of **44a**. Interestingly, the effects on withdrawal threshold were maximal for test drug **44a** when measured at the 3 hour time point, compared to 1 hour post drug dosing for the positive control, (2*R*,4*R*)-APDC. This observation is difficult to explain, apart from potential differences in the polarizability and lipophilicity of the two compounds, which may have affected their distribution and absorption. Slight sedation was noted after both test drug and positive control treatment, an effect which has not been reported previously. Generally, metabotropic glutamate receptor ligands are reported to not produce sedation, thus further investigation is needed to verify that this effect was, in actual fact, drug related.[52,54]

Endogenous glutamate within the dorsal horn is known to act pro-nociceptively on glutamatergic neurons which project to the brain stem and higher brain centres.[234] Hence, pre-synaptic modulation of these projecting neurons is capable of attenuating pain signalling. Since mGluR2 and R3 have been identified on glutamatergic primary afferent neurons, it is reasonable to assume that mGluR2/R3 ligands could modulate signalling in these projecting neurons, thus resulting in anti-nociception (See Figure 4.3).[207,232]

It is well known that there exists descending inhibitory pathways which serve to dampen and attenuate pain signalling at the spinal dorsal horn level.[6] Research by Zhou and colleagues has highlighted the action of endogenous glutamate, acting by stimulation of Group II mGluRs in the spinal dorsal horn, in causing a decrease in GABAergic neuron activity and a subsequent decrease in GABA inhibition due to nociceptive input.[235] Their data suggests that GABA inhibition in the dorsal horn is anti-nociceptive and hence is evidence for disinhibition of descending anti-nociceptive neurons which would result in analgesia (See Figure 4.3).

Referring to Figure 4.3, metabotropic glutamate receptors 2 and 3 have been identified both on glutamatergic primary afferent neurons and GABAergic axon terminals. Binding to excitatory glutamatergic neurons would result in decreased ascending nerve transmission via ascending projecting neurons, whereas binding to inhibitory GABAergic neurons likely causes disinhibition of descending inhibitory neurons. Thus, these tandem mechanisms are partly responsible for the observed reversal of mechanical allodynia.

Figure 4.3. Neuronal and Glial Pathways in the Spinal Dorsal Horn
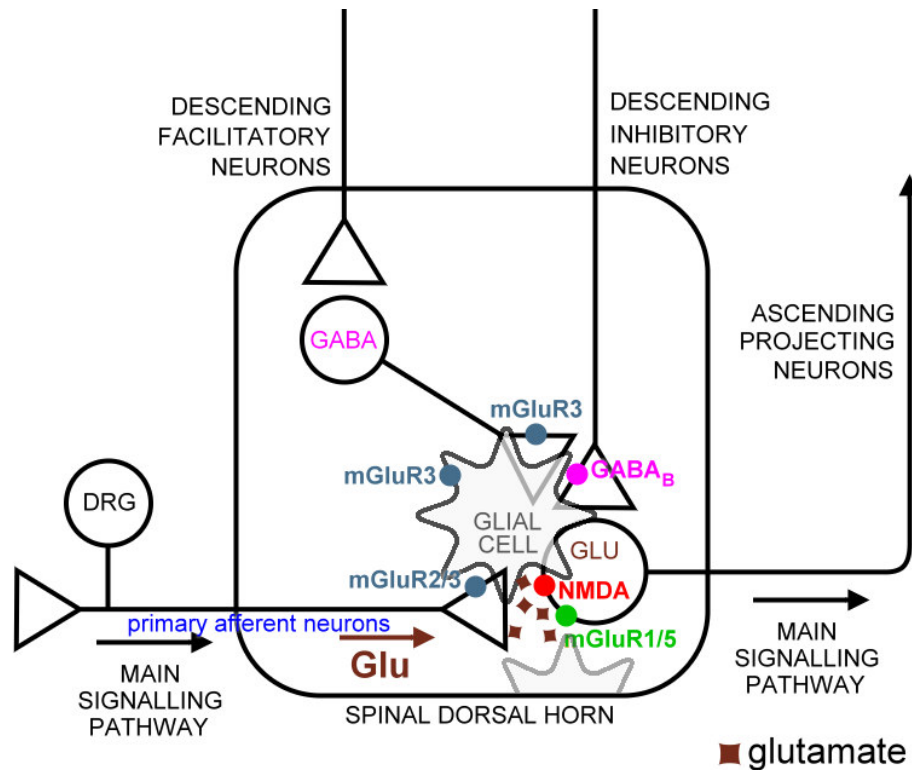
Involvement of Glial Cells

Glial cells are also known to be present in the spinal dorsal horn and much accumulating evidence points to the presence of mGluR3 receptors on glia.[79,80,236-238] Recent research has demonstrated the important contribution of glial cell activation and consequent changes to glial and neuronal signalling to the development and maintenance of neuropathic pain.[42,226-229,239] Considering this, it is essential that the mechanism of action of any new pharmacological agent be discussed, not only in terms of possible neuronal actions, but also in light of its potential effects on glial cells.

Illustrated as a simplified schematic in Figure 4.4, glial cell activation leads to increased release of pro-inflammatory cytokines such as tumour necrosis factor alpha (TNFα), interleukin 1 beta (IL-1β) and interleukin 6 (IL-6).[239] It has been shown that levels of pro-inflammatory cytokines are increased both centrally and spinally due to chronic constriction injury of the sciatic nerve.[240,241] These cytokines cause inflammation responses that result in changes to nerve signalling function which contributes to the

allodynia and hyperalgesia which is evident in the neuropathic pain state.[41,242] Not only this, but under these circumstances, neurons can release fractalkine, which creates a positive feedback loop by binding to fractalkine receptors on glia and further increasing release of pro-inflammatory cytokines.[226] The activation of Group II metabotropic glutamate receptors has been demonstrated to modulate glial cell activation and play a role in alterations to levels of pro-inflammatory cytokines.[44,243]

Figure 4.4. Changes to Glial Cell Function and Neuronal Excitability Due to Nerve Damage
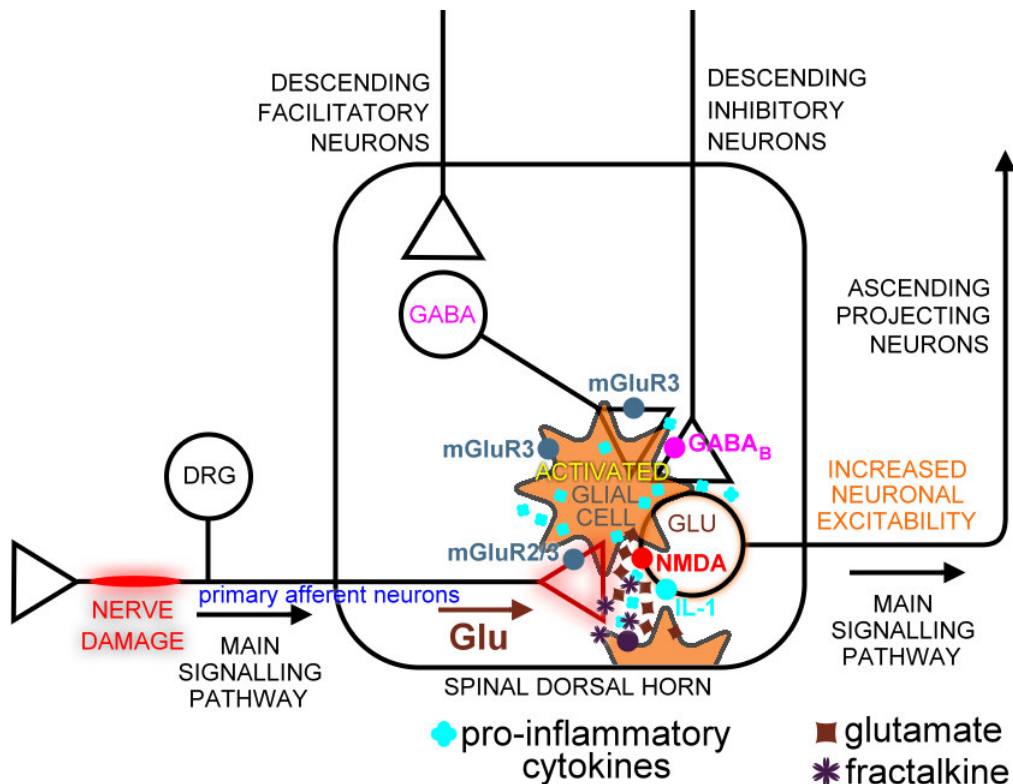
Further evidence to support this hypothesis regards the activation of glia and release of cytokines induced by morphine.[244] It is by this mechanism that chronic opioid administration is now believed to result in opioid tolerance.[244-246] Work by Popik *et al.* has revealed that the potent, selective Group II metabotropic glutamate agonist, LY354740, is able to reverse opioid tolerance *in vivo*; an effect which is quite feasibly due to the drug's action at glial mGlu receptors.[247] In the present study, it is likely that the selective mGlu2/3 receptor agonist, **44a**, is acting to reverse mechanical allodynia by interactions with both neurons and glia. Compound **44a** may have caused a decrease

in cytokine levels through activation of glial metabotropic glutamate receptors, which in turn decreased neuronal cell activation and led to an attenuation of pain signalling.

The pharmacological action of compound **44a** on metabotropic glutamate receptors 2 and 3 expressed both on glutamatergic and GABAergic neurons and on glial cells within the dorsal horn of the spinal cord, most likely mediated the reversal of mechanical allodynia observed in this study.

4.5 Summary

In vitro drug screening at NMDA, kainate and AMPA ionotropic glutamate receptor subtypes revealed activity of compound **45** with an EC_{50} value of 63 μM and compound **48** with an EC_{50} value of 49 μM at AMPA receptors. All other compounds showed no activity at any of these receptor subtypes as indicated by $EC_{50} > 100$ μM. *In vitro* drug screening at metabotropic glutamate receptor subtypes 1, 2 and 4 revealed agonist activity for compound **44a** at mGluR2 with an EC_{50} value of 0.05 μM and weak antagonist activity of compound **44d** at mGluR2 with an EC_{50} value of 62 μM. All other compounds tested, apart from the positive control, were found to be inactive at all subtypes of the metabotropic receptors which were tested as indicated by $EC_{50} > 100$ μM. Compound **44a** was then tested *in vivo* in a rodent model of neuropathic pain and was found to significantly and dose-dependently decrease mechanical allodynia, measured at one hour and three hours post intrathecal dosing. It is highly likely that this effect is due to activation of mGlu2 and 3 receptors located on both neuronal and glial cells within the dorsal horn of the spinal cord.

Chapter 5 : *In Silico* Docking Simulations

5.1 Introduction

In an effort to rationalize the results obtained from the *in vitro* binding assays, *in silico* docking simulations were carried out using Autodock 4. A library was constructed consisting of known active compounds, newly synthesized compounds and theoretical compounds and were docked into mGluR1, mGluR3, NMDA receptor (NMDAR) and AMPA receptor (AMPAR).

There were 100 simulations carried out for each ligand with 5 million iterations each over a cubic grid with a 0.375 Å spacing resolution. The grid box was sufficiently large so as to encompass the entire extracellular domain. Two different versions of the NMDA x-ray crystal structure were used as found in the Protein Data Bank (PDB). The first was the NR2A type (NMDA: PDB code 2A5S) and the second consisted of an NR1/NR2A ligand-binding cores complex (NMDA2: PDB code 2A5T).[248] The AMPAR ligand binding domain used was the GluR4$_{flip}$ subunit (PDB code 3EPE).[249] Two versions of the mGluR1 receptor were also used, the 1ISR (mGluR1) and the 1EWK (mGluR1a) x-ray structures.[105,250] Finally, the mGluR3 x-ray crystal structures used were PDB entries 2E4X and 2E4U.[251] All receptors were prepared beforehand by removal of any ligands and co-factors present, followed by re-docking of the glutamate ligand to ensure reliable results could be obtained. In order to further confirm the reliability of the docking, a comparison was made between the docking of known ligands and the available x-ray crystal structures of the same ligand bound to the receptor.

The results were analysed using Autodock Tools by comparison of the docked position of glutamate to that of the particular compound. The mean lowest docked energy structures were considered with docking frequency and total number of docked positions also being taken into account.

The amino acid (AA) residues involved in receptor / ligand interactions for each receptor, NMDA AMPA, mGluR3 and mGluR1 are outlined in Table 5.1. The data was

obtained from the literature and comparison to the *in silico* data revealed identical amino acid residues within the ligand binding region.[248,249,252]

Table 5.1. Amino Acid Residues Involved in Receptor Binding

Receptor	AA residue	Receptor	AA residue
NMDA[248]	Ser114	AMPA[249]	Tyr451 (57)*
	Thr116		Pro479 (85)*
	Arg121		Thr656 (87)*
	Ser173		Arg486 (92)*
	Thr174		Gly452 (137)*
	Thr174		Ser655 (138)*
	Tyr214		Glu706 (189)*
mGluR1[252]	Arg78	mGluR3[252]	Arg68
	Ser165		Arg68
	Thr188		Ser151
	Asp318		Thr174
	Lys409		Thr174
			Asp301
			Lys389

*Numbering in parentheses is taken from the PDB x-ray crystal structure (3EPE) and will be used throughout this chapter.

5.2 Results and Discussion

5.2.1 Docking Validation

Before screening of new structures, it was necessary to ensure the docking simulation could correctly predict the receptor binding position and orientation in a reliable and repeatable manner. As such, some known ligands including the endogenous ligand, glutamate, were first docked *in silico*. As is depicted in Figure 5.1, when docked into NMDAR, there was excellent overlap between the docked position of the ligand glutamate and the position of the same molecule in the x-ray crystal structure. Glutamate docked to this position with a frequency of 7 out of 100 dockings, with a

mean lowest docking energy of −5.90 kcal/mol. For these dockings, the frequency was low, since glutamate is a highly flexible molecule. However, in this case the docking energy holds more weight than the docking frequency and so the NMDA receptor docking was validated.

Figure 5.1. Comparison of glutamate docked position in NMDA receptor to x-ray crystal structure (PDB code: 2A5S) glutamate position.
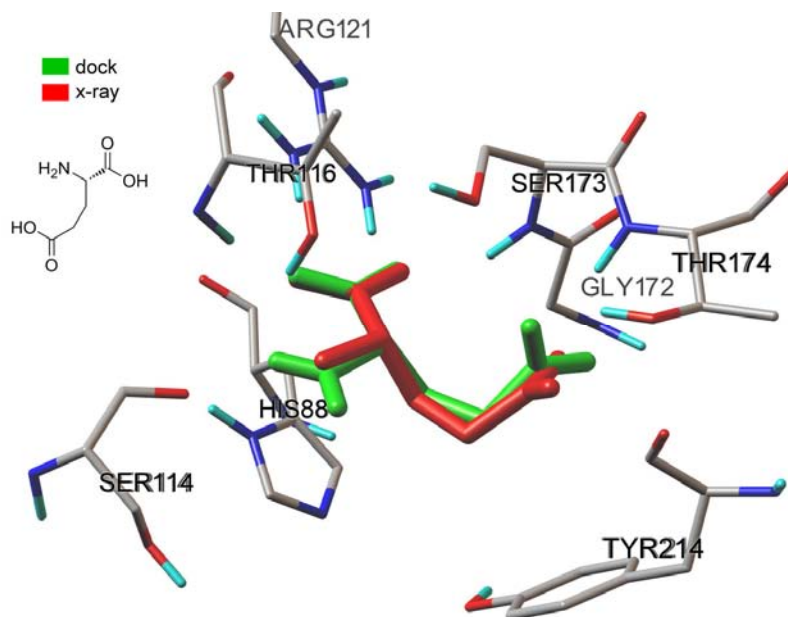
Depicted in Figure 5.2, when docked into AMPAR, there was excellent overlap between the docked position of the ligand glutamate and the position of the same molecule in the x-ray crystal structure. Glutamate docked to this position with a frequency of 64 out of 100 dockings, with a mean lowest docking energy of −6.14 kcal/mol. Figure 5.3 illustrates the docked position of the ligand AMPA compared to the position of glutamate from the x-ray crystal structure; there was good overlap between the two molecules. AMPA docked to this position with a frequency of 95 out of 100 dockings, with a mean lowest docking energy of −9.60 kcal/mol. Thus, the AMPA receptor docking was validated.

Figure 5.2. Comparison of glutamate docked position in AMPA receptor to x-ray crystal structure (PDB code: 3EPE) glutamate position.
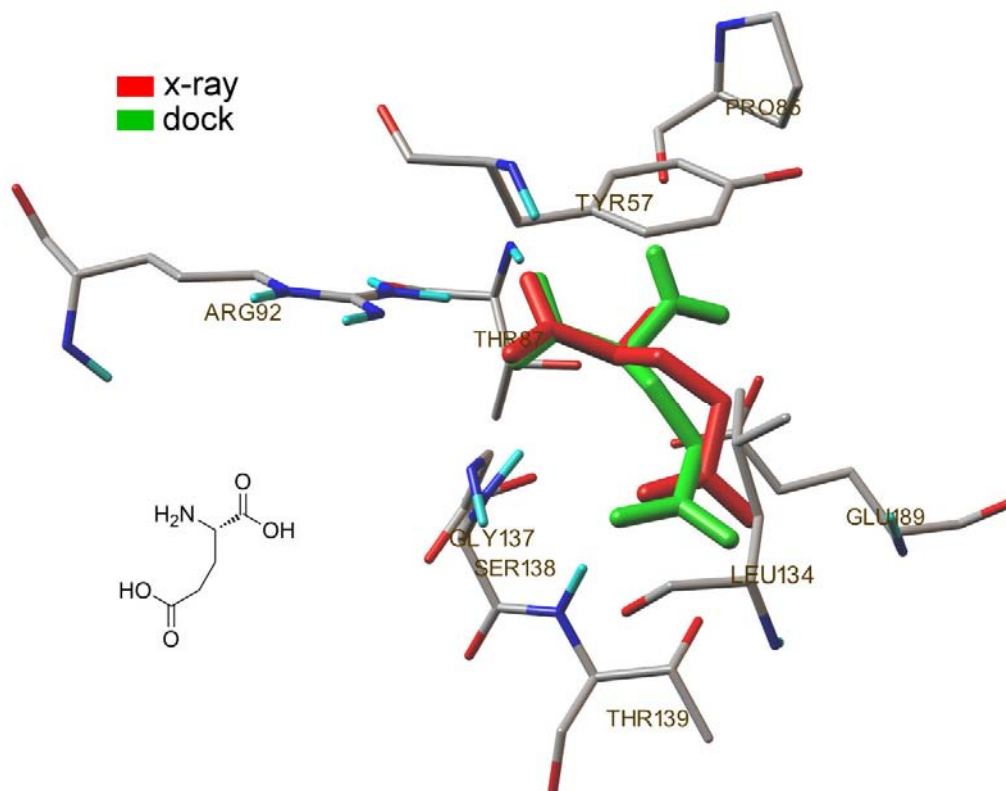
Figure 5.3. Comparison of AMPA docked position in AMPA receptor to x-ray crystal structure (PDB code: 3EPE) glutamate position.

Figure 5.4 shows that the docked position of the ligand glutamate and the position of the same molecule in the x-ray crystal structure of subtype 1 of the metabotropic glutamate receptor were significantly different. This immediately rendered the mGluR1 *in silico* docking invalid. Attempts were made, by decreasing the size of the docking grid box, to improve the docking data, however, this also failed. Due to this, the mGluR1 docking was abandoned.

Figure 5.4. Comparison of glutamate docked position in mGluR1 receptor to x-ray crystal structure (PDB code: 1ISR) glutamate position.

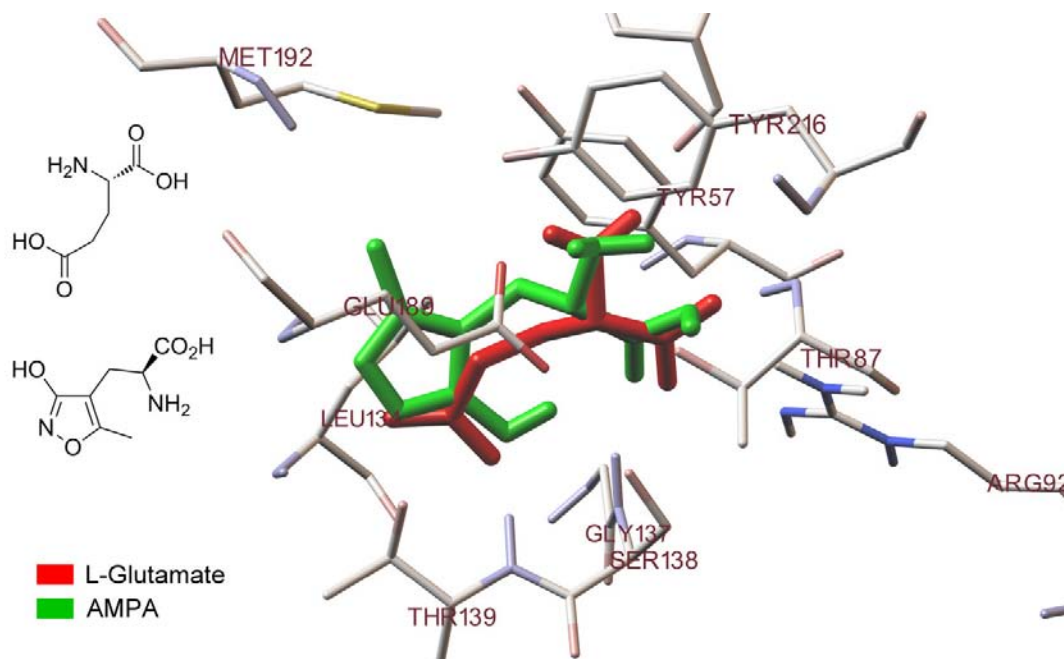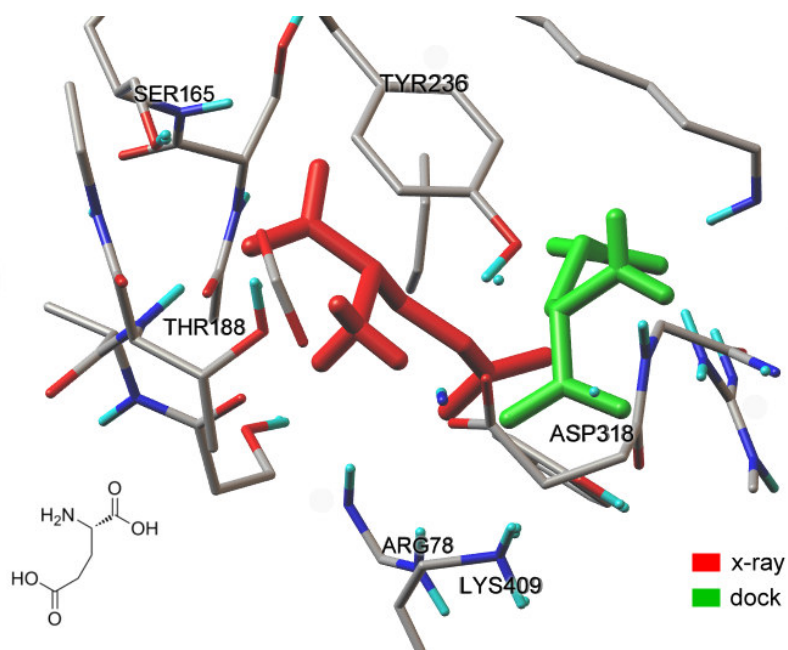Figure 5.5 depicts the overlap of the docked position of the ligand glutamate and the position of the same molecule in the x-ray crystal structure of subtype 3 of the metabotropic glutamate receptor. The docked position agrees very well with the x-ray crystal structure; thus, the mGluR3 docking was validated. Glutamate docked to this position with a frequency of 30 out of 100 dockings, with a mean lowest docking energy of −6.20 kcal/mol.

Figure 5.5. Comparison of glutamate docked position in mGluR3 to x-ray crystal structure (PDB code: 2E4U) glutamate position.
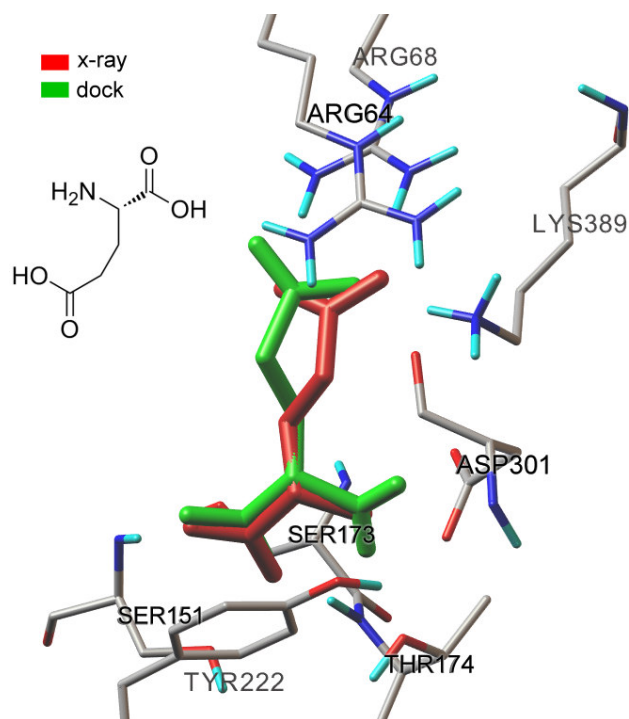
Figure 5.6 shows very good overlap of the docked position of the receptor agonist, (1*S*,3*R*)-1-aminocyclopentane-1,3-dicarboxylic acid ((1*S*,3*R*)-ACPD) and the position of the same molecule in the x-ray crystal structure of subtype 3 of the metabotropic glutamate receptor. The ligand (1*S*,3*R*)-ACPD docked to this position with a frequency of 31 out of 100 dockings, with a mean lowest docking energy of −8.23 kcal/mol. Thus, the mGluR3 docking was validated.

Figure 5.6. Comparison of (1*S*,3*R*)-ACPD docked position in mGluR3 to x-ray crystal structure (PDB code: 2E4X) (1*S*,3*R*)-ACPD position.
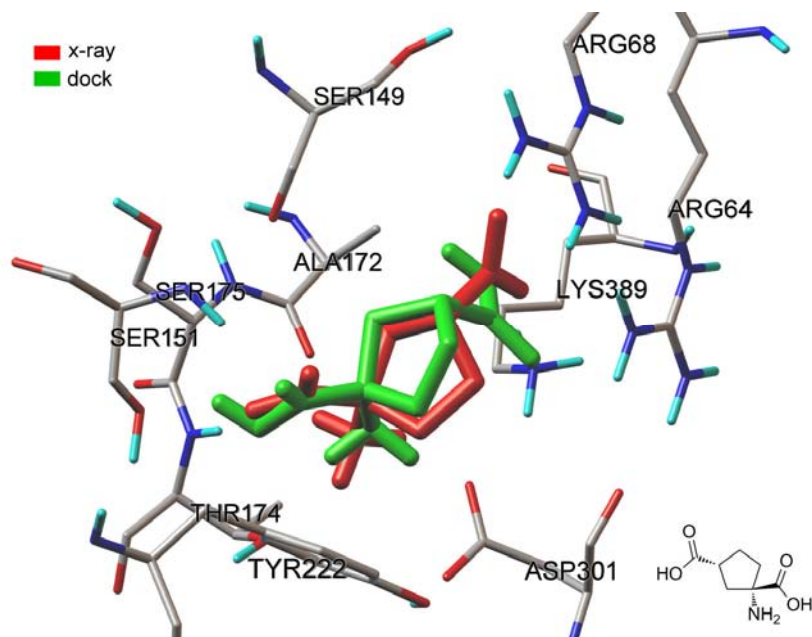

Figure 5.7 illustrates the docked positions of glutamate and several carboxycyclopropylglycine analogues. For comparison, the position of glutamate from the x-ray crystal structure is shown in red. As would be expected, substitution in the 3'-position of the cyclopropane ring causes the ligand to occupy a new region of space within the binding pocket of the receptor. The substitution patterns on the ligands shown are either small and non-polar (methyl), or slightly larger and polar (hydroxymethyl and carboxy (DCG-IV)). These molecules all docked in the correct location and with the correct orientation. However, when docking was attempted on compounds having larger or bulkier groups in the 3'-position, such as cycloalkyl, phenyl and xanthenyl groups, the structures docked at a location distant from the competitive binding site (Figure 5.8). The reason for this was the docking was initially carried out using a rigid receptor protein structure, whereas in an *in vitro* or *in vivo* system, the receptor would be flexible and able to accommodate different structures. It was hypothesized, based on work by Yao and co-workers, that the position of tyrosine 150 (Tyr150) in the rigid receptor binding site may have been at least partly responsible for the inaccurate docking.[253] In an effort to provide a more reliable system in which new compounds could be docked, amino acid residues in the binding site of the receptor and known to be involved in binding were made flexible. Thus, the docking was

repeated with glutamate and known ligands to verify that the model was reliable. Even so, when the docking simulation was run with flexible residues, the mean docking energy increased dramatically, providing essentially meaningless data. Finally, the docking was attempted with a smaller grid box so as to restrict possible docking locations and increase the likelihood of the ligand docking in the correct position; however, this also failed to give accurate results. As a consequence of this, the mGluR3 docking work was also abandoned.

Figure 5.7. Overlap of glutamate with several carboxycyclopropylglycine ligands in mGluR3 x-ray crystal structure (PDB code: 2E4U).
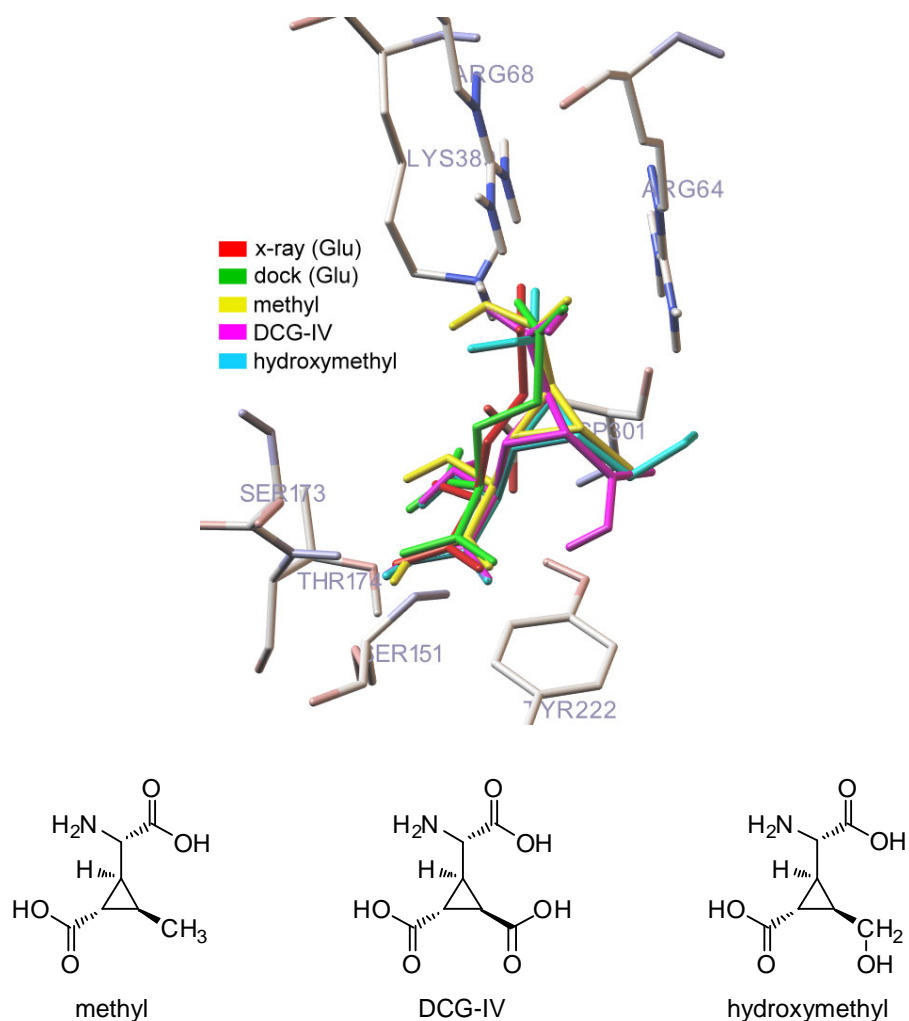
Figure 5.8. Structures of Incorrectly Docked Cyclopropane Amino Acids

| cyclopropyl | phenyl | cyclohexyl | xanthenylmethyl |
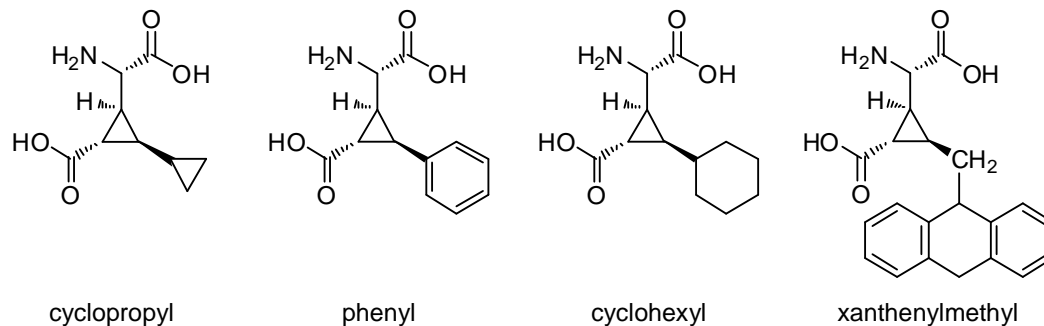
Overall, only the NMDA and AMPA receptor docking provided reliable results, whereas limited data was obtained for the metabotropic glutamate receptor 3 and the metabotropic glutamate receptor 1 docking was not further investigated.

5.2.2 Docking Active Compounds

There were few novel compounds screened *in silico* for which the docking suggested favourable interactions. There was indication that triazoles **48** and **49** (Figure 5.9) could potentially bind to NMDA receptors; however, the *in vitro* data indicated that this was not significant. It's possible that the receptor adopts a different conformation *in vitro*, which prevents the molecules from either accessing the binding site or binding as predicted by the *in silico* docking. The docking indicated that glutamate made eight hydrogen bonds, whereas triazole **48** made seven and triazole **49** made five. Although the mean lowest docking energies for these triazoles were lower than that for glutamate (−5.48 kcal/mol) at −7.91 and −9.04 kcal/mol respectively, there were particular interactions not present, such as hydrogen bonds to the amine group of the ligand. Triazole **49** is shown docked to the NMDA receptor in Figure 5.9 along with glutamate for comparison; there was good overlap between the two structures.

Figure 5.9. Comparison of Triazole **49** docked position in NMDA receptor 2 (PDB code: 2A5T) to glutamate docked position.
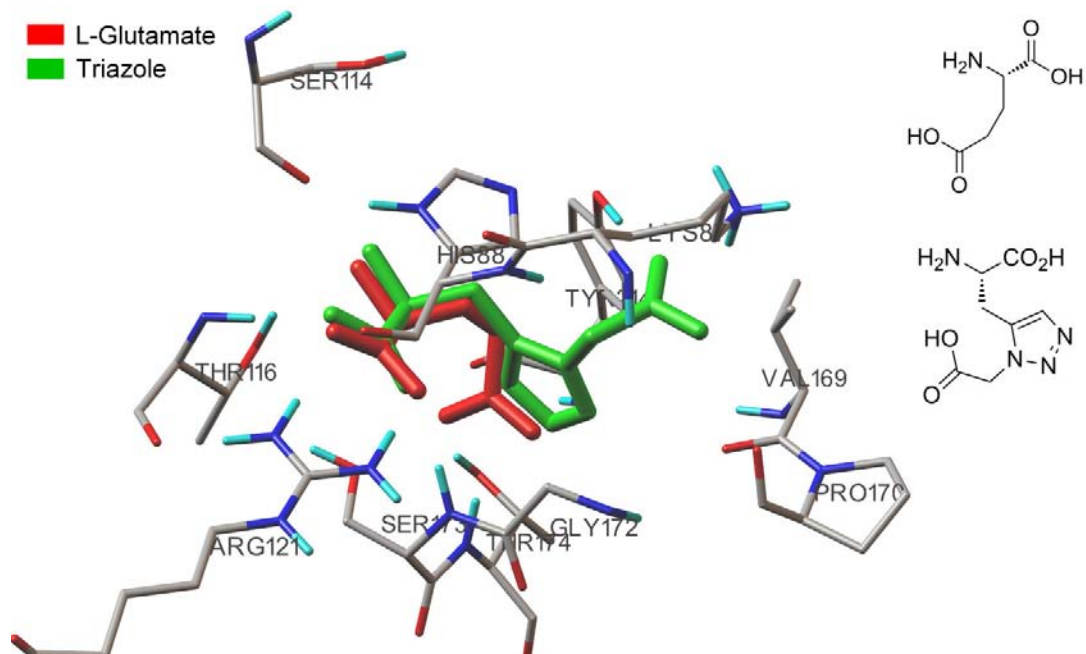
An example of the hydrogen bonding interactions between triazole **49** and key amino acid residues within the NMDA receptor binding pocket are depicted in Figure 5.10. Hydrogen bonds are indicated as dotted green lines. Note the lack of hydrogen bonding between Ser114 and the amine group of triazole **49**.

Figure 5.10. Triazole **49** docked interactions in NMDA receptor 2 (PDB code: 2A5T).

The *in vitro* binding assays showed weak activity for triazoles **45** and **48** at AMPA receptors. Triazole **48** was the more potent compound with an IC_{50} of 49 μM at AMPA receptors. It can be observed from Figure 5.11 that there was good overlap of the glutamate (red) docked position to the docked position of triazole **48** (green).
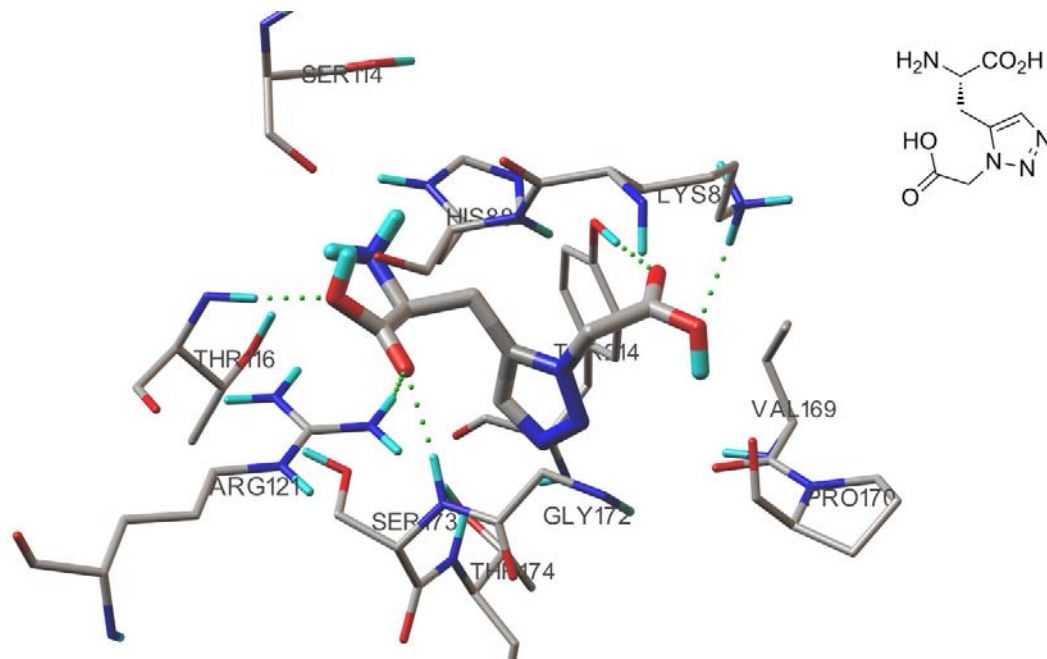
Figure 5.11. Comparison of Triazole **48** docked position in AMPA receptor (PDB code: 3EPE) to glutamate docked position.
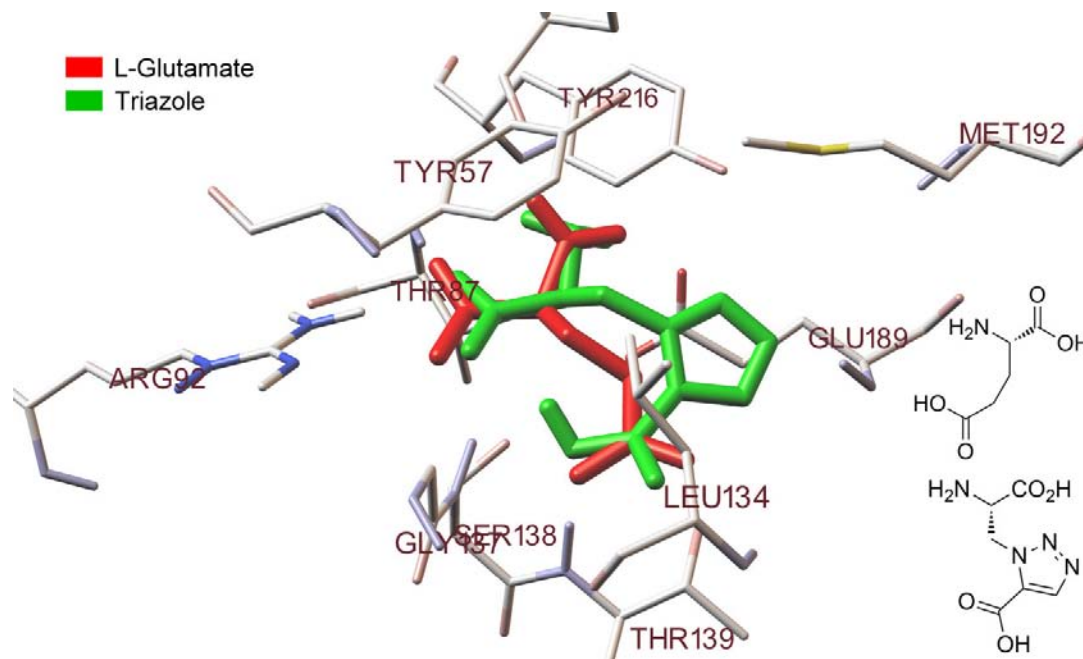
Triazole **48** docked to this location with a frequency of 75 out of 100 dockings. Examination of the receptor-ligand interactions reveals strong agreement with the interactions for glutamate (See Figure 5.12 and Table 5.2). On comparison of the mean lowest docking energies, it was discovered that the binding of triazole **48** (−8.71 kcal/mol) was more favourable energetically than glutamate (−6.14 kcal/mol). Triazole **48** makes six hydrogen bonds with the receptor as does glutamate. The amino acid residues involved in binding are outlined in Table 5.2 and compared to those for both the endogenous ligand glutamate and AMPA.

Figure 5.12. Triazole **48** docked interactions in AMPA receptor (PDB code: 3EPE).
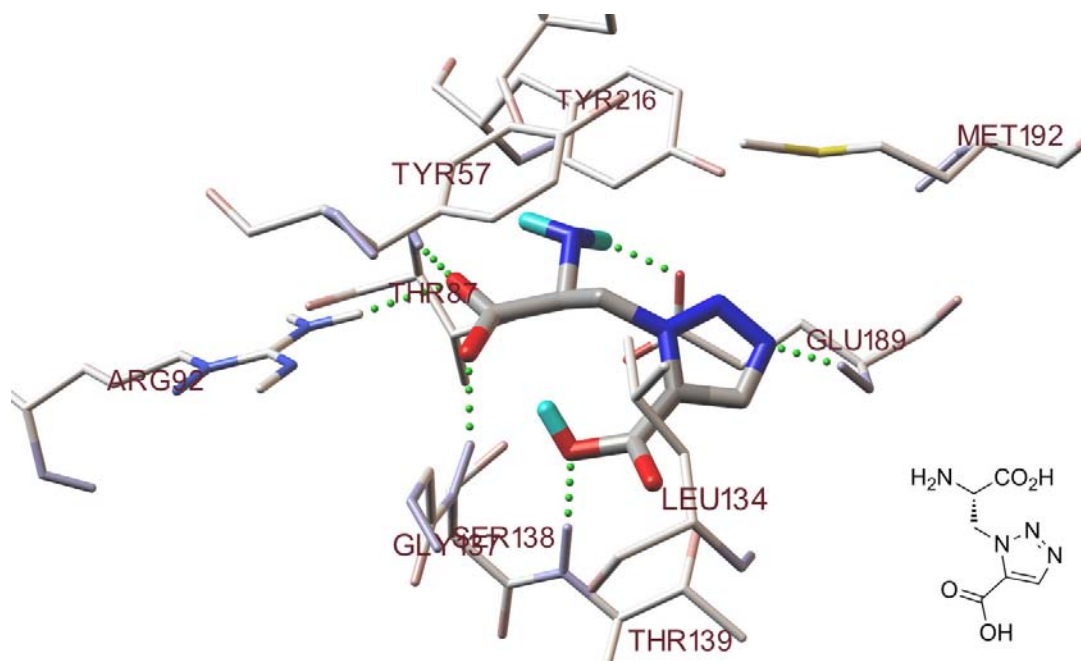
Triazole **45** was slightly less potent than triazole **48**, with an IC_{50} of 63 μM at AMPA receptors. It can be observed from Figure 5.13 that there was good overlap of the glutamate (red) docked position to the docked position of triazole **45** (green). Triazole **45** docked to this location with a frequency of 55 out of 100 dockings. Examination of the receptor-ligand interactions reveals strong agreement with the interactions for glutamate (See Figure 5.14). A comparison of the mean lowest docking energies suggests that the binding of triazole **45** (−8.48 kcal/mol) was more favourable energetically than glutamate (−6.14 kcal/mol). Triazole **45** makes seven hydrogen bonds with the receptor, which is one more than glutamate.

Figure 5.13. Comparison of Triazole **45** docked position in AMPA receptor (PDB code: 3EPE) to glutamate docked position.

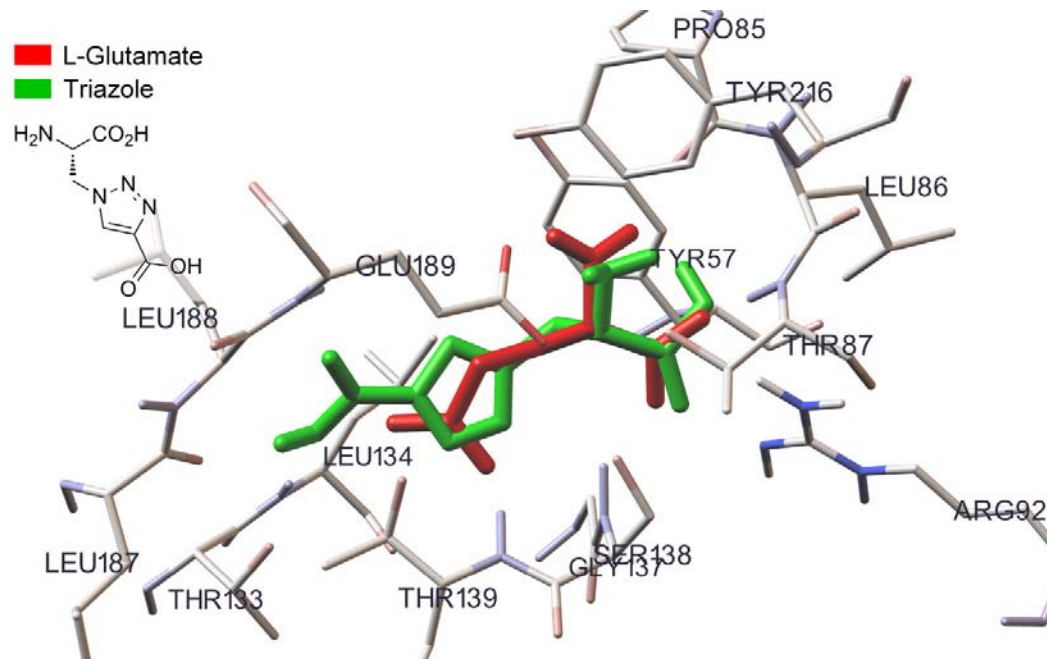The low docking energy of glutamate is no doubt mainly attributable to its very flexible structure. Upon examination of the amino acid residues involved in binding, it seems as if hydrogen bonding with Pro85 also has a negative effect in terms of docking energy. Triazole **45** also interacts with Pro85 and is the less potent of the two active compounds. AMPA is the potent, selective agonist after which the receptor is named and upon binding does not appear to interact with Pro85 and neither does the more active of the tested compounds, triazole **48** (Compare Figures 5.15 and 5.12). However, the docking was carried out employing a rigid receptor x-ray crystal structure form which glutamate was removed. The literature sheds some light on this by clearly stating that AMPA does in fact interact with Pro85 upon binding and thus the lack of Pro85 hydrogen bonding observed here is due to the rigid receptor that was used.[249,254] Future work making use of flexible amino acid residues in the ligand binding domain may serve to improve the docking data obtained.

Figure 5.14. Triazole **45** docked interactions in AMPA receptor (PDB code: 3EPE).
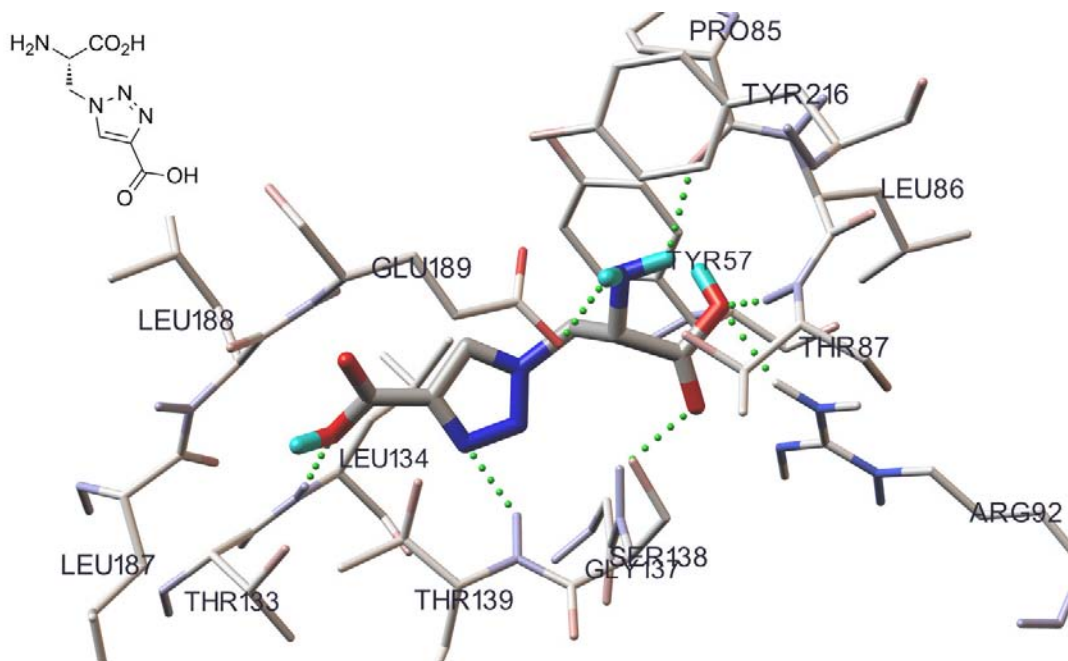
Figure 5.15. AMPA docked interactions in AMPA receptor (PDB code: 3EPE).
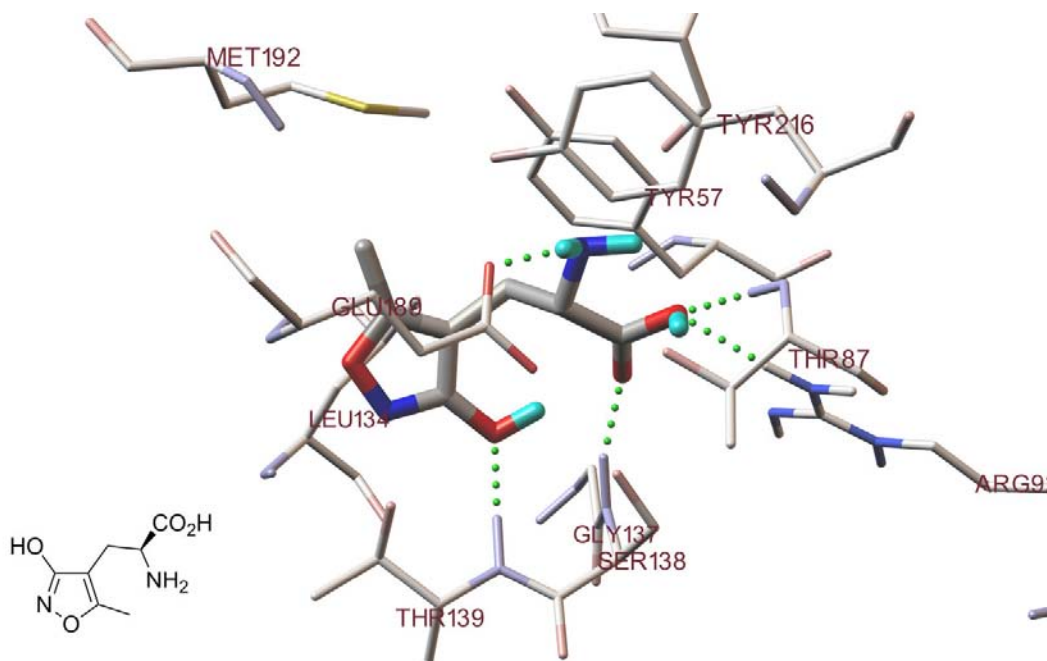
The amino acid residues involved in binding are outlined in Table 5.2 and compared to those for both the endogenous ligand glutamate and AMPA. Amino acid resides involved in hydrogen bonding are listed in red; other residues are involved in van der Waals-type interactions.

Table 5.2. Interactions of Glutamate, AMPA, Triazole **45** and Triazole **48** in the AMPA Receptor

Compound	Amino Acid Residue	Receptor Interactions	Ligand Interactions	Hydrogen Bonds	Mean Lowest Docking Energy
Glutamate	Tyr57	phenyl ring	hydrophobic	6	−6.14 kcal/mol
(Agonist)	Pro85	C=O	NH		
	Thr87	NH	OH / C=O (prox)		
	Arg92	NH (dist)	OH / C=O (prox)		
	Leu134	alkyl chain	hydrophobic		
	Ser138	NH	OH / C=O (prox)		
	Thr139	NH	C=O (dist)		
	Glu189	C=O (dist)	NH		
Triazole **45**	Tyr57	phenyl ring	hydrophobic	7	−8.48 kcal/mol
(Active)	Pro85	C=O	NH		
	Thr87	NH	OH (prox)		
	Arg92	NH (dist)	OH / C=O (prox)		
	Thr133	NH	OH (dist)		
	Ser138	NH	OH / C=O (prox)		
	Thr139	NH	N (triazole)		
	Glu189	C=O (dist)	NH		
Triazole **48**	Tyr57	phenyl ring	hydrophobic	6	−8.71 kcal/mol
(Active)	Thr87	NH	OH (prox)		
	Arg92	NH (dist)	OH / C=O (prox)		
	Ser138	NH	C=O (prox)		
	Thr139	NH	OH (dist)		
	Glu189	C=O (dist)	NH		
	Glu189	NH	N (triazole)		
AMPA	Tyr57	phenyl ring	hydrophobic	5	−9.60 kcal/mol
(Agonist)	Thr87	NH	OH (prox)		
	Arg92	NH (dist)	OH (prox)		
	Ser138	NH	C=O (prox)		
	Thr139	NH	OH (phenolic)		
	Glu189	C=O (dist)	NH		

dist: distal; prox: proximal

117

5.3 Summary

In an effort to rationalize the *in vitro* binding data, the newly synthesized cyclopropane and triazole amino acids were docked *in silico* into the NMDA, AMPA, mGluR1 and mGluR3 receptors available as x-ray crystal structures. The mGluR1 *in silico* docking could not be successfully validated. The endogenous ligand, glutamate, failed to dock in the correct location, even when a small docking grid box was employed. Due to this, no further useful data could be gained regarding docking to the mGlu1 receptor. The mGluR3 *in silico* docking was successfully validated. However, certain known receptor ligands, particularly those with bulky side groups and including the new biologically active cyclopropane amino acid, failed to dock correctly. This is suggested to be due to the receptor structure being rigid and unable to accommodate these structures. As a consequence of this, limited data was obtained from the mGluR3 docking. Both the NMDA and AMPA *in silico* docking models were validated successfully. AMPA receptor docking of the new *in vitro* active triazole amino acids **45** and **48** revealed positive docking interactions in agreement with those seen for the endogenous ligand, glutamate and the selective agonist AMPA. The docking of these new compounds was also computed to be highly energetically favourable, thus suggesting plausible binding modes.

Chapter 6 : Experimental

General Experimental

Diethyl ether and dichloromethane were dried over 4Å sieves. Methanol was dried over 3Å sieves. THF was dried over sodium wire with benzophenone as indicator and distilled just prior to use. All organic extracts were dried over anhydrous magnesium sulfate. Thin layer chromatography was carried out using aluminium sheets coated with silica gel 60 F_{254} (40 × 80 mm) from Merck and visualized under 254 nm light, or developed in either vanillin or ninhydrin dip. Flash chromatography was accomplished using Merck silica gel 60 (230–400 mesh). All yields reported refer to isolated material judged to be >95% homogenous by TLC and NMR spectroscopy.

^{1}H and ^{13}C NMR spectra were obtained using either a Bruker ACP-300 (300 MHz) or Varian INOVA (600 MHz) instrument. NMR spectra were recorded in $CDCl_3$ solution using TMS (0 ppm) and $CDCl_3$ (77.0 ppm) as internal standards and D_2O (4.87 ppm) using t-butanol as external zero for ^{13}C NMR. NMR spectra collected in CD_3OD were calibrated to CD_3OD (3.31 and 49.0 ppm). NMR spectra collected in d_6-DMSO were calibrated to d_6-DMSO (2.50 and 39.5 ppm). All resonances are given in parts per million (ppm). ^{1}H multiplicities are given the following abbreviations: singlet (s), doublet (d), triplet (t), multiplet (m) and broad (br) referring to broadened signals. All coupling constants are reported in Hertz (Hz).

Infrared spectra were recorded on an ATI Mattson Genesis Series FTIR spectrophotometer between solid plates (NaCl) as a nujol mull or thin film. Melting points were taken on a Reichert Thermovar Kofler apparatus and are uncorrected. Electron impact (EI) mass spectra were recorded using a VG ZAB 2HF mass spectrometer operating at 70 eV. Accurate mass measurements were performed at the School of Chemistry, Monash University, Victoria, Australia using electrospray ionisation (ESI). Elemental analysis was conducted in the Department of Chemistry, University of Otago, Dunedin, New Zealand. X-ray crystallography was performed by Edward R. T. Tiekink at The University of Texas, San Antonio, USA, using a Bruker AXS SMART CCD.

The following compounds were purchased from Sigma Aldrich Fine Chemicals and used without further purification: rose bengal *bis*(triethylammonium)salt, *trans* cinnamyl chloride, *trans* 2-methoxycinnamaldehyde, cyclopropanecarboxaldehyde, cyclobutanecarboxylic acid, cyclopentanecarboxaldehyde, cyclohexanecarboxaldehyde, cycloheptanecarboxylic acid, (±)-Cbz-α-phosphonoglycine trimethyl ester, vanillin, *tert*-butyl bromoacetate, *tert*-butyl propiolate and HOBt. (*S*)-Propargyl glycine, Boc-L-2,3-diaminopropionic acid, (*S*)-Boc-serine methyl ester and EDC hydrochloride were purchased from Chem Impex International and used without further purification.

General Procedure for the Preparation of Cycloalkanemethanols. Anhydrous diethyl ether (100 mL) was cooled to 0 ^{o}C under an N_2 atmosphere. $LiAlH_4$ (0.1 mol) was added in one portion with stirring followed by dropwise addition of the cycloalkanecarboxylic acid (0.09 mol) in diethyl ether (50 mL). Once addition was complete, the mixture was heated under reflux overnight. The reaction was allowed to cool to rt before being diluted with ether and cooled to 0 ^{o}C. Water was slowly added dropwise followed by 15% $NaOH_{(aq)}$ and further addition of water. The solution was allowed to warm to rt and stirred for 15 minutes at which point formation of a white precipitate was observed and anhydrous $MgSO_{4(s)}$ was added. After stirring for an additional 15 minutes, the solution was filtered through a pad of kenite and the ether removed *in vacuo* to afford the desired pure cycloalkanemethanol.

General Procedure for the Preparation of Cycloalkanecarboxaldehydes. The cycloalkanemethanol (0.03 mol) was dissolved in anhydrous dichloromethane (150 mL) to which was added freshly prepared pyridinium dichromate (0.04 mol) in one portion and the solution was stirred under an N_2 atmosphere for 8–24 h. Upon consumption of the starting material and formation of the aldehyde, as monitored by TLC (30% ethyl acetate in hexanes, v/v), the solvent was carefully removed *in vacuo*. The remaining brown residue was taken up in 50:50 diethyl ether:*n*-pentane and filtered through a pad of silica (4 cm × 5 cm ID) to remove all insoluble chromium salts. The filtrate was collected and the volatiles removed *in vacuo* to afford the desired pure cycloalkanecarboxaldehyde.

Cinnamyltriphenylphosphonium chloride. The phosphonium salt was prepared by reaction of neat cinnamyl chloride (36.8 g, 0.2 mol) with triphenylphosphine (76 g, 0.2

mol) at ~90 $^{\circ}$C. Heating was continued until formation of the salt as a glass. The glass was broken up and a small amount of toluene added followed by further heating to ensure the reaction was complete. The salt was then ground to a fine powder, vacuum filtered and washed with ether to afford pure cinnamyl triphenylphosphonium chloride as an off-white solid (90 g, 90%); ^{1}H NMR (300 MHz, CDCl$_3$) δ 5.10–5.17 (m, 2H), 5.71−6.04 (m, 1H), 6.72−6.79 (m, 1H), 7.18−7.25 (m, 5H), 7.64−7.94 (m, 15H).

Cycloheptyliodomethane[255]

Method A (78a).[169] Cycloheptanemethanol (6.5 g, 50 mmol) and *N*-iodosuccinimide (17 g, 75 mmol) were dissolved in anhydrous dichloromethane (60 mL) under a N$_2$ atmosphere. The solution was cooled to *ca.* 5 $^{\circ}$C. Triphenylphosphine (19.8 g, 75 mmol) dissolved in anhydrous dichloromethane (60 mL) was added dropwise over approximately 20 minutes. The reaction was then stirred for 1 h at 5 $^{\circ}$C followed by stirring for 1 h at room temperature. Solvents were stripped under vacuum and the residue taken up in 10% ether / *n*-pentane to precipitate all TPPO by-product, followed by vacuum filtration through a silica pad. The filter cake was rinsed with further 10% ether / *n*-pentane and the solvents removed from the filtrate *in vacuo* to afford the pure iodo compound as a pale yellow oil (8 g, 67%). The crude product was used without further purification.

Method B (78b).[170] Cycloheptanemethanol (7.0 g, 55 mmol) was dissolved in anhydrous THF (130 mL). To the stirred solution was added triphenylphosphine (17.2 g, 66 mmol) and imidazole (7.4 g, 110 mmol) followed by cooling to 0 $^{\circ}$C. Elemental iodine (16.6 g, 66 mmol) was added and the stirred reaction allowed to warm to rt overnight. The reaction was quenched with saturated sodium metabisulfite solution and washed with saturated sodium bicarbonate solution followed by extraction with diethyl ether. Ether extracts were combined, dried over MgSO$_{4(s)}$, filtered and volatiles removed *in vacuo* providing cycloheptyliodomethane as a pale yellow oil (12.5 g, 96%) which was used without further purification.

Attempted Preparation of Cyclopentanecarboxaldehyde by Swern Oxidation[171] **(76c).** To a 0.5 M solution of oxalyl chloride (2.5 g, 20 mmol) in DCM (40 mL) held at −78 $^{\circ}$C was added anhydrous DMSO (3.1 g, 40 mmol) with stirring for 10 min.

Cyclopentanemethanol (1.0 g, 10 mmol) in DCM (10 mL) was added dropwise followed by stirring for 1 h. TEA (4.6 g, 45 mmol) was added and the reaction stirred at −78 °C for a further 5 min before being allowed to warm to rt at which point stirring was continued for another 15 min. The reaction was diluted with H_2O (80 mL) and extracted with DCM (2 × 50 mL) and the combined organic extracts washed with brine (80 mL). Drying of the DCM solution, filtration and removal of the solvent *in vacuo* provided the crude aldehyde. ^{1}H NMR, however, revealed only traces of desired product, approximately 50 % remaining starting material and significant amounts of ester.

Attempted Preparation of Cyclopentanecarboxaldehyde by Parikh-Doering Oxidation[172] (76c). To a stirred slurry of sulfur trioxide pyridine complex (3.2 g, 20 mmol) and DMSO (3.1 g, 40 mmol) in DCM (16 mL) was added dropwise cyclopentanemethanol (1.0 g, 10 mmol) and TEA (6.0 g, 60 mmol) in DCM (16 mL) at 0 °C under an N_2 blanket. After 1 h, the reaction was allowed to warm to rt and stirring was continued for a further 3 h. The solution was washed with H_2O (50 + 50 mL) and extracted with DCM (50 + 50 mL). The organic extracts were combined, washed with brine (50 mL), dried over $MgSO_{4(s)}$, filtered and the solvent carefully removed under reduced pressure to give the crude aldehyde. ^{1}H NMR, however, revealed only traces of desired product and mostly starting material.

General Procedure for the Preparation of 1-cycloalkyl-4-phenyl-1,3-butadienes (75a−f). Cinnamyl triphenylphosphonium chloride (36 mmol) was added to anhydrous diethyl ether or anhydrous THF (150 mL). Whilst the slurry was stirred under N_2, potassium *tert*-butoxide (39 mmol) was added in one portion. After stirring for 15 minutes, the cycloalkanecarboxaldehyde (30 mmol), dissolved in anhydrous ether (50 mL), was added dropwise over approximately 20 minutes. The reaction was stirred overnight at which point the excess base was quenched with half-saturated $NH_4Cl_{(aq)}$, the volatiles removed *in vacuo*, the residue diluted with water (100 mL) and extracted with dichloromethane (3 × 100 mL). After drying over anhydrous $MgSO_{4(s)}$, filtering and removal of the solvent *in vacuo*, the residue was taken up in hexanes and filtered through a pad of silica (4 cm × 5 cm ID) to remove all triphenylphosphine oxide. Removal of the hexanes *in vacuo* afforded the desired crude 1,3-butadienes.

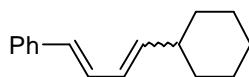**[(1_E_,3_E_)-4-Cyclopropylbuta-1,3-dien-1-yl]benzene (75a).** Colourless oil (17 g, 90%);
^{1}H NMR (300 MHz, CDCl$_3$) δ 0.43−0.48 (m, 2H), 0.77−0.90 (m, 2H), 1.42−1.54 (m, 1H), 1.83−1.93 (m, 1H), 4.85−4.92 (m, 1H), 5.27−5.39 (m, 2H), 6.07−6.15 (m, 1H), 6.25−6.55 (m, 3H), 6.68−6.76 (m, 1H), 7.14−7.44 (m, 10H). The crude product was used without further purification.
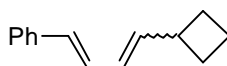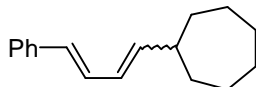

[(1_E_,3_E_)-4-Cyclobutylbuta-1,3-dien-1-yl]benzene (75b). Colourless oil (4.73 g, 74%);
^{1}H NMR (300 MHz, CDCl$_3$) δ 1.73−2.31 (m, 14H), 2.96−3.07 (m, 1H), 3.39 (d, *J* = 13.8 Hz, 2H), 3.40−3.55 (m, 1H), 5.04−5.11 (m, 2H), 5.63 (t, *J* = 9.6 Hz, 1H), 5.88−6.05 (m, 2H), 6.10−6.29 (m, 2H), 6.37−6.51 (m, 3H), 6.75 (dd, *J* = 10.2, 5.4 Hz, 1H), 7.01 (ddd, *J* = 9.9, 3.6, 1.2 Hz, 1H), 7.14−7.41 (m, 20H); ^{13}C NMR (75 MHz, CDCl$_3$) δ 18.7, 19.2, 29.1, 30.3, 34.7, 38.8, 40.5, 116.0, 124.9, 125.9, 126.0, 126.3, 126.3, 126.5, 126.9, 127.2, 127.3, 127.5, 128.6, 128.8, 129.5, 130.6, 131.2, 132.2, 137.7, 137.8, 138.6, 140.3. The crude product was used without further purification.
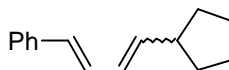

[(1_E_,3_E_)-4-Cyclopentylbuta-1,3-dien-1-yl]benzene (75c). Colourless oil (12 g, 93%);
IR (film): 3080, 3060, 3024, 3003, 2953, 2867, 1641, 1595, 1494, 1448, 1295, 1265 cm^{-1}; ^{1}H NMR (300 MHz, CDCl$_3$) δ 1.25−1.40 (m, 4H), 1.56−1.92 (m, 12H), 2.53 (sextet, *J* = 8.4, 8.1, 7.8 Hz, 1H), 3.00 (sextet, *J* = 8.4 Hz, 1H), 5.46 (dd, *J* = 10.2 Hz, 1H), 5.82 (dd, *J* = 8.1, 7.2 Hz, 1H), 6.02−6.29 (m, 2H), 6.47 (dd, *J* = 15.3, 7.2 Hz, 2H), 6.75 (dd, *J* = 10.5, 5.1 Hz, 1H), 7.18−7.43 (m, 10H); ^{13}C NMR (75 MHz, CDCl$_3$) δ 25.2, 25.4, 33.2, 34.0, 38.9, 43.6, 124.8, 125.8, 126.1, 126.3, 127.0, 127.2, 127.3, 128.5, 128.6, 129.5, 129.9, 131.8, 137.4, 138.7, 140.6. The crude product was used without further purification.

[(1*E*,3*E*)-4-Cyclohexylbuta-1,3-dien-1-yl]benzene (75d). Colourless oil (22 g, 97%); R_f 0.81 (35% dichloromethane in hexanes, v/v). All other physical and chemical properties were identical with those previously reported.[256] The crude product was used without further purification.


[(1*E*,3*E*)-4-Cycloheptylbuta-1,3-dien-1-yl]benzene (75e). Colourless oil (3.75 g, 58%); R_f 0.81 (35% dichloromethane in hexanes, v/v) IR (film): 3080 (weak), 3060 (weak), 3025, 3003 (weak), 2923, 2853, 1639 (weak), 1596 (weak), 1494, 1447 cm^{-1}. The crude product was used without further purification.
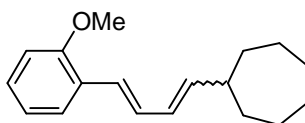
**2-[(1*E*,3*E*)-4-Cycloheptylbuta-1,3-dien-1-yl]phenyl methyl ether (75f).** Colourless oil (5.2 g, 86%); ^{1}H NMR (300 MHz, CDCl$_3$) δ 1.26−1.82 (m, 12H), 2.68−2.79 (m, 1H), 3.84 (s, 3H), 5.41−5.48 (m, 1H), 6.00−6.07 (m, 1H), 6.75−6.95 (m, 3H), 7.01−7.24 (m, 2H), 7.49−7.51 (m, 1H). The crude product was used without further purification.

General Procedure for the Preparation of 1,2-dioxines (80a−f). All 1,2-dioxines were prepared by the rose bengal bis(triethylammonium)salt sensitized [4π + 2π] cycloaddition of singlet oxygen to the corresponding 1,3-butadiene. The 1,3-butadiene (3 g, 15 mmol) and rose bengal bis(triethylammonium)salt (100 mg, 0.09 mmol) were dissolved in dichloromethane (100 mL) and the reaction vessel semi-immersed in an ice bath so that the reaction mixture was maintained at a temperature of *ca.* 5−10 ^{o}C. A stream of oxygen was then passed through the solution, whilst irradiating with two or three tungsten halogen lamps (500 W) at a distance of 10 cm from the reaction vessel for 6−12 h. Upon consumption of the diene, as monitored by TLC (35% dichloromethane in hexanes, v/v), the volatiles were then removed *in vacuo* and the residue subjected to flash column chromatography (10% ethyl acetate in hexanes, v/v) which afforded the pure 1,2-dioxine.
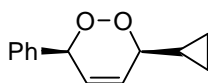
(±) **(3*S*,6*S*)-3-Cyclopropyl-6-phenyl-3,6-dihydro-1,2-dioxine (80a).** Recrystallization from hot hexanes gave the title compound as colourless needles (15.4 g, 69%); mp: 54−55 ^{o}C; R_f 0.49 (10% ethyl acetate in hexanes, v/v); IR (nujol): 2922, 2852, 2725, 2672, 1715, 1455, 1378, 1305, 1256, 1190, 1160 cm^{-1}; ^{1}H NMR (300 MHz, CDCl$_3$) δ 0.31−0.67 (m, 4H), 1.02−1.13 (m, 1H), 3.87−3.92 (m, 1H), 5.48 (dd, *J* = 1.8, 2.1 Hz, 1H), 6.09−6.20 (m, 2H), 7.30−7.43 (m, 5H); ^{13}C NMR (75 MHz, CDCl$_3$) δ 1.7, 3.4, 13.2, 79.9, 82.7, 137.8; MS (EI) (C$_{13}$H$_{14}$O$_2$) *m/z* (%): (M$^+$ 202, < 1%), 173 (10), 160 (20), 133 (10), 118 (20), 105 (100), 97 (5), 77 (40), 69 (35), 51 (10); HRMS (ESI, [M + Na]$^+$) calcd for C$_{13}$H$_{14}$O$_2$Na$_1$: 225.0894, found 225.0884; Anal. Calcd. for C$_{13}$H$_{14}$O$_2$: C, 77.20; H, 6.98. Found: C, 77.48; H, 6.88.
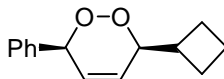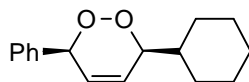

(±) **(3*S*,6*S*)-3-Cyclobutyl-6-phenyl-3,6-dihydro-1,2-dioxine (80b).** Colourless oil (2.11 g, 40%); R_f 0.54 (10% ethyl acetate in hexanes, v/v); IR (film): 3032, 2976, 2863, 1603 (weak), 1493, 1454, 1385, 1291, 1257 cm^{-1}; ^{1}H NMR (300 MHz, CDCl$_3$) δ 1.83−2.14 (m, 6H), 2.56−2.65 (m, 1H), 4.55 (dd, *J* = 6.3, 2.1 Hz, 1H), 5.46−5.47 (m, 1H), 6.07−6.15 (m, 2H), 7.31−7.40 (m, 5H); MS (EI) (C$_{14}$H$_{16}$O$_2$) *m/z* (%): (M$^+$ 216, < 1%), 172 (8), 161 (100), 145 (8), 133 (16), 115 (14), 105 (100), 91 (8), 83 (22), 77 (60), 55 (60).
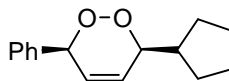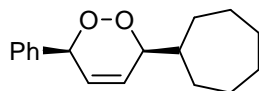

(±) **(3*S*,6*S*)-3-Cyclopentyl-6-phenyl-3,6-dihydro-1,2-dioxine (80c).** Colourless oil (1.43 g, 21%); R_f 0.57 (10% ethyl acetate in hexanes, v/v); IR (film): 3032, 2953, 2868, 2360 (weak), 1603 (weak), 1493, 1453, 1387, 1258 cm^{-1}; ^{1}H NMR (300 MHz, CDCl$_3$) δ 1.24−1.90 (m, 8H), 2.18 (sextet, *J* = 8.4, 8.4, 8.1 Hz, 1H), 4.37 (ddd, *J* = 2.4, 2.1, 1.8 Hz, 1H), 5.48 (dd, *J* = 2.4, 2.1 Hz, 1H), 6.08−6.21 (m, 2H), 7.30−7.42 (m, 5H); ^{13}C NMR (75 MHz, CDCl$_3$) δ 25.5, 25.7, 28.7, 29.6, 43.0, 80.4, 82.5, 126.8, 128.3, 128.7, 128.8, 128.9, 138.1; MS (EI) (C$_{15}$H$_{18}$O$_2$) *m/z* (%): (M$^+$ 230, 5%), 189 (10), 161 (100), 145 (5),

133 (15), 115 (5), 105 (45), 97 (12), 91 (5), 77 (25), 69 (30), 51 (5); HRMS (ESI, [M + Na]$^+$) calcd for $C_{15}H_{18}O_2Na_1$: 253.1204, found 253.1198.

(±) (3*S*,6*S*)-3-Cyclohexyl-6-phenyl-3,6-dihydro-1,2-dioxine (80d). Colourless solid (2.05 g, 59%); R_f 0.84 (30% ethyl acetate in hexanes, v/v); IR (nujol): 3082, 3054, 3032, 2932, 2862, 1491, 1453, 1337, 1316, 1292, 1272, 1254 cm^{-1}; ^{1}H NMR (300 MHz, CDCl$_3$) δ 1.30–1.90 (m, 10H), 2.18 (sextet, *J* = 8.7, 8.4, 8.1 Hz, 1H), 4.37 (ddd, *J* = 2.1, 2.1 Hz, 1H), 5.48 (dd, *J* = 2.4, 2.1 Hz, 1H), 6.08–6.18 (m, 2H), 7.35–7.47 (m, 5H); ^{13}C NMR (75 MHz, CDCl$_3$) δ 25.3, 25.4, 28.4, 29.4, 42.7, 80.1, 82.3, 126.6, 128.0, 128.4, 128.6, 128.6, 137.8; MS (EI) (C$_{16}$H$_{20}$O$_2$) *m/z* (%): (M$^+$ 244, < 1%), 198 (100), 169 (15), 156 (30), 142 (30), 129 (73), 115 (25), 105 (12), 79 (10); HRMS (ESI, [M + H]$^+$) calcd for C$_{16}$H$_{21}$O$_2$: 248.1776, found 248.1647. All data was identical to that reported previously.[128]


(±) (3*S*,6*S*)-3-Cycloheptyl-6-phenyl-3,6-dihydro-1,2-dioxine (80e). Colourless oil (1.90 g, 44%); R_f 0.60 (10% ethyl acetate in hexanes, v/v); IR (film): 3086, 3063, 3032, 2920, 2854, 2685, 1950, 1883, 1806, 1602, 1492, 1454, 1258 cm^{-1}; ^{1}H NMR (300 MHz, CDCl$_3$) δ 1.33–1.94 (m, 13H), 4.40–4.44 (m, 1H), 5.46 (dd, 1H), 6.10–6.21 (m, 2H), 7.33–7.42 (m, 5H); ^{13}C NMR (75 MHz, CDCl$_3$) δ 26.8, 26.9, 28.5, 28.8, 29.7, 30.5, 43.0, 127.1, 128.0, 128.7, 128.8, 138.3; MS (EI) (C$_{17}$H$_{22}$O$_2$) *m/z* (%): (M$^+$ 258, < 1%), 226 (100), 170 (12), 130 (55), 129 (55), 128 (55), 115 (35), 105 (30), 93 (8), 91 (10), 79 (8), 77 (8); HRMS (ESI, [M + NH$_4$]$^+$) calcd for C$_{17}$H$_{26}$O$_2$N$_1$: 276.1964, found 276.1962.
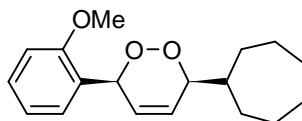
(±) (3*S*,6*S*)-3-Cycloheptyl-6-(2-methoxyphenyl)-3,6-dihydro-1,2-dioxine (80f). Colourless oil (2.8 g, 48%); R_f 0.57 (10% ethyl acetate in hexanes, v/v); IR (film): 3047, 3002, 2918, 2857, 2687, 2045, 1904, 1724, 1601, 1589, 1493, 1463, 1439, 1387, 1331, 1287, 1241, 1191 cm^{-1}; ^{1}H NMR (300 MHz, CDCl$_3$) δ 1.35–1.93 (m, 13H), 3.85 (s, 3H),

4.49 (dd, J = 1.5, 2.0 Hz, 1H), 5.90 (m, 1H), 6.07−6.16 (m, 2H), 6.88−6.98 (m, 2H), 7.26−7.32 (m, 2H), 7.40−7.43 (m, 1H); ^{13}C NMR (75 MHz, CDCl$_3$) δ 26.7, 26.7, 28.3, 28.5, 29.3, 30.2, 42.6, 55.4, 74.2, 82.5, 110.5, 120.3, 126.5, 127.0, 127.5, 129.2, 129.6, 157.3; MS (EI) (C$_{18}$H$_{24}$O$_3$) m/z (%): (M$^+$ 288, < 1%), 256 (100), 213 (8), 200 (20), 185 (8), 159 (25), 148 (12), 134 (30), 121 (22), 107 (8), 93 (10), 91 (10), 79 (5); HRMS (ESI, [M + NH$_4$]$^+$) calcd for C$_{18}$H$_{28}$O$_3$N$_1$: 306.2069, found 306.2070.

General Procedure for Construction of the Cyclopropane Core (81a–j). The phosphonate, (±)-Cbz-α-phosphonoglycine trimethyl ester (15 mmol) was dissolved in anhydrous, freshly distilled THF, under N$_2$. The solution was cooled to ca. −78 ^{o}C and freshly prepared, titrated LDA (mono-tetrahydrofuran complex in cyclohexane) (13 mmol) was added dropwise. After *ca.* 30 minutes, the 1,2-dioxine (14 mmol) was added and allowed to react for *ca.* 15 minutes before the reaction was warmed to *ca.* −15 to −10 ^{o}C. The reaction was maintained at this temperature for at least 4 hours and then allowed to warm to rt overnight. The reaction was quenched with half-saturated NH$_4$Cl$_{(aq)}$, extracted with diethyl ether, dried over MgSO$_{4(s)}$, filtered and the solvents removed *in vacuo* to yield the crude reaction extract containing a 1:1 mixture of diastereoisomers. Flash column chromatography (20% ethyl acetate in hexanes, v/v) afforded the desired pure diastereoisomers.
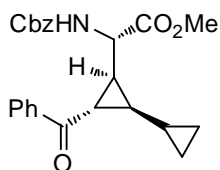
Methyl (2S)-[(1R,2S,3S)-3-benzoyl-1,1'-bi(cyclopropyl)-2-yl]{[(benzyloxy)carbonyl]amino}ethanoate (81a). Colourless needles (500 mg, 27%); mp: 84−85 ^{o}C; R$_f$ 0.25 (20% ethyl acetate in hexanes, v/v); IR (nujol): 3384, 3073, 2924, 2727, 1740, 1704, 1662, 1597, 1580, 1520, 1456, 1377, 1294, 1284, 1230 cm^{-1}; ^{1}H NMR (600 MHz, CDCl$_3$) δ 0.28−0.31 (m, 1H), 0.39−0.42 (m, 1H), 0.61−0.68 (m, 2H), 1.01−1.06 (m, 1H), 1.67 (ddd, J = 6.0, 3.6, 1.8 Hz, 1H), 2.02 (ddd, J = 6.0, 4.8, 3.0 Hz, 1H), 2.88 (dd, J = 4.8, 4.8 Hz, 1H), 3.82 (s, 3H), 4.51 (dd, J = 9.0, 1.8 Hz, 1H), 5.10 (dd, J = 12.6, 12.6 Hz, 1H), 5.57 (d, J = 8.4 Hz, 1H), 7.26−7.30 (m, 4H), 7.34−7.37 (m, 1H), 7.42−7.45 (m, 2H), 7.54−7.57 (m, 1H), 7.96−7.97 (m, 2H); ^{13}C NMR (150 MHz,

CDCl$_3$) δ 4.8, 8.8, 28.1, 34.2, 34.3, 52.7, 53.0, 67.1, 127.9, 128.2, 128.5, 128.6, 133.0, 136.1, 137.4, 156.1, 171.6, 198.3; MS (EI) (C$_{24}$H$_{25}$O$_5$N) *m/z* (%): (M$^+$ 407, < 1%), 240 (6), 185 (100), 167 (6), 157 (6), 144 (12), 129 (8), 115 (9), 105 (100), 91 (9), 77 (70), 59 (4), 51 (8); HRMS (ESI, [M + H]$^+$) calcd for C$_{24}$H$_{26}$O$_5$N: 408.1811, found 408.1813; Anal. Calcd. for C$_{24}$H$_{25}$O$_5$N: C, 70.74; H, 6.18; N, 3.44. Found: C, 70.74; H, 6.13; N, 3.48.
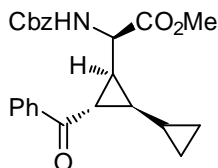

Methyl (2R)-[(1R,2S,3S)-3-benzoyl-1,1'-bi(cyclopropyl)-2-yl]{[(benzyloxy)carbonyl]amino}ethanoate (81b). Colourless needles (500 mg, 27%); mp: 104−105 ^{o}C; R$_f$ 0.18 (20% ethyl acetate in hexanes, v/v); IR (nujol): 3342, 3181, 2924, 2727, 2671, 1749, 1725, 1716, 1648, 1596, 1577, 1531, 1462, 1377, 1340, 1270, 1202 cm$^-$1; ^{1}H NMR (600 MHz, CDCl$_3$) δ 0.22−0.26 (m, 1H), 0.29−0.33 (m, 1H), 0.53−0.57 (m, 1H), 0.59−0.63 (m, 1H), 0.81−0.82 (m, 1H), 1.54 (ddd, *J* = 8.4, 7.2, 4.8 Hz, 1H), 1.95 (ddd, *J* = 4.8, 4.2, 2.4 Hz, 1H), 2.80 (dd, *J* = 4.8, 4.2 Hz, 1H), 3.69 (s, 3H), 4.33−4.36 (m, 1H), 5.14 (dd, *J* = 21, 12 Hz, 2H), 5.45 (d, *J* = 7.8 Hz, 1H), 7.31−7.59 (m, 8H), 7.98−8.00 (m, 2H); ^{13}C NMR (150 MHz, CDCl$_3$) δ 4.9, 5.1, 8.3, 29.5, 31.9, 33.1, 52.5, 53.3, 67.1, 128.0, 128.1, 128.2, 128.5, 128.6, 133.1, 136.2, 137.4, 155.6, 172.1, 197.9; MS (EI) (C$_{24}$H$_{25}$O$_5$N) *m/z* (%): (M$^+$ 407, < 1%), 240 (3), 185 (100), 167 (6), 157 (6), 144 (15), 129 (8), 115 (8), 105 (100), 91 (9), 77 (65), 59 (4), 51 (6); HRMS (ESI, [M + H]$^+$) calcd for C$_{24}$H$_{26}$O$_5$N: 408.1811, found 408.1816; Anal. Calcd. for C$_{24}$H$_{25}$O$_5$N: C, 70.74; H, 6.18; N, 3.44. Found: C, 70.66; H, 6.20; N, 3.46.
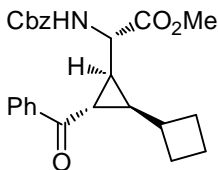
Methyl (2S)-[(1S,2S,3R)-2-benzoyl-3-cyclobutylcyclopropyl]{[(benzyloxy)carbonyl]amino}ethanoate (81c). Colourless needles (230 mg, 14%); mp: 115−117 ^{o}C; R$_f$ 0.28 (20% ethyl acetate in hexanes, v/v); IR (nujol): 3383, 2926, 2727, 2671, 1737, 1703, 1662, 1596, 1579, 1520, 1463, 1377,

1288 cm^{-1}; ^{1}H NMR (300 MHz, CDCl$_3$) δ 1.81–2.24 (m, 8H), 2.46–2.51 (m, 1H), 2.78–2.81 (m, 1H), 3.77 (s, 3H), 4.21–4.28 (m, 1H), 5.04–5.13 (m, 2H), 5.50 (d, J = 8.7 Hz, 1H), 7.27–7.59 (m, 8H), 7.96–7.99 (m, 2H); MS (EI) (C$_{25}$H$_{27}$O$_5$N) m/z (%): (M$^+$ 421, < 1%), 254 (9), 199 (50), 171 (40), 105 (100), 91 (55), 77 (50), 65 (5), 51 (6); HRMS (ESI, [M + Na]$^+$) calcd for C$_{25}$H$_{27}$O$_5$N$_1$Na$_1$: 444.1787, found 444.1779; Anal. Calcd. for C$_{25}$H$_{27}$O$_5$N: C, 71.24; H, 6.46; N, 3.32. Found: C, 71.52; H, 6.38; N, 3.29.
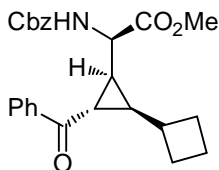
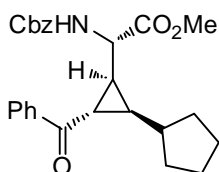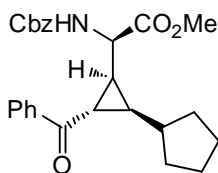
Methyl   (2R)-[(1S,2S,3R)-2-benzoyl-3-cyclobutylcyclopropyl]{[(benzyloxy)carbonyl]amino}ethanoate (81d). Colourless needles (436 mg, 27%); mp: 127–128 ^{o}C; R$_f$ 0.19 (20% ethyl acetate in hexanes, v/v); IR (nujol): 3352, 2921, 2727, 2671, 2363, 1741, 1696, 1657, 1597, 1578, 1518, 1460, 1377, 1269, 1240, 1213 cm^{-1}; ^{1}H NMR (600 MHz, CDCl$_3$) δ 1.77–1.96 (m, 6H), 1.98–2.03 (m, 1H), 2.10–2.16 (m, 1H), 2.26–2.32 (m, 1H), 2.69 (dd, J = 4.8, 4.8 Hz, 1H), 3.66 (s, 3H), 4.12 (dd, J = 10.2, 9.0 Hz, 1H), 5.13 (dd, J = 17.4, 12.6 Hz, 2H), 5.33 (br d, J = 8.4 Hz, 1H), 7.30–7.38 (m, 5H), 7.47–7.49 (m, 2H), 7.56–7.59 (m, 1H), 7.98–7.99 (m, 2H); ^{13}C NMR (150 MHz, CDCl$_3$) δ 18.5, 28.1, 28.6, 29.7, 31.6, 34.5, 35.5, 52.5, 53.2, 67.2, 128.1, 128.2, 128.5, 128.6, 133.0, 136.1, 137.5, 155.5, 172.0, 198.0; MS (EI) (C$_{25}$H$_{27}$O$_5$N) m/z (%): (M$^+$ 421, < 1%), 362 (2), 318 (2), 270 (2), 254 (5), 242 (2), 199 (57), 171 (43), 157 (3), 143 (2), 128 (3), 115 (3), 105 (100), 91 (50), 77 (45), 65 (3), 51 (6); HRMS (ESI, [M + Na]$^+$) calcd for C$_{25}$H$_{27}$O$_5$N$_1$Na$_1$: 444.1787, found 444.1783; Anal. Calcd. for C$_{25}$H$_{27}$O$_5$N$_1$: C, 71.24; H, 6.46; N, 3.32. Found: C, 71.32; H, 6.45; N, 3.33.

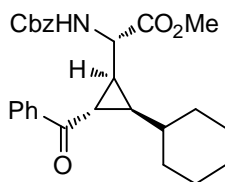**Methyl   (2S)-[(1S,2S,3R)-2-benzoyl-3-cyclopentylcyclopropyl]{[(benzyloxy)carbonyl]amino}ethanoate (81e).** Fine, colourless needles (294 mg, 17%); mp: 153–154 ^{o}C; R$_f$ 0.65 (30% ethyl acetate in

petroleum spirit, v/v); IR (nujol): 3462, 3381, 2923, 2854, 2728, 1956, 1900, 1813, 1738, 1704, 1662, 1596, 1580, 1520, 1456, 1377, 1290 cm^{-1}; ^{1}H NMR (600 MHz, CDCl$_3$) δ 1.34–1.38 (m, 2H), 1.39–1.54 (m, 1H), 1.58–1.75 (m, 4H), 1.88–1.95 (m, 3H), 2.08–2.12 (m, 1H), 2.80–2.81 (m, 1H), 3.80 (s, 3H), 4.33–4.36 (m, 1H), 5.09 (dd, J = 12.6 6.6 Hz, 2H), 5.48 (d, J = 9.0 Hz, 1H), 7.26–7.28 (m, 5H), 7.43–7.45 (m, 2H), 7.55–7.58 (m, 1H), 7.97–7.99 (m, 2H); ^{13}C NMR (150 MHz, CDCl$_3$) δ 25.1, 25.5, 29.2, 32.2, 33.6, 34.4, 38.3, 39.3, 52.6, 52.9, 67.1, 128.1, 128.2, 128.5, 128.6, 132.9, 136.0, 137.4, 156.0, 171.4, 198.6; MS (EI) (C$_{26}$H$_{29}$O$_5$N) m/z (%): (M$^+$ 435, < 1%), 213 (100), 145 (10), 105 (80), 91 (20), 77 (30), 67 (5), 51 (5); HRMS (ESI, [M + Na]$^+$) calcd for C$_{26}$H$_{29}$O$_5$N$_1$Na$_1$: 458.1943, found 458.1941.

Methyl (2R)-[(1S,2S,3R)-2-benzoyl-3-cyclopentylcyclopropyl]{[(benzyloxy)carbonyl]amino}ethanoate (81f). Fine, colourless needles (255 mg, 15%); mp: 115–117 °C; R$_f$ 0.56 (30% ethyl acetate in petroleum spirit, v/v); IR (nujol): 3373, 3063, 2922, 2728, 1737, 1698, 1658, 1598, 1581, 1528, 1456, 1377, 1283 cm^{-1}; ^{1}H NMR (600 MHz, CDCl$_3$) δ 1.28–1.37 (m, 2H), 1.47–1.86 (m, 8H), 1.94–1.98 (m, 1H), 2.74–2.76 (m, 1H), 3.65 (s, 3H), 4.20 (dd, J = 9.0, 1.8 Hz, 1H), 5.13 (dd, J = 31.8, 12 Hz, 2H), 5.39 (br d, J = 8.4 Hz, 1H), 7.31–7.37 (m, 5H), 7.47–7.49 (m, 2H), 7.57–7.59 (m, 1H), 7.99–8.01 (m, 2H); ^{13}C NMR (150 MHz, CDCl$_3$) δ 25.1, 25.5, 30.0, 32.0, 32.5, 33.3, 36.2, 38.7, 52.5, 53.2, 67.2, 128.1, 128.2, 128.5, 128.6, 133.0, 136.2, 137.5, 155.6, 172.1, 198.2; MS (EI) (C$_{26}$H$_{29}$O$_5$N) m/z (%): (M$^+$ 435, < 1%), 344 (8), 300 (8), 283 (8), 268 (8), 213 (100), 195 (20), 145 (20), 105 (75), 91 (40); HRMS (ESI, [M + NH$_4$]$^+$) calcd for C$_{26}$H$_{33}$O$_5$N$_2$: 453.2389, found 453.2391.
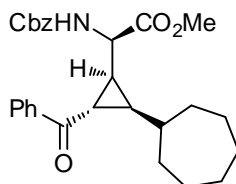
Methyl   **(2S)-[(1S,2S,3R)-2-benzoyl-3-cyclohexylcyclopropyl]{[(benzyloxy)carbonyl]amino}ethanoate (81g).** White solid (642 mg, 19%); mp: 150−151 ^{o}C; R_f 0.62 (30% ethyl acetate in hexanes, v/v); IR (nujol): 3387, 2926, 2727, 2669, 1737, 1708, 1659, 1595, 1580, 1519, 1455, 1377, 1292 cm^{-1}; ^{1}H NMR (600 MHz, CDCl$_3$) δ 1.08–2.13 (m, 13H), 2.74–2.76 (m, 1H), 3.79 (s, 3H), 4.29–4.32 (m, 1H), 5.07 (d, J = 12.0 Hz, 1H), 5.12 (d, J = 12.0 Hz, 1H), 5.48 (d, J = 8.4 Hz, 1H), 7.26–7.57 (m, 8H), 7.98–7.99 (m, 2H); ^{13}C NMR (150 MHz, CDCl$_3$) δ 25.8, 26.1, 26.2, 28.0, 32.9, 33.6, 34.3, 37.0, 39.0, 52.6, 52.9, 67.1, 128.0, 128.1, 128.2, 128.5, 128.6, 133.0, 136.0, 137.3, 156.0, 171.4, 198.6; MS (EI) (C$_{27}$H$_{29}$O$_5$N) m/z (%): (M$^+$ 450, < 1%), 227 (100), 209 (20), 145 (30), 105 (90), 91 (30); HRMS (ESI, [M + NH$_4$]$^+$) calcd for C$_{27}$H$_{35}$O$_5$N$_2$: 467.2546, found 467.2548. Data were identical to that previously reported.[128]
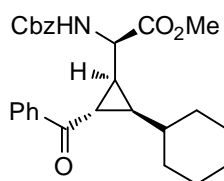
Methyl   **(2R)-[(1S,2S,3R)-2-benzoyl-3-cyclohexylcyclopropyl]{[(benzyloxy)carbonyl]amino}ethanoate (81h).** White solid (638 mg, 19%); mp: 156−158 ^{o}C; R_f 0.44 (30% ethyl acetate in hexanes, v/v); IR (nujol): 3349, 2924, 2854, 2727, 2668, 1774, 1742, 1696, 1670, 1598, 1581, 1518, 1456, 1378, 1286 cm^{-1}; ^{1}H NMR (600 MHz, CDCl$_3$) δ 1.07–1.28 (m, 6H), 1.06–1.76 (m, 6H), 1.93–1.97 (m, 1H), 2.70–2.72 (m, 1H), 3.65 (s, 3H), 4.17–4.21 (m, 1H), 5.08 (d, J = 12.6 Hz, 1H), 5.18 (d, J = 12.6 Hz, 1H), 5.36 (br d, J = 8.4 Hz, 1H), 7.31–7.37 (m, 5H), 7.47–7.50 (m, 2H), 7.56–7.59 (m, 1H), 8.00–8.01 (m, 2H); ^{13}C NMR (150 MHz, CDCl$_3$) δ 25.8, 26.0, 26.1, 28.8, 32.3, 33.3, 33.6, 36.7, 37.1, 52.5, 53.2, 67.2, 128.0, 128.1, 128.2, 128.5, 128.6, 133.0, 136.2, 137.4, 155.5, 172.2, 198.3; MS (EI) (C$_{27}$H$_{29}$O$_5$N) m/z (%): (M$^+$ 450, < 1%), 390 (7), 358 (5), 346 (7), 329 (8), 297 (7), 265 (5), 239 (15), 227 (75), 209 (25), 145 (30), 131 (15), 105 (100), 91 (60); HRMS (ESI, [M + NH$_4$]$^+$) calcd for C$_{27}$H$_{35}$O$_5$N$_2$: 467.2546, found 467.2547. Data were identical to that previously reported.[128]
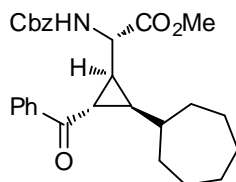
Methyl **(2S)-[(1S,2S,3R)-2-benzoyl-3-cycloheptylcyclopropyl]{[(benzyloxy)carbonyl]amino}ethanoate (81i).** Off-white solid (45 mg, 10%); R_f 0.36 (3% diethyl ether in dichloromethane, v/v); ^{1}H NMR (300 MHz, CDCl$_3$) δ 1.33−1.90 (m, 14H), 2.11 (dddd, J = 4.5, 4.2, 3.0, 1.5 Hz, 1H), 2.76 (dd, J = 4.8, 4.8 Hz, 1H), 3.78 (s, 3H), 4.31 (dd, J = 9.9, 9.6 Hz, 1H), 5.09 (dd, J = 12.3, 3.9 Hz, 2H), 5.47 (br d, J = 8.4 Hz, 1H), 7.28−7.56 (m, 8H), 7.97−8.00 (m, 2H).

Methyl **(2R)-[(1S,2S,3R)-2-benzoyl-3-cycloheptylcyclopropyl]{[(benzyloxy)carbonyl]amino}ethanoate (81j).** Off-white solid (33 mg, 7%); R_f 0.25 (3% diethyl ether in dichloromethane, v/v); ^{1}H NMR (300 MHz, CDCl$_3$) δ 1.36−1.96 (m, 15H), 2.71−2.74 (m, 1H), 3.65 (s, 3H), 4.20 (dd, J = 9.3, 1.2 Hz, 1H), 5.13 (dd, J = 15.6, 12.3 Hz, 2H), 5.40 (br d, J = 8.7 Hz, 1H), 7.31−7.61 (m, 8H), 7.99−8.02 (m, 2H).

General Procedures for the Preparation of Baeyer-Villiger Oxidation Products (87a−h).

Method A.[176] To a stirred mixture of 30% H$_2$O$_2$ (29 mmol) and dichloromethane (10 mL), cooled to 0 °C was added trifluoroacetic anhydride (92 mmol) dropwise. On completion of addition, temperature was maintained at 0 °C with the dropwise addition of the phenyl ketone (0.44 mol) dissolved in dichloromethane (10 mL). The reaction was stirred under nitrogen and allowed to warm to rt overnight. Following this, the reaction was quenched by pouring into 2% K$_2$CO$_{3(aq)}$ solution and extracting with dichloromethane. The organic extracts were pooled, dried over MgSO$_4$, filtered and the volatiles removed *in vacuo*. Flash column chromatography (30% ethyl acetate in hexanes, v/v) afforded the pure phenyl ester.

Method B. The phenyl ketone (3 mmol) along with *meta*-chloroperbenzoic acid (20 mmol), were dissolved in chloroform and the solution left in the dark at rt for 1 month. After quenching the reaction with saturated sodium thiosulfate solution, the resulting solution was extracted with dichloromethane. The organic extracts were washed with saturated $NaHCO_{3(aq)}$ solution followed by saturated $NaCl_{(aq)}$ solution. The organic extracts were pooled, dried over $MgSO_4$, filtered and the volatiles removed *in vacuo*. Flash column chromatography (30% ethyl acetate in hexanes, v/v) afforded the pure phenyl ester.
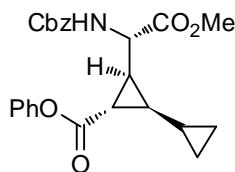
Phenyl (1*R*,2*S*,3*S*)-3-[(1*S*)-1-{[(benzyloxy)carbonyl]amino}-2-methoxy-2-oxoethyl]-1,1'-bi(cyclopropyl)-2-carboxylate (87a). Prepared via method A: Pale yellow oil (75 mg, 24%); Prepared via method B: Colourless, sticky, viscous oil (954 mg, 77%); R_f 0.45 (5% diethyl ether in dichloromethane, v/v); IR (nujol): 3351, 3066, 3033, 3004, 2954, 2850, 1732, 1593, 1494, 1456, 1376 cm^{-1}; ^{1}H NMR (300 MHz, CDCl$_3$) δ 0.35−0.43 (m, 2H), 0.65−0.68 (m, 2H), 0.96−0.98 (m, 1H), 1.64 (ddd, *J* = 5.4, 3.6, 1.5 Hz, 1H), 1.87−1.96 (m, 2H), 3.82 (s, 3H), 4.41 (t, *J* = 9.6 Hz, 1H), 5.15 (dd, *J* = 12.0, 9.9 Hz, 2H), 5.53 (d, *J* = 8.1 Hz, 1H), 7.04−7.07 (m, 2H), 7.19−7.39 (m, 3H); ^{13}C NMR (75 MHz, CDCl$_3$) δ 4.6, 4.8, 8.3, 23.3, 31.1, 31.7, 52.6, 52.7, 67.2, 121.4, 125.8, 128.1, 128.2, 128.6, 129.3, 136.1, 150.6, 155.9, 171.5, 171.6; MS (EI) (C$_{24}$H$_{25}$O$_6$N) *m/z* (%): (M$^+$ 423, < 1%), 201 (50), 162 (6), 134 (5), 119 (6), 107 (20), 91 (100), 79 (25), 65 (10), 51 (5); HRMS (ESI, [M + NH$_4$]$^+$) calcd for C$_{24}$H$_{29}$O$_6$N$_2$: 441.2026, found 441.2027.
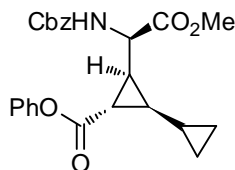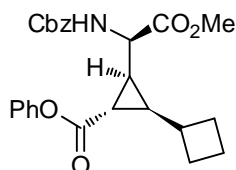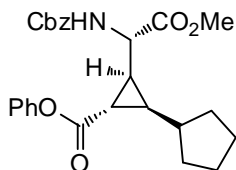

Phenyl (1*R*,2*S*,3*S*)-3-[(1*R*)-1-{[(benzyloxy)carbonyl]amino}-2-methoxy-2-oxoethyl]-1,1'-bi(cyclopropyl)-2-carboxylate (87b). Prepared via method A: Pale yellow oil (57 mg, 11%); ^{1}H NMR (300 MHz, CDCl$_3$) δ 0.23−0.79 (m, 5H), 1.45−1.52 (m, 1H), 1.82−1.97 (m, 2H), 3.82 (s, 3H), 4.25−4.31 (m, 1H), 5.08−5.18 (m, 2H), 5.40 (d, *J* = 8.1

Hz, 1H), 6.99−7.04 (m, 2H), 7.07−7.43 (m, 8H). Compound decomposition prevented further analysis.

Phenyl (1S,2S,3R)-2-[(1S)-1-{[(benzyloxy)carbonyl]amino}-2-methoxy-2-oxoethyl]-3-cyclobutylcyclopropanecarboxylate (87d). Prepared via method B: Yellow-brown solid (145 mg, 47%); ^{1}H NMR (300 MHz, CDCl$_3$) δ 0.23−0.79 (m, 5H), 1.45−1.52 (m, 1H), 1.82−1.97 (m, 2H), 3.82 (s, 3H), 4.25−4.31 (m, 1H), 5.08−5.18 (m, 2H), 5.40 (d, J = 8.1 Hz, 1H), 6.99−7.04 (m, 2H), 7.07−7.43 (m, 8H). Compound decomposition prevented further analysis.

Phenyl (1S,2S,3R)-2-[(1S)-1-{[(benzyloxy)carbonyl]amino}-2-methoxy-2-oxoethyl]-3-cyclopentylcyclopropanecarboxylate (87e). Prepared via method A: White solid (334 mg, 64% + 84 mg starting material, inseparable); R$_f$ 0.64 (30% ethyl acetate in petroleum spirit, v/v); IR (film): 3337, 3033, 2952, 2866, 1747, 1722, 1704, 1667, 1597, 1524, 1496, 1453, 1437, 1340, 1277, 1233, 1198, 1150, 1051 cm^{-1}; ^{1}H NMR (300 MHz, CDCl$_3$) δ 1.26−2.15 (m, 12H), 3.80 (s, 3H), 4.20−4.26 (m, 1H), 5.08−5.20 (m, 2H), 5.53 (d, J = 8.1 Hz, 1H), 7.05−7.07 (m, 2H), 7.11−7.59 (m, 8H); ^{13}C NMR (75 MHz, CDCl$_3$) (partial) δ 24.4, 25.0, 25.5, 31.4, 32.1, 33.5, 35.3, 38.9, 52.5, 52.6, 67.3, 121.5, 125.7, 128.1, 128.3, 128.5, 129.3, 132.6, 136.0, 150.6, 155.7, 171.5.
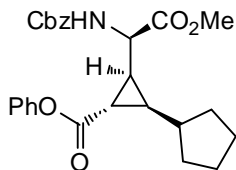
Phenyl (1S,2S,3R)-2-[(1R)-1-{[(benzyloxy)carbonyl]amino}-2-methoxy-2-oxoethyl]-3-cyclopentylcyclopropanecarboxylate (87f). Prepared via method A: White solid

(135 mg, 19%); mp: 117–118 °C; R_f 0.59 (30% ethyl acetate in petroleum spirit, v/v); IR (nujol): 3372, 3065, 2920, 2727, 1732, 1698, 1592, 1520, 1456, 1377, 1285 cm^{-1}; ^{1}H NMR (300 MHz, CDCl$_3$) δ 1.28–1.30 (m, 1H), 1.41–1.70 (m, 8H), 1.80–1.92 (m, 3H), 3.81 (s, 3H), 4.12 (dd, J = 3, 8.1 Hz, 1H), 5.13 (dd, J = 12.3 Hz, 2H), 5.33 (d, J = 9 Hz, 1H), 7.04–7.07 (m, 2H), 7.19–7.24 (m, 1H), 7.30–7.40 (m, 7H); ^{13}C NMR (75 MHz, CDCl$_3$) δ 25.0, 25.3, 25.5, 29.6, 32.3, 33.2, 33.6, 38.3, 52.6, 52.8, 67.2, 121.4, 125.8, 128.0, 128.2, 128.5, 129.3, 136.1, 150.6, 155.6, 171.5, 172.1; MS (EI) (C$_{26}$H$_{29}$O$_6$N) m/z (%): (M$^+$ 452, < 1%), 358 (15), 250 (15), 222 (33), 190 (8), 162 (8), 135 (10), 119 (8), 108 (25), 91 (100), 79 (30), 65 (10), 51 (8); HRMS (ESI, [M + Na]$^+$) calcd for C$_{26}$H$_{29}$O$_6$N$_1$Na$_1$: 474.1893, found 474.1890.
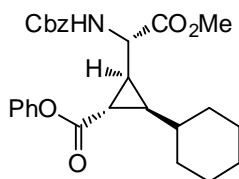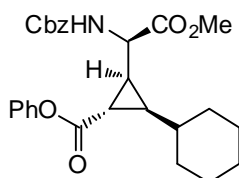

Phenyl (1S,2S,3R)-2-[(1S)-1-{[(benzyloxy)carbonyl]amino}-2-methoxy-2-oxoethyl]-3-cyclohexylcyclopropanecarboxylate (87g). Prepared via method A: Colourless needles (415 mg, 73%); mp: 143–145 °C; R_f 0.67 (30% ethyl acetate in petroleum spirit, v/v); IR (nujol): 3387, 3069, 2922, 2727, 2671, 1740, 1702, 1656, 1590, 1520, 1499, 1460, 1377, 1346, 1293 cm^{-1}; ^{1}H NMR (300 MHz, CDCl$_3$) δ 0.88–2.03 (m, 14H), 3.79 (s, 3H), 4.16–4.23 (m, 1H), 5.15 (dd, J = 10.2, 12.3 Hz, 2H), 5.51 (d, J = 8.4 Hz, 1H), 7.03–7.07 (m, 2H), 7.18–7.38 (m, 8H); ^{13}C NMR (75 MHz, CDCl$_3$) δ 23.4, 25.7, 26.0, 26.1, 30.9, 32.7, 33.3, 36.1, 36.7, 52.4, 52.7, 67.2, 121.4, 125.7, 128.1, 128.3, 128.6, 129.3, 136.0, 150.6, 155.9, 171.5, 171.8; MS (EI) (C$_{27}$H$_{31}$O$_6$N) m/z (%): (M$^+$ 466, < 1%), 372 (30), 344 (8), 328 (25), 310 (23), 268 (15), 251 (15), 223 (20), 91 (100); HRMS (ESI, [M + H]$^+$) calcd for C$_{27}$H$_{32}$O$_6$N$_1$: 466.2230, found 466.2233; Anal. calcd for C$_{27}$H$_{31}$O$_6$N$_1$: C, 69.66; H, 6.71; N, 3.01. Found: C, 69.40; H, 6.98; N, 2.97.


Phenyl (1S,2S,3R)-2-[(1R)-1-{[(benzyloxy)carbonyl]amino}-2-methoxy-2-oxoethyl]-3-cyclohexylcyclopropanecarboxylate (87h). Prepared via method A: White solid (97

mg, 47%); mp: 134−135°C; R_f 0.63 (30% ethyl acetate in petroleum spirit, v/v); IR (nujol): 3350, 3065, 2922, 2728, 2668, 1746, 1732, 1699, 1592, 1518, 1496, 1459, 1377, 1345, 1286, 1286, 1202 cm^{-1}; ^{1}H NMR (300 MHz, CDCl$_3$) δ 1.12−1.89 (m, 14H), 3.81 (s, 3H), 4.07−4.14 (m, 1H), 5.05−5.20 (m, 2H), 5.37 (d, J = 9 Hz, 1H), 7.04−7.06 (m, 2H), 7.19−7.39 (m, 8H); ^{13}C NMR (75 MHz, CDCl$_3$) δ 24.4, 25.7, 25.9, 26.1, 29.6, 33.2, 33.5, 34.5, 36.4, 52.7, 52.8, 67.2, 121.4, 125.8, 128.0, 128.2, 128.5, 129.4, 136.1, 150.6, 155.5, 155.5, 171.6, 172.2; MS (EI) (C$_{27}$H$_{31}$O$_6$N) m/z (%): (M$^+$ 466, < 1%), 372 (9), 344 (5), 328 (30), 310 (45), 268 (9), 250 (13), 223 (10), 142 (9), 91 (100); HRMS (ESI, [M + NH$_4$]$^+$) calcd for C$_{27}$H$_{35}$O$_6$N$_2$: 483.2495, found 483.2497.

General Procedure for Bis Methyl Ester Formation (88a−d). The phenyl ester was dissolved in anhydrous methanol and concentrated H$_2$SO$_4$ (2 drops) was added. The solution was heated under reflux for 16 h at which point solid NaHCO$_3$ (120 mg) was added and the methanol removed in vacuo until a volume of 5 mL remained. Dichloromethane was added and the solution extracted with sat. NaHCO$_3$ solution. The aqueous extract was extracted with further dichloromethane, the organic extracts pooled, dried over MgSO$_4$, filtered and the volatiles removed *in vacuo*. Flash column chromatography (5% diethyl ether in dichloromethane, v/v) of the residue afforded the pure methyl ester.
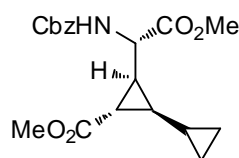
Methyl (1R,2S,3S)-3-[(1S)-1-{[(benzyloxy)carbonyl]amino}-2-methoxy-2-oxoethyl]-1,1'-bi(cyclopropyl)-2-carboxylate (88a). Colourless, viscous oil (385 mg, 96%); R_f 0.43 (5% diethyl ether in dichloromethane, v/v); IR (film): 3345, 3066, 3034, 3006, 2954, 2903, 2846, 1724, 1709, 1587, 1526, 1455, 1395 cm^{-1}; ^{1}H NMR (600 MHz, CDCl$_3$) δ 0.26−0.28 (m, 1H), 0.32−0.35 (m, 1H), 0.57−0.63 (m, 2H), 0.90−0.91 (m, 1H), 1.49 (ddd, J = 6.0, 3.0, 1.8 Hz, 2H), 1.70 (t, J = 4.2 Hz, 1H), 1.76 (dddd, J = 4.8, 4.8, 3.0, 1.2 Hz, 1H), 3.64 (s, 3H), 3.79 (s, 3H), 4.31 (t, J = 9.6 Hz, 1H), 5.12 (dd, J = 14.4, 12.0 Hz, 2H), 5.44 (d, J = 8.4 Hz, 1H), 7.34 (m, 5H); ^{13}C NMR (150 MHz, CDCl$_3$) δ 0.2, 4.7, 4.8, 8.4, 23.2, 30.5, 31.0, 52.1, 52.8, 67.3, 128.3, 128.4, 128.7, 136.3, 156.1, 171.9, 173.5; MS (EI) (C$_{19}$H$_{23}$O$_6$N) m/z (%): (M$^+$ 361, < 1%), 258 (5), 226 (3), 194 (3),

166 (4), 139 (70), 107 (24), 91 (100), 79 (45), 59 (10); HRMS (ESI, [M + Na]$^+$) calcd for $C_{19}H_{23}O_6N$: 384.1423, found 384.1421.
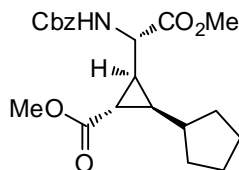
Methyl (1S,2S,3R)-2-[(1S)-1-{[(benzyloxy)carbonyl]amino}-2-methoxy-2-oxoethyl]-3-cyclopentylcyclopropanecarboxylate (88b). White solid (316 mg, 80%); mp: 96−97.5 ^{o}C; R$_f$ 0.57 (30% ethyl acetate in petroleum spirit, v/v); IR (nujol): 3348, 2919, 1746, 1723, 1705, 1525, 1463, 1377, 1351, 1285 cm^{-1}; ^{1}H NMR (600 MHz, CDCl$_3$) δ 1.30−1.91 (m, 12H), 3.66 (s, 3H), 3.78 (s, 3H), 5.08−5.15 (m, 2H), 5.39 (d, J = 7.8 Hz, 1H), 7.31−7.38 (m, 5H); ^{13}C NMR (150 MHz, CDCl$_3$) δ 24.2, 25.0, 25.5, 30.6, 32.1, 33.3, 34.4, 38.9, 51.9, 52.5, 52.6, 67.2, 128.1, 128.2, 128.5, 136.1, 155.9, 171.6, 173.7; MS (EI) ($C_{21}H_{27}O_6N$) m/z (%): (M$^+$ 389, < 1%), 330 (4), 286 (3), 250 (3), 222 (12), 194 (10), 167 (100), 154 (6), 135 (75), 126 (9), 119 (19), 108 (55), 91 (100), 79 (74), 67 (35), 59 (19), 51 (13); HRMS (ESI, [M + Na]$^+$) calcd for $C_{21}H_{27}O_6N_1Na_1$: 412.1736, found 412.1734; Anal. calcd for $C_{21}H_{27}O_6N_1$: C, 64.77; H, 6.99; N, 3.60. Found: C, 64.86; H, 7.19; N, 3.62.
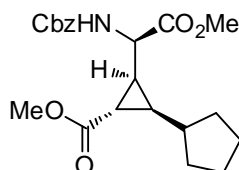
Methyl (1S,2S,3R)-2-[(1R)-1-{[(benzyloxy)carbonyl]amino}-2-methoxy-2-oxoethyl]-3-cyclopentylcyclopropanecarboxylate (88c). White solid (96 mg, 82%); mp: 95−97 ^{o}C; R$_f$ 0.53 (30% ethyl acetate in petroleum spirit, v/v); IR (nujol): 3435, 3385, 2958, 2926, 2857, 1747, 1719, 1702, 1516, 1456, 1377, 1338, 1204, 1048 cm^{-1}; ^{1}H NMR (600 MHz, CDCl$_3$) δ 1.22−1.84 (m, 12H), 3.66 (s, 3H), 3.76 (s, 3H), 4.01−4.04 (m, 1H), 5.07−5.16 (m, 2H), 5.27 (d, J = 8.4 Hz, 1H), 7.31−7.36 (m, 5H); ^{13}C NMR (150 MHz, CDCl$_3$) δ 0.0, 25.0, 25.5, 28.8, 32.4, 32.9, 33.1, 38.3, 52.0, 52.6, 52.9, 67.2, 128.1, 128.2, 128.5, 136.1, 155.6, 172.2, 173.3; MS (EI) ($C_{21}H_{27}O_6N$) m/z (%): (M$^+$ 389, < 1%), 330 (10), 286 (4), 254 (5), 222 (3), 204 (3), 194 (4), 167 (26), 135 (19), 119 (6),

108 (22), 91 (100), 79 (30), 67 (10), 59 (6), 51 (6); HRMS (ESI, $[M + H]^+$) calcd for $C_{21}H_{28}O_6N_1$: 390.1917, found 390.1916.
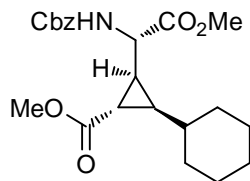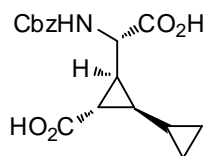

Methyl (1S,2S,3R)-2-[(1S)-1-{[(benzyloxy)carbonyl]amino}-2-methoxy-2-oxoethyl]-3-cyclohexylcyclopropanecarboxylate (88d). Colourless solid (258 mg, 76%); mp: 129−130 °C; R_f 0.64 (30% ethyl acetate in petroleum spirit, v/v); IR (nujol): 3345, 2916, 2728, 2671, 2360, 1751, 1718, 1706, 1523, 1461, 1377, 1364, 1344, 1282, 1231 cm^{-1}; ^{1}H NMR (600 MHz, CDCl$_3$) δ 1.07−1.25 (m, 6H), 1.39−1.41 (m, 1H), 1.55−1.91 (m, 7H), 3.65 (s, 3H), 3.77 (s, 3H), 4.08−4.11 (m, 1H), 5.09−5.15 (m, 2H), 5.37 (d, J = 7.8 Hz, 1H), 7.32−7.38 (m, 5H); ^{13}C NMR (150 MHz, CDCl$_3$) δ 0.0, 23.2, 25.8, 26.0, 26.2, 30.2, 32.8, 33.3, 35.2, 36.6, 51.9, 52.6, 67.2, 128.1, 128.3, 128.6, 136.1, 155.8, 171.7, 173.7; MS (EI) ($C_{21}H_{27}O_6N$) m/z (%): (M^+ 403, < 1%), 344 (6), 300 (5), 268 (5), 236 (4), 204 (5), 181 (33), 149 (16), 133 (6), 121 (6), 108 (26), 91 (100), 79 (32), 67 (10), 55 (7); HRMS (ESI, $[M + H]^+$) calcd for $C_{22}H_{30}O_6N_1$: 404.2073, found 404.2076.

General Procedure for Ester Hydrolysis (89a−d). The methyl ester (1.0 mol) was dissolved in THF (5 mL) and stirred with 2.5M LiOH (10 mL, 25 mmol) solution at rt overnight. Brine (10 mL) was added followed by acidification with concentrated HCl (2 drops). The solution was then extracted with ether (2 × 15 mL), dried over MgSO$_4$, filtered and the solvents removed *in vacuo*.

(1R,2S,3S)-3-[(S)-{[(Benzyloxy)carbonyl]amino}(carboxy)methyl]-1,1'-bi(cyclopropyl)-2-carboxylic acid (89a). White solid (298 mg, 92%); mp: 130−132 °C; IR (nujol): 3303, 2922, 2727, 2672, 1702, 1456, 1377, 1301, 1245 cm^{-1}; ^{1}H NMR (600 MHz, CD$_3$OD) δ 0.25−0.30 (m, 2H), 0.54−0.62 (m, 2H), 0.95−0.96 (m, 1H), 1.50−1.53 (m, 2H), 1.83−1.87 (m, 1H), 4.14 (d, J = 10.2 Hz, 1H), 5.10 (dd, J = 12.6, 10.2 Hz, 2H),

7.28–7.36 (m, 5H); ^{13}C NMR (150 MHz, CD_3OD) δ 5.5, 5.6, 9.6, 24.7, 31.7, 32.7, 68.1, 129.2, 129.4, 130.0, 138.8, 159.2, 177.4, 210.3; MS (EI) ($C_{17}H_{19}O_6N$) m/z (%): (M^+ 333, 7%), 328 (14), 310 (10), 239 (14), 212 (27), 166 (45), 152 (14), 107 (100), 91 (55), 79 (36); HRMS (ESI, $[M + H]^+$) calcd for $C_{17}H_{20}O_6N_1$: 334.1291, found 334.1289.
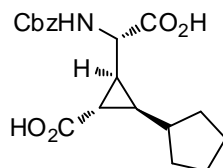
(1S,2S,3R)-2-[(S)-{[(Benzyloxy)carbonyl]amino}(carboxy)methyl]-3-cyclopentylcyclopropanecarboxylic acid (89b). Off-white solid (238 mg, 99%); mp: 165−167 ^{o}C; IR (nujol): 3335, 2924, 2858, 2727, 2677, 1710, 1694, 1678, 1535, 1464, 1377, 1342, 1298, 1254, 1224 cm^{-1}; ^1H NMR (600 MHz, CD_3OD) δ 1.28−1.98 (m, 12H), 3.98 (d, J = 10.2 Hz, 1H), 5.10 (dd, J = 15.6, 12.6 Hz, 2H), 7.26−7.36 (m, 5H); ^{13}C NMR (150 MHz, CD_3OD) δ 26.0, 26.4, 26.9, 31.8, 33.8, 34.8, 36.1, 40.9, 54.6, 68.2, 129.1, 129.4, 130.0, 138.7, 159.1, 174.9, 177.8; MS (EI) ($C_{19}H_{22}O_6N$) m/z (%): (M^+ 361, < 1%), 343 (4), 236 (4), 226 (8), 210 (7), 208 (7), 180 (10), 164 (8), 135 (7), 117 (7), 91 (100); HRMS (ESI, $[M + 2H]^+$) calcd for $C_{19}H_{24}O_6N_1$: 362.1604, found 362.1603.

(1S,2S,3R)-2-[(R)-{[(Benzyloxy)carbonyl]amino}(carboxy)methyl]-3-cyclopentylcyclopropanecarboxylic acid (89c). Off-white solid (68 mg, 96%); dec: 210 ^{o}C; IR (nujol): 3307, 2924, 2862, 2727, 2671, 1714, 1694, 1652, 1538, 1464, 1377, 1342, 1297, 1226 cm^{-1}; ^1H NMR (300 MHz, CD_3OD) δ 1.26−1.85 (m, 12H), 3.75−3.82 (m, 1H), 4.99−5.14 (m, 2H), 7.26−7.35 (m, 5H); ^{13}C NMR (75 MHz, CD_3OD) δ 26.1, 26.6, 26.8, 29.8, 30.9, 33.6, 34.3, 40.1, 54.6, 67.8, 129.0, 129.1, 129.6, 138.4, 158.4, 175.5, 177.2; MS (EI) ($C_{19}H_{22}O_6N$) m/z (%): (M^+ 361, < 1%), 313 (1), 285 (2), 239 (8), 212 (23), 166 (45), 152 (15), 107 (100); HRMS (ESI, $[M + 2H]^+$) calcd for $C_{19}H_{24}O_6N_1$: 362.1604, found 362.1600.
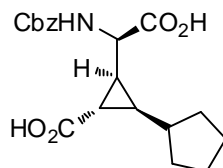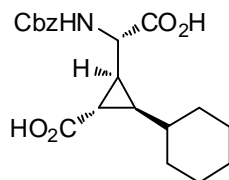
(1S,2S,3R)-2-[(S)-{[(Benzyloxy)carbonyl]amino}(carboxy)methyl]-3-cyclohexylcyclopropanecarboxylic acid (89d). White solid (185 mg, 97%); mp: 160–167 $^{\circ}$C; IR (nujol): 3306, 2923, 2854, 2729, 1728, 1694, 1682, 1538, 1463, 1409, 1377, 1326, 1285, 1246 cm^{-1}; ^{1}H NMR (600 MHz, CD$_3$OD) δ 1.06–1.41 (m, 8H), 1.63–2.02 (m, 6H), 3.93–3.95 (m, 1H), 5.05–5.12 (m, 2H), 7.25–7.35 (m, 5H); ^{13}C NMR (150 MHz, CD$_3$OD) δ 25.1, 27.4, 27.7, 27.9, 31.7, 34.4, 34.9, 37.0, 38.5, 54.6, 68.2, 129.2, 129.4, 130.0, 138.7, 159.1, 175.4, 178.1; MS (EI) (C$_{20}$H$_{25}$O$_6$N) *m/z* (%): (M$^+$ 375, < 1%), 357 (12), 250 (15), 240 (15), 224 (16), 194 (14), 178 (32), 131 (35), 108 (47), 91 (100), 79 (70); HRMS (ESI, [M + H]$^+$) calcd for C$_{20}$H$_{26}$O$_6$N$_1$: 376.1760, found 376.1760.

General Procedure for Amine Deprotection. The protected amine (0.8 mmol) was dissolved in methanol (10 mL) to which 5% Pd/C (20 wt%) was added. The reaction was purged of air by placing under vacuum and subsequently filled with H$_{2(g)}$ held in a hydrogen balloon. The reaction was stirred at rt for 48 h and then filtered through a pad of kenite, using methanol and water to flush the product off of the catalyst. All solvents were removed *in vacuo* and the residue completely dried under a hard vacuum.

General Procedure for Purification of Free Amine

To the crude residue obtained after hydrogenation was added water (5 mL) and conc. HCl (2 drops). The solvent was then stripped under hard vacuum and the residue (0.5 mmol) dissolved in methanol (0.6 mmol). Anhydrous propylene oxide (25 mL/mmol) was then added and the solution stirred under an N$_2$ atmosphere at rt overnight. The precipitated solid was collected and washed with ethyl acetate to give the pure free amine.
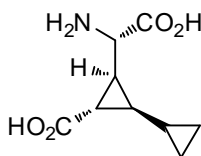
(1*R*,2*S*,3*S*)-3-[(*S*)-Amino(carboxy)methyl]-1,1'-bi(cyclopropyl)-2-carboxylic acid (90a). Compound was prepared according to the general procedure for amine deprotection. White solid (158 mg, 95%); dec: 234 °C; IR (solid): 3013, 1693, 1656, 1612, 1562, 1508, 1470, 1457, 1393, 1343, 1321, 1300, 1239 cm^{-1}; ^{1}H NMR (600 MHz, D$_2$O) δ 0.05−0.13 (m, 2H), 0.30−0.35 (m, 1H), 0.40−0.44 (m, 1H), 0.72−0.77 (m, 1H), 1.51−1.55 (m, 2H), 1.76 (ddd, *J* = 4.8, 4.2, 2.4 Hz, 1H), 3.82 (d, *J* = 11.4 Hz, 1H); ^{13}C NMR (150 MHz, D$_2$O) δ 5.5, 9.1, 25.1, 28.7, 32.6, 54.0, 172.4, 178.0; HRMS (ESI, [M + H]$^+$) calcd for C$_9$H$_{14}$O$_4$N$_1$: 200.0923, found 200.0917.
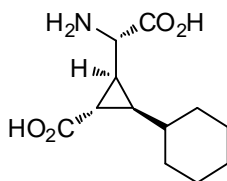
(1*S*,2*S*,3*R*)-2-[(*S*)-Amino(carboxy)methyl]-3-cyclohexylcyclopropanecarboxylic acid (91d). Compound was prepared according to the general procedure for amine deprotection and purification of free amine. Off-white solid (16 mg, 16%); IR (solid): 2924, 2851, 1680, 1586, 1554, 1451, 1391, 1320, 1231 cm^{-1}; ^{1}H NMR (600 MHz, D$_2$O) δ 0.80−0.93 (m, 6H), 1.27−1.43 (m, 6H), 1.64−1.73 (m, 2H), 3.60 (d, *J* = 10.8, 1H); ^{13}C NMR (150 MHz, D$_2$O) δ 25.2, 27.3, 29.1, 33.8, 34.3, 37.1, 37.2, 37.8, 53.6, 53.8, 172.2, 178.5; HRMS (ESI, [M + H]$^+$) calcd for C$_{12}$H$_{20}$O$_4$N$_1$: 242.1392, found 242.1387.
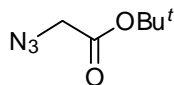
Preparation of *tert*-Butyl azidoacetate (94). *tert*-Butyl bromoacetate (2.5 g, 13 mmol) was dissolved in chloroform (100 mL) and sodium azide (2.5 g, 39 mmol) was added at 0 °C with stirring, followed by tetrabutylammonium bromide (40 mg, 0.13 mmol). The resulting slurry was stirred at 0 °C for 20 min, followed by heating to 40 °C under an inert atmosphere overnight. The reaction was then diluted with CH$_2$Cl$_2$ (100 mL), washed with 2M HCl$_{(aq)}$ (2 × 200 mL) and brine (200 mL) and the organic extract dried over MgSO$_{4(s)}$. Filtration and removal of solvents *in vacuo* yielded the crude product. Flash column chromatography (10% diethyl ether in petroleum spirit, v/v) afforded the pure azide (**94**) as a colourless, volatile oil (4.00 g, 38%); R$_f$ 0.49 (10% diethyl ether in petroleum spirit, v/v); IR (film): 3004, 2982, 2935, 2108, 1740, 1479, 1457, 1425, 1394,

1370, 1356, 1299, 1258, 1227, 1157, 1111, 953, 842 cm^{-1}; ^{1}H NMR (300 MHz, CDCl$_3$) δ 1.49 (s, 9H), 3.76 (s, 2H); ^{13}C NMR (75 MHz, CDCl$_3$) δ 27.8, 50.9, 82.8, 166.2; MS (EI) (C$_6$H$_{11}$O$_2$N$_3$) m/z (%): (M$^+$ 157, < 1%), 59.2 (35), 57.2 (100). Spectral data matched that reported previously.[183]
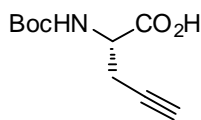
(2S)-2-[(tert-Butoxycarbonyl)amino]pent-4-ynoic acid (96). (S)-Propargyl glycines (**111**) (500 mg, 4.4 mmol) was dissolved in a 2:1 mix of 1,4-dioxane/H$_2$O (9 mL) and cooled to 0 °C. 2M NaOH solution (2.2 mL, 4.4 mmol) was added dropwise followed by di-tert-butyl dicarbonate (1.1 g, 4.9 mmol) as a solid in one portion. The reaction was stirred for 15 min at 0 °C, then allowed to warm to rt and stirred for an additional 2 h. The 1,4-dioxane was removed *in vacuo* and the resulting aqueous residue cooled to 0 °C and washed with ethyl acetate (20 mL). The aqueous solution was acidified to pH 2−3 with NaHSO$_4$ solution and extracted with ethyl acetate (3 × 40 mL). The combined organics were washed with water, dried over MgSO$_{4(s)}$, filtered and the solvent stripped to afford the target material (**96**) as a colourless gum (923 mg, 98%); R$_f$ 0.25 (20% ethyl acetate in hexanes, v/v); IR (film): 3414, 3303, 3114, 3055, 2981, 2934, 1715, 1513, 1456, 1429, 1396, 1370, 1344, 1253, 1224, 1162, 1064, 1027 cm^{-1}; ^{1}H NMR (300 MHz, CDCl$_3$) δ 1.47 (s, 9H), 2.06−2.12 (m, 1H), 2.77−2.86 (m, 2H), 4.50−4.56 (m, 1H), 5.36 (d, J = 8.1 Hz, 1H); ^{13}C NMR (75 MHz, CDCl$_3$) δ 22.5, 28.2, 51.8, 71.2, 78.3, 80.7, 155.4, 175.2; MS (EI) m/z (%): (M$^+$ 213, < 1%), 157(60), 129(20), 115(2), 101(5), 87(22), 57(100); HRMS (ESI, [M − H]$^+$) calcd for C$_{10}$H$_{14}$O$_4$N: 212.0923, found 212.0931.
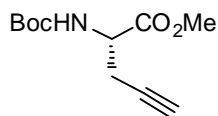
Methyl (2S)-2-[(tert-butoxycarbonyl)amino]pent-4-ynoate (97). (S)-Propargyl glycine (**111**) (500 mg, 4.4 mmol) was dissolved in anhydrous methanol (15 mL) and cooled to 0 °C. Thionyl chloride (1.05 g, 8.8 mmol) was added dropwise. After 15 min, cooling was removed and the solution was heated under reflux conditions for 2 h. Removal of volatiles *in vacuo* gave a syrupy residue which was dissolved in 1:1 1,4-

dioxine/H_2O (30 mL) and cooled to 0 ^{o}C. Solid $NaHCO_3$ (1.1 g, 13 mmol) was added with stirring, followed by di-*tert*-butyl dicarbonate (1.9 g, 8.8 mmol) as a solid in one portion. Cooling was removed and the reaction was stirred at rt for a further 2 h at which time the 1,4-dioxane was stripped under vacuum. The aqueous residue was extracted with ethyl acetate (3 × 25 mL), organic extracts combined, dried over $MgSO_4$ and filtered. Crude product was stripped of solvent under vacuum and subjected to flash column chromatography (15% ethyl acetate in petroleum spirit, v/v) to afford the pure target material as a colourless oil (838 mg, 83%); R_f 0.22 (15% ethyl acetate in petroleum spirit, v/v); IR (film): 3378, 3295, 2979, 2934, 1749, 1726, 1506, 1454, 1439, 1393, 1367, 1357, 1284, 1251, 1220, 1166, 1063, 1026, 994, 869, 780, 646 cm^{-1}; ^{1}H NMR (300 MHz, CDCl$_3$) δ 1.46 (s, 9H), 2.05 (t, J = 5.4 Hz, 1H), 2.67–2.82 (m, 2H), 3.79 (s, 3H), 4.46–4.52 (m, 1H), 5.36 (d, J = 7.5 Hz, 1H); ^{13}C NMR (75 MHz, CDCl$_3$) δ 22.7, 28.2, 51.8, 52.5, 71.5, 78.4, 80.0, 155.0, 171.0. All other chemical and physical properties were identical to those previously reported.[202]
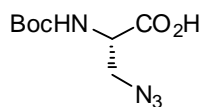
3-Azido-*N*-(*tert*-butoxycarbonyl)-L-alanine (98). As per Yan *et al.*[184] Sodium azide (3.8 g, 58 mmol) was suspended in anhydrous acetonitrile (60 mL) and cooled to 0 ^{o}C with stirring under a nitrogen atmosphere. Triflic anhydride (13.7 g, 49 mmol) was added dropwise over 10 min and the cooled solution stirred for 2 h. The mixture was filtered through cotton wool to give crude triflic azide in solution. A suspension of Boc-L-2,3-diaminopropionic acid (**112**) (8.3 g, 41 mmol) was vigorously stirred in acetonitrile (100 mL) and water (40 mL) to which was added triethylamine (12.3 g, 122 mmol) and $CuSO_{4(s)}$ (0.1 g, 0.4 mmol). The resulting solution was cooled to 0 ^{o}C and the triflic azide solution added dropwise. The reaction was allowed to stir overnight and warm to rt. The acetonitrile was removed *in vacuo* and the remaining aqueous solution washed with ethyl acetate (3 × 200 mL). The aqueous phase was then acidified with 2M HCl and extracted with ethyl acetate, dried over $MgSO_{4(s)}$, filtered and the solvent stripped under vacuum and subjected to dry column vacuum chromatography (5−10% methanol in chloroform containing 0.5% acetic acid, v/v) which afforded crude product. Addition of cold chloroform to precipitate the triflyl amide by-product, followed by filtration through cotton wool and removal of volatiles under hard vacuum gave pure

azide as a yellow, viscous oil (2.96 g, 32%); R_f 0.56 (20% methanol in chloroform, v/v); IR (film): 3386, 3279, 3041, 2983, 2938, 2109, 1724, 1694, 1612, 1520, 1450, 1351, 1236, 1187, 1070, 1030, 955, 868 cm^{-1}; ^{1}H NMR (300 MHz, CDCl$_3$) δ 1.47 (s, 9H), 3.74–3.87 (m, 2H), 4.51–4.54 (m, 1H), 5.38 (d, J = 7.8 Hz, 1H); ^{13}C NMR (75 MHz, CDCl$_3$) δ 28.2, 52.3, 53.3, 81.1, 155.5, 174.0; MS (EI) m/z (%): (M$^+$ 230, 1%), 202(5), 185(6), 174(2), 157(3), 147(8), 130(10), 111(2), 102(35), 85(10), 74(5), 57(100). All other chemical and physical properties were identical to those previously reported.[257]
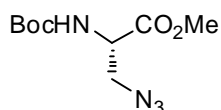
Methyl 3-azido-N-(*tert*-butoxycarbonyl)-L-alaninate (99). As per Gomez-Vidal and Silverman:[203] (*S*)-Boc-serine methyl ester (**113**) (3.0 g, 14 mmol) and triphenylphosphine (4.3 g, 16 mmol) were dissolved in anhydrous THF (100 mL) under an inert atmosphere and cooled to 0 °C. Diisopropyl azodicarboxylate (3.6 g, 18 mmol) was added dropwise followed by diphenyl phosphorylazide (4.5 g, 16 mmol). After 1h, the reaction was allowed to warm to rt and left stirring overnight. Volatiles were stripped *in vacuo* and the bright yellow syrupy residue was subjected to flash column chromatography (20% ethyl acetate in petroleum spirit, v/v) to afford pure target material as a colourless oil (2.29g, 69%); R_f 0.38 (20% ethyl acetate in petroleum spirit, v/v); IR (film): 3362, 2980, 2936, 2108, 1749, 1716, 1506, 1449, 1393, 1368, 1252, 1211, 1164, 1066, 1048 cm^{-1}; ^{1}H NMR (300 MHz, CDCl$_3$) δ 1.46 (s, 9H), 3.73 (d, J = 3.6 Hz, 2H), 4.46–4.49 (m, 1H), 5.37 (d, J = 6.3 Hz, 1H); ^{13}C NMR (75 MHz, CDCl$_3$) δ 28.2, 52.6, 52.8, 53.5, 80.4, 155.0, 170.2; HRMS (ESI, [M + Na]$^+$) calcd for C$_9$H$_{16}$O$_4$N$_4$Na: 267.1069, found 267.1066.
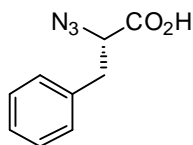
(2S)-2-Azido-3-phenylpropanoic acid (100). As per Yan *et al.*[184] Sodium azide (2.3 g, 35 mmol) was suspended in anhydrous acetonitrile (35 mL) and cooled to 0 °C with stirring. Triflic anhydride (8.2 g, 29 mmol) was added dropwise over 10 min and the cooled solution stirred for 1.5 h followed by 30 min at rt. The mixture was filtered through cotton wool to give crude triflic azide in solution. A suspension of L-

phenylalanine (**114**) (4.0 g, 24 mmol) was vigorously stirred in acetonitrile (50 mL) and water (20 mL) to which was added triethylamine (7.4g, 73 mmol) and $CuSO_{4(s)}$ (60 mg, 0.24 mmol). The resulting solution was cooled to 0 °C and the triflic azide solution added dropwise. After 30 min, cooling was removed and the reaction was allowed to stir at rt overnight. The acetonitrile was removed *in vacuo* and the remaining aqueous solution washed with ethyl acetate (2 × 100 mL). The aqueous phase was then acidified with 2M HCl followed by conc. HCl and extracted with ethyl acetate (3 × 100 mL), dried over $MgSO_{4(s)}$, filtered and the solvent stripped to afford crude target material. Chloroform was added and the solution refrigerated and filtered to remove some triflyl amine by-product. Removal of the solvent *in vacuo*, followed by flash column chromatography (5% methanol in chloroform, v/v) afforded the pure azide as a pale yellow oil (2.05 g, 44%); IR (film): 3089, 3068, 3032, 2928, 2118, 1720, 1497, 1456, 1441, 1420, 1264, 1228, 1081, 1030, 751, 700 cm^{-1}; ^{1}H NMR (300 MHz, CDCl$_3$) δ 3.04 (dd, *J* = 5.1, 8.7, 9.0 Hz, 1H), 3.24 (dd, *J* = 5.1, 5.1, 9.0 Hz, 1H), 4.16 (dd, *J* = 3.9, 5.1 Hz, 1H), 7.24–7.38 (m, 5H), 10.68 (s, 1H); ^{13}C NMR (75 MHz, CDCl$_3$) δ 37.4, 63.0, 127.4, 128.8, 129.2, 135.5, 176.0.
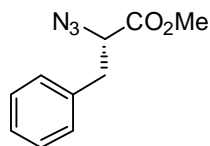
Methyl (2*S*)-2-azido-3-phenylpropanoate (101). To a well stirred solution of (2*S*)-2-azido-3-phenylpropanoic acid (**100**) (223mg, 1.2 mmol) in anhydrous methanol (5 mL) was added thionyl chloride (2 drops) at 0 °C. The solution was stirred at rt under an inert atmosphere overnight. Volatiles were carefully removed under vacuum to yield pure target material as a colourless oil (233 mg, 97%); R$_f$ 0.74 (40% ethyl acetate in petroleum spirit, v/v); IR (film): 3088, 3065, 3031, 2955, 2112, 1747, 1605, 1498, 1456, 1437, 1357, 1278, 1262, 1210, 1176, 1081, 1030, 1017, 750, 700 cm^{-1}; ^{1}H NMR (300 MHz, CDCl$_3$) δ 3.01 (dd, *J* = 5.4, 8.7, 8.7 Hz, 1H), 3.18 (dd, *J* = 5.7, 5.7, 8.4 Hz, 1H), 3.77 (s, 3H), 4.07 (dd, *J* = 3.3, 5.4, 5.4 Hz, 1H), 7.20–7.36 (m, 5H); ^{13}C NMR (75 MHz, CDCl$_3$) δ 37.5, 52.6, 63.1, 127.2, 128.6, 129.1, 135.8, 170.3; MS (EI) *m/z* (%): (M$^+$ 205, <1%), 177(7), 162(13), 118(20), 91(100), 65(10); HRMS (ESI, [M + Na]$^+$) calcd for $C_{10}H_{11}O_2N_3Na$: 228.0749, found 228.0746. Data were identical to that previously reported.[184]
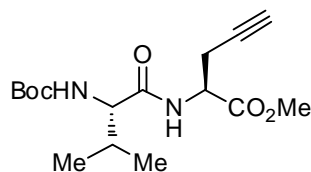
Methyl (2S)-2-{[N-(*tert*-butoxycarbonyl)-L-valyl]amino}pent-4-ynoate (117). To a stirred solution of (S)-2-*tert*-Butoxycarbonylamino-pent-4-ynoic acid methyl ester (**97**) (15 mg, 0.07 mmol) in anhydrous CH_2Cl_2, (2 mL) was added conc. HCl (0.6 mL) and H_2O (4 drops). The resulting solution was stirred at rt overnight followed by removal of solvent and excess HCl *in vacuo* to provide the crude hydrochloride salt (9 mg, 82%). To this was added Boc-L-valine (**116**) (12 mg, 0.06 mmol), EDC hydrochloride (14 mg, 0.07 mmol) and HOBt (11 mg, 0.08 mmol) and the solids dissolved in anhydrous CH_2Cl_2 (1.5 mL). Diisopropylethylamine (7.8 mg, 0.06 mmol) was added dropwise with stirring and the solution allowed to stir overnight at rt. After dilution with CH_2Cl_2, the solution was washed with sat. $NaHCO_3$ solution (2 × 10 mL), 1M HCl (2 × 10 mL) and brine (2 × 10 mL). Drying over $MgSO_{4(s)}$, filtering and removal of volatiles *in vacuo* gave crude di-peptide **117** (16 mg, 89%).

General Procedure for Amino Acid Coupling (120–123).

The carboxylic acid, amine hydrochloride salt, EDC hydrochloride and HOBt were combined and dissolved in anhydrous CH_2Cl_2 with stirring at rt. Upon dissolution, TEA was added dropwise. The reaction was allowed to stir at rt overnight at which point the solution was diluted with CH_2Cl_2 and washed alternately with 1M HCl (10 mL) and saturated sodium bicarbonate solution (10 mL). This process was repeated followed by washing with brine (15 mL), drying over $MgSO_{4(s)}$, filtering and removal of all volatiles *in vacuo*. The product amino acid was analysed without further purification.
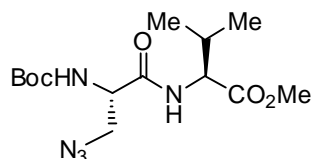
Methyl 3-azido-N-(*tert*-butoxycarbonyl)-L-alanyl- L-valinate (120). Compound was prepared according to the general procedures for ester hydrolysis and amino acid coupling. Isolated yield: 70 mg, 92% (pale yellow gum); ^{1}H NMR (600 MHz, CDCl$_3$) δ

0.92 (d, J = 6.6 Hz, 3H), 0.95 (d, J = 7.2 Hz, 3H), 1.47 (s, 9H), 2.18–2.21 (m, 1H), 3.54−3.57 (m, 1H), 3.75 (s, 3H), 3.86−3.89 (m, 1H), 4.28 (m, 1H), 4.53−4.55 (m, 1H), 5.29 (d, J = 8.4 Hz, 1H), 6.81 (d, J = 1.2 Hz, 1H); ^{13}C NMR (150 MHz, CDCl$_3$) δ 17.6, 18.9, 28.4, 32.2, 51.8, 52.2, 53.6, 57.4, 80.9, 155.4, 169.4, 171.8.
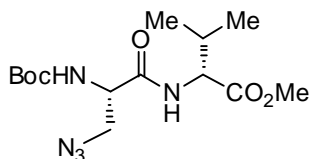
Methyl 3-azido-*N*-(*tert*-butoxycarbonyl)-L-alanyl-D-valinate (121). Compound was prepared according to the general procedures for ester hydrolysis and amino acid coupling. Isolated yield: 54 mg, 77% (pale yellow gum); ^{1}H NMR (600 MHz, CDCl$_3$) δ 0.91 (d, J = 6.6 Hz, 3H), 0.96 (d, J = 7.2 Hz, 3H), 1.47 (s, 9H), 2.18–2.21 (m, 1H), 3.55−3.58 (m, 1H), 3.75 (s, 3H), 3.84−3.87 (m, 1H), 4.33 (m, 1H), 4.55 (dd, J = 4.8, 4.2 Hz, 1H), 5.32 (m, 1H), 6.78 (d, J = 6.6 Hz, 1H); ^{13}C NMR (150 MHz, CDCl$_3$) δ 17.5, 18.9, 28.2, 31.2, 51.9, 52.2, 57.2, 155.8, 169.3, 172.0.
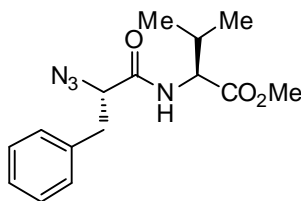
Methyl *N*-[(2*S*)-2-azido-3-phenylpropanoyl]-L-valinate (122). Compound was prepared according to the general procedures for ester hydrolysis and amino acid coupling. Isolated yield: 70 mg, 92% (pale yellow gum); ^{1}H NMR (600 MHz, CDCl$_3$) δ 0.81 (d, J = 7.2 Hz, 3H), 0.82 (d, J = 7.2 Hz, 3H), 2.07–2.12 (m, 1H), 3.02–3.36 (m, 2H), 3.74 (s, 3H), 4.25 (dd, J = 4.2, 3.6 Hz, 1H), 4.47 (dd, J = 5.4, 3.0 Hz, 1H), 7.25−7.33 (m, 5H); ^{13}C NMR (150 MHz, CDCl$_3$) δ 17.7, 18.7, 31.1, 38.6, 52.2, 57.1, 65.5, 127.2, 128.6, 129.6, 135.9, 168.3, 171.8.
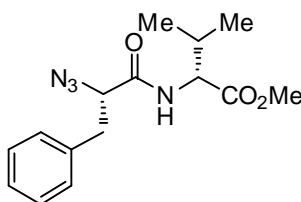
Methyl *N*-[(2*S*)-2-azido-3-phenylpropanoyl]-D-valinate (123). Compound was prepared according to the general procedures for ester hydrolysis and amino acid coupling. Isolated yield: 74 mg, 86% (pale yellow gum); ^{1}H NMR (600 MHz, CDCl$_3$) δ 0.88 (d, *J* = 6.6 Hz, 3H), 0.90 (d, *J* = 7.2 Hz, 3H), 2.13−2.16 (m, 1H), 2.98−3.36 (m, 2H), 3.72 (s, 3H), 4.20 (dd, *J* = 4.8, 3.6 Hz, 1H), 4.50 (dd, *J* = 5.4, 3.6 Hz, 1H), 7.26−7.33 (m, 5H); ^{13}C NMR (150 MHz, CDCl$_3$) δ 17.8, 18.9, 31.2, 38.6, 52.2, 57.1, 65.5, 127.2, 128.7, 129.4, 136.1, 168.6, 171.6.

General Procedure for Copper-Catalysed Cycloaddition (124–126).

Alkyne (0.7 mmol) and azide (0.9 mmol) were dissolved in *t*-butanol (2 mL) and CuSO$_{4(s)}$ (0.04) was added in one portion followed by water (1 mL) and sodium ascorbate (0.15 mmol). The mixture was stirred at rt overnight at which point solvents were stripped under vacuum. The residue was taken up in ethyl acetate (15 mL) and washed with 0.5 M HCl (3 × 15 mL). The ethyl acetate extracts were washed with water and dried over MgSO$_{4(s)}$, filtered and the solvent removed *in vacuo* to afford crude triazole. Flash column chromatography (10% methanol in chloroform, v/v) provided the pure target material.
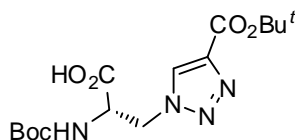
***N*-(*tert*-Butoxycarbonyl)-3-[4-(*tert*-butoxycarbonyl)-1*H*-1,2,3-triazol-1-yl]-L-alanine (124).** Compound was prepared according to the general procedure for copper-catalysed cycloaddition from alkyne **95** and azide **98**. Isolated yield: 135 mg, 96% (white solid); mp: 85−87 °C (water); IR (nujol): 3396, 3147, 2927, 2854, 1714, 1615, 1538, 1461, 1377, 1247, 1167, 1058, 1028, 908, 842, 779, 735 cm^{-1}; ^{1}H NMR (300 MHz, CDCl$_3$) δ 1.45 (s, 9H), 1.59 (s, 9H), 4.71−4.73 (m, 1H), 4.91−5.06 (m, 2H), 5.49 (d, *J* = 5.7 Hz, 1H), 8.04 (s, 1H); ^{13}C NMR (75 MHz, CDCl$_3$) δ 28.1, 28.2, 51.6, 55.4, 79.5, 82.3, 128.7, 140.4, 155.6, 160.3, 174.2; HRMS (ESI, [M + H]$^+$) calcd for C$_{15}$H$_{25}$O$_6$N$_4$: 357.1774, found 357.1770.
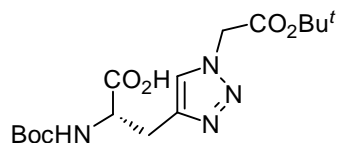
***N*-(*tert*-Butoxycarbonyl)-3-[1-(2-*tert*-butoxy-2-oxoethyl)-1*H*-1,2,3-triazol-4-yl]-L-alanine (125).** Compound was prepared according to the general procedure for copper-catalysed cycloaddition from alkyne **96** and azide **94**. Isolated yield: 82 mg, 85% (white solid); R_f 0.38 (10% methanol in chloroform, v/v); mp: 59−61 ^{o}C (water); IR (nujol): 3354, 3148, 2954, 2922, 2852, 2726, 1743, 1714, 1464, 1455, 1377, 1302, 1169, 1151, 1052, 858, 722 cm^{-1}; ^{1}H NMR (300 MHz, CDCl$_3$) δ 1.45 (s, 9H), 1.48 (s, 9H), 3.27−3.44 (m, 2H), 4.56−4.57 (m, 1H), 5.04 (s, 2H), 5.62 (d, *J* = 6.6 Hz, 1H), 7.58 (s, 1H); ^{13}C NMR (75 MHz, CDCl$_3$) δ 27.5, 27.9, 28.3, 51.7, 52.9, 80.3, 84.0, 124.4, 142.7, 155.8, 165.0, 172.7; HRMS (ESI, [M + Na]$^+$) calcd for C$_{16}$H$_{26}$O$_6$N$_4$Na: 393.1750, found 393.1745.
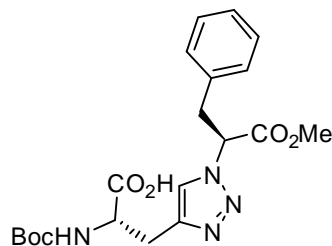
***N*-(*tert*-Butoxycarbonyl)-3-{1-[(2*S*)-1-methoxy-1-oxo-3-phenylpropan-2-yl]-1*H*-1,2,3-triazol-4-yl}-L-alanine (126).** Compound was prepared according to the general procedure for copper-catalysed cycloaddition from alkyne **96** and azide **101**. Isolated yield: 101 mg, 64% (white solid); $[\alpha]_D^{25}$ −39.0 (*c* 0.6, MeOH); mp: 52−55 ^{o}C (water); IR (neat): 3417, 3329, 3145, 3062, 3032, 1979, 2932, 1749, 1713, 1499, 1456, 1438, 1393, 1368, 1266, 1168, 1054, 1029, 802, 738, 702 cm^{-1}; ^{1}H NMR (300 MHz, CDCl$_3$) δ 1.43 (s, 9H), 3.24−3.53 (m, 4H), 3.74 (s, 3H), 4.53−4.55 (m, 1H), 5.44−5.52 (m, 2H), 6.96−6.99 (m, 2H), 7.18−7.28 (m, 3H), 7.49 (s, 1H); ^{13}C NMR (75 MHz, CDCl$_3$) δ 27.4, 28.3, 38.5, 53.1, 64.4, 80.1, 123.4, 127.6, 128.8, 128.9, 134.5, 142.2, 155.7, 168.3, 173.0; HRMS (ESI, [M + H]$^+$) calcd for C$_{20}$H$_{27}$O$_6$N$_4$: 419.1931, found 419.1924.

Attempted Preparation of [Cp*RuCl]$_4$ Catalyst (108).

According to Fagan *et al.*[204] To a stirred solution of Cp*RuCl$_2$ (60 mg, 0.20 mmol) in anhydrous THF (2 mL) under a nitrogen blanket was added 1M LiEt$_3$BH in THF (0.2

mL, 0.20 mmol). The brown solution was stirred for 1 hour and then filtered, however no product could be isolated.

Preparation of Cp*Ru(PPh₃)₂Cl Catalyst (109).

According to Morandini *et al.*[205] Triphenylphosphine (170 mg, 0.65 mmol) and Cp*RuCl₂ (77 mg, 0.25 mmol) were dried under a hard vacuum overnight. Anhydrous ethanol (3 mL) was added with stirring and the solution heated under reflux for 6 h under a nitrogen atmosphere. The solids were collected by vacuum filtration and washed with minimal petroleum spirit. Drying under hard vacuum overnight afforded the product as a brick red / orange solid (98 mg, 49%).

General Procedure for Ruthenium-Catalysed Cycloaddition (128–130).

According to Boren *et al.*[199] Alkyne (0.5–0.6 mmol) and azide (0.5–0.7 mmol) were dissolved in anhydrous THF (4 mL) and the solvent deoxygenated by bubbling nitrogen through the solution. The catalyst, Cp*Ru(PPh₃)₂Cl (2 mol%) was added in one portion with stirring and the reaction heated under reflux conditions for 3 h. Volatiles were stripped under vacuum and the residue subjected to two passes of flash column chromatography (50% ethyl acetate in petroleum spirit, v/v) to provide pure target material.
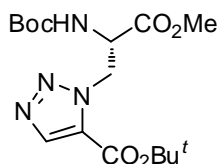
tert-**Butyl** **1-{(2*S*)-2-[(*tert*-butoxycarbonyl)amino]-3-methoxy-3-oxopropyl}-1*H*-1,2,3-triazole-5-carboxylate (128).** Compound was prepared according to the general procedure for ruthenium-catalysed cycloaddition from alkyne **95** and azide **99**. Isolated yield: 58 mg, 33% (pale yellow gum); R_f 0.62 (50% ethyl acetate in petroleum spirit, v/v); IR (film): 3378, 2980, 2935, 1745, 1720, 1529, 1508, 1454, 1438, 1394, 1369, 1325, 1255, 1211, 1163, 1124, 1096, 1057 cm^{-1}; ^{1}H NMR (300 MHz, CDCl₃) δ 1.38 (s, 9H), 1.60 (s, 9H), 3.78 (s, 3H), 4.86–4.93 (m, 1H), 5.00–5.18 (m, 2H), 5.37 (d, *J* = 8.4 Hz, 1H), 8.02 (s, 1H); ^{13}C NMR (75 MHz, CDCl₃) δ 28.1, 28.1, 50.5, 52.8, 53.1, 80.3, 83.9, 129.8, 137.6, 154.9, 157.6, 169.8; HRMS (ESI, [M + H]$^+$) calcd for C₁₆H₂₇O₆N₄: 371.1931, found 371.1928.
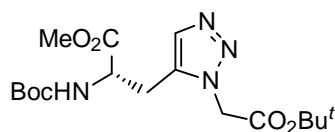
Methyl *N*-(*tert*-butoxycarbonyl)-3-[1-(2-*tert*-butoxy-2-oxoethyl)-1*H*-1,2,3-triazol-5-yl]-L-alaninate (129). Compound was prepared according to the general procedure for ruthenium-catalysed cycloaddition from alkyne **97** and azide **94**. Isolated yield: 158 mg, 85% (colourless gum); $[\alpha]_D^{25}$ −12.1 (*c* 1.6, MeOH); R$_f$ 0.36 (50% ethyl acetate in petroleum spirit, v/v); IR (film): 3370, 2981, 2937, 2252, 1747, 1712, 1518, 1458, 1438, 1394, 1369, 1289, 1246, 1160 cm^{-1}; ^{1}H NMR (300 MHz, CDCl$_3$) δ 1.44 (s, 9H), 1.48 (s, 9H), 3.13−3.27 (m, 2H), 4.56−4.58 (m, 1H), 5.06 (dd, *J* = 16.5, 17.7 Hz, 2H), 5.34 (d, *J* = 6.6 Hz, 1H), 7.49 (s, 1H); ^{13}C NMR (75 MHz, CDCl$_3$) δ 25.9, 27.9, 28.2, 49.6, 52.5, 52.8, 80.6, 83.8, 133.2, 133.3, 155.0, 165.3, 171.0; HRMS (ESI, [M + H]$^+$) calcd for C$_{17}$H$_{29}$O$_6$N$_4$: 385.2087, found 385.2087.
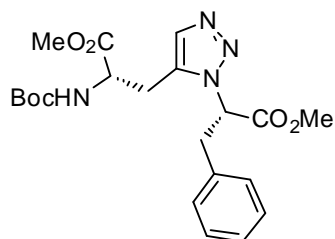
Methyl *N*-(*tert*-butoxycarbonyl)-3-{1-[(2*S*)-1-methoxy-1-oxo-3-phenylpropan-2-yl]-1*H*-1,2,3-triazol-5-yl}-L-alaninate (130). Compound was prepared according to the general procedure for ruthenium-catalysed cycloaddition from alkyne **97** and azide **101**. Isolated yield: 194 mg, 92% (pale yellow gum); $[\alpha]_D^{25}$ −9.7 (*c* 0.6, MeOH); R$_f$ 0.25 (50% ethyl acetate in petroleum spirit, v/v); IR (film): 3422, 3376, 3031, 3005, 2980, 2956, 1748, 1711, 1515, 1498, 1456, 1438, 1393, 1368, 1352, 1286, 1253, 1166, 1098, 1056, 1015, 986, 913, 733, 702, 648 cm^{-1}; ^{1}H NMR (300 MHz, CDCl$_3$) δ 1.45 (s, 9H), 2.65−2.78 (m, 2H), 3.60−3.73 (m, 2H), 3.67 (s, 3H), 3.77 (s, 3H), 5.07 (d, J = 6.9 Hz, 1H), 5.28−5.33 (m, 1H), 6.97−7.00 (m, 2H), 7.18−7.20 (m, 3H), 7.37 (s, 1H); ^{13}C NMR (75 MHz, CDCl$_3$) δ 25.3, 28.1, 37.6, 52.2, 52.5, 53.0, 61.6, 80.4, 127.1, 128.5, 128.9, 132.8, 133.6, 135.8, 154.8, 168.0, 170.8; HRMS (ESI, [M + H]$^+$) calcd for C$_{21}$H$_{29}$O$_6$N$_4$: 433.2087, found 433.2086.

General Procedure for Ester Hydrolysis (131–134).

The triazole ester was dissolved in THF (5 mL) and cooled to 0 °C. Pre-cooled 1M LiOH$_{(aq)}$ (8.0 equiv.) was added dropwise with stirring and the reaction allowed to stir at rt overnight. The suspension was diluted with water and washed with ethyl acetate before being acidified with 1M HCl and extracted with ethyl acetate. The ethyl acetate extracts were combined and washed with brine, dried over MgSO$_{4(s)}$, filtered and the solvent removed *in vacuo*. The residue was re-dissolved in toluene and the solvent stripped under hard vacuum to provide the pure desired triazolyl carboxylic acid.
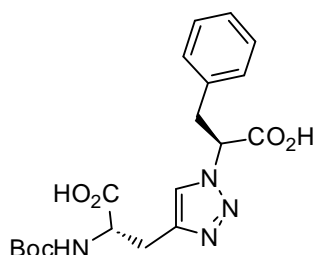
***N*-(*tert*-Butoxycarbonyl)-3-{1-[(1*S*)-1-carboxy-2-phenylethyl]-1*H*-1,2,3-triazol-4-yl}-L-alanine (131).** Compound was prepared according to the general procedure for ester hydrolysis from compound **126**. Isolated yield: 50 mg, quantitative (white solid); IR (nujol): 3352, 3148, 2925, 2854, 1714, 1513, 1457, 1394, 1369, 1255, 1165, 1058, 1026 cm^{-1}; ^{1}H NMR (300 MHz, CD$_3$OD) δ 1.30 (s, 9H), 2.89–3.19 (m, 2H), 3.27–3.48 (m, 2H), 4.14–4.23 (m, 1H), 5.38–5.39 (m, 1H), 6.90–6.98 (m, 2H), 7.01–7.15 (m, 3H), 7.68 (s, 1H); ^{13}C NMR (75 MHz, CD$_3$OD) δ 23.89, 28.94, 39.43, 53.88, 66.29, 80.85, 124.78, 128.25, 129.77, 130.16, 130.51, 137.48, 157.99, 171.56, 174.92; HRMS (ESI, [M + H]$^+$) calcd for C$_{19}$H$_{25}$O$_6$N$_4$: 405.1774, found 405.1768. The crude product was used without further purification.
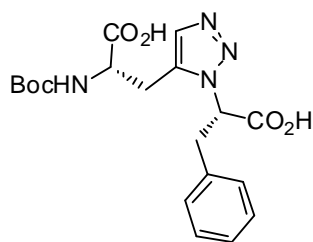
***N*-(*tert*-Butoxycarbonyl)-3-{1-[(1*S*)-1-carboxy-2-phenylethyl]-1*H*-1,2,3-triazol-5-yl}-L-alanine (132).** Compound was prepared according to the general procedure for

ester hydrolysis from compound **130**. Isolated yield: 134 mg, 96% (white solid); mp: 130−134 $^{\circ}$C; IR (nujol): 3334, 2927, 2600, 1916, 1714, 1652, 1496, 1457, 1376, 1278, 1250, 1155, 1113, 1055, 1028 cm^{-1}; ^{1}H NMR (300 MHz, CD$_3$OD) δ 1.43 (s, 9H), 2.68−2.94 (m, 2H), 3.48−3.74 (m, 2H), 4.10−4.23 (m, 1H), 5.43−5.49 (m, 1H), 7.01−7.05 (m, 2H), 7.17−7.20 (m, 3H), 7.45 (s, 1H); ^{13}C NMR (75 MHz, CD$_3$OD) δ 26.25, 28.79, 38.83, 53.60, 63.37, 80.96, 128.25, 128.29, 129.77, 130.21, 137.85, 137.88, 157.86, 170.90, 173.95; HRMS (ESI, [M + H]$^{+}$) calcd for C$_{19}$H$_{25}$O$_6$N$_4$: 405.1774, found 405.1772. The crude product was used without further purification.
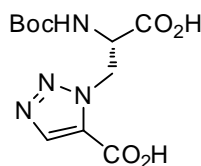
1-{(2S)-2-[(*tert*-Butoxycarbonyl)amino]-2-carboxyethyl}-1*H*-1,2,3-triazole-5-carboxylic acid (133a,b). Compound was prepared according to the general procedure for ester hydrolysis from compound **128** and isolated as a mix of free carboxylic acid and *t*-butyl ester. The crude mix of products was used without further purification.
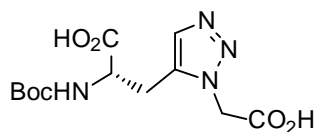
N-(*tert*-Butoxycarbonyl)-3-[1-(carboxymethyl)-1*H*-1,2,3-triazol-5-yl]-L-alanine (134a,b).** Compound was prepared according to the general procedure for ester hydrolysis from compound **129** and isolated as a mix of free carboxylic acid and *t*-butyl ester; white solid (66 mg, 65%). The crude mix of products was used without further purification.

General Procedure for Boc Deprotection (45a–50a).

The Boc-protected triazolyl amino acid was dissolved in 1,4-dioxane (4 mL) and cooled to 0 $^{\circ}$C with stirring. 6M HCl (2 mL) was added dropwise and the reaction allowed to stir at rt overnight. All volatiles were removed under vacuum and the residue re-dissolved in dry benzene or toluene followed by removal of solvent *in vacuo*. Washing with ether and thorough drying under hard vacuum provided the pure target triazole amino acids as hydrochloride salts.
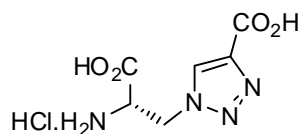
1-[(2S)-2-Amino-2-carboxyethyl]-1H-1,2,3-triazole-4-carboxylic acid hydrochloride (45a). Compound was prepared according to the general procedure for Boc deprotection. Isolated yield: 42 mg, quantitative (pale brown solid); $[\alpha]_D^{25}$ −7.1 (c 1.0, 5% NaOH$_{(aq)}$); IR (nujol): 3121, 3030, 2920, 2854, 2688, 2628, 2562, 2463, 1743, 1688, 1600, 1556, 1543, 1492, 1459, 1421, 1377, 1350, 1259, 1231, 1051 cm^{-1}; ^{1}H NMR (300 MHz, d_6-DMSO) δ 4.56–4.59 (m, 1H), 4.92–5.05 (m, 2H), 8.72 (s, 1H); ^{13}C NMR (75 MHz, d_6-DMSO) δ 48.65, 51.75, 130.51, 139.74, 161.63, 168.17. Due to the extremely hygroscopic nature of this material, no further analysis could be undertaken.
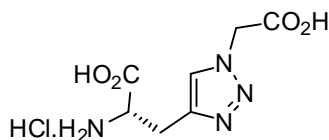
3-[1-(Carboxymethyl)-1H-1,2,3-triazol-4-yl]-L-alanine hydrochloride (46a). Compound was prepared according to the general procedure for Boc deprotection. Isolated yield: 49 mg, quantitative (off white solid); $[\alpha]_D^{25}$ +4.6 (c 0.9, MeOH); ^{1}H NMR (300 MHz, D$_2$O) δ 3.38–3.51 (m, 2H), 4.22–4.44 (m, 1H), 5.34 (s, 2H), 7.98 (s, 1H); ^{13}C NMR (75 MHz, D$_2$O) δ 26.24, 51.65, 53.22, 126.94, 141.67, 171.41, 171.52. Due to the extremely hygroscopic nature of this material, no further analysis could be undertaken.
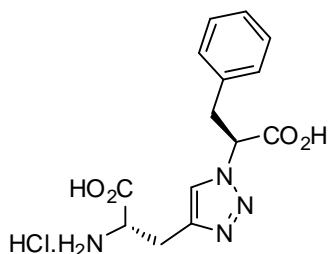
3-{1-[(1S)-1-Carboxy-2-phenylethyl]-1H-1,2,3-triazol-4-yl}-L-alanine hydrochloride (47a). Compound was prepared according to the general procedure for Boc deprotection. Isolated yield: 27 mg, quantitative (white solid); $[\alpha]_D^{25}$ −5.1 (c 0.5,

MeOH); IR (solid crystal): 3392, 2936, 2527, 1744, 1631, 1497, 1456, 1439, 1296, 1249, 1143, 1083, 1057 cm^{-1}; ^{1}H NMR (600 MHz, CD$_3$OD) δ 3.27–3.37 (m, 2H), 3.60–3.65 (m, 2H), 4.31–4.33 (m, 1H), 5.72–5.74 (m, 1H), 7.08–7.11 (m, 2H), 7.16–7.22 (m, 3H), 7.98 (s, 1H); ^{13}C NMR (150 MHz, CD$_3$OD) δ 27.52, 39.36, 54.00, 66.07, 125.98, 128.78, 130.17, 130.18, 130.53, 137.23, 170.68, 171.02; HRMS (ESI, [M + H]$^+$) calcd for C$_{14}$H$_{16}$O$_4$N$_4$Cl: 339.0860, found 339.1936.
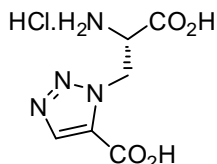
1-[(2S)-2-Amino-2-carboxyethyl]-1H-1,2,3-triazole-5-carboxylic acid hydrochloride (48a). Compound was prepared according to the general procedure for Boc deprotection. Isolated yield: 28 mg, quantitative (off white solid); ^{1}H NMR (300 MHz, D$_2$O) δ 4.66–4.69 (m, 1H), 5.21–5.40 (m, 2H), 8.24 (s, 1H); ^{13}C NMR (75 MHz, D$_2$O) δ 49.17, 53.25, 131.66, 138.55, 161.31, 169.47. Due to the extremely hygroscopic nature of this material, no further analysis could be undertaken. Spectral data were identical to that previously reported.[185]
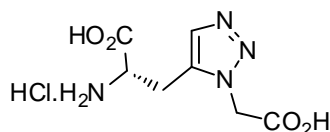
3-[1-(Carboxymethyl)-1H-1,2,3-triazol-5-yl]-L-alanine hydrochloride (49a). Compound was prepared according to the general procedure for Boc deprotection. Isolated yield: 62 mg, 90% (over two steps) (off white solid); $[\alpha]_D^{25}$ +8.4 (c 1.0, MeOH); ^{1}H NMR (300 MHz, CDCl$_3$) δ 3.46–3.70 (m, 2H), 4.51–4.52 (m, 1H), 5.60 (s, 2H), 8.36 (s, 1H);); ^{13}C NMR (75 MHz, CD$_3$OD) δ (partial) 25.18, 56.42, 102.81; HRMS (ESI, [M + H]$^+$) calcd for C$_7$H$_{12}$O$_4$N$_4$Cl: 251.0547, found 251.0953. Due to the extremely hygroscopic nature of this material, no further analysis could be undertaken.
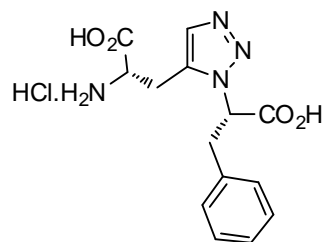
3-{1-[(1*S*)-1-Carboxy-2-phenylethyl]-1*H*-1,2,3-triazol-5-yl}-L-alanine hydrochloride (50a). Compound was prepared according to the general procedure for Boc deprotection. Isolated yield: 70 mg, 92% (pale yellow solid); $[\alpha]_D^{25}$ −1.4 (*c* 1.2, MeOH); IR (solid crystal): 3584, 3402, 2919, 2362, 1738, 1604, 1497, 1456, 1236, 1143, 1081, 963 cm^{-1}; ^{1}H NMR (300 MHz, D$_2$O) δ 2.77–3.06 (m, 2H), 3.38–3.56 (m, 1H), 3.59–4.17 (m, 2H), 5.50–5.62 (m, 1H), 6.94–6.97 (m, 2H), 7.18–7.19 (m, 3H), 7.66 (s, 1H); ^{13}C NMR (75 MHz, D$_2$O) δ 4.79, 8.79, 28.06, 34.20, 34.34, 52.68, 53.01, 65.36, 67.07, 126.95, 127.62, 127.93, 128.16, 128.50, 128.54, 128.58, 132.97, 136.07, 137.37, 140.89; HRMS (ESI, [M − Cl + NH$_3$]$^+$) calcd for C$_{14}$H$_{20}$O$_4$N$_5$: 322.1515, found 322.1591.

References

1. MBF Foundation Ltd *First study of Australia's high cost of pain reveals $34 billion price tag* **2007**, Media Release, Accessed: 03/07/09

2. Bonica J.J. *Pain* **1979**, *6*, 247-252.

3. Anaesthesia UK *Pain Pathways (edited)* **2009**, Web Resource, Accessed: 7/12/09

4. DeLeo J.A. *J. Bone Joint Surg. Am.* **2006**, *88 Suppl 2*, 58-62.

5. Gauriau C. and Bernard J.F. *Exp. Physiol.* **2002**, *87*, 251-258.

6. Millan M.J. *Prog. Neurobiol.* **2002**, *66*, 355-474.

7. Torrance N., Smith B.H., Bennett M.I., and Lee A.J. *J. Pain* **2006**, *7*, 281-289.

8. McCarberg B.H. and Billington R. *Am. J. Manag. Care* **2006**, *12*, S263-268.

9. Tang N.K. and Crane C. *Psychol. Med.* **2006**, *36*, 575-586.

10. McQuay H.J. *Eur. J. Pain* **2002**, *6 Suppl A*, 11-18.

11. Sen D. and Christie D. *Best Prac. Res. Clin. Rheum.* **2006**, *20*, 369-386.

12. Colombo B., Annovazzi P.O., and Comi G. *Neurol. Sci.* **2006**, *27 Suppl 2*, S183-189.

13. Ossipov M.H. and Porreca F. *J. Am. Soc. Exp. NeuroTher.* **2005**, *2*, 650-661.

14. Jensen T.S., Gottrup H., Sindrup S.H., and Bach F.W. *Eur. J. Pharmacol.* **2001**, *429*, 1-11.

15. Suzuki R., Rygh L.J., and Dickenson A.H. *Trends Pharmacol. Sci.* **2004**, *25*, 613-617.

16. Porreca F., Ossipov M.H., and Gebhart G.F. *Trends Neurosci.* **2002**, *25*, 319-325.

17. Kim S.J., Calejesan A.A., and Zhuo M. *Pharmacol. Biochem. Behav.* **2002**, *73*, 429-437.

18. Gebhart G.F. *Neurosci. Biobehav. Rev.* **2004**, *27*, 729-737.

19. Neubert M.J., Kincaid W., and Heinricher M.M. *Pain* **2004**, *110*, 158-165.

20. Urban M.O. and Gebhart G.F. *PNAS* **1999**, *96*, 7687-7692.

21. Mason P. *Annu. Rev. Neurosci.* **2001**, *24*, 737-777.

22. Vera-Portocarrero L.P., Zhang E.T., Ossipov M.H., Xie J.Y., King T., Lai J., and Porreca F. *Neurosci.* **2006**, *140*, 1311-1320.

23. Polomano R.C. and Farrar J.T. *Am. J. Nurs.* **2006**, *106*, 39-47.

24. Kalso E., Edwards J.E., Moore R.A., and McQuay H.J. *Pain* **2004**, *112*, 372-380.

25.   Abs R., Verhelst J., Maeyaert J., Van Buyten J.P., Opsomer F., Adriaensen H., Verlooy J., Van Havenbergh T., Smet M., and Van Acker K. *J. Clin. Endocr. Metab.* **2000**, *85*, 2215-2222.

26.   Compton P., Charuvastra V.C., and Ling W. *Drug Alcohol Depend.* **2001**, *63*, 139-146.

27.   Kouyanou K., Pither C.E., and Wessely S. *J. Psychosom. Res.* **1997**, *43*, 497-504.

28.   Porreca F., Burgess S.E., Gardell L.R., Vanderah T.W., Malan T.P., Jr., Ossipov M.H., Lappi D.A., and Lai J. *J. Neurosci.* **2001**, *21*, 5281-5288.

29.   Lai J., Ossipov M.H., Vanderah T.W., Malan T.P., Jr., and Porreca F. *Mol. Interventions* **2001**, *1*, 160-167.

30.   Mao J., Sung B., Ji R.R., and Lim G. *J. Neurosci.* **2002**, *22*, 7650-7661.

31.   Doverty M., White J.M., Somogyi A.A., Bochner F., Ali R., and Ling W. *Pain* **2001**, *90*, 91-96.

32.   Chong M.S. and Brandner B. *Biomed. Pharmacother.* **2006**, *60*, 318-322.

33.   Martin T.J. and Eisenach J.C. *J. Pharmacol. Exp. Ther.* **2001**, *299*, 811-817.

34.   Mico J.A., Ardid D., Berrocoso E., and Eschalier A. *Trends Pharmacol. Sci.* **2006**, *27*, 348-354.

35.   Visser E. and Schug S.A. *Biomed. Pharmacother.* **2006**, *60*, 341-348.

36.   Azevedo F.A., Carvalho L.R., Grinberg L.T., Farfel J.M., Ferretti R.E., Leite R.E., Jacob Filho W., Lent R., and Herculano-Houzel S. *J. Comp. Neurol.* **2009**, *513*, 532-541.

37.   Bruno V., Battaglia G., Casabona G., Copani A., Caciagli F., and Nicoletti F. *J. Neurosci.* **1998**, *18*, 9594-9600.

38.   Allen N.J. and Barres B.A. *Curr. Opin. Neurobiol.* **2005**, *15*, 542-548.

39.   Araque A., Carmignoto G., and Haydon P.G. *Annu. Rev. Physiol.* **2001**, *63*, 795-813.

40.   Verkhratsky A. and Kirchhoff F. *J. Anat.* **2007**, *210*, 651-660.

41.   Watkins L.R., Hutchinson M.R., Milligan E.D., and Maier S.F. *Brain Res. Rev.* **2007**, *56*, 148-169.

42.   Watkins L.R., Milligan E.D., and Maier S.F. *Trends Neurosci.* **2001**, *24*, 450-455.

43.   Hutchinson M.R., Bland S.T., Johnson K.W., Rice K.C., Maier S.F., and Watkins L.R. *ScientificWorldJournal* **2007**, *7*, 98-111.

44. Aronica E., Gorter J.A., Rozemuller A.J., Yankaya B., and Troost D. *Neurosci.* **2005**, *130*, 927-933.

45. Corlew R., Brasier D.J., Feldman D.E., and Philpot B.D. *Neuroscientist* **2008**, *14*, 609-625.

46. Anwyl R. *Neuropharmacol.* **2009**, *56*, 735-740.

47. Bliss T.V. and Collingridge G.L. *Nature* **1993**, *361*, 31-39.

48. Kim S.J. and Linden D.J. *Neuron* **2007**, *56*, 582-592.

49. Kullmann D.M. and Lamsa K.P. *Nat. Rev. Neurosci.* **2007**, *8*, 687-699.

50. Kew J.N. and Kemp J.A. *Psychopharmacol.* **2005**, *179*, 4-29.

51. Chen S.R. and Pan H.L. *J. Pharmacol. Exp. Ther.* **2005**, *312*, 120-126.

52. Simmons R.M., Webster A.A., Kalra A.B., and Iyengar S. *Pharmacol. Biochem. Behav.* **2002**, *73*, 419-427.

53. Zheng G.Z., Bhatia P., Kolasa T., Patel M., El Kouhen O.F., Chang R., Uchic M.E., Miller L., Baker S., Lehto S.G., Honore P., Wetter J.M., Marsh K.C., Moreland R.B., Brioni J.D., and Stewart A.O. *Bioorg. Med. Chem. Lett.* **2006**, *16*, 4936-4940.

54. Fisher K., Lefebvre C., and Coderre T.J. *Pharmacol. Biochem. Behav.* **2002**, *73*, 411-418.

55. Collado I., Pedregal C., Mazon A., Espinosa J.F., Blanco-Urgoiti J., Schoepp D.D., Wright R.A., Johnson B.G., and Kingston A.E. *J. Med. Chem.* **2002**, *45*, 3619-3629.

56. Helton D.R., Tizzano J.P., Monn J.A., Schoepp D.D., and Kallman M.J. *J. Pharmacol. Exp. Ther.* **1998**, *284*, 651-660.

57. Johnson M.P., Barda D., Britton T.C., Emkey R., Hornback W.J., Jagdmann G.E., McKinzie D.L., Nisenbaum E.S., Tizzano J.P., and Schoepp D.D. *Psychopharmacol.* **2005**, *179*, 271-283.

58. Feeley Kearney J.A. and Albin R.L. *Exp. Neurol.* **2003**, *184 Suppl 1*, S30-36.

59. Ossowska K., Konieczny J., Wardas J., Golembiowska K., Wolfarth S., and Pilc A. *Amino Acids* **2002**, *23*, 193-198.

60. Senkowska A. and Ossowska K. *Pol. J. Pharmacol.* **2003**, *55*, 935-950.

61. Gonzalez-Maeso J., Ang R.L., Yuen T., Chan P., Weisstaub N.V., Lopez-Gimenez J.F., Zhou M., Okawa Y., Callado L.F., Milligan G., Gingrich J.A., Filizola M., Meana J.J., and Sealfon S.C. *Nature* **2008**, *452*, 93-97.

62. Moghaddam B. *Psychopharmacol.* **2004**, *174*, 39-44.

63.   Alexander G.M. and Godwin D.W. *Epilepsy Res.* **2006**, *71*, 1-22.

64.   Chaki S., Yoshikawa R., Hirota S., Shimazaki T., Maeda M., Kawashima N., Yoshimizu T., Yasuhara A., Sakagami K., Okuyama S., Nakanishi S., and Nakazato A. *Neuropharmacol.* **2004**, *46*, 457-467.

65.   Markou A. *Biol. Psych.* **2007**, *61*, 17-22.

66.   Pilc A., Chaki S., Nowak G., and Witkin J.M. *Biochem. Pharmacol.* **2008**, *75*, 997-1006.

67.   Spillson A.B. and Russell J.W. *Exp. Neurol.* **2003**, *184 Suppl 1*, S97-105.

68.   Kenny P.J., Boutrel B., Gasparini F., Koob G.F., and Markou A. *Psychopharmacol.* **2005**, *179*, 247-254.

69.   Kenny P.J. and Markou A. *Trends Pharmacol. Sci.* **2004**, *25*, 265-272.

70.   Peters J. and Kalivas P.W. *Psychopharmacol.* **2006**, *186*, 143-149.

71.   Fisher K. and Coderre T.J. *Pain* **1996**, *68*, 255-263.

72.   Chizh B.A. *Amino Acids* **2002**, *23*, 169-176.

73.   Willis W.D. *Brain Res. Rev.* **2002**, *40*, 202-214.

74.   Sandkuhler J. *Pain* **2000**, *88*, 113-118.

75.   Anwyl R. *Brain Res. Rev.* **1999**, *29*, 83-120.

76.   Carlsson K.C., Hoem N.O., Moberg E.R., and Mathisen L.C. *Acta Anaesthesiol. Scand.* **2004**, *48*, 328-336.

77.   Bhave G., Karim F., Carlton S.M., and Gereau R.W.t. *Nat. Neurosci.* **2001**, *4*, 417-423.

78.   Jang J.H., Kim D.W., Sang Nam T., Se Paik K., and Leem J.W. *Neurosci.* **2004**, *128*, 169-176.

79.   Jia H., Rustioni A., and Valtschanoff J.G. *J. Comp. Neurol.* **1999**, *410*, 627-642.

80.   Azkue J.J., Mateos J.M., Elezgarai I., Benitez R., Osorio A., Diez J., Bilbao A., Bidaurrazaga A., and Grandes P. *Neurosci. Lett.* **2000**, *287*, 236-238.

81.   De Blasi A., Conn P.J., Pin J., and Nicoletti F. *Trends Pharmacol. Sci.* **2001**, *22*, 114-120.

82.   Neugebauer V., Li W., Bird G.C., and Han J.S. *Neuroscientist* **2004**, *10*, 221-234.

83.   Neugebauer V. and Li W. *J. Neurophysiol.* **2002**, *87*, 103-112.

84.   Nandigama P. and Borszcz G.S. *Brain Res.* **2003**, *959*, 343-354.

85.   LeDoux J.E. *Annu. Rev. Neurosci.* **2000**, *23*, 155-184.

86.   Han J.S., Li W., and Neugebauer V. *J. Neurosci.* **2005**, *25*, 10717-10728.

87.   Li W. and Neugebauer V. *J. Neurophysiol.* **2004**, *91*, 13-24.

88.   Han J.S., Fu Y., Bird G.C., and Neugebauer V. *Mol. Pain* **2006**, *2*, 18.

89.   Han J.S., Bird G.C., and Neugebauer V. *Neuropharmacol.* **2004**, *46*, 918-926.

90.   Linden A.M., Baez M., Bergeron M., and Schoepp D.D. *Neuropharmacol.* **2006**,

91.   Lin H.C., Wang S.J., Luo M.Z., and Gean P.W. *J. Neurosci.* **2000**, *20*, 9017-9024.

92.   Lin C.H., Lee C.C., Huang Y.C., Wang S.J., and Gean P.W. *Learn. Memory* **2005**, *12*, 130-137.

93.   Maione S., Marabese I., Leyva J., Palazzo E., de Novellis V., and Rossi F. *Neuropharmacol.* **1998**, *37*, 1475-1483.

94.   Maione S., Oliva P., Marabese I., Palazzo E., Rossi F., Berrino L., and Filippelli A. *Pain* **2000**, *85*, 183-189.

95.   Budai D. and Larson A.A. *Neurosci.* **1998**, *83*, 571-580.

96.   Sharpe E.F., Kingston A.E., Lodge D., Monn J.A., and Headley P.M. *Br. J. Pharmacol.* **2002**, *135*, 1255-1262.

97.   Sugiyama H., Ito I., and Hirono C. *Nature* **1987**, *325*, 531-533.

98.   Palmer E., Monaghan D.T., and Cotman C.W. *Eur. J. Pharmacol.* **1989**, *166*, 585-587.

99.   Masu M., Tanabe Y., Tsuchida K., Shigemoto R., and Nakanishi S. *Nature* **1991**, *349*, 760-765.

100.   Houamed K.M., Kuijper J.L., Gilbert T.L., Haldeman B.A., O'Hara P.J., Mulvihill E.R., Almers W., and Hagen F.S. *Science* **1991**, *252*, 1318-1321.

101.   Pin J.P. and Duvoisin R. *Neuropharmacol.* **1995**, *34*, 1-26.

102.   Schoepp D.D. *Neurochem. Int.* **1994**, *24*, 439-449.

103.   Schoepp D.D., Jane D.E., and Monn J.A. *Neuropharmacol.* **1999**, *38*, 1431-1476.

104.   O'Hara P.J., Sheppard P.O., Thogersen H., Venezia D., Haldeman B.A., McGrane V., Houamed K.M., Thomsen C., Gilbert T.L., and Mulvihill E.R. *Neuron* **1993**, *11*, 41-52.

105.   Kunishima N., Shimada Y., Tsuji Y., Sato T., Yamamoto M., Kumasaka T., Nakanishi S., Jingami H., and Morikawa K. *Nature* **2000**, *407*, 971-977.

106.   Desai M.A. and Conn P.J. *Neurosci. Lett.* **1990**, *109*, 157-162.

107.   Bräuner-Osborne H., Egebjerg J., Nielsen E.O., Madsen U., and Krogsgaard-Larsen P. *J. Med. Chem.* **2000**, *43*, 2609-2045.

108.   Watkins J. and Collingridge G. *Trends Pharmacol. Sci.* **1994**, *15*, 333-342.

109. Hayashi Y., Sekiyama N., Nakanishi S., Jane D.E., Sunter D.C., Birse E.F., Udvarhelyi P.M., and Watkins J.C. *J. Neurosci.* **1994**, *14*, 3370-3377.

110. Eaton S.A., Jane D.E., Jones P.L., Porter R.H., Pook P.C., Sunter D.C., Udvarhelyi P.M., Roberts P.J., Salt T.E., and Watkins J.C. *Eur. J. Pharmacol.* **1993**, *244*, 195-197.

111. Caveney S. and Starratt A. *Nature* **1994**, *372*, 509.

112. Fowden L. and Smith A. *Phytochem.* **1969**, *8*, 1043-1045.

113. Millington D.S. and Sheppard R.C. *Phytochem.* **1969**, *8*, 437-443.

114. Starratt A.N. and Caveney S. *Phytochem.* **1995**, *40*, 479-481.

115. Bessis A.S., Jullian N., Coudert E., Pin J.P., and Acher F. *Neuropharmacol.* **1999**, *38*, 1543-1551.

116. Costantino G., Macchiarulo A., and Pellicciari R. *J. Med. Chem.* **1999**, *42*, 2816-2827.

117. Jullian N., Brabet I., Pin J.P., and Acher F.C. *J. Med. Chem.* **1999**, *42*, 1546-1555.

118. Kawai M., Horikawa Y., Ishihara T., Shimamoto K., and Ohfune Y. *Eur. J. Pharmacol.* **1992**, *211*, 195-202.

119. Pellicciari R., Costantino G., Marinozzi M., Macchiarulo A., Amori L., Josef Flor P., Gasparini F., Kuhn R., and Urwyler S. *Bioorg. Med. Chem. Lett.* **2001**, *11*, 3179-3182.

120. Thomsen C., Bruno V., Nicoletti F., Marinozzi M., and Pellicciari R. *Mol. Pharmacol.* **1996**, *50*, 6-9.

121. Collado I., Pedregal C., Bueno A.B., Marcos A., Gonzalez R., Blanco-Urgoiti J., Perez-Castells J., Schoepp D.D., Wright R.A., Johnson B.G., Kingston A.E., Moher E.D., Hoard D.W., Griffey K.I., and Tizzano J.P. *J. Med. Chem.* **2004**, *47*, 456-466.

122. Gonzalez R., Collado I., de Uralde B.L., Marcos A., Martin-Cabrejas L.M., Pedregal C., Blanco-Urgoiti J., Perez-Castells J., Fernandez M.A., Andis S.L., Johnson B.G., Wright R.A., Schoepp D.D., and Monn J.A. *Bioorg. Med. Chem.* **2005**, *13*, 6556-6570.

123. Amori L., Serpi M., Marinozzi M., Costantino G., Diaz M.G., Hermit M.B., Thomsen C., and Pellicciari R. *Bioorg. Med. Chem. Lett.* **2006**, *16*, 196-199.

124. Pellicciari R., Marinozzi M., Natalini B., Costantino G., Luneia R., Giorgi G., Moroni F., and Thomsen C. *J. Med. Chem.* **1996**, *39*, 2259-2269.

125. Monn J.A., Valli M.J., Massey S.M., Wright R.A., Salhoff C.R., Johnson B.G., Howe T., Alt C.A., Rhodes G.A., Robey R.L., Griffey K.R., Tizzano J.P., Kallman M.J., Helton D.R., and Schoepp D.D. *J. Med. Chem.* **1997**, *40*, 528-537.

126. Monn J.A., Valli M.J., Massey S.M., Hansen M.M., Kress T.J., Wepsiec J.P., Harkness A.R., Grutsch J.L., Jr., Wright R.A., Johnson B.G., Andis S.L., Kingston A., Tomlinson R., Lewis R., Griffey K.R., Tizzano J.P., and Schoepp D.D. *J. Med. Chem.* **1999**, *42*, 1027-1040.

127. Monn J.A., Massey S.M., Valli M.J., Henry S.S., Stephenson G.A., Bures M., Herin M., Catlow J., Giera D., Wright R.A., Johnson B.G., Andis S.L., Kingston A., and Schoepp D.D. *J. Med. Chem.* **2007**, *50*, 233-240.

128. Avery T.D., Greatrex B.W., Pedersen D.S., Taylor D.K., and Tiekink E.R. *J. Org. Chem.* **2008**, *73*, 2633-2640.

129. Gerwick W.H., Proteau P.J., Nagle D.G., Hamel E., Blokhin A., and Slate D.L. *J. Org. Chem.* **1994**, *59*, 1243-1245.

130. Gu L., Jia J., Liu H., Hakansson K., Gerwick W.H., and Sherman D.H. *J. Am. Chem. Soc.* **2006**, *128*, 9014-9015.

131. Nagle D.G. and Gerwick W.H. *J. Org. Chem.* **1994**, *59*, 7227-7237.

132. Wallock N.J. and Donaldson W.A. *J. Org. Chem.* **2004**, *69*, 2997-3007.

133. Tokiwano T., Watanabe H., Seo T., and Oikawa H. *Chem. Comm.* **2008**, 6016-6018.

134. Yoshida M., Ezaki M., Hashimoto M., Yamashita M., Shigematsu N., Okuhara M., Kohsaka M., and Horikoshi K. *J. Antibiot.* **1990**, *43*, 748-754.

135. Deng X.-M., Cai P., Ye S., Sun X.-L., Liao W.-W., Li K., Tang Y., Wu Y.-D., and Dai L.-X. *J. Am. Chem. Soc.* **2006**, *128*, 9730-9740.

136. Hartikka A. and Arvidsson P.I. *J. Org. Chem.* **2007**, *72*, 5874-5877.

137. Denmark S.E., Christenson B.L., O'Connor S.P., and Murase N. *Pure Appl. Chem.* **1996**, *68*, 23-27.

138. Denmark S.E., Edwards J.P., and Wilson S.R. *J. Am. Chem. Soc.* **1992**, *114*, 2592-2602.

139. Doyle M.P. and Protopopova M.N. *Tetrahedron* **1998**, *54*, 7919-7946.

140. Furukawa J., Kawabata N., and Nishimura J. *Tetrahedron Lett.* **1966**, 3353-3354.

141. Nishimura J., Kawabata N., and Furukawa J. *Tetrahedron* **1969**, *25*, 2647-2659.

142. Salaun J. *Chem. Rev.* **1989**, *89*, 1247-1270.

143. Long J., Du H., Li K., and Shi Y. *Tetrahedron Lett.* **2005**, *46*, 2737-2740.

144. Doyle M.P., Austin R.E., Bailey A.S., Dwyer M.P., Dyatkin A.B., Kalinin A.V., Kwan M.M.Y., Liras S., and Oalmann C.J. *J. Am. Chem. Soc.* **1995**, *117*, 5763-5775.

145. Nishiyama H., Itoh Y., Matsumoto H., Park S.-B., and Itoh K. *J. Am Chem. Soc.* **1994**, *116*, 2223-2224.

146. Ichiyanagi T., Shimizu M., and Fujisawa T. *Tetrahedron* **1997**, *53*, 9599-9610.

147. Park S.-W., Son J.-H., Kim S.-G., and Ahn K.H. *Tetrahedron: Asymmetry* **1999**, *10*, 1903-1911.

148. Reissig H.-U. *Angew. Chem. Int. Ed.* **1996**, *35*, 971-973.

149. Struempel M., Ondruschka B., Daute R., and Stark A. *Green Chem.* **2008**, *10*, 41-43.

150. Barluenga J., de Prado A., Santamaria J., and Tomas M. *Chem.* **2007**, *13*, 1326-1331.

151. Li A.-H., Dai L.-X., and Aggarwal V.K. *Chem. Rev.* **1997**, *97*, 2341-2372.

152. Little R.D. and Dawson J.R. *Tetrahedron Lett.* **1980**, *21*, 2609-2612.

153. Su J., Qiu G., Liang S., and Hu X. *Syn. Comm.* **2005**, *35*, 1427-1433.

154. Sun X.-L. and Tang Y. *Acc. Chem. Res.* **2008**, *41*, 937-948.

155. Mazon A., Pedregal C., and Prowse W. *Tetrahedron* **1999**, *55*, 7057-7064.

156. Pajouhesh H., Curry K., Pajouhesh H., Meresht M.H., and Patrick B. *Tetrahedron: Asymmetry* **2003**, *14*, 593-596.

157. Aggarwal V.K. and Grange E. *Chem.* **2006**, *12*, 568-575.

158. Avery T.D., Culbert J.A., and Taylor D.K. *Org. Biomol. Chem.* **2006**, *4*, 323-330.

159. Avery T.D., Fallon G., Greatrex B.W., Pyke S.M., Taylor D.K., and Tiekink E.R.T. *J. Org. Chem.* **2001**, *66*, 7955-7966.

160. Avery T.D., Haselgrove T.D., Rathbone T.J., Taylor D.K., and Tiekink E.R.T. *Chem. Comm.* **1998**, 333-334.

161. Avery T.D., Taylor D.K., and Tiekink E.R.T. *J. Org. Chem.* **2000**, *65*, 5531-5546.

162. Brown Rachel C., Taylor Dennis K., and Elsey Gordon M. *Org. Lett.* **2006**, *8*, 463-466.

163. Greatrex B.W. and Taylor D.K. *J. Org. Chem.* **2005**, *70*, 470-476.

164. Greatrex B.W., Kimber M.C., Taylor D.K., Fallon G., and Tiekink E.R.T. *J. Org. Chem.* **2002**, *67*, 5307-5314.

165. Greatrex B.W., Kimber M.C., Taylor D.K., and Tiekink E.R.T. *J. Org. Chem.* **2003**, *68*, 4239-4246.

166. Greatrex B.W., Taylor D.K., and Tiekink E.R.T. *J. Org. Chem.* **2004**, *69*, 2580-2583.

167. Kimber M.C. and Taylor D.K. *J. Org. Chem.* **2002**, *67*, 3142-3144.

168. Kornblum N. and DeLaMare H.E. *J. Am. Chem. Soc.* **1951**, *73*, 880-881.

169. Guan H.-P., Qiu Y.-L., Ksebati M.B., Kern E.R., and Zemlicka J. *Tetrahedron* **2002**, *58*, 6047-6059.

170. Fujiwara N., Kinoshita M., and Akita H. *Tetrahedron: Asymmetry* **2006**, *17*, 3037-3045.

171. Omura K. and Swern D. *Tetrahedron* **1978**, *34*, 1651-1660.

172. Banwell M.G., McLeod M.D., Premraj R., and Simpson G.W. *Aust. J. Chem.* **2000**, *53*, 659-664.

173. Parikh J.R. and Doering W.v.E. *J. Am. Chem. Soc.* **1967**, *89*, 5505-5507.

174. Wakamatsu K., Takahashi Y., Kikuchi K., and Miyashi T. *J. Chem. Soc.* **1996**, 2105-2109.

175. Meijere A.D. *Angew. Chem.* **1979**, *91*, 867-884.

176. Anastasia M., Allevi P., Ciuffreda P., Fiecchi A., and Scala A. *J. Org. Chem.* **1985**, *50*, 321-325.

177. Huisgen R. *1,3-Dipolar Cycloadd. Chem.* **1984**, *1*, 1-176.

178. Krogsgaard-Larsen P., Honore T., Hansen J.J., Curtis D.R., and Lodge D. *Nature* **1980**, *284*, 64-66.

179. Hansen J.J., Lauridsen J., Nielsen E., and Krogsgaard-Larsen P. *J. Med. Chem.* **1983**, *26*, 901-903.

180. Madsen U., Slok F.A., Stensbol T.B., Brauner-Osborne H., Lutzhoft H.H., Poulsen M.V., Eriksen L., and Krogsgaard-Larsen P. *Eur. J. Med. Chem.* **2000**, *35*, 69-76.

181. Ebert B., Lenz S., Brehm L., Bregnedal P., Hansen J.J., Frederiksen K., Bogeso K.P., and Krogsgaard-Larsen P. *J. Med. Chem.* **1994**, *37*, 878-884.

182. Rosenberg S.H., Spina K.P., Woods K.W., Polakowski J., Martin D.L., Yao Z., Stein H.H., Cohen J., Barlow J.L., Egan D.A., and et al. *J. Med. Chem.* **1993**, *36*, 449-59.

183. Afonso C.A.M. *Syn. Comm.* **1998**, *28*, 261 - 276.

184. Yan R.-B., Yang F., Wu Y., Zhang L.-H., and Ye X.-S. *Tetrahedron Lett.* **2005**, *46*, 8993-8995.

185. Gajewski M., Seaver B., and Esslinger C.S. *Bioorg. Med. Chem. Lett.* **2007**, *17*, 4163-4166.

186. Hou D.-R., Alam S., Kuan T.-C., Ramanathan M., Lin T.-P., and Hung M.-S. *Bioorg. Med. Chem. Lett.* **2009**, *19*, 1022-1025.

187. Ito S., Satoh A., Nagatomi Y., Hirata Y., Suzuki G., Kimura T., Satow A., Maehara S., Hikichi H., Hata M., Kawamoto H., and Ohta H. *Bioorg. Med. Chem. Lett.* **2008**, *16*, 9817-9829.

188. Srinivasan R., Tan L.P., Wu H., Yang P.-Y., Kalesh K.A., and Yao S.Q. *Org. Biomol. Chem.* **2009**, *7*, 1821-1828.

189. Lewis W.G., Green L.G., Grynszpan F., Radic Z., Carlier P.R., Taylor P., Finn M.G., and Sharpless K.B. *Angew. Chem. Int. Ed.* **2002**, *41*, 1053-1057.

190. Krasinski A., Radic Z., Manetsch R., Raushel J., Taylor P., Sharpless K.B., and Kolb H.C. *J. Am. Chem. Soc.* **2005**, *127*, 6686-6692.

191. Kolb H.C., Finn M.G., and Sharpless K.B. *Angew. Chem. Int. Ed.* **2001**, *40*, 2004-2021.

192. Kolb H.C. and Sharpless K.B. *Drug Discovery Today* **2003**, *8*, 1128-1137.

193. Breinbauer R. and Koehn M. *ChemBioChem* **2003**, *4*, 1147-1149.

194. Hotha S. and Kashyap S. *J. Org. Chem.* **2006**, *71*, 364-367.

195. Lutz J.-F. *Angew. Chem. Int. Ed.* **2007**, *46*, 1018-1025.

196. Vora A., Singh K., and Webster D.C. *Polymer* **2009**, *50*, 2768-2774.

197. Ahlquist M. and Fokin V.V. *Organometallics* **2007**, *26*, 4389-4391.

198. Himo F., Lovell T., Hilgraf R., Rostovtsev V.V., Noodleman L., Sharpless K.B., and Fokin V.V. *J. Am. Chem. Soc.* **2005**, *127*, 210-216.

199. Boren B.C., Narayan S., Rasmussen L.K., Zhang L., Zhao H., Lin Z., Jia G., and Fokin V.V. *J. Am. Chem. Soc.* **2008**, *130*, 8923-8930.

200. Conrow R.E. and Dean W.D. *Org. Process Res. Dev.* **2008**, *12*, 1285-1286.

201. Vollmar A. and Dunn M.S. *J. Org. Chem.* **1960**, *25*, 387-390.

202. Van Esseveldt B.C.J., Van Delft F.L., Smits J.M.M., De Gelder R., Schoemaker H.E., and Rutjes F.P.J.T. *Adv. Syn. Catal.* **2004**, *346*, 823-834.

203. Gomez-Vidal J.A. and Silverman R.B. *Org. Lett.* **2001**, *3*, 2481-2484.

204. Fagan P.J., Ward M.D., and Calabrese J.C. *J. Am. Chem. Soc.* **1989**, *111*, 1698-1719.

205. Morandini F., Dondana A., Munari I., Pilloni G., Consiglio G., Sironi A., and Moret M. *Inorg. Chim. Acta* **1998**, *282*, 163-172.

206. Bleakman D., Alt A., and Nisenbaum E.S. *Semin. Cell Dev. Biol.* **2006**, *17*, 592-604.

207. Gerber G., Zhong J., Youn D., and Randic M. *Neurosci.* **2000**, *100*, 393-406.

208. Ahn D.K., Kim K.H., Jung C.Y., Choi H.S., Lim E.J., Youn D.H., and Bae Y.C. *Pain* **2005**, *118*, 53-60.

209. Ransom R.W. and Stec N.L. *J. Neurochem.* **1988**, *51*, 830-836.

210. Honoré T. and Nielsen M. *Neurosci. Lett.* **1985**, *54*, 27-32.

211. Braitman D.J. and Coyle J.T. *Neuropharmacol.* **1987**, *26*, 1247-1251.

212. Sills M.A., Fagg G., Pozza M., Angst C., Brundish D.E., Hurt S.D., Wilusz E.J., and Williams M. *Eur. J. Pharmacol.* **1991**, *192*, 19-24.

213. Bradford M.M. *Anal. Biochem.* **1976**, *72*, 248-254.

214. Aramori I. and Nakanishi S. *Neuron* **1992**, *8*, 757-765.

215. Tanabe Y., Masu M., Ishii T., Shigemoto R., and Nakanishi S. *Neuron* **1992**, *8*, 169-179.

216. Hayashi Y., Tanabe Y., Aramori I., Masu M., Shimamoto K., Ohfune Y., and Nakanishi S. *Br. J. Pharmacol.* **1992**, *107*, 539-543.

217. Craig D.A. *Trends Pharmacol. Sci.* **1993**, *14*, 89-91.

218. Milligan E.D., Hinde J.L., Mehmert K.K., Maier S.F., and Watkins L.R. *J. Neurosci. Method.* **1999**, *90*, 81-86.

219. Bennett G.J. and Xie Y.K. *Pain* **1988**, *33*, 87-107.

220. Milligan E.D., Maier S.F., and Watkins L.R. *Method. Mol. Med.* **2004**, *99*, 67-89.

221. Chaplan S.R., Bach F.W., Pogrel J.W., Chung J.M., and Yaksh T.L. *J. Neurosci. Method.* **1994**, *53*, 55-63.

222. Chacur M., Milligan E.D., Gazda L.S., Armstrong C., Wang H., Tracey K.J., Maier S.F., and Watkins L.R. *Pain* **2001**, *94*, 231-244.

223. Milligan E.D., O'Connor K.A., Nguyen K.T., Armstrong C.B., Twining C., Gaykema R.P., Holguin A., Martin D., Maier S.F., and Watkins L.R. *J. Neurosci.* **2001**, *21*, 2808-2819.

224. Treutwein B. and Strasburger H. *Percep. Psychophys.* **1999**, *61*, 87-106.

225. Milligan E.D., Mehmert K.K., Hinde J.L., Harvey L.O., Martin D., Tracey K.J., Maier S.F., and Watkins L.R. *Brain Res.* **2000**, *861*, 105-116.

226. Milligan E.D., Zapata V., Chacur M., Schoeniger D., Biedenkapp J., O'Connor K.A., Verge G.M., Chapman G., Green P., Foster A.C., Naeve G.S., Maier S.F., and Watkins L.R. *Eur. J. Neurosci.* **2004**, *20*, 2294-2302.

227. Milligan E.D., Twining C., Chacur M., Biedenkapp J., O'Connor K., Poole S., Tracey K., Martin D., Maier S.F., and Watkins L.R. *J. Neurosci.* **2003**, *23*, 1026-1040.

228. Wieseler-Frank J., Maier S.F., and Watkins L.R. *Neurochem. Int.* **2004**, *45*, 389-395.

229. Hansson E. *Acta Physiol.* **2006**, *187*, 321-327.

230. Jones C.K., Lutz Eberle E., Peters S.C., Monn J.A., and Shannon H.E. *Neuropharmacol.* **2005**, *49*, 206-218.

231. Ohishi H., Shigemoto R., Nakanishi S., and Mizuno N. *J. Comp. Neurol.* **1993**, *335*, 252-266.

232. Carlton S.M., Hargett G.L., and Coggeshall R.E. *Neurosci.* **2001**, *105*, 957-969.

233. Dolan S. and Nolan A.M. *Neuropharmacol.* **2000**, *39*, 1132-1138.

234. Fundytus M.E. *CNS Drugs* **2001**, *15*, 29-58.

235. Zhou H.Y., Zhang H.M., Chen S.R., and Pan H.L. *J. Neurophysiol.* **2007**, *97*, 871-882.

236. Aronica E., van Vliet E.A., Mayboroda O.A., Troost D., da Silva F.H., and Gorter J.A. *Eur. J. Neurosci.* **2000**, *12*, 2333-2344.

237. Petralia R.S., Wang Y.X., Niedzielski A.S., and Wenthold R.J. *Neurosci.* **1996**, *71*, 949-976.

238. Tamaru Y., Nomura S., Mizuno N., and Shigemoto R. *Neurosci.* **2001**, *106*, 481-503.

239. Watkins L.R. and Maier S.F. *Physiol. Rev.* **2002**, *82*, 981-1011.

240. Garrison C.J., Dougherty P.M., Kajander K.C., and Carlton S.M. *Brain Res.* **1991**, *565*, 1-7.

241. Üçeyler N., Tscharke A., and Sommer C. *Brain Behav. Immun.* **2007**, *21*, 553-560.

242. Cao H. and Zhang Y.Q. *Neurosci. Biobehav. Rev.* **2008**, *32*, 972-983.

243. Jung C.Y., Lee S.Y., Choi H.S., Lim E.J., Lee M.K., Yang G.Y., Han S.R., Youn D.H., and Ahn D.K. *Neurosci. Lett.* **2006**, *409*, 173-178.

244. Hutchinson M.R., Coats B.D., Lewis S.S., Zhang Y., Sprunger D.B., Rezvani N., Baker E.M., Jekich B.M., Wieseler J.L., Somogyi A.A., Martin D., Poole S.,

Judd C.M., Maier S.F., and Watkins L.R. *Brain Behav. Immun.* **2008**, *22*, 1178-1189.

245. Song P. and Zhao Z.Q. *Neurosci. Res.* **2001**, *39*, 281-286.

246. Watkins L.R., Hutchinson M.R., Johnston I.N., and Maier S.F. *Trends Neurosci.* **2005**, *28*, 661-669.

247. Popik P., Kozela E., and Pilc A. *Br. J. Pharmacol.* **2000**, *130*, 1425-1431.

248. Furukawa H., Singh S.K., Mancusso R., and Gouaux E. *Nature* **2005**, *438*, 185-192.

249. Gill A., Birdsey-Benson A., Jones B.L., Henderson L.P., and Madden D.R. *Biochem.* **2008**, *47*, 13831-13841.

250. Tsuchiya D., Kunishima N., Kamiya N., Jingami H., and Morikawa K. *PNAS* **2002**, *99*, 2660-2665.

251. Muto T., Tsuchiya D., Morikawa K., and Jingami H. *PNAS* **2007**, *104*, 3759-3764.

252. Bertrand H.O., Bessis A.S., Pin J.P., and Acher F.C. *J. Med. Chem.* **2002**, *45*, 3171-3183.

253. Yao Y., Pattabiraman N., Michne W.F., Huang X.P., and Hampson D.R. *J. Neurochem.* **2003**, *86*, 947-957.

254. Kasper C., Frydenvang K., Naur P., Gajhede M., Pickering D.S., and Kastrup J.S. *FEBS Lett.* **2008**, *582*, 4089-4094.

255. Webb H.K., Wu Z., Sirisoma N., Ha H.C., Casero R.A., Jr., and Woster P.M. *J. Med. Chem.* **1999**, *42*, 1415-1421.

256. Murakami M., Ubukata M., and Ito Y. *Tetrahedron Lett.* **1998**, *39*, 7361-7364.

257. Kim H., Cho Jin K., Aimoto S., and Lee Y.-S. *Org. Lett.* **2006**, *8*, 1149-1151.